History of the Fluids Associated with the Lode-Gold Deposits, and Complex U-PGE-Au Vein-Type Deposits, Goldfields Peninsula, Northern Saskatchewan, Canada

A Thesis Submitted to the Faculty of Graduate Studies and Research, in Partial Fulfillment of the Requirements for the Degree of

Master of Science
in Geology

at the
Department of Geological Sciences
University of Saskatchewan
Saskatoon, Canada

Matthew Ian Rees
May, 1992

Acknowledgements

The author would like to acknowledge the support and assistance provided by the faculty and staff in the Department of Geological Sciences over the last number of years. In particular, assistance from, or discussions with, Drs. H.E. Hendry, R.W. Kerrich, L.C. Coleman, M. Stauffer, M.J. Reeves, R.W. Renault, and G.R. Edwards were of great help. I am grateful to D. Pezderic, M. Novakowski, Z. Szczepanik, and J. Dubets for teaching me many laboratory and sample preparation techniques, which I was often able to teach to others. I am wholly indebted to D. Chipley, T. Kotzer, M. Powell, S. Whittaker, T. Cadrin, B. Janser, and G. Koehler for their technical assistance, and the many animated discussions over the years. This work has also benefited from many fruitful discussions with K. Ansdell, M.S. Ibrahim, D. O'Hanley, R. King, D. Wyman, J. Fedorowich, F. Hrdy, P. Field, D. Schultz and M. Fayek.

Many thanks to D. Quirt of the Saskatchewan Research Council for his help, both in the loaning of samples and data, as well as the many long discussions. The Saskatchewan Research Council, under the guidance of Dr. J. Hoeve, undertook the initial funding of the work. Later funding was provided by research grants to Dr. T.K. Kyser from NERSC and Saskatchewan Energy & Mines. Dr. T.I.I. Sibbald of SEM must be heartily thanked for his support and enthusiasm throughout the project.

I would like to extend my deepest gratitude to Dr. T.K.

Kyser, for his guidance and teaching, and for having the patience of a saint.

Finally, I have to express my deepest love and sympathy to my wife, Karen, who heroically withstood the pressures of an absent and delinquent husband for so long. You are the best.

Table of Contents

List of Figures.....i
List of Plates (Photomicrographs).....ii

Abstract.....1

1.0 Introduction
1.1 Location, Access, and Physiography.....4
1.2 Exploration History of the Beaverlodge Area.....4
1.3 Objective of Thesis.....10

2.0 Regional Geology
2.1 Tectonic Setting.....13
2.2 General Stratigraphy.....16
2.3 Geology of the Nevins Lake Block.....21
2.4 Economic Geology.....33

3.0 Field and Analytical Methods
3.1 Sample Collection.....37
3.2 Fluid Inclusion Techniques.....37
3.2.1 Polished Wafer Preparation.....37
3.2.2 Microthermometric Analysis.....48
3.3 Isotopic Methods.....49
3.3.1 Stable Isotopes.....49
3.3.2 Radiogenic Isotopes.....50
3.4 Geochemical Analyses.....51

4.0 Lode-Gold Deposits
4.1 Geology of Deposits.....52
4.1.1 Mine Granites.....52
4.1.2 Lode-Gold Veins.....57
4.2 Fluid Inclusions.....62
4.2.1 Inclusion Types & Petrography.....62
4.2.2 Microthermometric Data.....73
4.2.3 Discussion of Fluid Inclusion Data.....83

Table of Contents (continued)

4.3 Stable Isotopes.....96
4.3.1 Isotopic Compositions & Isotopic Geothermometry.....96
4.3.2 Fluids in Equilibrium with Minerals.....117
4.4 Radiogenic Isotopes.....122
4.5 Summary of Lode-Gold Deposits.....129

5.0 Au-PGE-U Mineralization
5.1 Geology of Deposits.....132
5.1.1 Nicholson & Fish Hook Bay Deposits.....132
5.1.2 Quartzite Ridge Showing.....135
5.1.3 Late U-bearing Veins ("Comb Veins").....137
5.1.4 Carbonate Albitite or "Sponge Rock".....137
5.2 Fluid Inclusions.....138
5.2.1 Fluid Inclusion Petrography.....138
5.2.2 Microthermometric Data.....149
5.2.3 Discussion of Data.....162
5.3 Stable Isotopic Data.....165
5.3.1 Isotopic Compositions & Isotopic Geothermometry.....165
5.3.2 Fluids in Equilibrium with Minerals.....171
5.4 Discussion and Summary.....173

6.0 Conclusion: Fluid History of the Goldfields Area.....178

References.....186

Appendix 1: Lithogeochemical Data.....200
Appendix 2: Summary of Type I Fluid Inclusion Data.....203
Appendix 3: Stable Isotope Data & Temperatures.....204
Appendix 4: Radiogenic Isotope Data.....206
Appendix 5: Sample List & Descriptions.....207

List of Figures

Figure 1: Schematic tectonic map of northern Saskatchewan.....5

Figure 2: Simplified geologic map of the Goldfields area; boxes outline the location of mineral deposits investigated in this study.....6

Figure 3: Simplified geologic map of the south end of Beaverlodge Lake, showing the location of the Quartzite Ridge showing.....11

Figure 4: Tectonic map of a portion of the Canadian Shield.....14

Figure 5: Simplified geologic map of the Beaverlodge area.....15

Figure 6: General stratigraphy, Beaverlodge area.....17

Figure 7: General geologic map of the Murmac Bay Group in the Goldfields area.....23

Figure 8: Compilation of published radiogenic ages of various rocks, Greater Beaverlodge area.....31

Figure 9: Simplified geologic map of the Goldfields area; numbered boxes refer to sample location maps.....38

Figure 10: Local geology and sample locations, Frontier lode-golddeposit.....39

Figure 11: Local geology and sample locations, 1986, Box lode-golddeposit.....40

Figure 12: Local geology and sample locations, 1987, Box lode-golddeposit.....41

Figure 13: Local geology and sample locations, Box Mine Docks, southeast of the Box Mine.....42

Figure 14: Local geology and sample locations, 1986, Athona lode-gold deposit.....43

Figure 15: Local geology and sample locations, 1987, Athona lode-gold deposit.....44

Figure 16: Local geology and sample locations, Melma lode-goldshowing.....45

Figure 17: Local geology and sample locations, Greenlee lode-goldshowing.....46

Figure 18: Local geology and sample locations, Nicholson Au-PGE-Udeposit.....47

Figure 19: Relation amoung normative quartz-albite-orthoclase compositions for samples of the Minegranites.....56

Figure 20: Paragenesis of minerals in lode-gold veins, Box and Athona mines.....59

Figure 21: Summary of fluid inclusion data from the Goldfields lode-gold quartz veins (Box, Athona,Frontier).....65

Figure 22: Type I fluid inclusions, showing examples of bimodal distribution of CO_2-H_2O ratios within a group of inclusions.....68

Figure 23: Histogram of combined Type I low temperature microthermometric data from the Box, Athona, and Frontier quartz veins.....74

Figure 24: Histogram of homogenization temperatures and low temperature microthermometric properties of Type II inclusions from the Box, Athona, and Frontier quartz veins.....75

Figure 25: Histogram of Type III and IV homogenization temperatures and low temperature microthermometric data from the Box quartz veins.....76

Figure 26: Histogram of homogenization temperatures of Type I inclusions from the Box, Athona, and Frontier quartz veins.....81

Figure 27: Relation between CO_2-H_2O homogenization temperatures and mole fraction (X) CO_2 of Type Iinclusions.....85

Figure 28: Two examples of morphology of Type I inclusions from the Box and Athona quartz veins.....88

Figure 29: Minimum pressure estimates based on CO_2 densities and CO_2-H_2O homogenization temperatures of Type I inclusions.....91

Figure 30: Summary of fluid inclusion data from the lode-gold veins, showing relation between homogenization temperatures and salinities of the various types of inclusions.....93

Figure 31: Summary of $\delta^{18}O$ values of minerals from lode-veins and Mine granites.....97

Figure 32: Al-Fe-Mg ternary diagram of chemical compositions of tourmalines from Goldfields lode-goldveins.....105

Figure 33: Relation between $\delta^{18}O$ quartz and $\delta^{18}O$ feldspar for coexisting quartz-feldspar pairs from the Box and Athona mine granites.....109

Figure 34: Relation between $\delta^{18}O$ quartz and $\delta^{18}O$ feldspar for coexisting quartz-feldspar pairs from the Goldfields lode-gold veins.....111

Figure 35: Compilation of $\delta^{34}S$ values for sulphide minerals in lode-veins from the Goldfields deposits.....113

Figure 36: Paragenesis of vein sulphides from the Box and Athona lode-gold deposits.....115

Figure 37: Relation between $\delta^{18}O$ and δD values of water in equilibrium with minerals from the Goldfields lode-golddeposits.....120

Figure 38: Rb/Sr isochrons for lode-gold vein minerals and Box mine granite feldspars.....124

Figure 39: Model of $^{87}Sr/^{86}Sr$ evolution of basement rocks, mine granites, and lode-gold vein minerals in the Goldfields area.....127

Figure 40: Schematic diagram of primary fluid inclusion locations on growth planes within euhedral quartz and dolomite crystals from the Au-PGE-U deposits in the Goldfields area.....140

Figure 41: Schematic diagram of primary and secondary fluid inclusion types from the Au-PGE-U deposits in the Goldfields area.....145

Figure 42: Schematic diagram of primary and secondary fluid inclusions from the Nicholson and Fish Hook Bay deposits that have overgrown an already formed solid phase.....147

Figure 43: Compilation histogram of homogenization temperatures and halite dissolution temperatures from primary and secondary fluid inclusions, Nicholson, Fish Hook Bay, and Quartzite Ridge deposits.....151

Figure 44: Histogram of homogenization temperatures of primary fluid inclusions from the cross-cutting comb veins, Box Mine.....152

Figure 45: Histogram of homogenization and NaCl dissolution temperatures of primary and secondary fluid inclusions in dolomite, Nicholson No.4 zone.....153

Figure 46: Histogram of homogenization and NaCl dissolution temperatures of primary and secondary inclusions in dolomite, Nicholson No.2zone.....155

Figure 47: Histogram of NaCl dissolution temperatures and low temperature microthermetric data from primary fluid inclusions in early quartz, Nicholson No.4 zone.....156

Figure 48: Histogram of homogenization and NaCl dissolution temperatures of primary and secondary inclusions in dolomite, Fish Hook Baydeposit.....157

Figure 49: Histogram of homogenization and NaCl dissolution temperatures of primary and secondary inclusions in quartz, Quartzite Ridgeshowing.....158

Figure 50: Summary of fluid inclusion data from the Au-PGE-U deposits, Goldfields area, showing relation between approximate homogenization temperatures and fluid salinities.....164

Figure 51: Summary of $\delta^{18}O$ values of vein minerals from the Au-PGE-U deposits, Goldfields area.....166

Figure 52: Relation between $\delta^{18}O$ and δD values of water in equilibrium with vein minerals from Au-PGE-U deposits, Goldfields area.....174

Figure 53: Summary diagram of fluid events in the Goldfieldsarea.....179

Figure 54: Summary diagram of geological events in the Goldfields and greater Beaverlodge region..180

Figure 55: Generalized cross-sectional models of the geologic evolution of the Goldfields area..182

List of Plates (Photomicrographs)

Plate 1: Fluid inclusion petrography and relationships in lode-gold veins, Box mine.....63

Plate 2: Examples of Type I, Ia, and II fluid inclusions in lode-gold veins, Box mine.....67

Plate 3: Examples of muscovite alteration of tourmaline in lode-gold veins, Frontier property and Box mine.....103

Plate 4: Relationships of primary inclusions to crystal growth planes, and types of growth planes in complex Au-PGE-U vein-type deposits and late combveins.....141

Plate 5: Examples fluid inclusion necking in complex Au-PGE-U vein-type deposits and comb veins.....143

Plate 6: Examples of inclusion types and their variable phase ratios in complex Au-PGE-U vein-type deposits and comb veins.....146

Abstract

The varied mineral deposit types of the Beaverlodge area, Northern Saskatchewan, indicate that the rocks have undergone a complex and protracted fluid history. All of the deposits studied are physically hosted in a variably metamorphosed sedimentary sequence, the Aphebian-aged Murmac Bay Group (complex Au-PGE-U vein-type deposits, e.g. Nicholson, Fish Hook), or within granites "intrusive" into the Group (lode-gold deposits, e.g. Box, Athona, Frontier). The complex Au-PGE-U vein-type deposits, and other minor mineralizations, are genetically associated with later, overlying sedimentary sequences such as the Late Aphebian to Helikian-aged Martin and Athabasca Groups. The succession of sedimentary basins was probably controlled by the virtually continuous tectonic evolution of the area prior to, and during, the Thelon-Talston (ca. 2.0 Ga), and Hudsonian (ca. 1.8 Ga) orogenies.

The first fluid event identified is F1, which occurred at ca. 1.97 to 1.95 Ga, when the mine granites were formed as nearly in-situ melts in the presence of a "metasomatic" fluid. The origin of the event is attributed to the burial of the Murmac Bay Group, presumably in a subduction-related setting, during the Thelon-Talston orogeny at ca. 2.0 to 1.9 Ga. $\delta^{18}O$ values of the granite minerals indicate an isotopic closure temperature for this event of 550 to 650°C, and that the "metasomatic" fluids may have been related to magmatic activity that occurred at deeper structural levels in the subduction zone. The development of a regional foliation, D1, may have occurred during the earlier stages of this event as well. The Thluicho Lake Group may be the remnants of a turbidite basin that developed in the back-arc area of the subduction zone.

The next fluid event documented is that which produced lode-gold quartz vein mineralization, associated with D2 deformation. This event is recorded in the veins by Type I and Ia fluid inclusions, and by the stable isotopic compositions of vein minerals as fluid events F2 and F3 (which are likely parts of the same overall fluid event). This fluid, at least during the late stage of vein development, is suspected to have been associated with gold deposition, and is indicated to have had minimum temperatures of about 300°C, and minimum pressures of 2.5 to 3.0 kbars. As the fluid was CO_2-bearing, and the inclusion populations appear to indicate pre-entrapment immiscibility, these temperatures and pressures are trapping conditions. This is confirmed by some stable isotopic fractionations between quartz and chlorite gangue minerals that yield temperatures of 300 to 400°C. The minerals were in equilibrium with a fluid of metamorphic origin. Rb/Sr ages of vein minerals indicate they are at

least 1.84 Ga, and probably between 1.855 and 1.84 Ga, suggesting that the D2 folding, and the retrograde metamorphic fluid that likely caused the lode-gold mineralization, were related to uplift during early Hudsonian collision. The source of the retrograde fluids is not clear, but the fluids may have been derived from the dehydration of material that was subducted during the Thelon-Talston orogeny, as the high initial $^{87}Sr/^{86}Sr$ ratios of the vein minerals, as well as feldspar from the Mine granites, imply that F1 to F3 fluids were derived from, or interacted with significantly older (i.e. deeply buried) crustal material.

The fluid represented by Type II inclusions is of an uncertain origin, but clearly post-dated the lode-gold veins (1.84 Ga), and pre-dated the Au-PGE-U mineralization (ca. 1.75 Ga?). This fluid event appears to have been regionally extensive, however, and may be related to events in the Beaverlodge area that are thought to have occurred ca. 1.78 to 1.74 Ga, such as regional albitization, or the simple vein-type uranium deposits. This age of approximately 1.75 Ga is often referred to as the "late overprint", suggested to be related to the later stages of the Hudsonian Orogen. The "late overprint" is also recorded by feldspars from the Box mine granite, which yield an Rb/Sr age of ca. 1.77 Ga. The Martin basin may have started to form at this time, due to epeirogenic fault movement during the waning stages of the Hudsonian Orogen, and this fluid event may also be related to early diagenesis within the basin.

The next fluid event, F4, is recorded by primary fluid inclusions in the complex Au-PGE-U vein-type deposits, which contain fluids of a moderately high salinity (28 to 36 wt % NaCl eq.). A similar fluid is found in secondary Type IV inclusions from the lode-gold veins, and in fluid inclusions from the "sponge rock" zones that have locally altered the mine granites. Stable isotopic equilibration temperatures of vein minerals from the Nicholson and Quartzite Ridge deposits indicate that the fluid was at a temperature of 100 to 120°C. The age of this fluid event may be as old as ca. 1.8 to 1.7 Ga, because the depleted δD value of the fluid, at approximately -90 permil, implies a high latitude for the area. The area was only located at the required high latitudes during two periods of time. For this reason, it is possible that Au-PGE mineralization, such as the Nicholson and Quartzite Ridge deposits, may have formed from diagenetic basinal fluids derived from, or influenced by, the Martin basin, or an unrecognized "proto-Athabasca" basin. Whether or not uranium accompanied the gold and platinoids, or was later overprinted on pre-existing Au-PGE mineralization is not presently known.

F5 is the youngest fluid event, recorded by the late U-bearing comb veins. The fluids were of a high salinity (40 wt. % NaCl eq.), and stable isotopic equilibrium

fractionations between vein minerals indicate a temperature of approximately 175°C. The calculated stable isotopic values of the fluid are similar to those of the diagenetic fluids in the Athabasca basin between ca. 1.6 and 1.0 Ga, during which time the unconformity-type and complex vein-type uranium deposits were formed. As mentioned above, this may be the time during which uranium mineralization overprinted the Au-PGE mineralization, forming "hybrid" complex Au-PGE-U vein-type deposits. An early stage of the F5 fluid event is represented by Type III secondary inclusions in the lode-gold veins. The moderate salinity of the fluid (10 to 15 wt. % NaCl eq.) is similar to fluid inclusions observed in quartz overgrowths from the Athabasca basin, where the fluid is interpreted to be of an early diagenetic origin.

1. Introduction

1.1 Location, Access, and Physiography

The Goldfields area is located on the north shore of Lake Athabasca, Saskatchewan, approximately 14.5 kilometres southeast of Uranium City, at latitude 59° 27' N and longitude 108° 30' W (Figure 1). Access to the Goldfields Peninsula is provided by a gravel road from Uranium City. From the end of the road, the Box, Athona, and Frontier properties (Figure 2) may be reached on foot, via old roads and trails, or by boat. The use of a helicopter in September 1987, greatly improved access to the Nicholson property (Figure 2), which would otherwise have required a lengthy boat trip.

The topography of the Goldfields area is grossly similar to that of the Canadian Shield in general, but is atypical due to its considerable ruggedness. Ridges have a relief of 30 to 100m, with local relief as much as 200m around Beaverlodge Mountain, which has an elevation of approximately 396m above sea level. Lake Athabasca has a mean elevation of 213m above sea level.

1.2 Exploration History of the Beaverlodge Area

The Beaverlodge area has a long and sporadic history of exploration and mining. Tyrrell (1894) reported the occurrence of iron formations near Fish Hook Bay (Figure 2),

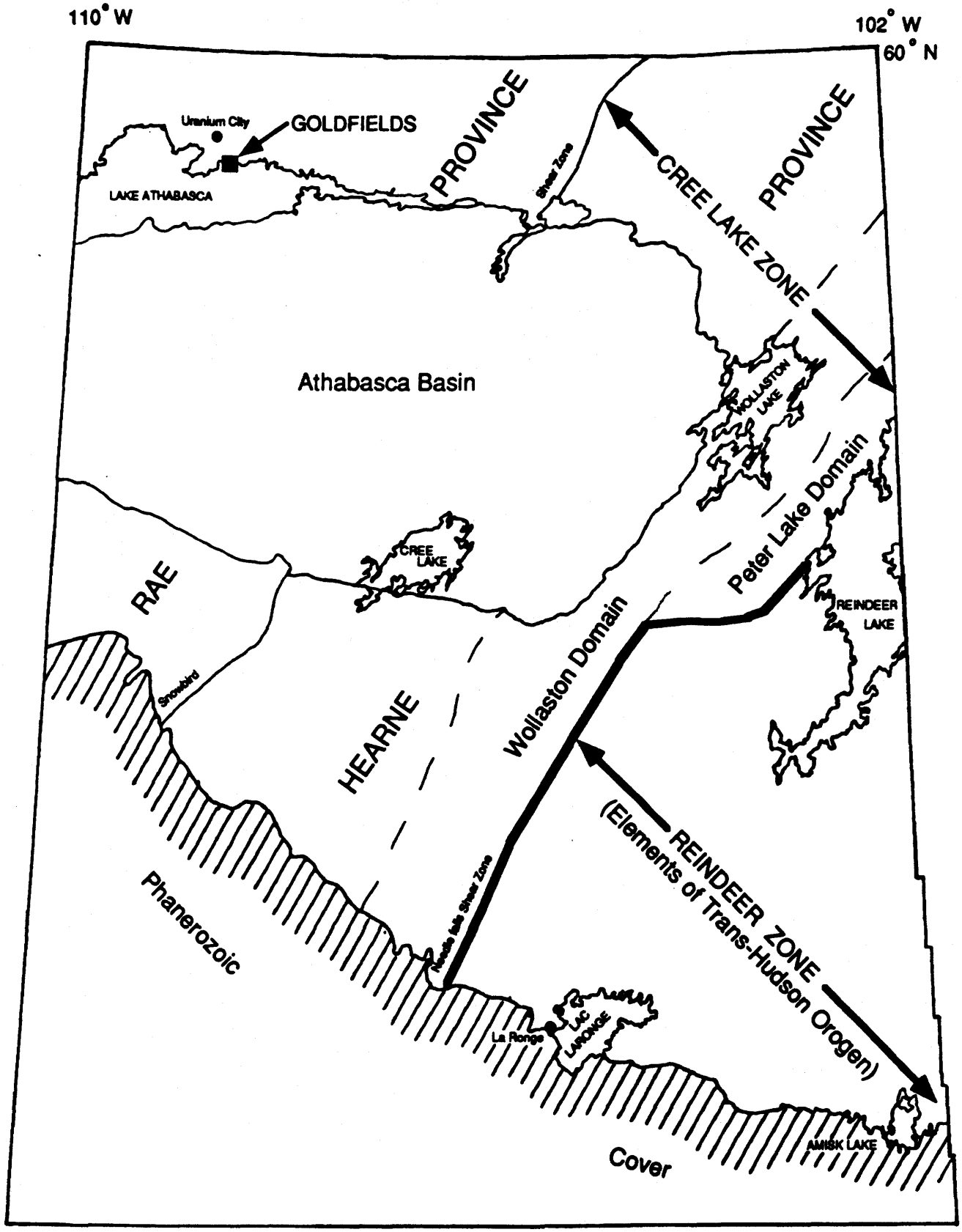

Figure 1: Schematic tectonic map of northern Saskatchewan, showing the location of the Goldfields area within the Rae Province, and its relationship to the other major tectonic and geologic subdivisions of the Churchill Craton. The hatched pattern indicates the northern limit of Phanerozoic strata.

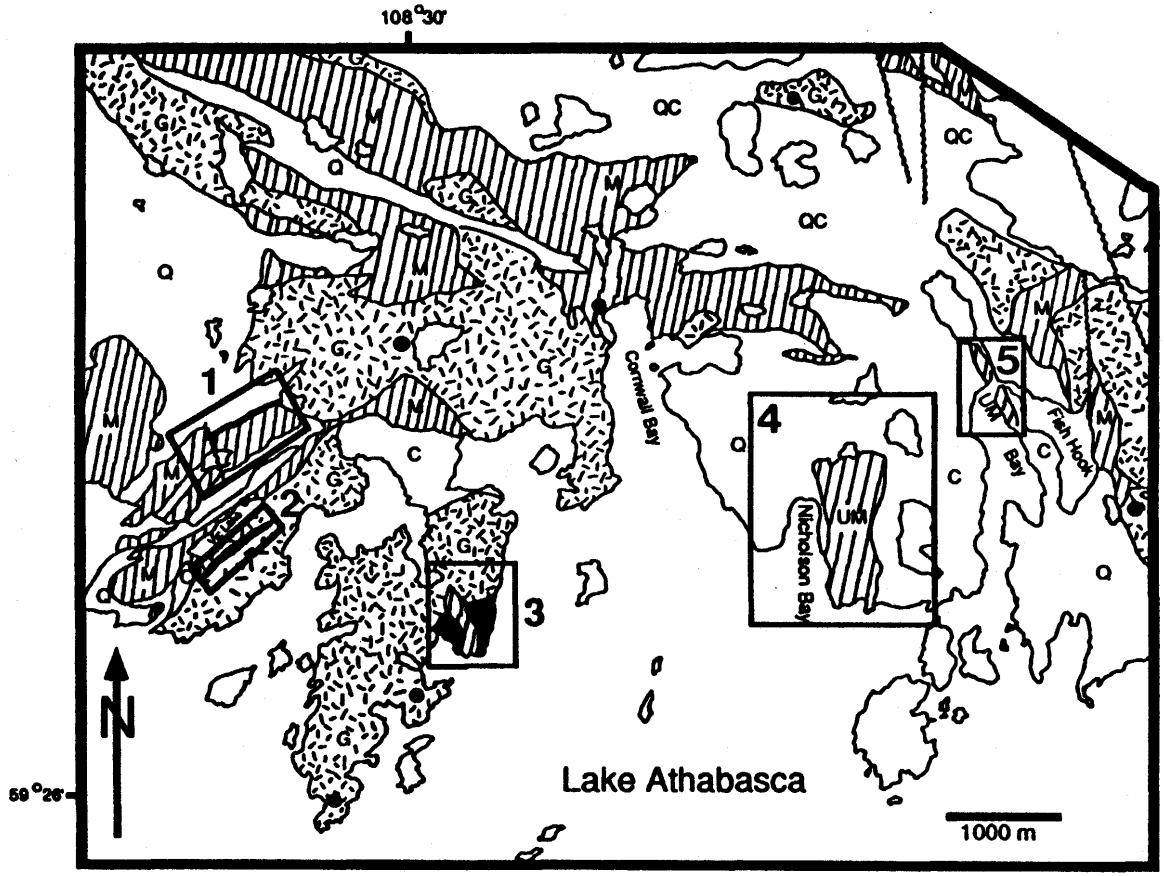

Figure 2: Simplified geologic map of the Goldfields area. Boxes outline the location of mineral deposits investigated in this study. 1 - Frontier property, 2 - Box Mine, 3 - Athona Mine, 4 - Nicholson Mine, 5 - Fish Hook Bay property. Black shaded units are the Mine granites. Black dots are other gold showings. Q - quartzite, C - carbonate and calc-silicate, M - amphibolite, UM - ultramafic, G - granitic gneiss ("Older Granite"). After Coombe (1984).

after his examination of the Lake Athabasca area in 1892 and 1893. Subsequent investigation of these in 1922 revealed their unsuitability for iron ore (Beck, 1969). In 1930, gold and base metal mineralization was discovered on the Nicholson property (Figure 2).

Intense exploration of the Beaverlodge area started in 1934, when gold was discovered in granite-hosted quartz veins on what was to become the Box property (Figure 2). A staking rush ensued, and by 1937 the town of Goldfields was well established. During this period, detailed prospecting of the Goldfields Peninsula and surrounding area resulted in the discovery of several gold showings similar to the Box discovery (Figure 2). All of the showings but one are located in an arc (Goldfields Synclinorium) centred on Cornwall Bay (Beck, 1959). Only the Box, Athona, and Frontier deposits (Figure 2) were subsequently developed to any extent.

Underground exploration for gold on the Frontier property consisted of an adit, off of which a single drift was constructed, parallel to the strike of the mine granite (Jiricka, 1984). The Athona property was explored with two vertical shafts and numerous drifts on the 38m and 76m levels (Christie, 1952). Neither of these prospects produced any gold. In 1939, the Athona workings were closed down, although there was an estimated 1,148,000 tonnes of probable and possible ore, at an overall grade of approximately 2.94 grams/tonne Au (Christie, 1952).

The Box property began gold production in 1939, but it closed in 1942, due to a manpower shortage and lower ore grades than were initially indicated. The mine workings consisted of two shafts, inclined at 42° and approximately 380m apart, which followed the footwall contact of the granite that hosted the gold-bearing, quartz vein stockwork. Three drift levels were constructed at 30m, 91m, and 152m, which followed the footwall contact for roughly 760m along strike. The mine produced a total of 1,992,645 grams of gold at an average grade of 1.55 grams/tonne Au (Cooke, 1946). Reported reserves in 1939 were 9.0 to 15.5 million tonnes of probable and possible ore, at grades ranging from 1.03 to 2.06 grams/tonne Au (Christie, 1952).

Fracture-hosted uranium mineralization in the Beaverlodge area was first discovered in 1935 on the Nicholson property while it was being evaluated for its gold potential. Later, in 1942, thucholite was discovered in late euhedral quartz-carbonate veins from the Box mine (Beck, 1986). At first considered uneconomic, uranium attained importance during WWII, which precipitated an examination of the area's uranium potential in 1944. The Crown company, Eldorado Mining and Refining Ltd. (now Cameco), held exclusive rights to prospect for uranium in Canada, and from 1945 to 1948 discovered many occurrences in the Beaverlodge area, including the Ace-Fay, Bolger, Martin Lake, and Hab deposits. The government opened public prospecting for uranium in 1948, resulting in the

discovery of several thousand radioactive occurrences (Christie, 1952). Underground exploration began on thirty-eight deposits, including the Ace-Fay (Eldorado), Martin Lake, Eagle, Gunnar, and Nicholson properties. Mining commenced in 1953, but only two deposits, the Gunnar and Eldorado, remained commercially viable beyond 1960. From 1953 to when the Eldorado mine closed in 1982, the Beaverlodge area produced almost 31 million kg of U_3O_8 (Beck, 1986).

Until recently, Platinum Group Element (PGE) mineralization on the Nicholson property had been treated as a curiosity. PGEs were first discovered there in 1950, when assays for samples from the Nicholson No.2 zone yielded average values of 13.8 ppm Pt, 17.3 ppm Pd, and 0.4 ppm Rh (Hulbert et al., 1988). As mentioned, gold had already been discovered on the property, and in 1935 two adits, with 107m of drifts were driven into the No.4 zone to evaluate this potential. The subsequent discovery of uranium mineralization in the zone resulted in the sinking of a shaft to 71m in the No.4 zone in 1949, and later, a shaft was sunk in the No.2 zone. By 1950, approximately 900m of drifting was completed on the 30m and 61m levels of the No.4 zone. Although the shaft was deepened to 100m and another drift level started, the Nicholson property did not become a lasting uranium producer.

Within the last five years, there has been a re-examination of the Goldfields area for its precious metal

potential. Drill core and surface sampling have confirmed the presence of PGE on the Nicholson property, as well as the Fish Hook Bay property, which was also explored underground for uranium in the past. Extensive drilling and bulk trench sampling on the Box and Athona properties have shown potential gold reserves of approximately 20 million tonnes combined, at approximately 1.9 grams/tonne. In 1983, underground drilling in the old Frontier workings suggested it to be uneconomic. Surface exploration of the area has discovered new mineralization, such as the Quartzite Ridge Au-PGE showing, 1.5km southwest of Beaverlodge Lake (Figure 3).

A recent summary of geological mapping by federal and provincial agencies in the Greater Beaverlodge area is provided by Macdonald & Slimmon (1986). A complete discussion of previous research and mapping, up to 1972, is provided by Trembly (1972). Current research in the Beaverlodge area (i.e. post-1985) is ongoing, funded by federal-provincial development agreements, of which this project is a part.

1.3 Objective of Thesis

The objective of this thesis is to elucidate some of the fluid history of the Beaverlodge area, particularly in the immediate Goldfields area. The variety and complexity of mineralization styles suggests that the Beaverlodge area has undergone several epigenetic mineralizing events involving hydrothermal fluids.

Fluid inclusion, stable isotope, and radiogenic isotope

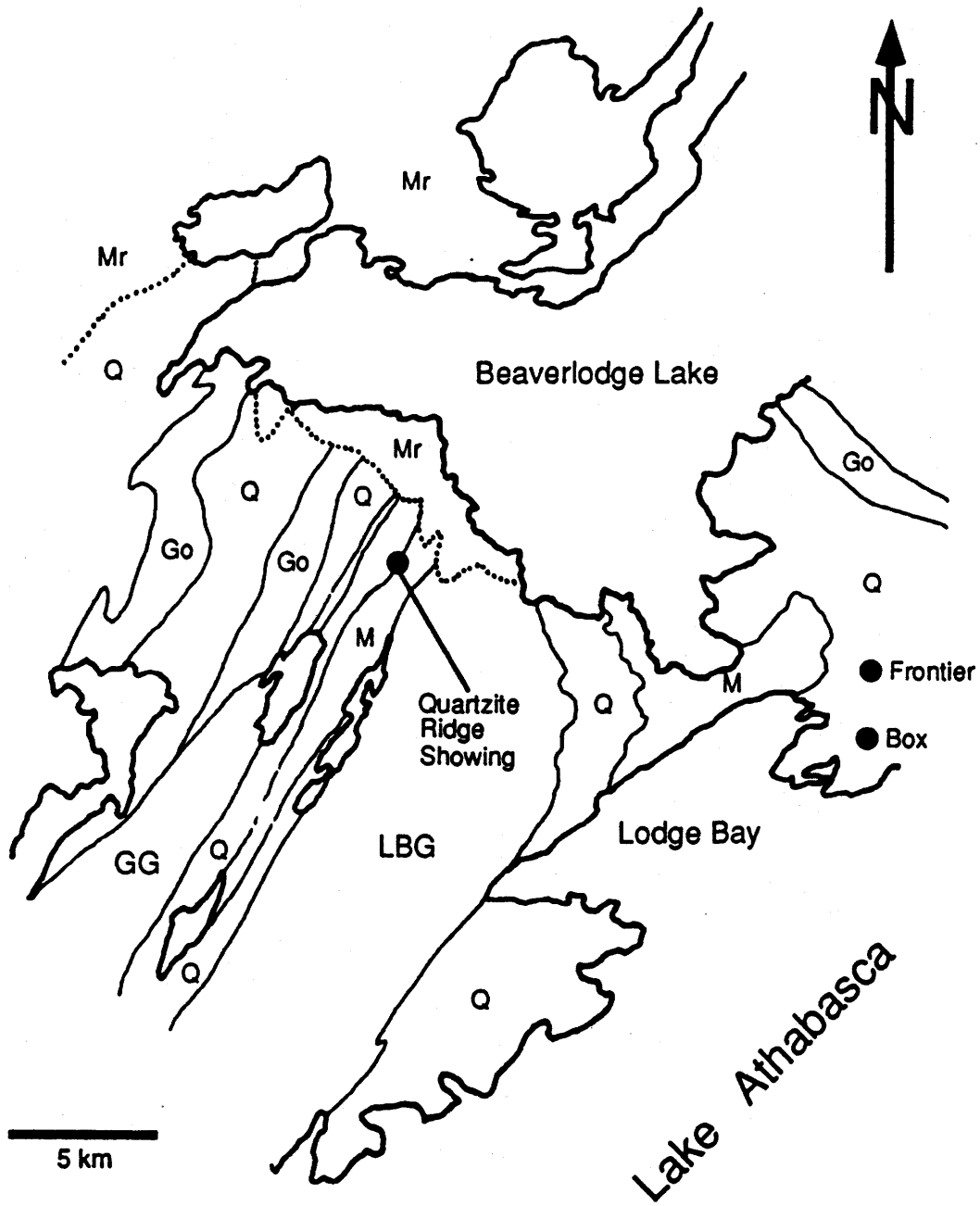

Figure 3: Simplified geologic map of the south end of Beaverlodge Lake, showing the location of the Quartzite Ridge showing. The locations of the Frontier and Box lode-gold deposits are shown for reference to Figure 2. Dotted line marks the contact with the Martin Group. Mr - Martin Group, GG - Gunnnar granite, LBG - Lodge Bay granite, M - amphibolite, Go - Older granite (granitic gneiss), Q - quartzite. After Sibbald & Lewry (1980).

data, as well as some chemical analyses are used to estimate fluid temperatures, pressures, compositions, and sources. Synthesis of these parameters provides constraints for genesis of the various types of mineralization.

A total of seven deposits in the Goldfields area were examined. The deposits can be grouped into two classes, based on their age and metal content. In general, the relative ages of the deposits can be determined by the amount of strain that the veins exhibit. Older deposits are characterized by strained quartz (e.g. undulose extinction, some recrystallization) in lode-type vein groups, whereas quartz in the younger veins is euhedral, and is not strained. The younger polymetallic veins occur as vuggy fissures of variable width and strike length. The older lode-Au deposits are the Box mine, the Athona property, and the Frontier property. The younger Au-PGE-U deposits are the Nicholson (Au-PGE-U), the Fish Hook Bay (Au-PGE-U), Quartzite Ridge (Au-PGE), and late euhedral quartz-carbonate veins containing uranium, which cross-cut the older gold mineralization on the Box and Athona properties (Figures 2 and 3).

2.0 Regional Geology

2.1 Tectonic Setting

The Goldfields area is located within the Rae Province of the Churchill Platform (Figure 4). In Saskatchewan, the Rae Province is largely composed of variably retrogressed granulite facies terrains, with a complex and poorly understood geology (Sibbald, 1987). Macdonald (1983, 1987) has subdivided the local terrains into a lithotectonic scheme (Figure 5), which is based on metamorphic facies, structural style, lithology, Rb/Sr radiometric ages (Bell & Blenkinsop, 1984; Bell & Bikerman, 1985), and U/Pb radiometric ages of zircons (Trembly et al., 1981; Van Schmus et al., 1986). The Nevins Lake block, Nolan block, Ena Lake complex, Tantato and Dodge domains all represent Archean basement blocks (ca. 2500 to 3000 Ma.), with or without overlying Lower Proterozoic supracrustals. The granitic migmatite Train Lake domain, situated between the Archean blocks, shows little evidence of an Archean history, and has an Rb/Sr age of 1950 +/- 125 Ma.

Domain and block boundaries are mostly defined by linear and curvilinear faults (Figure 5), commonly associated with cataclastic or mylonitic zones (e.g. Black Bay Fault-Beaverlodge Belt, Grease River Shear Zone, Oldman-Bulyea Lakes Shear Zone, St.Louis-Alces Lake Shear Zone). The domain boundries can be delineated on aeromagnetic maps, because high

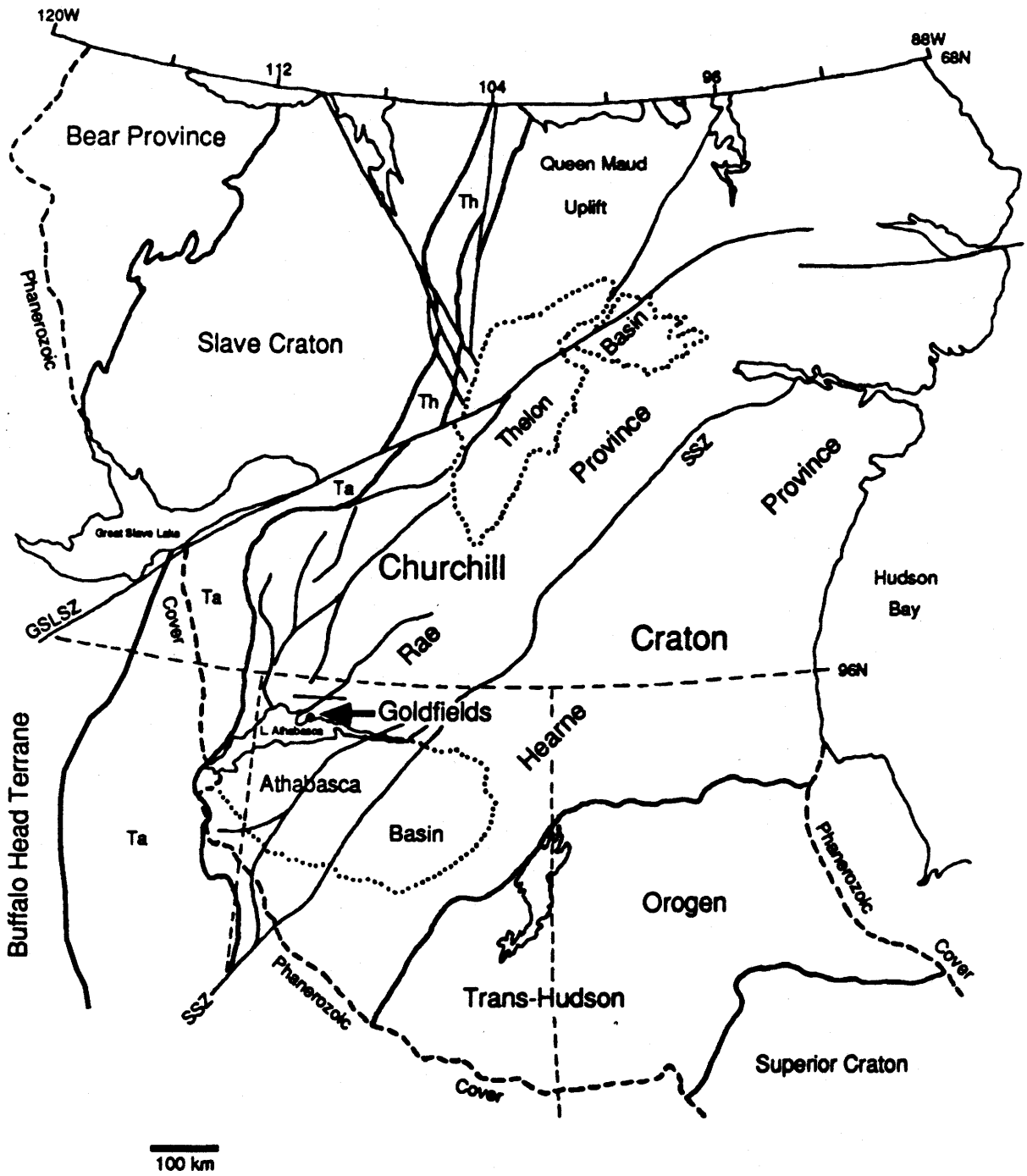

Figure 4: Tectonic map of a portion of the Canadian Shield, showing the location of the Goldfields area within the Churchill Craton. Th - Thelon Magmatic Zone, Ta - Talston Magmatic Zone, GSLSZ - Great Slave Lake Shear Zone, SSZ - Snowbird Shear Zone. After Hoffman (1988).

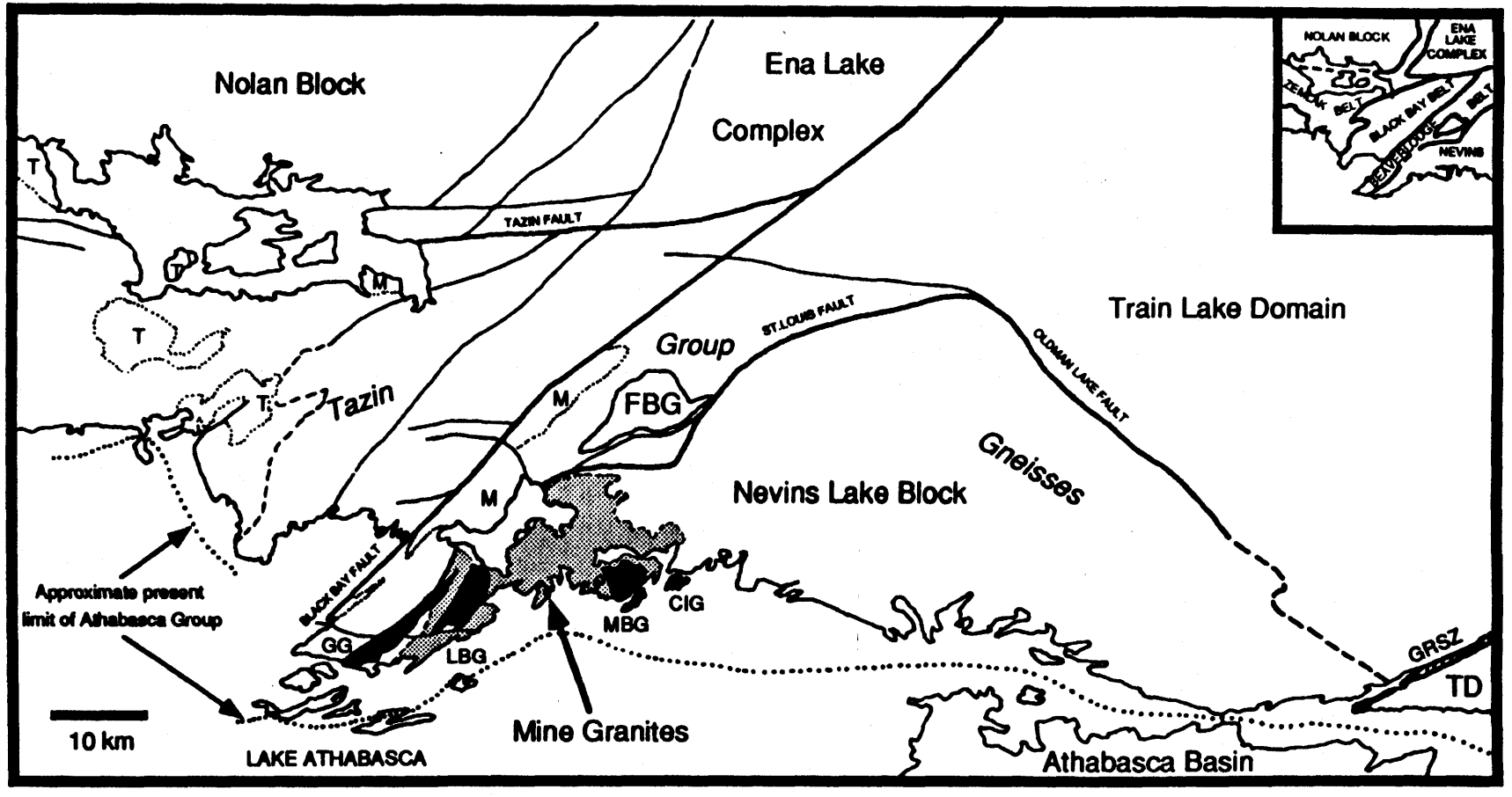

Figure 5: Simplified geologic map of the Beaverlodge area, showing the position of the Murmac Bay Group (shaded area) and the "North Shore Plutons" (black) within the Nevins Lake Block. Inset shows local lithotectonic subdivisions. TD - Tantato Domain, FBG - Foot Bay Gneiss, T - Thluicho Lake Group, M - Martin Lake Group, GG - Gunner granite, LBG - Lodge Bay granite, MBG - MacIntosh Bay granite, CIG - Cameron Island granite, GRSZ - Grease River Shear Zone. After MacDonald (1983).

magnetic intensities correlate with the older cratonic blocks, and low intensities are associated with younger cross-cutting structures (Sibbald, 1987). Rocks in the shear zones often show evidence of strong retrograde metamorphism, and many of the faults appear to have been multiply reactivated (Trembly, 1972). Sibbald (1987) suggests the fault zones are part of the highly variable overprint of Hudsonian orogenesis, the Churchill Platform having been a western foreland for the Trans-Hudson Orogen to the southeast. The Snowbird Shear Zone (Figure 4) may be a manifestation of the Hudsonian collision, as movement along the shear zone has been constrained to approximately 1.82 Ga, by the U/Pb dating of zircons within the syndeformational Junction granite (Bickford et al, 1987). The reactivation of cross cutting structures, and the range of radiometric ages (approximately 3.0 to 1.7 Ga.) in the area suggests that the Rae Province has undergone several periods of orogenesis, both before and after the accumulation of Lower Proterozoic sediments (Sibbald, 1987). Hoffman (1990) suggests that the Rae Province acted as an eastern foreland to the Thelon-Talston orogen, which occurred at ca. 2.0 Ga (Figure 4).

2.2 General Stratigraphy of the Greater Beaverlodge Area

The succession of metamorphosed sedimentary rocks in the Greater Beaverlodge area represent extended periods of deposition in four different sedimentary basins (Figure 6). The oldest recognizable sedimentary package is the variably

Stratigraphic Column: Beaverlodge Area

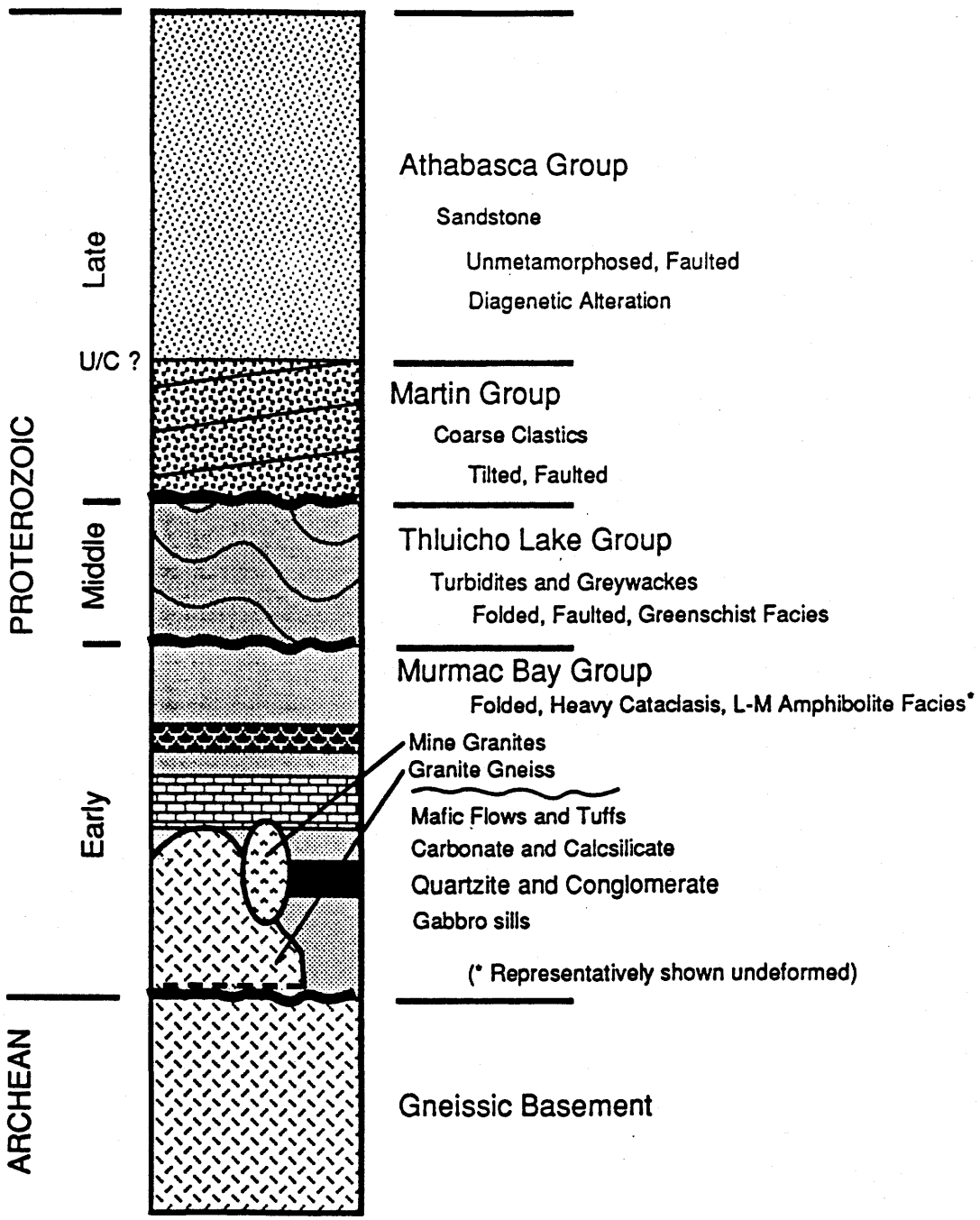

Figure 6: General stratigraphy of the Beaverlodge area, showing the succession of basin development through the Proterozoic. The Murmac Bay Group is representatively shown undeformed, and the rock types within it are shown schematically. Although age relationships of the granitic gneisses ("Older Granite") are not clear, they are shown associated with Mine granite emplacement.

metamorphosed and deformed Murmac Bay Group (Macdonald, 1983; Macdonald, 1987) and its lateral equivalent, the Tazin Group (Figure 5). The Murmac Bay and Tazin Groups are believed to lie unconformably on an older Archean basement, although an unconformity has not been positively identified. The age of the Murmac Bay Group is tentatively bracketed between 2.4 Ga. and 1.95 Ga. (O'Hanley et al., 1991). Tremblay (1972) suggests the rocks represent sediments deposited on a shallow shelf platform. A complete description of the Murmac Bay Group will be given in a later section, as these rocks host the mineral deposits under investigation.

Unconformably overlying the Murmac Bay Group are the complexly folded greenschist grade metasedimentary rocks of the Thluicho Lake Group, now exposed only to the northwest of the Goldfields area (Figures 5 and 6). This sequence of metamorphosed conglomerate, arkose, greywacke, feldspathic quartzite, argillite, and occasional tuffaceous horizons, is probably Aphebian in age, ca. 1.8 to 2.0 Ga. (Macdonald 1987). Scott (1978) suggests that some of these rocks display features consistent with a turbidite origin.

The Martin Group, which is dominantly an arkosic redbed sequence, is believed to have been deposited in a terrestrial, fault-bounded basin (Figures 5 and 6). The Group contains abundant conglomerate, breccia, sandstone, siltstone and mudstone, which were deposited as talus slopes, alluvial fans and lacustrine braided streams beds. A small volcanic

component is represented by basaltic flows and gabbroic dikes. Showing little evidence of metamorphism, but folded and faulted, the Martin Group is at least 5000m thick (Trembly, 1972). It is observed to uncomformably overlie the Thluicho Lake Group in only one location, other visible contacts being faulted and unclear (P. Mazimhaka, pers. comm.). The age of the Martin Group is estimated at ca. 1.7 to 1.8 Ga. (Macdonald, 1987).

Unconformably overlying the Martin Group are the mature quartzose sedimentary rocks of the Mid-Proterozoic Athabasca Group (Figures 5 and 6). The Athabasca Group also contains units of conglomerate, siltstone, oolitic and stromatilitic dolomite, and phosphatic horizons that locally preserve tuffs. These rocks comprise a fining upwards sequence at least 1400m thick. Two environments of deposition are recognized; fluviatile plains subject to aeolian erosion, and a warm shallow marine shelf setting. The relationship between these environments is unclear. Rameakers (1981) suggests a dominantly marine setting, with four transgressive marine sequences and one regressive fluvial wedge. Hoeve & Quirt (1986) recognize only two marine dominated environments, the remainder being fluviatile terrestrial deposits. They also state that 2200m of the Athabasca Group are preserved, with fluid inclusion data (Pagel, 1975) and clay mineral studies (Hoeve et al. 1981, Hoeve 1984) indicating an original thickness of as much as 4 to 5km.

Although the Athabasca Group presently represents a mature sedimentary sequence, there are several different concepts regarding its original composition. Fahrig (1961) proposed that they were deposited as "super-mature, multicycle" sediments. Rameakers (1981) argues deposition occurred rapidly as immature first cycle sediments in a tectonically active area. Original aeolian activity, fluvial winnowing, and a long and intense diagenesis have produced the maturity now seen. Similarly, Hoeve & Quirt (1986) proposed deposition of immature sediments, followed by protracted, but episodic diagenetic activity (low temperature hydrothermal alteration) which produced the mature sequence.

Tuffaceous units within the Wolverine Point Formation of the Athabasca Group have provided Rb/Sr dates of ca. 1430 to 1515 Ma. (Bell & Blenkinsop, 1980; Bell & Macdonald, 1982; Armstrong & Rameakers, 1985). An upper age limit is provided by an Rb/Sr date of 1310 +/- 70 Ma. on diabase dikes which intrude the Athabasca Group (Armstrong & Rameakers, 1985). This would constrain the Athabasca Group sediments as having formed in 100 to 200 million years, ca. 1500 to 1340 Ma. New Sm-Nd dates on diagenetic clay minerals, and paleomagnetic data from diagenetic hematite (Kotzer et al., 1992) indicate that the Athabasca sediments were subjected to diagenesis as early as ca. 1.6 Ga., suggesting that the basin may have been forming as early as ca. 1.7 Ga.

Ramaekers (1981) suggests that all the basins in the

Athabasca area (represented by Thluicho, Martin, and Athabasca Groups) were tectonically generated by transcurrent faulting, during and following the Hudsonian Orogeny. As well, the Athabasca Basin was particularly focused on epeirogenic uplift and subsidence zones, these being adjustments to the Hudsonian orogeny. Macdonald (1987) proposes a similar origin, citing the Thluicho Basin as the first of several successor basins focused on Early Proterozoic fault zones. Based on Hoffman's (1988) modelling of the tectonic events during the Proterozoic in the Beaverlodge area, the successor basin system may have been initiated as early as ca. 2.0 Ga. (i.e. Thluicho Group), during the Thelon-Talston orogeny, overlapping with, and continued, during the Hudsonian Orogeny.

2.3 Geology of the Nevins Lake Block

The rocks of the Goldfields Peninsula form part of the Nevins Lake block (Macdonald, 1983), which extends eastward from Beaverlodge Lake to the Grease River Shear Zone (Figure 5). The northern limit of the block is defined by the connecting curvilinear cataclastic zones of the Oldman-Bulyea Lakes Shear Zone to the northeast, and the St. Louis-Alces Lake Shear Zone to the northwest. The northwest edge of the Nevins Lake block is in contact with the Beaverlodge Cataclastic Belt (Figure 5).

Peak metamorphic grade in the Nevins Lake block increases from lower amphibolite in the southwest to granulite in the northeast. Peak metamorphic grade in the Goldfields area was

lower to middle amphibolite facies. In a wide zone along the northeast margin of the Nevins Lake block, rocks have been regionally retrogressed to amphibolite facies, and the effects of the retrogressive event are seen toward the southwest of the block to a lesser degree. Rocks in the Goldfields area record regression to upper greenschist facies. Macdonald (1983) concludes this retrogressive event may be contemporaneous with an amphibolite grade metamorphic event in the Train Lake Block, or to regional uplift during cataclastic events along the north boundary lineaments (Figure 5).

Christie (1952) named the supracrustals of the Beaverlodge area the Tazin Group. The lithologically distinct sequence of supracrustals that extend east from Beaverlodge Lake to Hill Lake, and south from the Fish Lake lineament to Lake Athabasca, were termed the Murmac Bay Formation of the Tazin Group by Tremblay (1972). Macdonald (1983, 1987) proposed that these supracrustals be called the Murmac Bay Group, with the dominantly quartzofeldspathic gneisses to the north and east (former Tazin Group) as possible lateral equivalents. Macdonald (1983) suggests that the gneisses express either a change of sedimentary environment, or exposure at a different stratigraphic level. Tremblay (1972) reports that the Murmac Bay and Tazin sedimentary rocks interfinger, indicating that they are laterally correlative.

The Murmac Bay Group in the Beaverlodge Lake area (Figure 7) is comprised of a thick sequence of quartzite, dolomitic

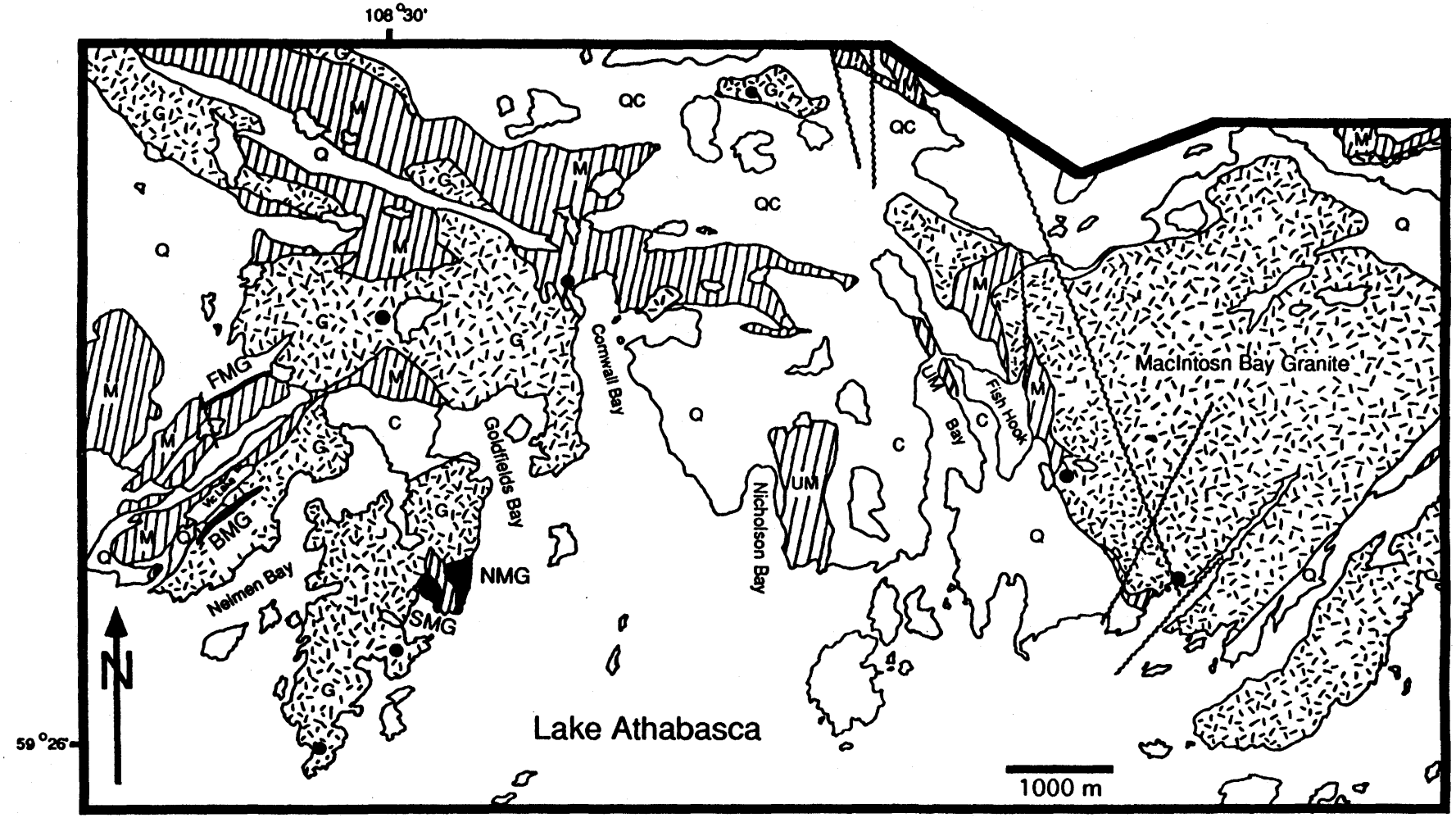

Figure 7: General geologic map of the Murmac Bay Group in the Goldfields area. Black shaded units are the Mine granites. Black dots are other gold showings. Q - quartzite, C - carbonate and calc-silicate, M - amphibolite, UM - ultramafic, G - granitic gneiss ("Older Granite"), FMG - Frontier mine granite, BMG - Box mine granite, NMG & SMG - northern and southern portions of the Athona mine granite. After Coombe (1984).

marble, amphibolite, various schists, and iron formation. There are also small ultramafic bodies, especially in the Nicholson Bay and Fish Hook Bay areas, which are locally associated with amphibolites. Amphibolites in the Murmac Bay Group show features that indicate the protoliths were flows, volcanic sediments, and shallow sill-like intrusions (Ross, 1949; Christie, 1952).

Christie (1952) and Tremblay (1972) agree that the sedimentary supracrustals of this sequence represent alternating units of dominantly chemical and clastic deposition, typical of a platform shelf environment. Tremblay (1972) suggests that the quartzofeldspathic gneisses to the north and east of the Beaverlodge Lake area are typical of a geosynclinal setting. Harper (1983) argues that conglomeratic layers, cross bedding and channel scours indicate a near-shore, high energy area of the shelf environment, with periodic transition to a quieter, perhaps lagoonal or deep basin environment, represented by the various pelitic schists and iron formations. Deposition of these units as argillites, and both oxide and sulphide facies iron formations, indicates a low energy environment must have existed during certain periods.

The mafic pyroclastics, flows and sills within this platform sedimentary succession have been attributed by Christie (1952) and Tremblay (1972) to either a deepening marine basin with rifting-associated volcanism, or a flanking

volcanic arc. Ross (1949), in a detailed stratigraphic study of the Goldfields area, was able to distingush two cycles of sedimentation, each followed by extrusive volcanic activity. He also concluded that the mafic sills were intruded during the latter stages of the second cycle. Associated ultramafic bodies, such as at Nicholson Bay, can not be clearly identified as intrusive or extrusive due to extensive serpentinization, and ambiguous contact relationships.

In the greater Goldfields area, two types of granite have been recognized (Sibbald, 1984). The two groups, "Older granites" and "Younger granites" are broadly based on the presence or absence, respectively, of foliation in the rock. This was originally thought to be related to their time of emplacement, either pre- or post-D1, but recent $^{207}Pb/^{206}Pb$ ages imply that the foliation in the "Older granites" may be inherited from the Murmac Bay Group protoliths, whereas the general absence of foliation in the leucocratic "Younger granites" is the result of a greater degree of recrystallization and metasomatism of the protolith (O'Hanley et al., 1991). This suggests that the "Older" and "Younger" granites may be contemporaneous, which is supported by field relations on the large island in Neimen Bay (Figure 7). According to Sibbald (pers. comm.), from west to east across the island, mixed Murmac Bay Group rocks become gradually "granitic" in appearance, similar to the foliated "Older granites", including some recognizable sills and dykes. On

the eastern side of the island, this "granitization" appears to culminate in a few small lenses (1m long) of "Younger granite", closely resembling the Box mine granite, and which may have been emplaced as "magmatic" fluids or melts. The foliated granitic gneisses, or "Older granites", form a large part of the Goldfields and Crackingstone Peninsulas. The gneissic character of the granite often makes it difficult to distingush from local paragneisses, further emphasizing its origin by "granitization" of the Murmac Bay Group metasediments. The leucocratic, weakly foliated "Younger granites" form a string of intrusives along the northern shore of Lake Athabasca. These North Shore Plutons (Figure 5) include the mine granites of the Goldfields Peninsula (Figure 7), and may represent the end result of the "granitization-plutonic" event. The origin of the mine granites will be discussed in more detail in section 4.0. Later minor intrusions reported in the Murmac Bay Group include pegmatite, lamprophyre and diabase dikes.

Deformation in the Nevins Lake Block is variable, but all supracrustal rocks have undergone at least two phases of deformation. In the northeast, Harper (1983) has identified three phases of folding, with complex interference fold patterns. Towards the southwest, deformation lessens, but intensity can vary dramatically over very short distances. In the Goldfields area, two events can be distingushed. The first (D1) gave rise to a moderately developed regional

foliation (S1), which generally parallels bedding (So). Occasional So/S1 intersections produce a "rodding lineation" (L1 of Sibbald, 1984). A second deformation (D2) has produced a weakly and only locally developed axial planar schistosity (S2). This event has folded the S1 foliation and lithologic layering into open folds. An L2 mineral lineation was developed, but generally is parallel to the first lineation. The rocks underlying the Goldfields Peninsula are folded (D2) into an open upright syncline, called the Goldfields Synclinorium (Sibbald, 1984), or the Athona Syncline (Roberts, 1990). The the syncline is centered around Goldfields Bay (Figure 7), with the axial trace trending north, and the hinge plunging moderately to the south. Clasts in the quartzites show only moderate flattening, which indicates a low strain state for the rocks of this area (Sibbald 1984).

Major faulting has occured in and around the Nevins Lake Block. Tremblay (1972) suggests faulting occured in two major stages. The first, which postdates or is syndepositional to his Tazin Group, has developed wide mylonitic zones. These trend northeast, such as the prominent Black Bay Fault (Figure 5). The second set of faults, which cut both Tazin and Martin Group rocks, are sharp and well defined, although they have associated cataclastic zones. Examples include the St.Louis-Alces Lake Shear Zone and the Oldman-Bulyea Lakes Shear Zone, which, as previously mentioned, define the northern boundry of the Nevins Lake block. Tremblay (1972), Macdonald (1983),

and others believe that regional uplift created movement along faults of this generation, with associated metamorphic retrogression. One minor (005°) and three major directions (085°, 105°, 130°) of these faults have been delineated by Tremblay (1972). It is also recognized that all faults have had a long history, with several periods of reactivation. The early stage Black Bay Fault was likely reactivated prior to, and along with, the later faults, and may have provided a locus of deposition for the Martin Group (P.Mazimhaka 1987, pers. comm.). This type of fault control for the development of basins in the Athabasca region was also suggested by Rameakers (1981) and Macdonald (1987), as previously discussed.

Alteration is widespread in the Beaverlodge area. Although local variations exist, hematization, chloritization, albitization, carbonitization, silicification, and epidotization have been recognized on a regional scale, and may inpart be related to regional metamorphism (Tremblay 1972). Hematization is almost ubiquitous and imparts a red colour to most rocks of the area. The hematite occurs as fine 'dusty' particles surrounding mineral grains and along cleavage planes, especially feldspars. Chloritization, attributed to regional retrograde metamorphism (uplift?) has partially or totally replaced most mafic minerals in the area. Epidotization, although widespread, is not intense. It occurs mainly as veinlets and seams throughout the rocks, dominantly

north of the St.Louis-Alces Lake Shear Zone. Amphibolites associated with the area's uranium deposits are especially epidotized.

Silicification appears mainly to be associated with cataclastic deformation which caused a local remobilization of quartz, on the centimeter to millimeter scale, into small, "sutured" patches. Tremblay (1972) recognizes another silicification event which he ascribes to "hydrothermal activity". This involved fracture filling by cryptocrystalline or vuggy, euhedral quartz. These veins are present within the study area, notably cross-cutting the Box and Athona mine granites. They are uranium-bearing, and are herein called euhedral quartz-carbonate veins, or comb veins.

Carbonate alteration is confined to granitic rocks within and near major faults. The final product of this alteration is a rock composed of carbonate, albite or oligoclase, and some chlorite. The carbonitized rocks exhibit anomalous radioactivity, and in some locations are cut by seams and veinlets of pitchblende. Similar zones, of very limited strike length, cross-cut the Athona mine granite, and there are referred to as "sponge rock", due to their distinctive weathered appearence. Carbonitization can also form fracture filling veins up to 0.3m wide, some with high grade pitchblende.

Albitization is widespread, in the form of thin albite or quartz/albite veinlets, as well as replacing pre-existing

potassic feldspars to a variable degree (i.e. perthitic, rimming, or complete replacement). Albitization is present in many of the uranium deposits in the Beaverlodge area, along with carbonitization. Hoeve (1982) suggests a relationship between vein-type pitchblende deposits of simple mineralogy and the albitization event. The mine granites have also been affected by albite alteration.

The Beaverlodge area has had a long geologic history, as evidenced by the wide range in ages of the rocks (Figure 8). Within the immediate area of the Nevins Lake Block, two Archean ages have been obtained from U/Pb dating of zircons. These include the Foot Bay Gneiss at 2513+36/-22 Ma (Tremblay et al. 1981) and the Lodge Bay Granite at ca. 3040 Ma (Van Schmus et al. 1986). However, the search for an underlying basement in the Beaverlodge area has met with little success, as these dates are not conclusive. For example, the Lodge Bay Granite had been classified with the North Shore Plutons because of its weak foliation and physical similarity to the other granites (Alcock, 1936). However, the ca. 3040 Ma U/Pb date may represent detrital zircons, as Pb/Pb dating of single zircons from rocks in the area indicate that many zircons are inherited (O'Hanley et al, 1991). Bikerman et al. (1990) obtained an Archean age for the Lodge Bay Granite of ca. 2900 Ma., using the whole rock Rb/Sr method. The initial ratio of 0.69134 is below meteorite values however, and Bikerman et al. suggest that the isochron has been rotated by an unknown

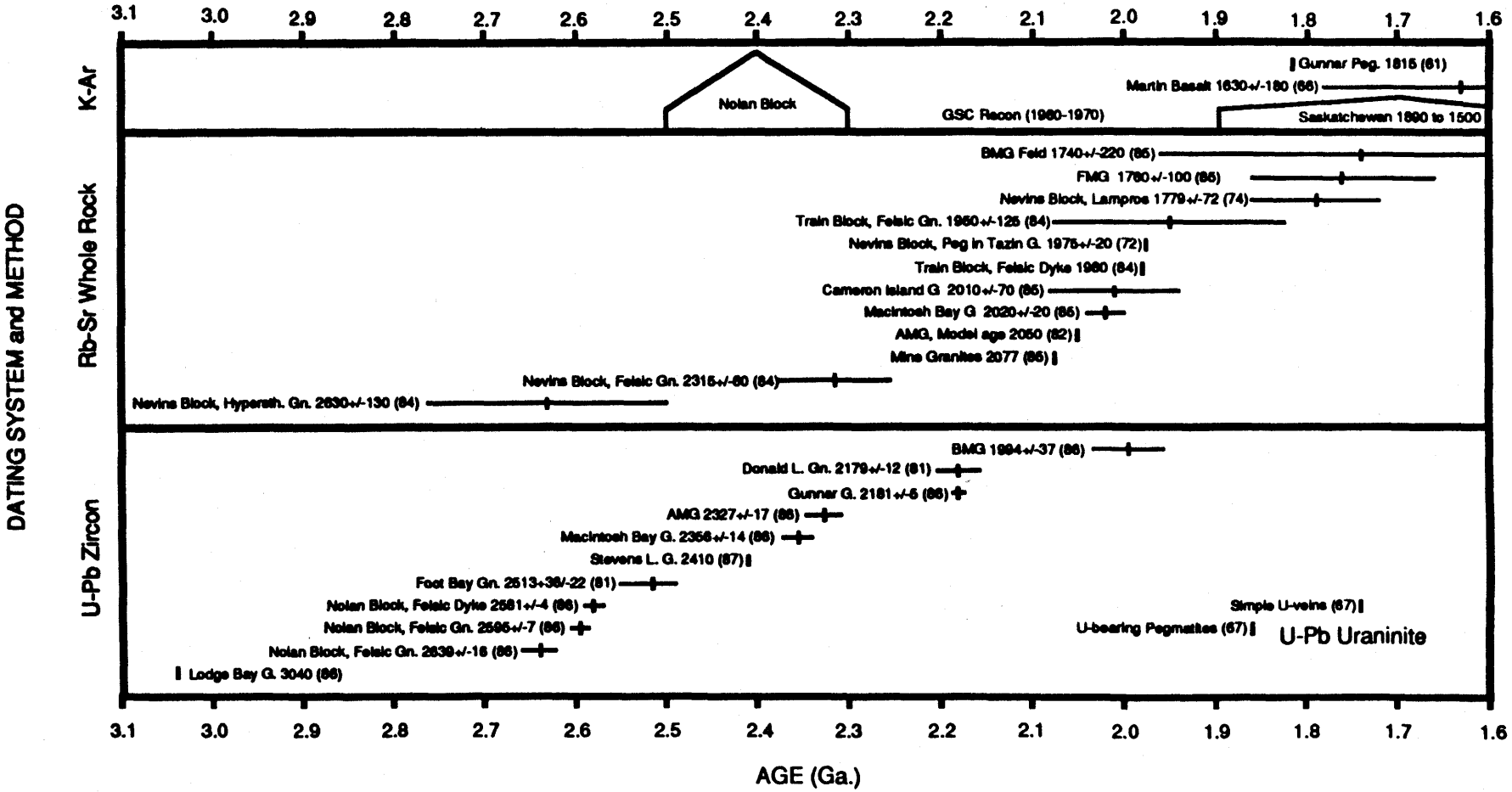

Figure 8: Compilation of published radiogenic ages of various rocks in the greater Beaverlodge area, arranged by age and radiogenic system. Error bars units are as quoted. Number in parentheses indicates the year the age was published (see reference list). FMG - Frontier mine granite, BMG - Box mine granite, AMG - Athona mine granite, Peg - pegmatite, Feld - feldspar seperate, G - granite, Gn - gneiss.

geologic event. If this is the case, then the ca. 2900 Ma. age represents a maximum age for the granite, further suggesting that the ca. 3040 Ma. age may be derived from a detrital zircon. The closest Archean terrane is probably the Nolan Lake block (Figure 5) to the north (Van Schmus et al. 1986).

Using U/Pb ages of zircons, Van Schmus et al. (1986) propose a model of evolution of the Beaverlodge area that starts ca. 3.0 Ga. as an age for Archean crust (Figure 8). A plutonic-metamorphic event, possibly Kenoran, is implied by the U/Pb ages derived from rocks of the Nolan Lake Block (Figure 5). The North Shore Plutons were then emplaced ca. 2.3 to 2.2 Ga. (Figure 8). This brackets the age of the Murmac Bay Group supracrustals between 3.0 to 2.3 Ga. They further suggest that hydrothermal activity at ca. 2.0 Ga. may have deposited gold in the mine granites and may be responsible for resetting the Rb/Sr system. Previously, Bell & Bikerman (1985) had suggested, using Rb/Sr results, that emplacement of the North Shore Plutons by metasomatism or "granitization" occurred at ca. 2100 to 2000 Ma. Later Hudsonian metamorphic overprinting then occurred at ca. 1760 to 1740 Ma.. The initial $^{87}Sr/^{86}Sr$ ratio for a combined Box, Athona, and Frontier isochron is 0.713 (Bell & Bikerman, 1985).

Van Schmus et al. (1986) report that most zircons from North Shore Plutons have low uranium contents (200 to 800

ppm), consistent with the contents in magmatic zircons. Zircons from the Box mine granite, however, have high uranium contents (1000 to 3000 ppm), usually indicative of a low temperature, hydrothermal formation. Cursory microprobe analysis of zircons in the Box mine granite has shown that there are at least two distinct zircon phases, as several zircon grains showed various rimming and replacement features. No grains had uranium contents as high as reported by Van Schmus et al. (1986), indicating the zircon populations are complex, involving the hydrothermal addition of at least one new phase of zircon. Recently, O'Hanley et al. (1991) have shown, using the single zircon Pb-evaporation technique, that the mine granites formed at about 1.95 Ga., and that many of the zircons are inherited, originating from Archean terranes with ages of ca. 2.5 and 3.0 Ga. As the mine granites post-date the Murmac Bay Group, this brackets the age of the Group between ca. 2.5, the age of the Foot Bay Gneiss (Figure 5), and 1.95 Ga. Furthermore, the zircon ages suggest that the lower age limit of the Group is younger than ca. 2.4 Ga., which is the youngest age of detrital zircons in the quartzites near the Frontier mine granite.

2.4 Economic Geology

Hoeve & Sibbald (1978) and Hoeve (1982) have classified uranium deposits in the Beaverlodge area into three types: syngenetic pegmatite, hydrothermal-metamorphic, and hydrothermal-diagenetic. The syngenetic type are uraninite-

bearing pegmatite dikes, thought to be associated with Hudsonian magmatic activity and the first peak of metamorphism at ca. 1860 Ma. (Figure 8). The next youngest are the simple vein-type which consist dominantly of pitchblende and minor uraninite and base metal sulphides, intimately associated with metasomatic albite alteration. U/Pb ages of the uraninite (Figure 8) indicate that these were formed during Hudsonian metamorphism at ca. 1740 Ma (Koeppel, 1968). During the interval of ca. 1400 to 1100 Ma. (Kyser et al., 1990), unconformity-type uranium deposits hosted within the Athabasca Basin, as well as the complex vein-type uranium deposits hosted in the Murmac Bay and Martin Groups were formed. In the Beaverlodge area, this event usually overprints the earlier, simple vein-type deposits, as well as forming new, mineralogically diverse (i.e. "complex") vein-type deposits. The complex vein-type deposits contain pitchblende and coffinite, Ni-Co-arsenides, -sulpharsenides, -sulphides, Co-Ni-Pb-Cu-Hg-selenides, Ag-antimonides, -sulphantimonides, base metal sulphides, native Au, Ag, Pt, Cu and thucholite. This assemblage is very similar to that of the unconformity-type deposits in the Athabasca Basin. Hematization, euhedral quartz-carbonate veining, and sericitization usually characterize the wall-rock alteration of the complex vein-type deposits, which is similar to parts of the alteration assemblage associated with the unconformity-type deposits.

There are several lode-gold deposits and occurrences in

the Beaverlodge area, which share many of the same characteristics, including their structural setting within the Goldfields Synclinorium (Figure 5). The gold is free, or associated with base metal sulphides, contained in approximately north-trending quartz veins. The veins form stockwork-like masses, or planar swarms, within small, usually red-coloured granitic bodies. The Box, Athona, and Frontier mine granites are examples. They are all generally leucocratic, and massive to weakly foliated, but have some mineralogical and textural differences, despite their gross similarity. They are classified as "Younger granites", and are members of the North Shore Pluton group, as previuosly indicated.

Anomalous PGE concentrations are known historically in the Nicholson Bay-Fish Hook Bay area, only four kilometers to the east of the Goldfields Peninsula. Platinum, palladium, gold and uranium are contained in fracture zones associated with ultramafic bodies. Hulbert (1986) considers the Nicholson occurence to be a hydrothermal-type deposit, possibly related to the complex vein-type uranium deposits. His work suggests that anomalous PGE concentrations only occur where the shears are in, or proximal to, ultramafic rock, whereas uranium and gold mineralization do not appear to be spatially controlled by ultramafic rock. Sibbald (1982) points out that the Au-U association here is similar to some of the unconformity-type uranium deposits.

In 1987, the Quartzite Ridge occurrence was discovered, where high Au, Pt, and Pd values were obtained from structurally brecciated, cherty quartzites of the Murmac Bay Group. The brecciated zone occurs along, and proximal to, the contact with a large mafic unit. Specular and red hematite, found along fractures and in the matrix of the rock are the only visible metallic minerals. Larger vuggy fractures are also coated with drusy, euhedral quartz. The lack of deformation in the quartz indicates the mineralization postdated peak metamorphism, and may be similar in age to the Nicholson Bay deposits. A similar, brecciated cherty quartzite with a hematitic matrix is the host lithology for several zones in the Nicholson deposit, again suggesting an overall similarity between the Quartzite Ridge and Nicholson deposits.

3. Field & Analytical Methods

3.1 Sample Collection

The field area is centered around Cornwall Bay on Lake Athabasca, from the Goldfields Peninsula to Fish Hook Bay (Figure 9), and was visited in 1986 and 1987. In July 1986, outcrop samples, and samples from old trenches were collected from the Box, Athona, Frontier, and Greenlee properties. Drill core samples from the Frontier property were collected from their storage site in Uranium City.

In September 1987, samples from outcrop and new trenches were collected from the Box and Athona properties, and samples from outcrop and old trenches were collected from the Frontier and Nicholson properties. Drill core from the Quartzite Ridge Au-PGE showing (Figure 3) was sampled, and a few surface samples were provided by Kasner Group geologists. Drill core samples from the Nicholson and Fish Hook Bay properties were obtained from L. Hulbert of the Geological Survey of Canada.

The geologic map of Sibbald (1984) was used to record sample locations. Figure 9 indicates areas that were sampled, shown in more detail by Figures 10 to 18, which are general geology maps of the deposits.

3.2 Fluid Inclusions

3.2.1 Polished Wafer Preparation

Doubly polished wafers for fluid inclusion analysis were

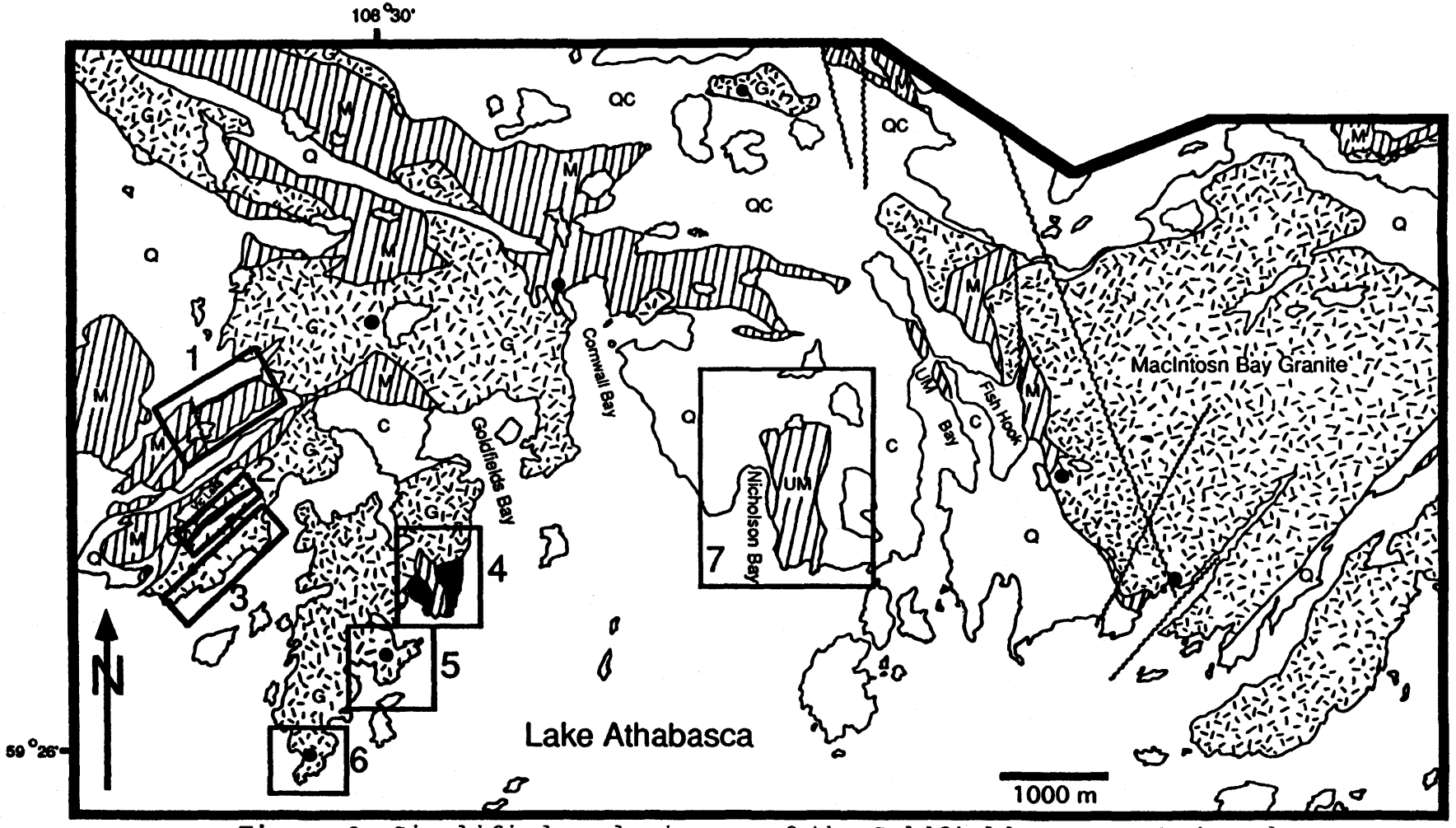

Figure 9: Simplified geologic map of the Goldfields area. Numbered boxes refer to sample location maps as follows: 1 - Frontier property (Figure 10), 2 - Box Mine (Figures 11 and 12), 3 - Box Mine Docks (Figure 13), 4 - Athona Mine (Figures 14 and 15), 5 - Melma showing (Figure 16), 6 - Greenlee showing (Figure 17), 7 - Nicholson Mine (Figure 18). Black shaded units are the Mine granites. Black dots are other gold showings. Q - quartzite, C - carbonate and calc-silicate, M - amphibolite, UM - ultramafic, G - granitic gneiss ("Older Granite"). After Coombe (1984).

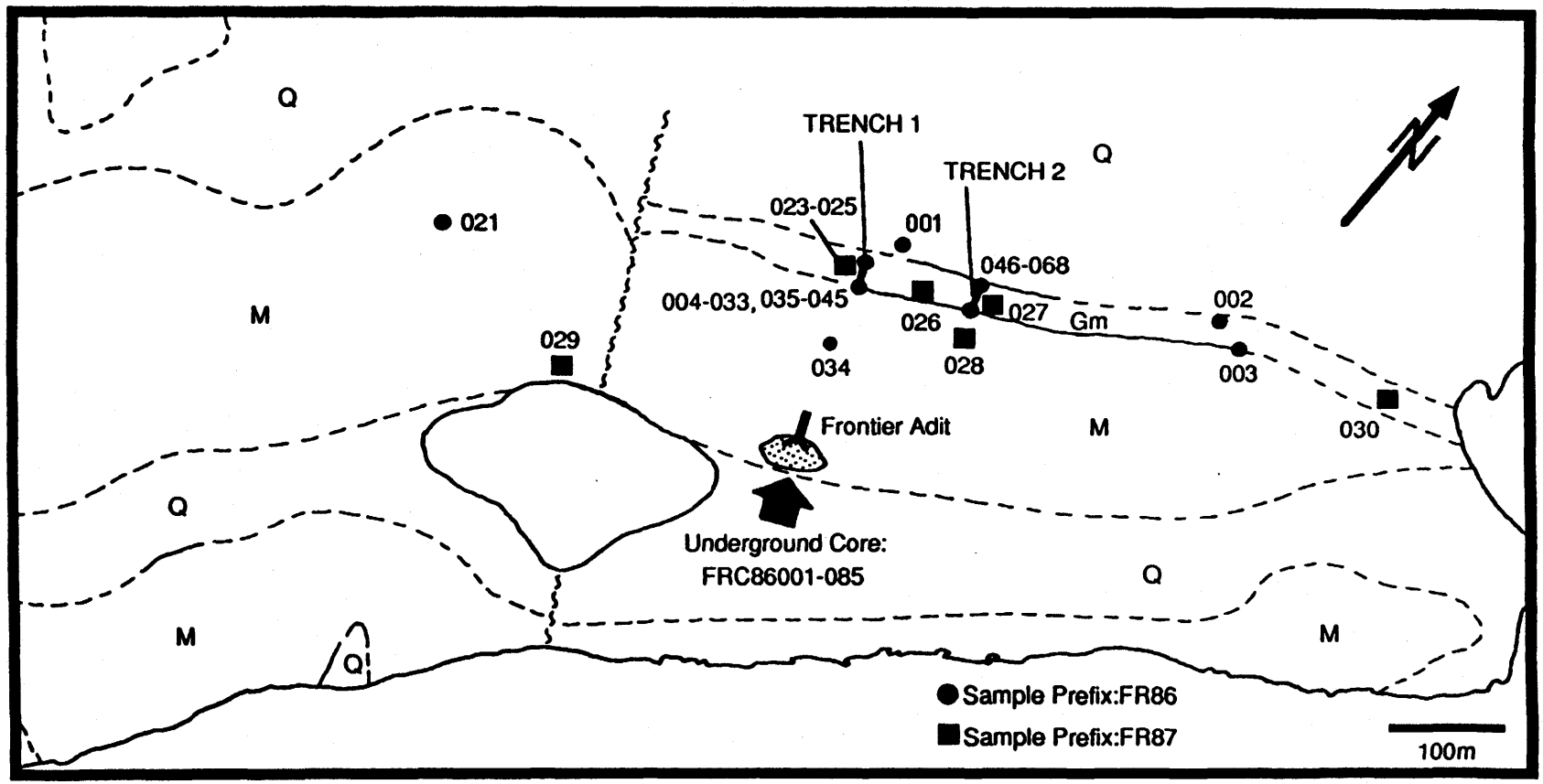

Figure 10: Local geology and sample locations, Frontier lode-gold deposit. D - diabase dyke, Gm - Mine granite, Ga - augen granite, Gl - leucogranite, Go - Older granite (granitic gneiss), M - Amphibolite (Mg - gabbroic, Md - dioritic), Q - quartzite, C - carbonate and calc-silicate. Stippled pattern indicates overburden, tailings, or waste rock. After Sibbald (1984).

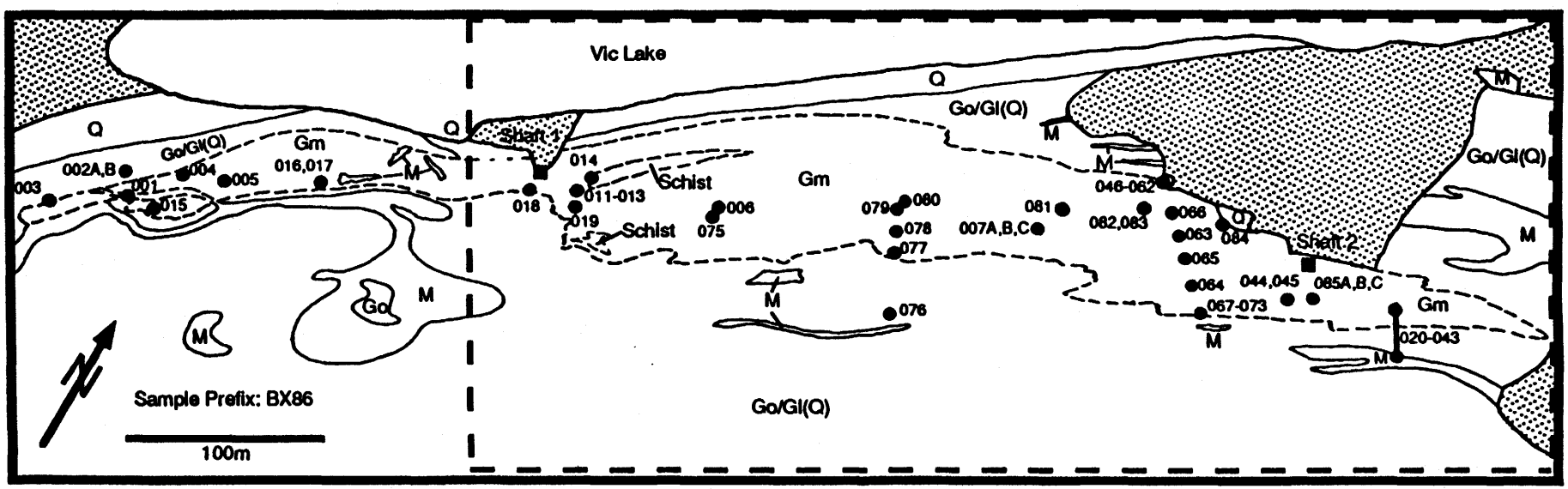

Figure 11: Local geology and sample locations, Box lode-gold deposit. D - diabase dyke, Gm - Mine granite, Ga - augen granite, Gl - leucogranite, Go - Older granite (granitic gneiss), M - Amphibolite (Mg - gabbroic, Md - dioritic), Q - quartzite, C - carbonate and calc-silicate. Stippled pattern indicates overburden, tailings, or waste rock. Dashed box outlines area of Figure 12. After Sibbald (1984), and Christie, 1952.

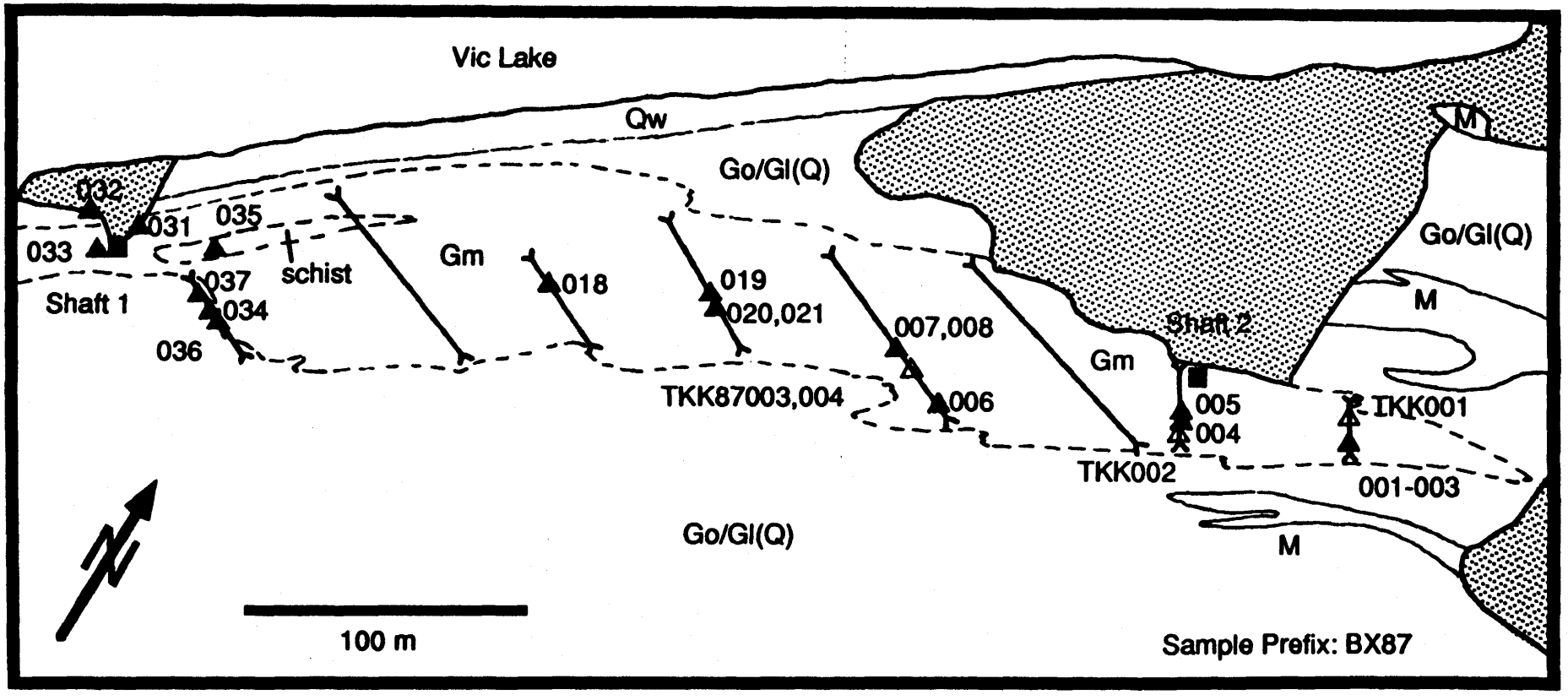

Figure 12: Local geology and sample locations, Box lode-gold deposit. D - diabase dyke, Gm - Mine granite, Ga - augen granite, Gl - leucogranite, Go - Older granite (granitic gneiss), M - Amphibolite (Mg - gabbroic, Md - dioritic), Q - quartzite, C - carbonate and calc-silicate. Stippled pattern indicates overburden, tailings, or waste rock. After Sibbald (1984).

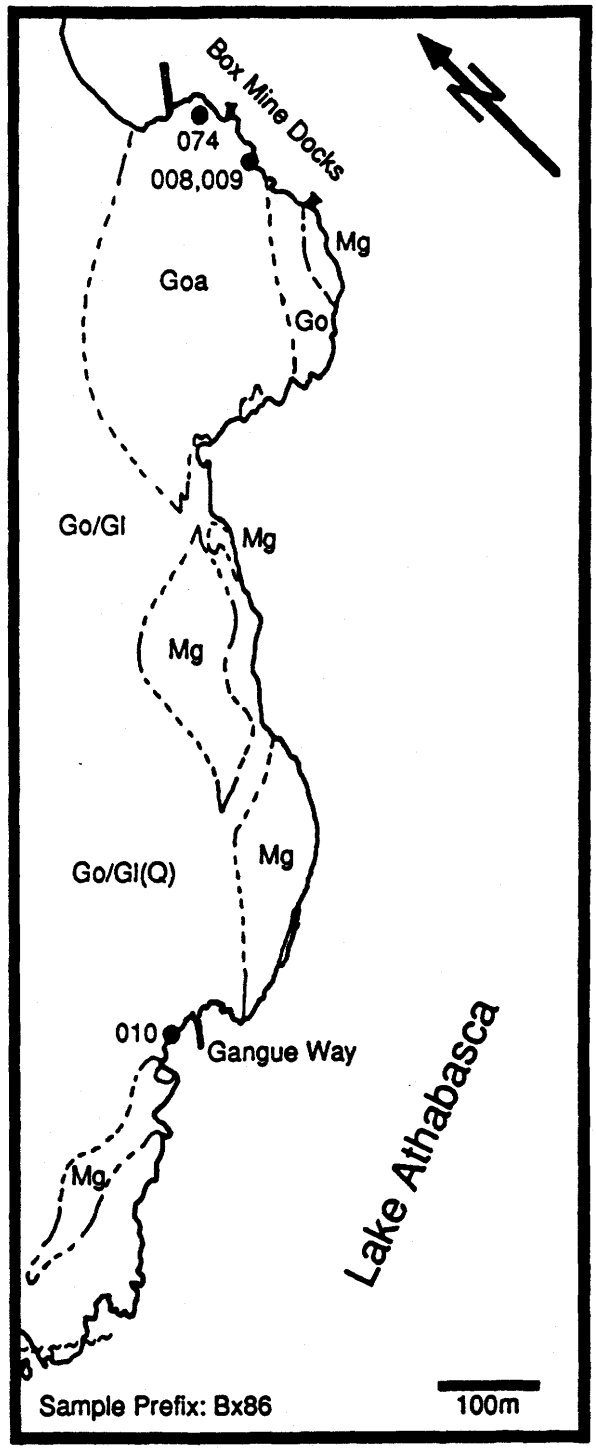

Figure 13: Local geology and sample locations, Box Mine Docks, southeast of the Box Mine. D - diabase dyke, Gm - Mine granite, Ga - augen granite, Gl - leucogranite, Go - Older granite (granitic gneiss), M - Amphibolite (Mg - gabbroic, Md - dioritic), Q - quartzite, C - carbonate and calc-silicate. Stippled pattern indicates overburden, tailings, or waste rock. After Sibbald (1984).

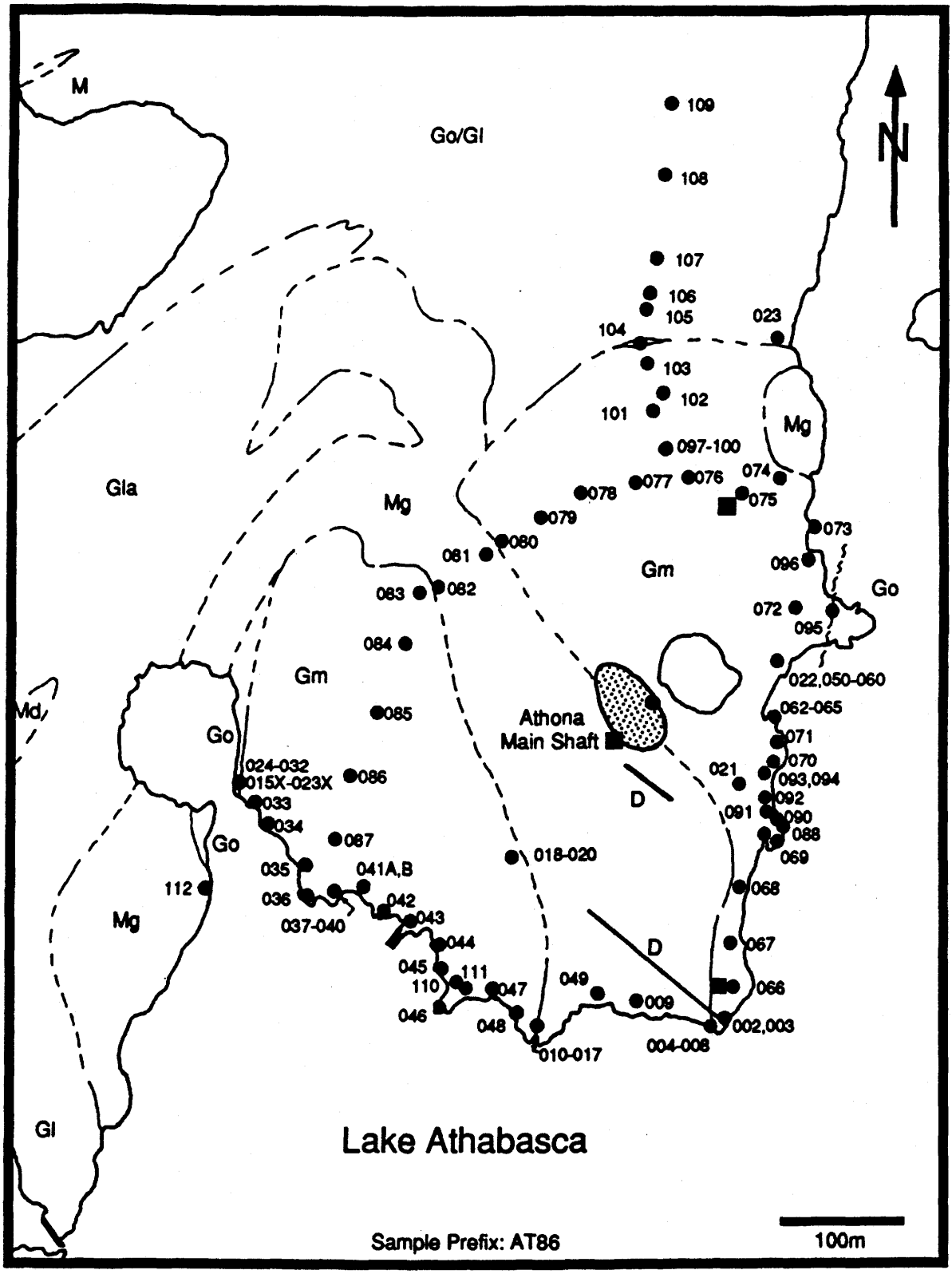

Figure 14: Local geology and sample locations, Athona lode-gold deposit. D - diabase dyke, Gm - Mine granite, Ga - augen granite, Gl - leucogranite, Go - Older granite (granitic gneiss), M - Amphibolite (Mg - gabbroic, Md - dioritic), Q - quartzite, C - carbonate and calc-silicate. Stippled pattern indicates overburden, tailings, or waste rock. After Sibbald (1984).

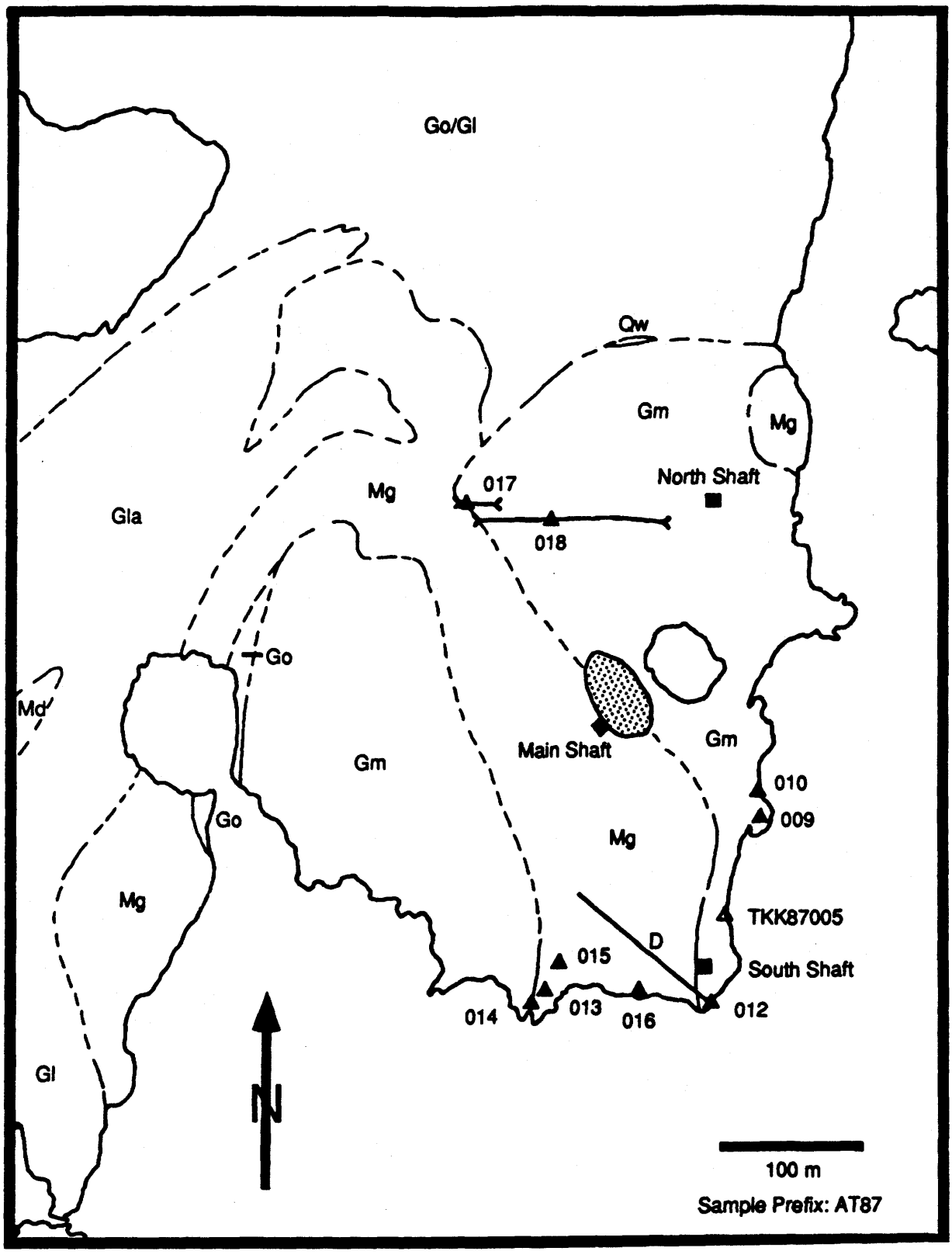

Figure 15: Local geology and sample locations, Athona lode-gold deposit. D - diabase dyke, Gm - Mine granite, Ga - augen granite, Gl - leucogranite, Go - Older granite (granitic gneiss), M - Amphibolite (Mg - gabbroic, Md - dioritic), Q - quartzite, C - carbonate and calc-silicate. Stippled pattern indicates overburden, tailings, or waste rock. After Sibbald (1984).

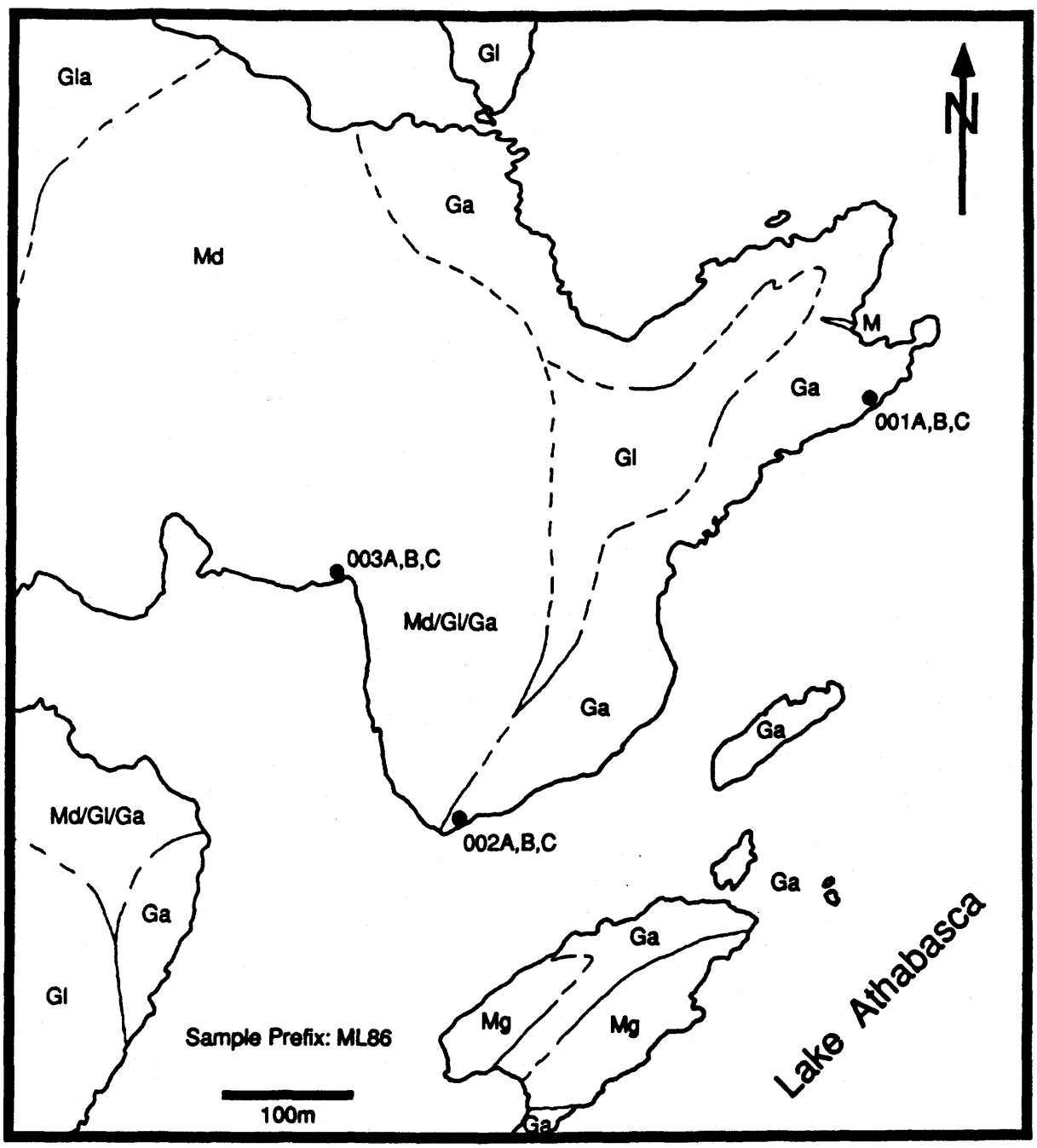

Figure 16: Local geology and sample locations, Melma lode-gold showing. D - diabase dyke, Gm - Mine granite, Ga - augen granite, Gl - leucogranite, Go - Older granite (granitic gneiss), M - Amphibolite (Mg - gabbroic, Md - dioritic), Q - quartzite, C - carbonate and calc-silicate. Stippled pattern indicates overburden, tailings, or waste rock. After Sibbald (1984).

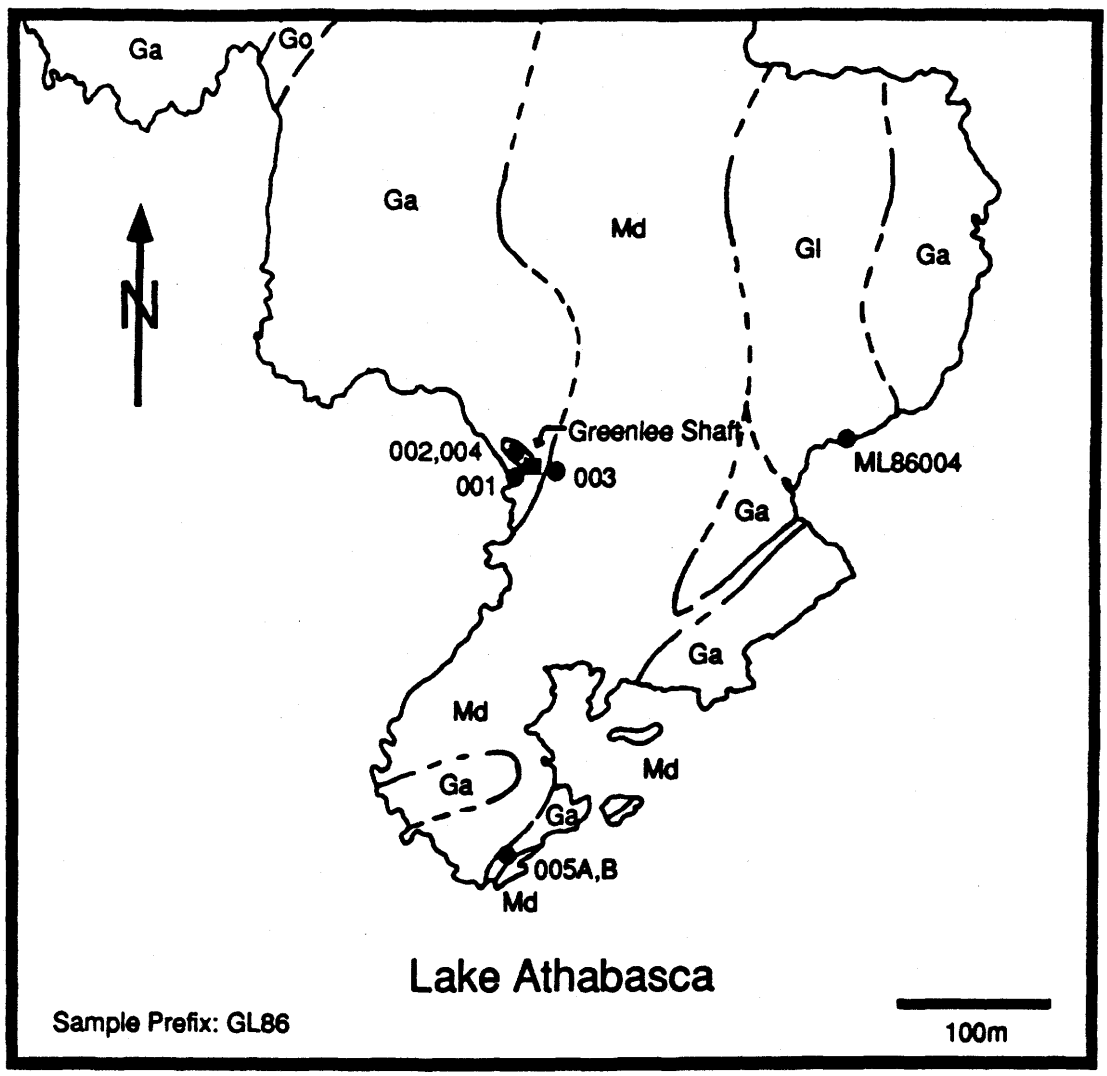

Figure 17: Local geology and sample locations, Greenlee lode-gold showing. D - diabase dyke, Gm - Mine granite, Ga - augen granite, Gl - leucogranite, Go - Older granite (granitic gneiss), M - Amphibolite (Mg - gabbroic, Md - dioritic), Q - quartzite, C - carbonate and calc-silicate. Stippled pattern indicates overburden, tailings, or waste rock. After Sibbald (1984).

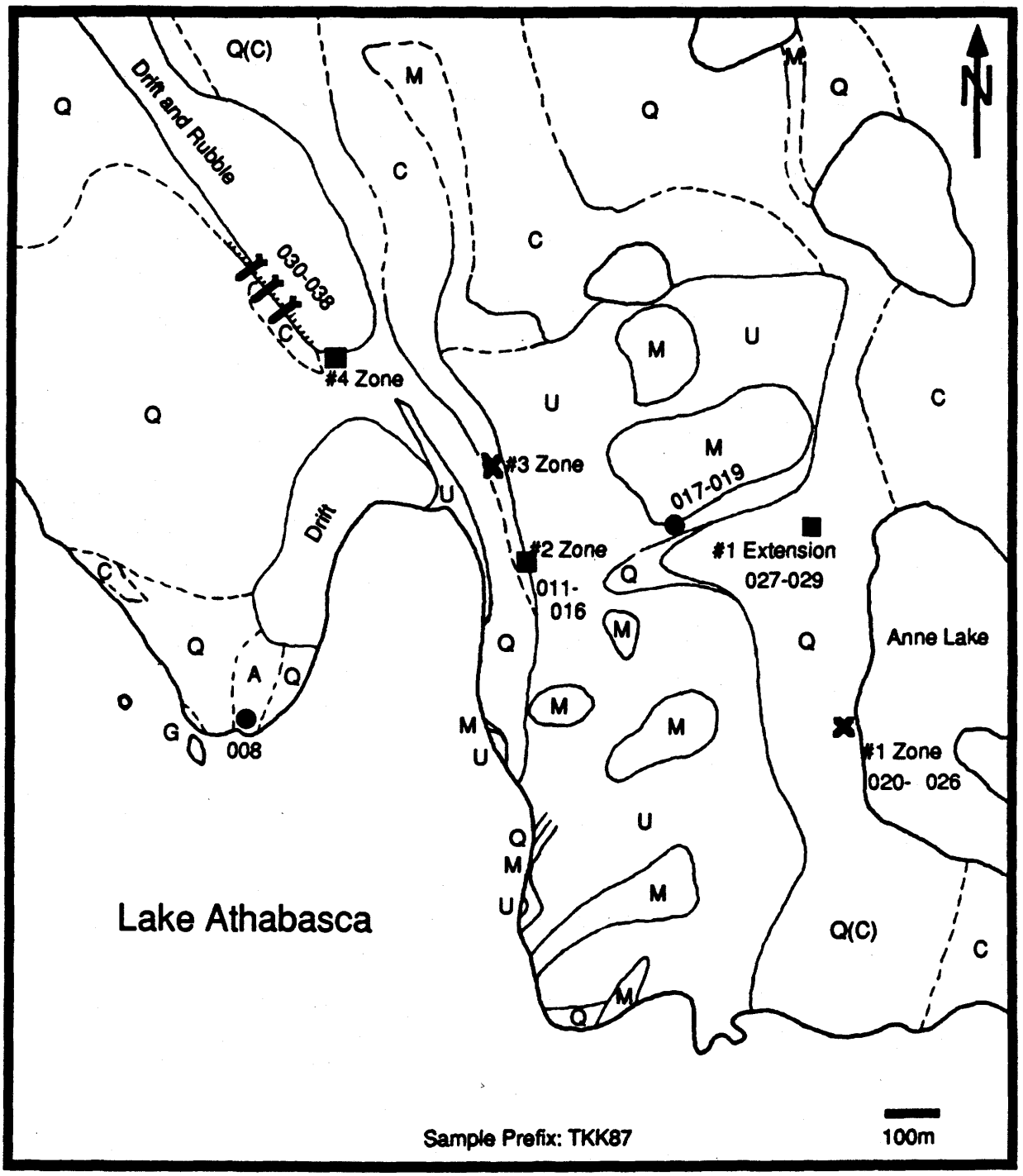

Figure 18: Local geology and sample locations, Nicholson U-PGE-Au deposit. A - Athabasca sandstone, G - granite, M - Amphibolite, U - ultramafic, Q - quartzite, C - carbonate and calc-silicate. After Sibbald (1984), and Sibbald et. al. (1983).

prepared in several ways, according to the tensile strength of the host mineral. Quartz vein material, either massive or euhedral, is sturdy enough to be prepared using conventional cutting, grinding and polishing equipment. Cryano-type adhesive was used to temporarily mount the wafer to a glass slide during preparation. After preparation, the adhesive was dissolved in acetone to release the finished wafer. The final thickness of the wafers is between 150 to 250 microns.

The lower tensile strength of dolomite requires sample preparation with minimal strain. Hand picked euhedral crystals were split along cleavage planes, into thin (approximately 1mm)slabs, using a sharp hobby knife. Cleavage surfaces are sufficiently smooth for microscopic viewing, eliminating the need for cutting, grinding and polishing. Dolomite samples from Fish Hook Bay were acquired from the Geological Survey of Canada (L. Hulbert) as commercially made wafers. Optical examination of the inclusions showed the petrographic lab was sufficiently cautious with the samples to prevent inclusion damage.

3.2.2 Microthermometric Analysis

Fluid inclusion analyses were made on an U.S.G.S. gas-flow heating and freezing stage, obtained from Fluid Inc. The digital temperature display and thermocouple are periodically calibrated at two points, -56.6°C and 0°C, using synthetic fluid inclusions. Error limits are within 0.1°C at low temperatures, and not more than 1°C at high temperatures.

3.3 Isotopic Methods

3.3.1 Stable Isotopes

Minerals were separates using standard laboratory techniques. Separates were washed, and sometimes leached in acids to remove contaminants (e.g. removing muscovite from tourmaline separates). The purity of the separations was rigourously checked, using a binocular microscope, and by XRD analysis.

All stable isotopic ratios are quoted in the standard per mil units, using the δ notation, and are relative to the V-SMOW (O,H), CDT (S), and PDB (C) standards. All measurements were done using a gas source ratio mass spectrometer (Finnigan Mat 251 or Micromass VG 602C) at the University of Saskatchewan. Laboratory values for analysed standards are 9.6 ± 0.2 per mil for NBS-28 quartz (O), -65 ± 5 per mil for NBS-30 biotite (H), and 16.8 ± 0.2 per mil for NBS-123 sphalerite (S).

Oxygen was extracted from silicates and oxides using the BrF_5 technique of Clayton and Mayeda (1963). Water from minerals was extracted and converted to hydrogen using the technique of Bigeleisen et al. (1952), with the modifications of Kyser and O'Neil (1984). Sulphides were crushed and mixed with cupric oxide, then heated to 1000°C, forming SO_2 (Rafter, 1965). Dolomite was reacted with 100 percent phosphoric acid for 24 to 48 hours at 25°C to form CO_2, after the method of McCrea (1950). Initial experimentation with dolomite splits

at reaction temperatures of 25°C and 50°C revealed no differences in the isotopic compositions of oxygen or carbon, once corrected for the temperature difference of the phosphoric acid.

Fluid inclusion water was extracted from hand picked, cleaned crystals of quartz and dolomite by thermal decrepitation, using a resistance furnace. Hydrogen was extracted from the liberated inclusion water by the same method used for minerals. Sample sizes ranged from 150 to 1500 mg. The temperature was increased to approximately 500°C over 15 to 30 minutes, then up to 600°C for a few minutes to ensure complete decrepitation (Shepard et al., 1986). Optical inspection of a dolomite sample brought to 400°C showed that only 20 to 30 percent of the inclusions had decrepitated. Mechanical decrepitation of one sample of dolomite, using an evacuated ball-mill type of container, yielded results similar to thermal decrepitation.

Fractionation factors for oxygen, hydrogen, and sulphur are those recommended by Kyser (1987). For discussion of the validity of the fractionation factors used, see Kyser (1987).

3.3.2 Radiogenic Isotopes

Mineral separates were washed to remove surface contaminants. Additionally, tourmalines were leached for 1 to 2 hours in agitated 50 percent HF to remove any muscovite alteration. After dissolution in $HF-HNO_3$ solutions for 24 hours, Rb and Sr were separated from minerals using standard

cation exchange chemical techniques. Rb and Sr abundances were calculated by isotope dilution, and mass ratios were analysed on a Finnigan Mat 261 solid source ratio mass spectrometer. The $^{87}Sr/^{86}Sr$ ratios were normalized to an 88/86 ratio of 8.3752. The $^{87}Sr/^{86}Sr$ ratio of NBS-987 standard was 0.710240 ± 0.000021.

3.4 Geochemical Analysis

Whole rock geochemical analyses were acquired from two sources. A few were published by Sibbald (1984), whereas the majority were obtained from D. Quirt at the Saskatchewan Research Council. The analyses are by standard Atomic Absorption and ICP-MS at the Saskatchewan Research Council. Samples were selected to exclude quartz veins and weathered material, crushed to powder in a tungsten mortar. Data for rare and trace elements are considered accurate to ± 2 ppm. Silica content was not analysed, but calculated by subtraction from 100 % of the total weight % of the other oxides, LOI, and trace elements. The resulting SiO_2 weight % is accurate to roughly 0.5 weight %.

4.0 Lode-Gold Deposits

4.1 Geology of Deposits

The general geology of the gold mineralization at the Box, Athona and Frontier deposits has been described in detail by Cooke (1937), Beavan (1938), Christie (1952), Sibbald (1984), and Sibbald & Jiricka (1986). Exploration, mining, and economic aspects of the deposits have been described by Byrne (1937), Jewitt & Gray (1940), and Swanson (1945). Alcock (1936) and Beck (1959) have provided short descriptions of all the lode-gold occurrences in the Goldfields area. The petrology and lithogeochemistry of the mine granites have been investigated recently by Quirt (1988, 1990), and Appleyard (1988, 1989, 1990), as well as a petrographic study of the Box mine granite by Killin (1939). A detailed structural study of the Box and Athona deposits was undertaken by Roberts (1990). As the geology has been well documented, only a pertinent summary is provided here, supplemented by field observations and petrographic examinations from this investigation.

4.1.1 Mine Granites

The mine granites are conformable, sill- or plate-like bodies that host lode-gold quartz veins (Figure 7), and are part of the North Shore Pluton group. They are typically leucocratic, and brick-red in colour. The Box and Athona granites are very similar petrographically, and are composed

of medium to coarse grained, euhedral to subhedral megacrysts of alkali feldspar (microcline perthites), albite, and quartz, set in a fine-grained granoblastic groundmass of the same three minerals, with minor accessory muscovite and pyrite. Trace biotite is present, but is usually altered to chlorite. Chlorite also occurs as thin coatings along later fractures, some of which are related to the lode-gold veins. Based on petrographic observations, Appleyard (1990) considers the megacrysts to be of igneous origin, but Sibbald (1984) reports some indications of a metamorphic origin (porphyroblasts). In either case, cataclastic fabrics have overprinted the granites, obscuring original textures, most prominently in the Athona granite. Albitization has variably affected the granites, a feature which is common to all rocks in the Beaverlodge area. The age of the albitization in the mine granites is unclear, as it cannot be definitely associated with: (1) the albitization associated with the simple-type uranium deposits, (2) the regional albitization, or (3) associated with the albite-bearing lode-gold veins that are hosted by the granites. As the late albite does not appear to be highly deformed, it was most likely developed after, or during the late stages of the D2 event with which the lode-gold veins are associated.

The Frontier granite is somewhat distinct from the Box and Athona granites, as it is fine-grained, and contains very little albite. Only small, anhedral megacrysts of alkali

feldspar are present, set in a fine-grained groundmass of quartz and alkali feldspar, with minor pyrite, and trace muscovite and chlorite. Cataclastic textures are least apparent within the Frontier granite, and later albitization has not affected the granite.

The postulated origins of the mine granites have been controversial from the time that the deposits were discovered. Theories for their origin range from classical intrusive magmas, to "magmatic fluid infiltration" (metasomatic granitization), to in situ melting (anatexis). These theories are summarized by Sibbald (1984), and Appleyard (1989, and 1990). Much of the confusion has arisen from the variation in both the internal appearance of the granites, as well as their contact relationships with surrounding country rocks, especially with the foliated granite gneisses ("Older Granite" of Sibbald, 1984). For example, although classical intrusive structures such as xenoliths and schlieren can be seen within the Box and Athona granites, the outer contacts are often gradational over several meters, especially where the granites are in contact with the foliated granitic gneisses. Of the three Mine granites, the Frontier granite bears the closest resemblance to a "metasomatic" granite, as relict sedimentary structures can be observed within marginal portions of the granite, and they can be traced laterally into the quartzites that host the granite. However, contradictory contact relationships exist, where apophyses of granite with sharp

contacts appear to push apart quartzite bedding. Quirt (1990) suggests that the Frontier granite is the result of potassic and silicic alteration that accompanied the emplacement of the lode-gold veins, based on mass balance calculations of whole rock geochemical data. If this were the case, the albitization observed in the Box and Athona granites could also be the result of vein-associated alteration. The correlation of the sodic or potassic character of the host mine granites with the albite or potassium feldspar gangue phases within the lode veins (see section 4.1.2) may be used as evidence of this, but it may also be the result of fluid-wall rock interaction. In either case, conclusive petrographic evidence of albitic or potassic alteration accompanying veining does not exist.

The variation of contact and internal field relationships of the mine granites, as well as the Neimen Bay "transect" described in section 2.3, are compatible with formation of the granites by a mixed process, involving melt generated by crustal anatexis, contemporaneous with autometasomatic "granitization". Such a process is favoured by Appleyard (1990).

Whether or not the melt was formed at depth as a minimum melt composition, or was formed "in situ" is not clear. Normative Quartz-Albite-Orthoclase compositions of the mine granites (Figure 19, and Appleyard, 1990, Figure 1) approach a minimum melt composition, but often show a wide scatter from

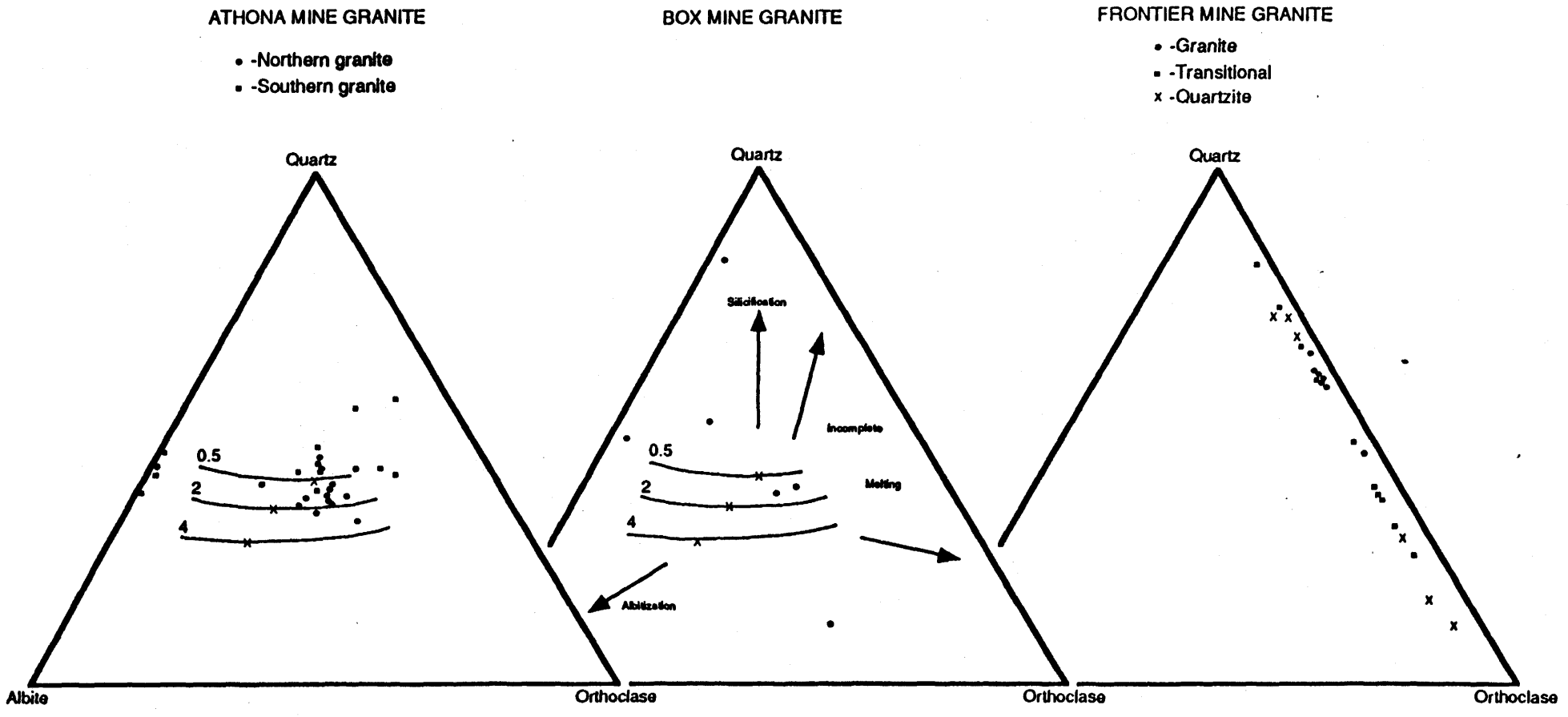

Figure 19: Relation amoung normative quartz-albite-orthoclase compositions for samples of the mine granites. Data from Appendix 1. Curved lines are isobars at 0.5, 2, and 4 kilobars, and X marks the ternary minimum melt composition at those pressures, in the presence of excess water (Tuttle & Bowen, 1958). Trend lines indicate the effects on ternary composition due to incomplete melting, or later alteration (silicification and albitization).

the minimum. Later alteration of the granites, such as silicification and albitization (Figure 19) may have produced some of the scatter, but incomplete melting, especially shown by the Frontier granite data (Figure 19), may explain why many of the normative compositions do not plot near minimum melt compositions. In contrast, normative compositions of samples from the Athona granite cluster near the minimum melt composition (Figure 19).

Although the exact formation mechanisms of the mine granites are not well defined, the tectonic setting in which they were generated seems clear. They are peraluminous (Appleyard, 1990, and confirmed using study data), and have an affinity with "S-type", syn-collisional, sedimentary-source granites, perhaps emplaced, or formed in situ, in a back-arc setting (Appleyard, 1990).

4.1.2 Lode-Gold Veins

Lode-gold veins hosted within the Box, Athona, and Frontier granites bear many similarities in mineralogy and structure, suggesting they are related to the same mineralizing process. The most detailed descriptions of the deposits are given by Cooke (1937), Beavan (1938), Jiricka (1984), and Roberts (1990), from which the following summary is derived, augmented by field observations from this study.

Veins hosted by the Box and Athona mine granites are dominantly quartz, with minor to trace amounts of chlorite, albite, microcline (rafted), tourmaline, muscovite, pyrite,

sphalerite, chalcopyrite, galena, gold. In the Athona veins, gangue minerals other than quartz are rare. Veins hosted within the Frontier mine granite are similar, but contain orthoclase instead of albite, and pyrite as the sole sulphide phase. Rare tremolite and calcite are also present in the Frontier veins.

Quartz in the veins appears to have been deposited continuously during the structural evolution of the vein-forming system (Figure 20). Feldspar, tourmaline, chlorite and pyrite are early formed phases, occuring as individual groups of subhedral to euhedral crystals, usually proximal to the vein selvages. Minor amounts of chlorite commonly occur as a very thin coating on the walls of the veins, indicating it formed early. It also occurs as a later phase that rims and crosscuts early-formed subhedral to euhedral pyrite, as well as along late micro-fractures in the quartz. Muscovite also occurs along the same late microfractures, as an alteration product of tourmaline. Minor pyrite deposition continued with the sequential deposition of sphalerite, chalcopyrite, and galena (Figure 20). Further details of vein paragenesis are described in section 4.3.1.

The bulk of the gold mineralization appears to have taken place during the latest stages of vein formation, as it occurs as coatings or fracture-fillings of the sulphide crystals, as well as within small internal fractures in the quartz veins. Although gold has not been found directly associated with the

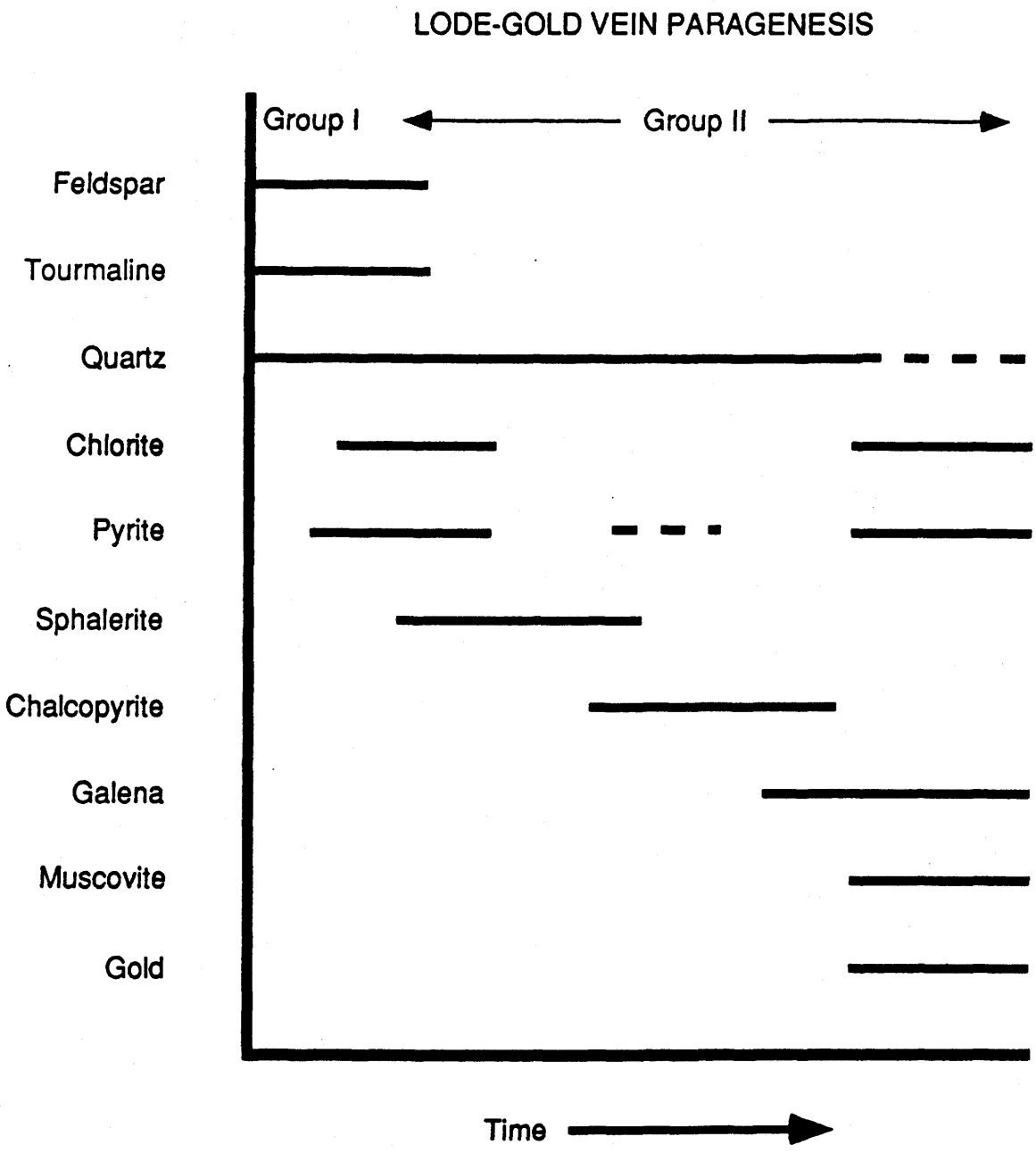

Figure 20: Paragenesis of minerals in lode-gold veins, Box and Athona mines. Paragenesis of minerals in Frontier veins discussed in text. Vein groups approximated from Roberts (1990). Dashed lines indicate weakly developed or uncertain development of the phase. Further details of paragenesis discussed in section 4.3. After Beavan (1938), with modifications.

late chlorite or muscovite along microfractures, its occurrence in the exact same settings implies they are contemporaneous.

Roberts (1990) has described the structure of the vein systems, and recognizes three groups of veins. Group I veins consist of an early set of small quartz pods and lenses within brittle-ductile shear zones that are parallel to lithological contacts (approximately 045°/40°SE), occuring along the footwall and hanging wall contacts of the mine granites. These shears and veins are weakly developed within the granites. The mineralogy of the Group I veins is consistent with their emplacement during the earliest stages of the vein-forming event (Figure 20). Group II veins are much more abundant than those of Group I, forming the bulk of the vein system. Group II veins are typically no more than 10cm in width, with strike lengths of up to 10m at the Box and Frontier deposits, and up to 100m at the Athona deposit. They variably crosscut, or are contemporaneous with, the Group I veins, but pass out of these into the stockworks (Box, Frontier) and planar swarms (Athona) that form the bulk of the deposits. Roberts (1990) has identified five, mutually crosscutting vein sets at the Box and Athona deposits. Three main sets, striking NNE, ENE, and N-S, with subvertical dips, are complemented by two minor sets of associated tension fractures with variably developed veining. The N-S veins are the best developed set at the Box deposit, where host

structures are dominantly of a brittle character. At the Athona deposit, the NNE set (parallel to the axial plane orientation of the Goldfields Synclinorium) is dominant, and structures are brittle-ductile. The structure of the vein system at the Frontier deposit is virtually identical to that at the Box deposit (Jiricka, 1984).

A later vein set crosscuts the lode-vein sets (Group III of Roberts, 1990) at the Box and Athona deposits. These are vuggy veins of euhedral quartz and dolomite which contain pitchblende, and are herein referred to as euhedral U-bearing, or comb veins. They occur as single narrow veins, or brecciated zones up to 1m wide, less than 50m in length, and typically strike E to SE, and have subvertical dips.

The emplacement of the lode-gold veins (D2b of Roberts, 1990) occured during the latter stages of D2, which formed the Goldfields Synclinorium (D2a of Roberts, 1990), as the veins have not been significantly deformed (Roberts, 1990). The geometry and crosscutting relationships of the vein sets suggest they were emplaced continually during compressional deformation within a slightly rotational strain regime (Roberts, 1990). Initially, Group I veins were emplaced in ductile-brittle shears that developed along lithologic contacts. As deformation progressed, strain could no longer be accomodated on these planes, resulting in brittle, to brittle-ductile deformation structures within the mine granites that host the Group II veins. Roberts (1990)

suggests that the preferential development of specific vein sets is related to local strain conditions, which may be dependant on the location of the deposit within the Goldfields Synclinorium.

4.2 Fluid Inclusions

4.2.1 Inclusion Types & Petrography

All fluid inclusions observed in the lode-gold veins occur in quartz. No inclusions could be seen in tourmaline and sphalerite, due to their dark colour and inability to take a good polish. No direct evidence linking gold deposition and any of the fluid inclusion types was found, because gold was never observed to be associated with specific fluid inclusions within a polished wafer. Quartz in the vein systems from all three deposits shows strain features such as undulose extinction, sutured grain boundries and sub-grain development. Complete polygonal recrystallization of the vein quartz is rare, and only locally developed. Subgrain boundries are evident in cross- polarized light, and can also be seen in plane light by the accumulation of dark, decrepitated inclusions, as well as numerous secondary fluid inclusions. In polished wafers, large areas of the vein quartz are essentially translucent, due to numerous small secondary inclusions along multiple fractures, as well as along grain and sub-grain boundries. Study of the inclusion populations was generally limited to clearer grains and patches of quartz between the translucent, or "cloudy" portions (Plate 1a).

Plate 1: a - photomicrograph showing a patch of clear, transparent quartz, surrounded by "cloudy", inclusion-filled quartz within a lode-gold vein (BX86085I). The contrast has been exaggerated in the photograph. Bottom edge of photograph is approximately 4mm long; **b** - photomicrograph of a subgrain of quartz within a lode-gold vein, showing hexagonally symmetric, pseudosecondary fracture planes (labelled 1, 2, and 3) bearing Type I and Ia fluid inclusions (BX87001). Note that the inclusion planes do not appear to crosscut the subgrain boundaries. Bottom edge of photograph is 1.35mm long.

1a

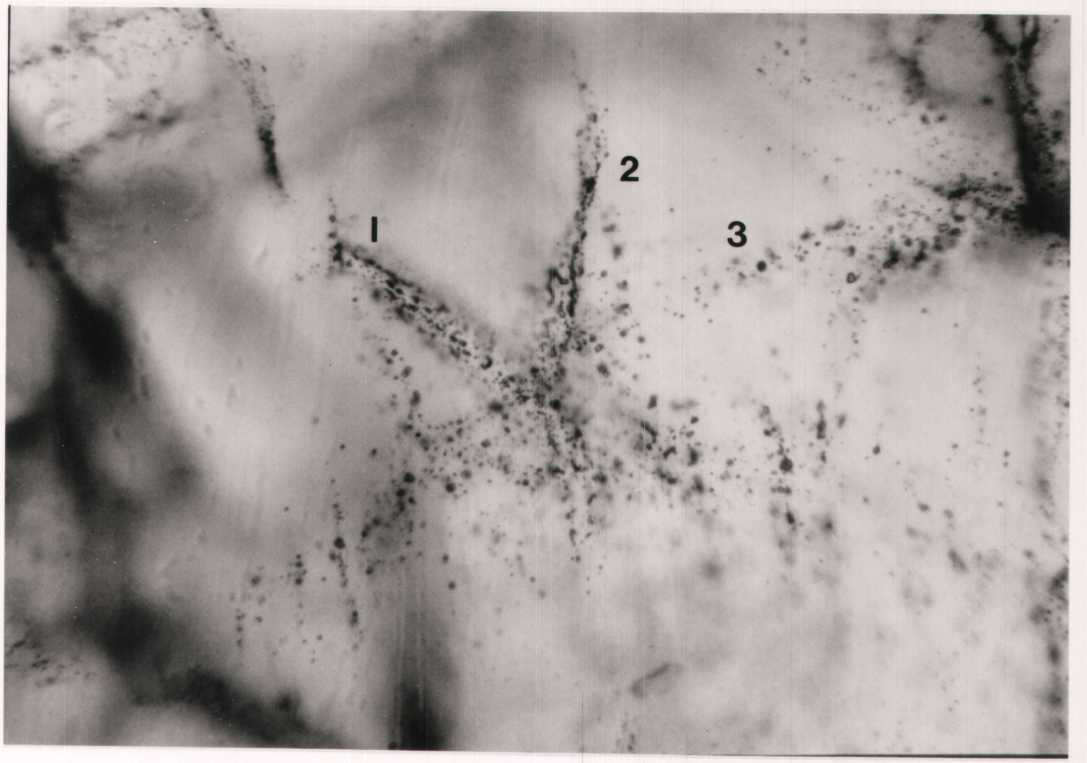

b

Petrographic relations imply that the clearer quartz grains most likely represent the latest additions of quartz to the veins, during crystallization in a rotational strain regime (Roberts, 1990) that deformed the earlier phases of quartz syn-depositionally in the developing fractures. The later quartz has escaped most of the deformation as it essentially represents the final stages of the vein-forming structural event (D2b).

A generalized inter-deposit comparison of petrographic strain indicators in the vein quartz (e.g. subgrain development, microfracture density, "degree of translucence") indicates that the degree of strain recorded increases in the order: Frontier < Box < Athona. The degree of strain correlates with the degree of cataclasis observed in the mine granites (Appleyard, 1990), as well as to the brittle or ductile character of the fractures that host the veins (Roberts, 1990).

Comparison of fluid inclusion data, both for different vein sets within a deposit, and among the deposits, indicates that the quartz veins in the three deposits all record similar fluid histories. Figure 21 summarizes the types of fluid inclusions observed in the lode-gold veins. They are arranged by relative age, so the type number equates to the relative age. An optical estimate of inclusion abundance roughly shows Type II >> Type I > Type III > or = Type IV.

Type I inclusions are CO_2 - H_2O bearing, with variable

Goldfields: Fluid Inclusions From Lode-gold Veins

TYPE	PICT	THERMOMETRIC DATA	LOCATION
I CO2-H2O PS & P ?		ThCO2 = 9 to 30 C ThCO2-H2O = 200 to 360 C 5 to 90 volume % CO2 total range, typically 20 volume % and 80 volume % bimodal distribution TmCO2 = -56.6 to -57.4 C 6 wt% NaCl eq. average (2 to 10 wt. %) CO2 density = 0.6 to0.9 g/cm3 Bulk density = 0.6 to 1.0 g/cm3	Box Athona Frontier
Ia CO2-H2O PS & P ?		75 to 95 volume % CO2 (Type Ia, or CO2-rich Type I)	
II H2O S	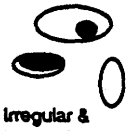 Irregular & Monophase	ThH2O = 100 to 400+ C (necking) = 125 to 175 C (Frontier) 0.5 to 6 wt. % NaCl eq.	Box Athona Frontier
III H2O S	 Liquid Mono-phase +/- daughter	ThH2O = 120 to 200 C (necking) 10 to 15 wt. % NaCl eq. Insoluable rhombic daughter mineral, possibly carbonate	Box
IV H2O S	 Often Liquid Monophase	ThH2O = 100 to 200 C (?, necking) Td = 150 C = ~30 wt% NaCl eq. Halite daughter mineral	Box
P = Primary PS = Psuedosecondary S = Secondary		○ = liquid H2O or CO2 ● = H2O vapour ● = CO2 vapour	

Figure 21: Summary of fluid inclusion data from the Goldfields lode-gold quartz veins (Box, Athona, Frontier). All data are discussed in the text, and are shown here for reference only. Pictoral representations of the inclusions are schematic, and not to scale. Type Ia inclusions are a sub-type of Type I, and have the same general characteristics as CO_2-rich Type I inclusions.

amounts of CO_2 (5 to 90 volume %). CO_2 is visually indicated by the presence of "double bubbles" (Plate 2), although some very CO_2-rich inclusions appear to have a single bubble (Type Ia), without much visible H_2O. Within a non-planar group, or short fracture-related group, Type I inclusions usually occur as a bimodal population of inclusions, some with high (approximately 80 volume % CO_2), and others with low (approximately 20 volume % CO_2) CO_2/H_2O ratios (Figure 22). Type Ia inclusions would belong to the CO_2-rich group, as their distinction as a subtype is based solely on the lack of visible water (Plates 2a & 2b). This distinction, however, is controlled to a great extent by the geometry of the inclusion, and the direction from which it is viewed, so that in an inclusion with a non-ideal shape (i.e. not a "negative crystal" shape), a small volume of water is often visible within a corner of the inclusion (see section 4.2.2). Some inclusions showed evidence of "necking" (Roedder, 1984) in their morphology, such as irregular inclusion shapes, short nipples or arms protruding from the inclusion, and a limited variablity of CO_2/H_2O ratios within the overall bimodal populations. This has had a limited influence on the microthermometric characteristics of the fluid (see section 4.2.2). Type I inclusions range in size from 2 to 40 microns (typically 10 to 20 microns), and contain no daughter minerals.

Type I inclusions occur in three configurations: (1) as

Plate 2: a - photomicrograph of a Type I (TI) fluid inclusion, showing outer CO_2 liquid and inner CO_2 vapour bubbles (C), with the bulk of the inclusion filled with H_2O liquid (H). Also in the photo are several Type Ia fluid inclusions (TIA), which appear to consist of only CO_2 liquid and vapour phases, with no visible H_2O. All of the inclusions are isolated, and do not appear to be related to a fracture plane (BX86085I). The Type I inclusion is approximately 26 microns in length; **b** - photomicrograph of Type I (TI) and Type Ia (TIA) fluid inclusions located along a short intragrain fracture (BX86085I). The Type I inclusion in the center of the photograph is approximately 35 microns in length; **c** - photomicrograph of an unusally large Type II fluid inclusion, consisting of a H_2O vapour bubble (V), and H_2O liquid (L). Type II inclusions of a typical size are located on the fracture plane (S), and have variable liquid to vapour ratios BX86085II). The large inclusion is approximately 25 microns in length.

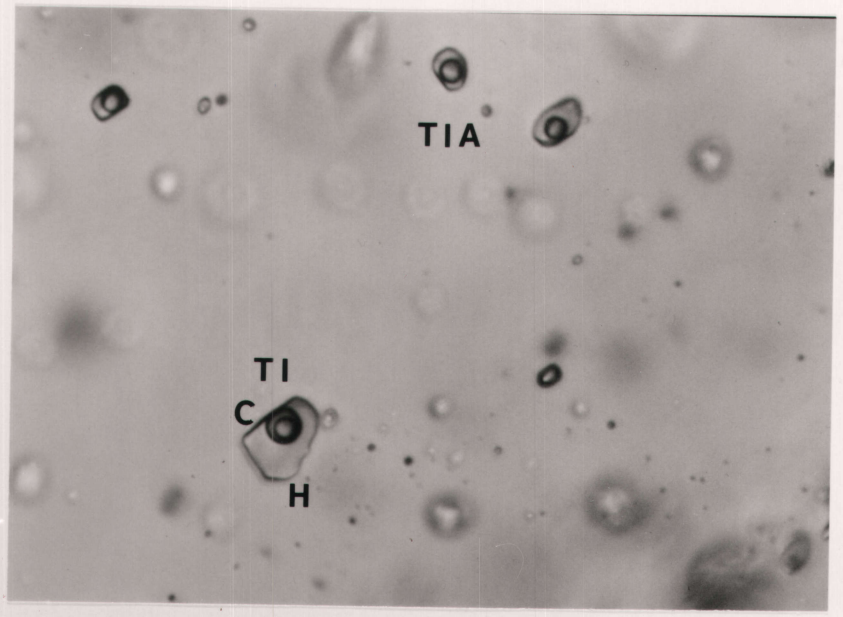

2a

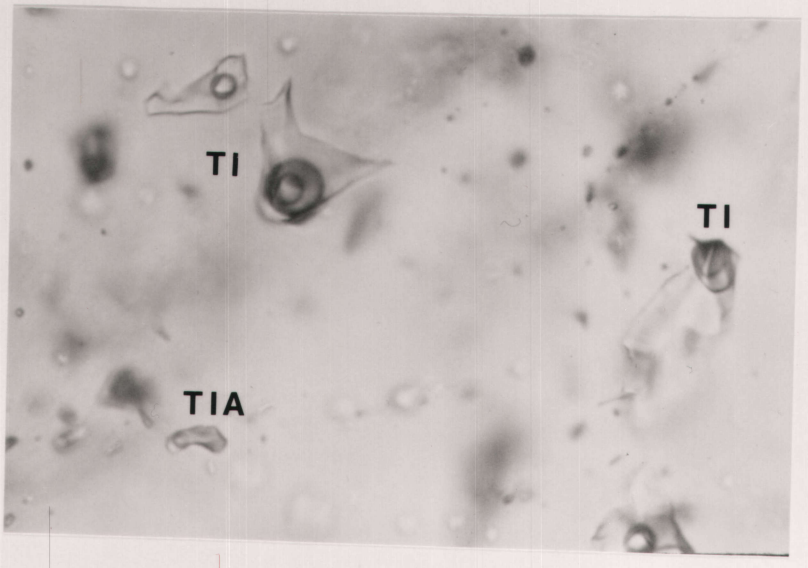

b

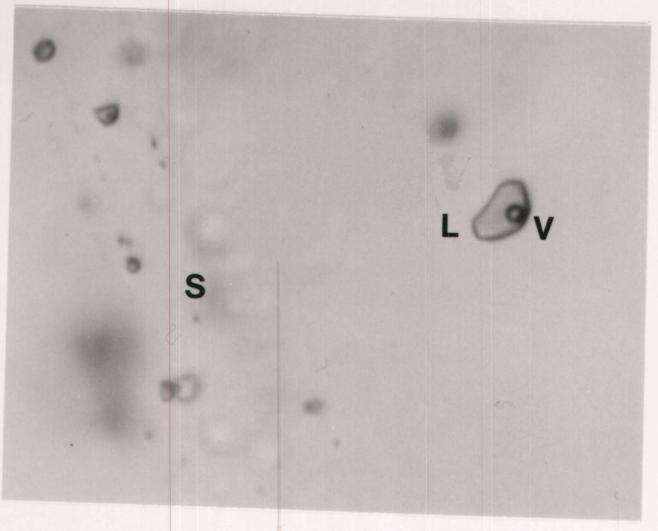

c

Figure 22: Type I fluid inclusions, showing examples of bimodal distribution of CO_2-H_2O ratios within a group of inclusions. A and B - two groups of inclusions from a Box quartz vein (BX87001), showing approximately 20 volume % and 80 volume % CO_2 contents in coexisting inclusions. Inclusions in A are not on a fracture plane, whereas those in B are along a fracture plane that does not leave the grain. C - a group of inclusions, not associated with a fracture, from a Frontier quartz vein (FR86040), also having approximately bimodal CO_2 contents. In all examples shown, volume % CO_2 is visually estimated, and depends on the geometry of the inclusion, as well as the effects of limited necking.

A - BX87001

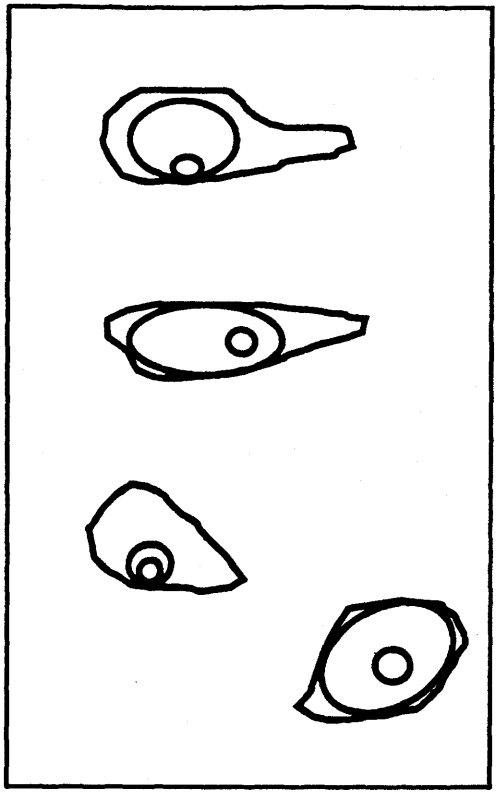

B - BX87001

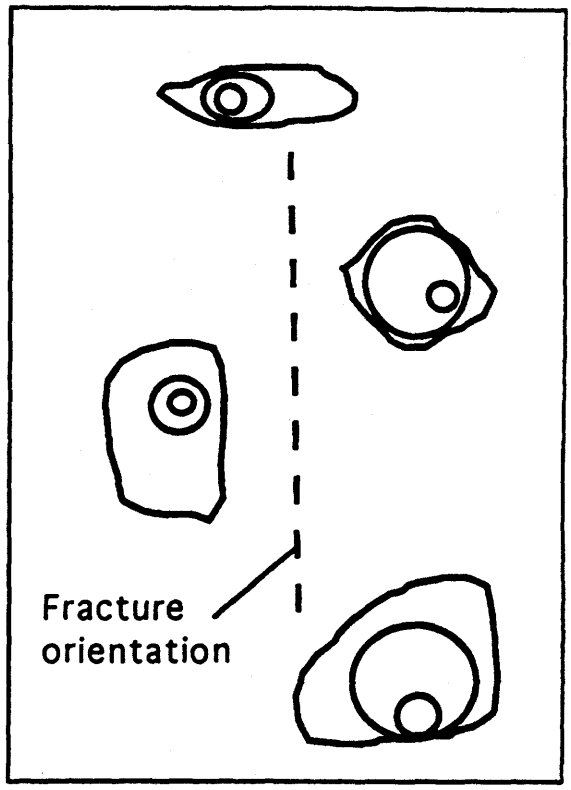

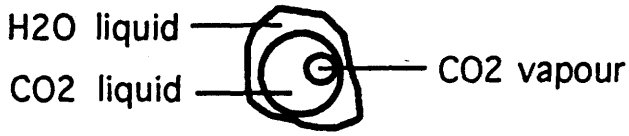

C - FR86040

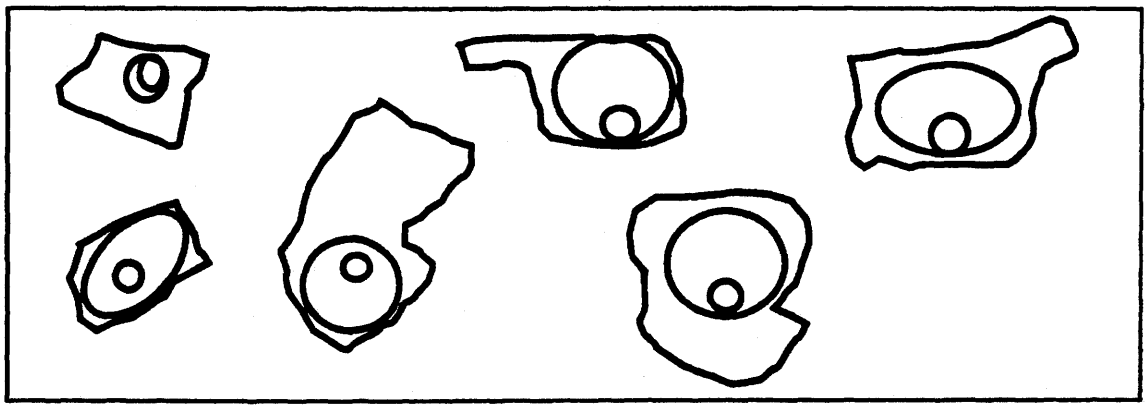

a single inclusion, or non-linear group of several inclusions, not obviously associated with a linear fracture plane (Plate 2a). They are separated from any fracture planes bearing obvious secondary inclusions (Type II). This indicates that Type I inclusions may be primary with respect to the quartz that hosts them. This is not conclusive evidence however, as original fracture planes may have completely healed, or been destroyed by deformation (i.e. sub-grain development). However, it does suggest that the inclusions are, in some way, associated with the overall veining and mineralizing sequence, because they could not post-date deformation; (2) alternately, one or two inclusions may be very close to a secondary fracture plane hosting Type II inclusions, but do not appear to be part of that plane; (3) Type I inclusions occur along short fracture planes that do not visibly cut across grain boundaries (Plate 2b). Although not conclusive, as mentioned in the first case, this latter occurrence would imply that the inclusions are "pseudosecondary" (essentially equivalent to primary inclusions), or that they are very early "secondary" inclusions that are associated with the later stages of the veining event. In a sample from the Box mine (BX87001), a six-pointed star-shaped structure of inclusions was seen in the centre of a grain (Plate 1b). The star-shape approximates hexagonal symmetry, reminiscent of the trigonal symmetry of quartz. None of the fracture planes (star points or arms) appear to leave the grain, which, along with the symmetry, may

imply a genesis not related to later secondary fracturing. The exact origin of the structure is unknown, but it suggests a pseudosecondary, and therefore primary, origin of the inclusions along it.

Although none of the above occurrences clearly indicate that the inclusions are truly primary, it is clear that the inclusions are the earliest population observed in the veins, and that they do not post-date vein deformation. As vein deformation appears to be essentially contemporaneous with emplacement, this implies that Type I inclusions are related to the later stages of the veining event (i.e. "pseudosecondary" or very early "secondary" inclusions), perhaps associated with the late brittle fracturing that hosts chlorite, muscovite, and gold.

Type II inclusions are aqueous (H_2O), and comprise the bulk of inclusions in the veins. They occur along extensive sub-parallel to random fracture networks, cross-cutting many grain or subgrain boundaries. They also occur along grain and subgrain boundaries. Type II inclusions are definitely later than Type I inclusions, as the fracture planes cross-cut the short fracture planes that host pseudosecondary Type I inclusions. As Type II fracture planes cross-cut subgrain boundries, and Type II inclusions occur along subgrain boundries, they post-date the majority of the strain that deformed the vein quartz, including the late brittle micro-fractures.

Type II inclusions are usually well formed, with negative crystal shapes, but show evidence of necking with variable liquid/vapour ratios along the same fracture plane, including monophase liquid or vapour inclusions (Plate 2c). Obvious necking morphology is commonly seen with the larger, irregularly shaped inclusions (approximately 30 microns in diameter), although most Type II inclusions have diameters of 2 (or less) to 10 microns. No daughter phases were observed.

Type III inclusions were observed only once, along several fracture planes in a sample fron the Box mine. The fractures appear to cross cut Type II fracture planes. The inclusions are usually well formed, and have variable but limited liquid/vapour ratios (vapour = 0 to 15 volume %) along the plane, indicating some degree of necking. The inclusions usually contain a small, virtually insoluble daughter phase, of a rhombic form. The mineral has a high relief, is strongly birefringent, and appears to be light green in plain light. A positive identification of the mineral could not be made, but it is most likely a carbonate (Ca/Mg), or an iron chloride ($FeCl_n$). The inclusions are from 5 to 20 microns in diameter.

Type IV inclusions were observed only in quartz samples from the Box mine, and only one inclusion was sufficiently exposed to be useful. The inclusions occur along fracture planes that did not indicate any clear crosscutting relationships, but they are proximal to, and parallel to, fractures of Type III inclusions, suggesting that they are of

a roughly similar provenance. Several potential Type IV's were seen in samples from the Athona mine, but they were not clearly visible, making confirmation impossible. Type IV inclusions are always large (25 microns +) and irregularly shaped, with obvious necking morphology. Liquid/vapour ratios are variable, commonly with no vapour phase at all. The striking feature of these inclusions is the presence of daughter halite cubes, commonly very large compared to the host inclusion. The morphological similarity of Type IV inclusions to those seen in the Au-PGE-U veins (e.g. Nicholson, U-bearing comb veins which cross-cut Au-bearing veins, and from "sponge rock" alteration zones in the granites), along with the crosscutting relationships, implies Type IV inclusions represent one of the youngest fluid events recorded by the Au-bearing veins.

A brief examination of two barren quartz veins (BX86074, AT86112) outside the mine granites showed an abundance of secondary Type II inclusions, but no obvious primary inclusions, including any with a CO_2 phase. Barren veins hosted by amphibolite, and exposed near the Athona property are very milky in appearance, and isoclinally folded in places. Although not all barren veins are folded, and unlikely to be of the same age, the presence of Type II inclusions in both auriferous and barren veins indicates that the fluids in these inclusions represent a diffuse, regional fluid event. As well, Type I inclusions represent a fluid

event restricted to the gold-bearing veins, because they do not show up as secondary inclusions in veins older than the Au-bearing veins.

4.2.2 Microthermometric Data

Low temperature (freezing) data can used to indicate the composition of the fluids in the inclusions, by observing the following phase changes:

Tm_{CO2}	melting point of CO_2 (if present)
Te or Tfm	temperature of "first melt", or the eutectic temperature
Tm_{ice} or Tlm	melting point of H_2O, or "last melt"
Tclath	melting point of clathrate (CO_2 $5.75H_2O$), if present

Freezing data for the fluid inclusions hosted in the lode-gold quartz veins are summarized in Figures 23, 24, and 25. All microthermometric data for Type I inclusions (Appendix 2) were processed using the computer programs of Nichols and Crawford (1985), with the corrections suggested by Brown and Lamb (1986).

Type I inclusions contain relatively pure CO_2, as indicated by the Tm_{CO2} which ranges from -56.6°C (the CO_2 triple point), to -57.4°C (Figure 23). The bulk of the inclusions melted at -57.0°C. Using the method of Shepard et al. (1986), the mole fraction CH_4 (or equivalent amount of another compound) dissolved in the CO_2 phase is only 0 to 0.045.

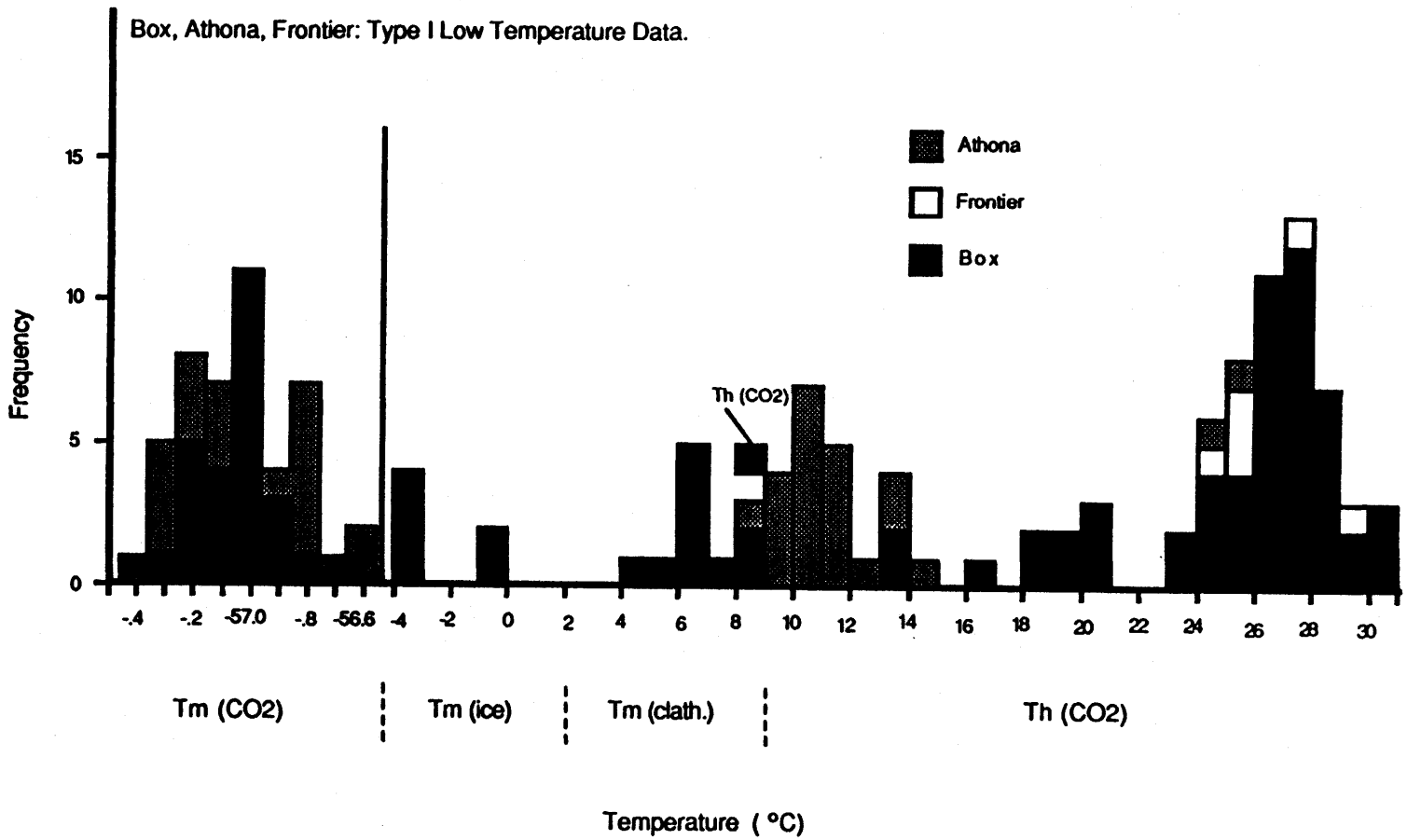

Figure 23: Histogram of combined Type I low temperature microthermetric data from the Box, Athona, and Frontier quartz veins. Tm (CO_2) - melting point of CO_2 ice, Tm (ice) - last melting of H_2O ice, Tm (clath.) - melting point of clathrate, a CO_2-H_2O compound, Th (CO_2) - homogenization temperature of CO_2 liquid and vapour to liquid.

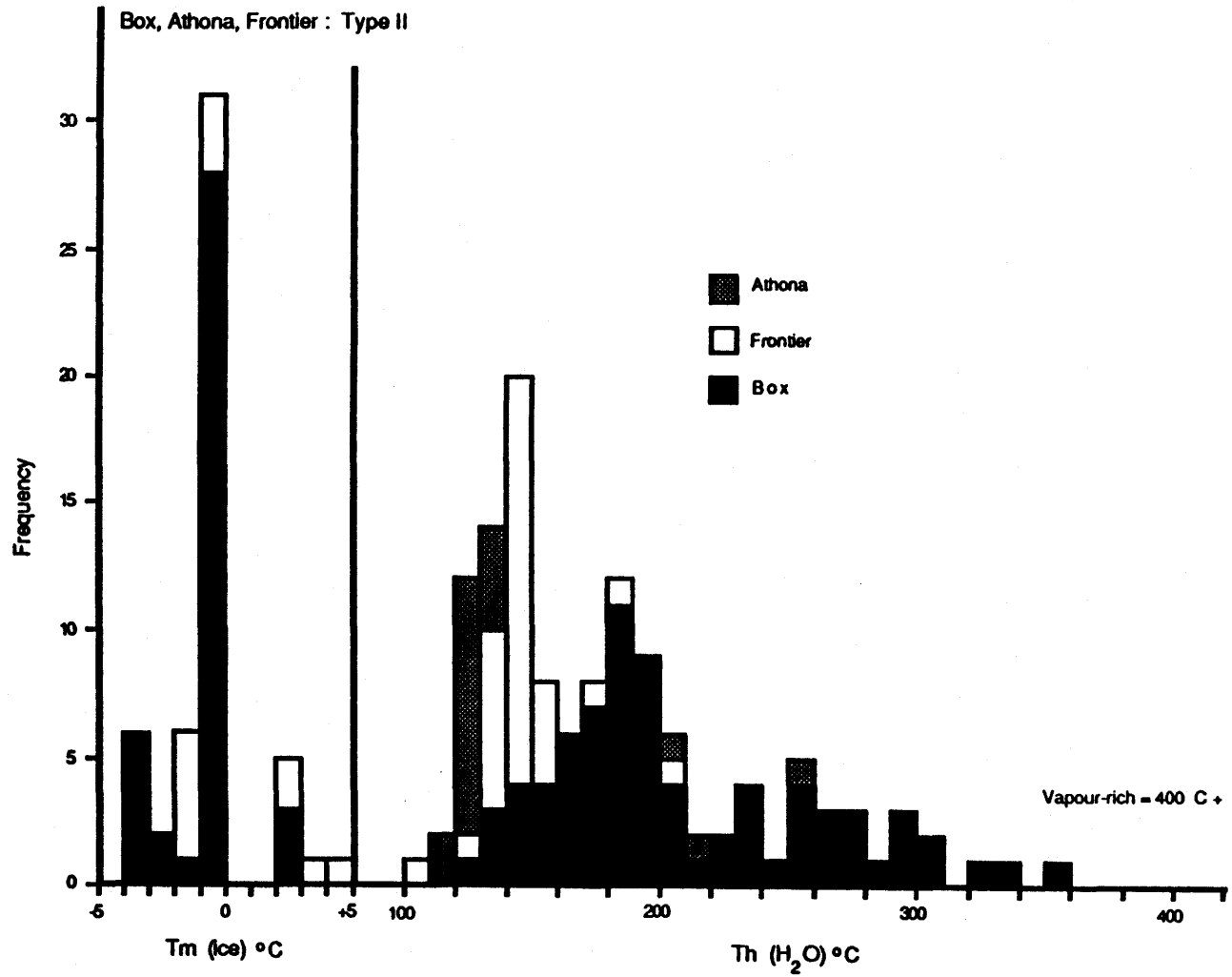

Figure 24: Histogram of homogenization temperatures and low temperature microthermetric properties of Type II inclusions from the Box, Athona, and Frontier quartz veins. Tm (ice) - last melting of H_2O ice, Th (H_2O) - homogenization temperature of liquid and vapour H_2O. Many vapour-rich inclusions homogenize at temperatures greater than 400°C, as indicated (see text).

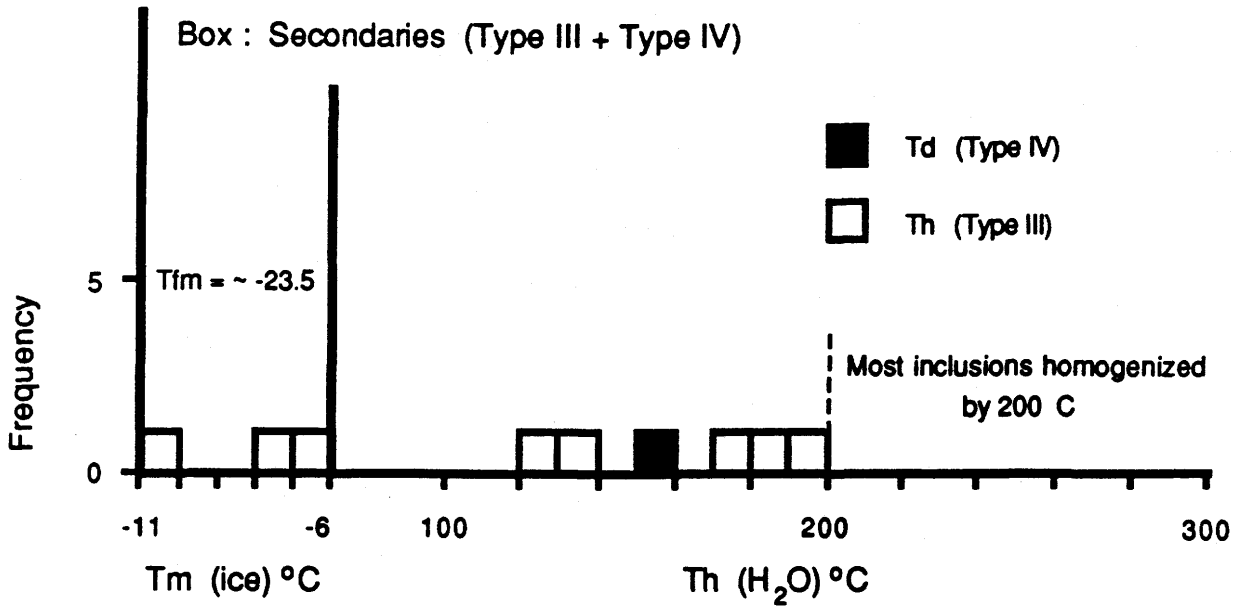

Figure 25: Histogram of Type III and IV homogenization temperatures and low temperature microthermetric data from the Box quartz veins. Tfm - first melt, or eutectic temperature, Tm (ice) - last melting of H_2O ice, Th (H_2O) - homogenization temperature of liquid and vapour H_2O (Type III only), Td - dissolution temperature of halite daughter mineral (Type IV only).

Depression of Tm_{CO2} is usually attributed to CH_4 impurities, although other components such as N_2, H_2S, and SO_2 can have a similar effect, and have been reported to be present in fluid inclusions from lode-gold veins (Roedder, 1984).

Water in Type II inclusions has a low salinity, as shown by Tm_{ice} of -4 to -0.4°C (Figure 24), corresponding to salinities of 0.5 to 6 wt. % NaCl eq. (Collins, 1979). Tm_{ice} in Type I inclusions is similar (Figure 23), but it was not used for salinity determination due to the interfering affects of the formation of CO_2-H_2O clathrates. Eutectic melting temperatures (Te) for Type I and II inclusions were not seen, so the cation and anion composition of the fluids could not be determined. A peculiar aspect of some Type II inclusions is the occasional melting, of what appears to be the ice phase, above 0°C (2.6 to 5.5°C). The most plausible explanation is the metastability of the ice phase above 0°C. Roedder (1984) cautions that upon freezing, if the vapour bubble is completely collapsed by the ice, melting causes high negative pressure, promoting metastability to as much as 6°C. The Type II inclusions in question do have small vapour bubbles, and other inclusions along the same plane behaved normally, suggesting metastability was responsible. "Cycling" the melting point was not effective in evaluating this phenomenon, as the inclusions were too small to see the melting of an individual ice crystal.

Type III inclusions have Tm_{ice} between -6.9 and -10.2°C (Figure 25), which correspond to salinities of 9.5 to 15 wt. % NaCl eq.. A Te of approximately -23.5°C roughly corresponds to the eutectic (-22.9°C) of the system H_2O - NaCl - KCl. However, accurate determination of a Te in small inclusions is extremely difficult and somewhat subjective, resulting in errors of several degrees. If the daughter mineral is a carbonate, a eutectic for the system H_2O - NaCl - Na_2CO_3 at -21.4°C, could be depressed slightly by the addition of minor Mg or Ca, and also produce the observed Te. When Type III inclusions are frozen, a brownish tint to the ice suggests the presence of Mg (Shepard et al., 1986).

Clathrate melting temperatures should be used to determine the salinity of the fluid in CO_2-bearing inclusions, as clathrates will incorporate NaCl from the H_2O phase during freezing (Collins, 1979). For Type I inclusions, salinities of 2 to 9 wt. % NaCl eq. are calculated for clathrate melting temperatures of 4.8 to 9°C (Figure 23), with an average of 5.8 wt. % NaCl eq. (7.0°C).

Minimum temperatures at which the fluids were trapped, the density of CO_2, and in some cases salinity, can be obtained by measurement of the following temperatures:

Th_{CO2}	homogenization of the CO_2 phases
Th	homogenization of liquid and vapour, or H_2O and CO_2 phases

Td dissolution temperature of daughter phases

Type I inclusions have Th_{CO2} temperatures from approximately 8 to 30°C (Figure 23), and always homogenized into the liquid phase. The CO_2 densities calculated from Th_{CO2} range from 0.6 to 0.9 g/cm^3. The average Th_{CO2}, and thus the average CO_2 densities of Type I inclusions from the Athona veins are somewhat higher than the Type I inclusions in the Box or Frontier veins (Figure 23). This may be a function of the structural styles in which the veins were emplaced. Tensional veins will result in an increase in the local volume of the system. This would promote a decrease and a variability of fluid density, as is observed in the higher and more variable Th_{CO2} for the Box vein samples, and similarly for the Frontier vein samples (Figure 23). The Athona veins are hosted in more ductile fractures, resulting in less of a local volume or pressure change, keeping fluid density more constant. Bulk fluid densities will not show this feature as readily, due to the added variablity of differing phase proportions. However, because the depth at which the veins were emplaced was probably similar for all three deposits, and thus similar confining pressures, the variable CO_2 densities may also reflect differences in the original composition of the fluids.

Homogenization temperatures (Th) of Type II and III inclusions can vary considerably, which is largely a result of necking during, or after, inclusion formation. Type II

inclusions have variable Th from 100 to 360°C (Figure 24), with some vapour-rich inclusions not yet homogenized at 400°C (when overall decepitation starts to occur). It appears that the more vapour-rich the inclusion, the higher its Th will be, consistent with the volume-temperature relationship that would be expected for necked inclusions. Type III inclusions homogenize between 120 and 200°C (Figure 25), reflecting a more restricted range of liquid/vapour ratios during the necking of the inclusions. Most inclusions homogenized in the upper portion of the Th range. No liquid-vapour homogenization temperatures were determined from Type IV inclusions, as necking was very obvious, and the vapour phase was commonly absent. Comparison to inclusions from the Au-PGE-U deposits (see section 5.2.2) would suggest that the bulk of the homogenization temperatures of Type IV inclusions should be in the range of 100 to 200°C.

Type I inclusions, although displaying some necking morphology, have a restricted range of Th, from 200 to 360°C (Figure 26), with the bulk of the homogenization temperatures between 270 and 300°C. These are comparable to the homogenization temperatures of "primary" CO_2-H_2O inclusions reported from other lode-gold deposits, both Archean and Proterozoic in age (see section 4.2.3). Type I inclusions homogenized into the dominant phase of the inclusion; in the bimodal population, CO_2-rich inclusions homogenized into the

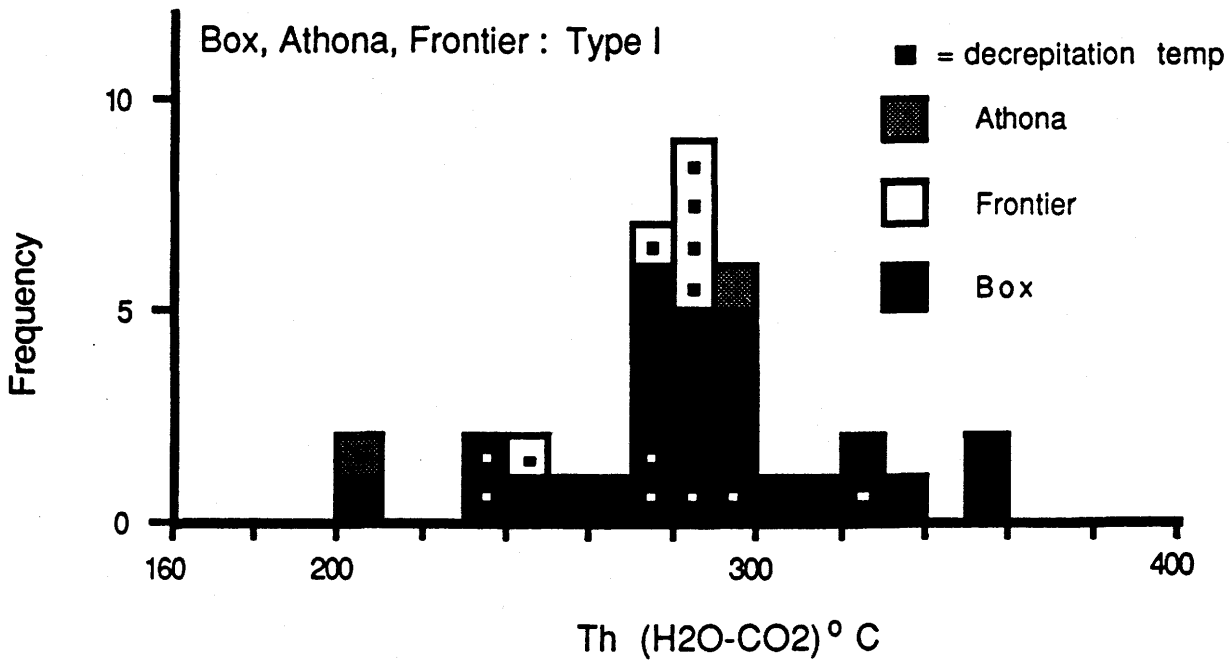

Figure 26: Histogram of homogenization temperatures (Th) of Type I inclusions from the Box, Athona, and Frontier quartz veins. Th (H_2O-CO_2) - homogenization temperature of the H_2O and CO_2 phases. Square dot indicates decrepitation temperature, which approximates homogenization temperature (see text).

CO_2 phase, and H_2O-rich into the H_2O phase. Several of the inclusions displayed critical homogenization, which indicates that the homogenization temperature is very close to the trapping temperature of the fluid, as the fluids must have been trapped near the critical point on the CO_2-H_2O solvus (Roedder, 1984). Some of the data are actually decrepitation temperatures, but for Type I inclusions, decrepitation and homogenization occured over the same temperature interval. Homogenization temperatures could not be determined for Type Ia inclusions, as the H_2O was not visible as a separate phase. Inclusions of this type may have up to 15 or 20 volume % water, which is not visible as it is spread over the walls of the inclusion as a thin film (Brown & Lamb, 1986; Roedder, 1984). As explained in the preceding section, some Type I inclusions are thought to be equivalent to Type Ia inclusions, as they contained 15 volume % H_2O, or less, but fortuituously concentrated in one corner of the inclusion. The resultant visiblity of the phase boundary allows the homogenization to be observed, and suggests that Type Ia inclusions would have similar homogenization temperatures, if they could be observed.

The salinity of a Type IV inclusion was determined by the dissolution of a halite daughter, at 152°C (Figure 25), corresponding to a salinity of 30 wt. % NaCl eq., using the appropriate graph from Shepard et al. (1986). The carbonate or iron chloride daughter minerals in Type III inclusions

appear to have slightly dissolved (rounding of rhomb) after heating to 350 or 400°C for a few minutes. Continued heating was not possible due to decrepitation.

4.2.3 Discussion of Fluid Inclusion Data

Four types of fluid inclusions, representing four different fluids, have been identified in quartz vein samples from the Box, Athona, and Frontier properties (Figure 21). As mentioned, Type I inclusions are the only possible candidates for primary inclusions. Whether or not the quartz that hosts them represents recrystallized and reformed patches of the main stage of vein emplacement, or less deformed late-stage quartz is not clear, as no discriminating petrographic evidence was found. If they are not truly primary, the petrographic evidence implies that they are at least associated with the later stages of veining, as pseudosecondary inclusions, which are essentially equivalent to primary inclusions, or can be thought of as very early "secondary" inclusions. In this case, as the gold mineralization also appears to be late, the Type I CO_2-H_2O fluid may have been responsible for the later stages of vein development, including gold mineralization. There is a striking similarity of Type I inclusions to those reported as primary, or associated with Au mineralization, from Archean mesothermal lode-gold deposits. Recent publications with summaries of fluid inclusion data (e.g. Ho, 1987; Ho et al. 1990; Robert & Kelly, 1987; or Guha et al., 1991), propose

that similar CO_2-H_2O fluids were involved in Archean lode gold deposits from Canada, Australia, India and South Africa. The lode gold deposits of the Goldfields Peninsula, although of Proterozoic age, appear to be associated with a very similar type of fluid. Recent investigations of Proterozoic lode gold deposits in the La Ronge Domain of northern Saskatchewan (Armstrong, 1990; Ibrahim & Kyser, 1991; Hrdy et al., 1991; Fayek et al., 1991) suggest that a similar CO_2-H_2O fluid is associated with these vein systems.

Additional interpretation of the microthermometric data from Type I inclusions can be used to characterize the nature of the H_2O-CO_2 fluid during veining and mineralization, and to relate Type I fluid inclusions from the Goldfields deposits to the fluid inclusions reported from other mesothermal lode-Au deposits. Figure 27 shows the relationship between Th and mole fraction CO_2 (mole fraction CO_2 calculated using the programs of Nichols & Crawford, 1985; see Appendix 2) in Type I inclusions. The H_2O-CO_2 solvus is shown for a pressure of 2.0 kb and 6 wt. % NaCl eq. salinity (Bowers & Helgeson, 1983) in the system H_2O-CO_2-NaCl. A pressure of 2 kb was chosen to represent the commonly estimated range at which mesothermal lode-gold deposits form, between 1 and 3 kb (e.g. Brown & Lamb, 1989). The immiscibility field at 1 kb would be slightly larger, and at 3 kb would be slightly smaller than the field shown at 2 kb (Bowers & Helgeson, 1983). The salinity of the system can have a large effect on the position

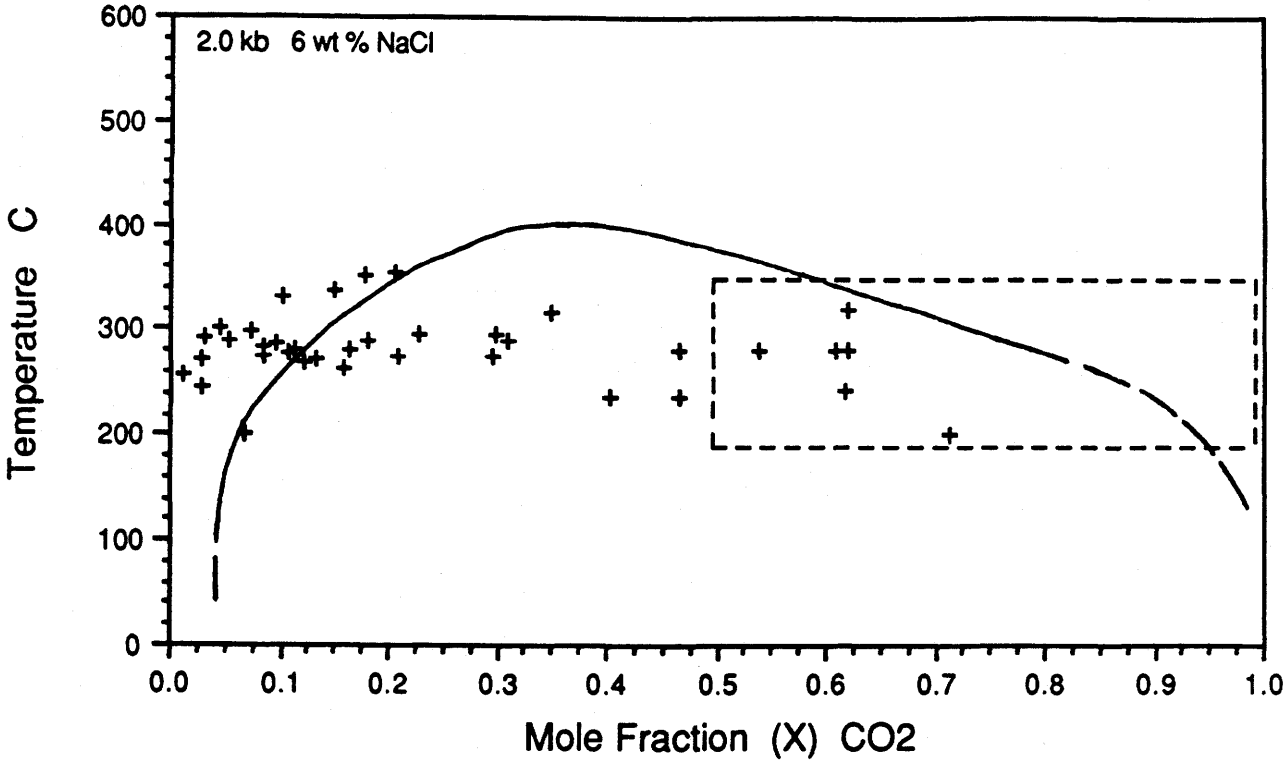

Figure 27: Relation between CO_2-H_2O homogenization temperatures and mole fraction (X) CO_2 of Type I inclusions. CO_2-H_2O solvus from Bowers & Helgeson (1983), for 2.0 kilobars and 6 wt. % NaCl (see text). Dashed box indicates probable relations for that Type Ia inclusions, assuming characteristics similar to six Type I inclusions with high CO_2-H_2O ratios (see text). Mole fraction of CO_2 calculated using computer programs of Nichols & Crawford (1985), with the corrections suggested by Lamb & Brown (1986). See text for further discussion.

of the solvus, but 6 wt. % NaCl eq. closely approximates the average salinity calculated for Type I inclusions. Type Ia inclusions would plot in the dashed box (calculated using "theoretical" Type Ia inclusions, see Appendix 2), assuming similar homogenization temperatures, and assuming mole fraction CO_2 (X_{CO2}) from 0.8 to 1.0. To support the assumption that Type I and Type Ia inclusions have similar Th and X_{CO2}, the highest X_{CO2} values calculated from Type I inclusions contained 85 to 90 volume % CO_2 (equivalent to the assumed CO_2 content of Type Ia inclusions), which plots just under the solvus, within the Type Ia box. Microthermometric data (except Th CO_2-H_2O) was acquired from thirty nine Type Ia inclusions, which would substantially increase the data population near the CO_2-rich end of the solvus, if they could be plotted.

The relationship between Th and X_{CO2} may be explained in several ways. The grouping of data around X_{CO2} of 0.15 and 0.7 suggests H_2O-CO_2 immiscibility may have occurred prior to fluid trapping (Roedder, 1984), from a homogeneous fluid with a bulk X_{CO2} of approximately 0.4. Limited necking may have partially masked a clear separation of the two populations, by creating inclusions with "non-immiscible" CO_2/H_2O ratios. Immiscibility of this type is rarely observed with certainty, and difficult to prove if necking has occurred (Roedder, 1984). Alternately, Ho (1987) suggests that a limited phase

separation may occur, in which immiscibility takes place sporadically and chaotically during vein formation and fluid trapping. This results in widely variable CO_2/H_2O ratios, which would be further compounded by necking. In contrast, trapping of an homogeneous fluid would normally yield inclusions with constant CO_2/H_2O ratios, variably modified by necking, but certainly not able to approximate a bimodal population.

If pre-entrapment immiscibility did not occur, then to produce inclusions similar to Types I and Ia in the Goldfields samples, necking would have to have occurred during or after post-entrapment immiscibility. This should have produced some monophase, H_2O-rich inclusions, which were not observed in direct association with Type I inclusions. Enlarged sketches of two Type I inclusions (Figure 28) show inclusion morphologies that indicate some degree of necking. This morphology could be created by slight "shrinkage" of the inclusion after entrapment of a heterogeneous fluid, or by the necking entrapment of an already separated CO_2 phase within a larger inclusion. Neither can be proven using individual inclusions, but the absence of any monophase, H_2O-rich inclusions within the Type I groups suggests that necking was not the only factor involved in producing variable CO_2/H_2O ratios, so that the variable ratios were created by a process other than necking. As the data dominantly conform to a bimodal population, perhaps modified by limited necking, some

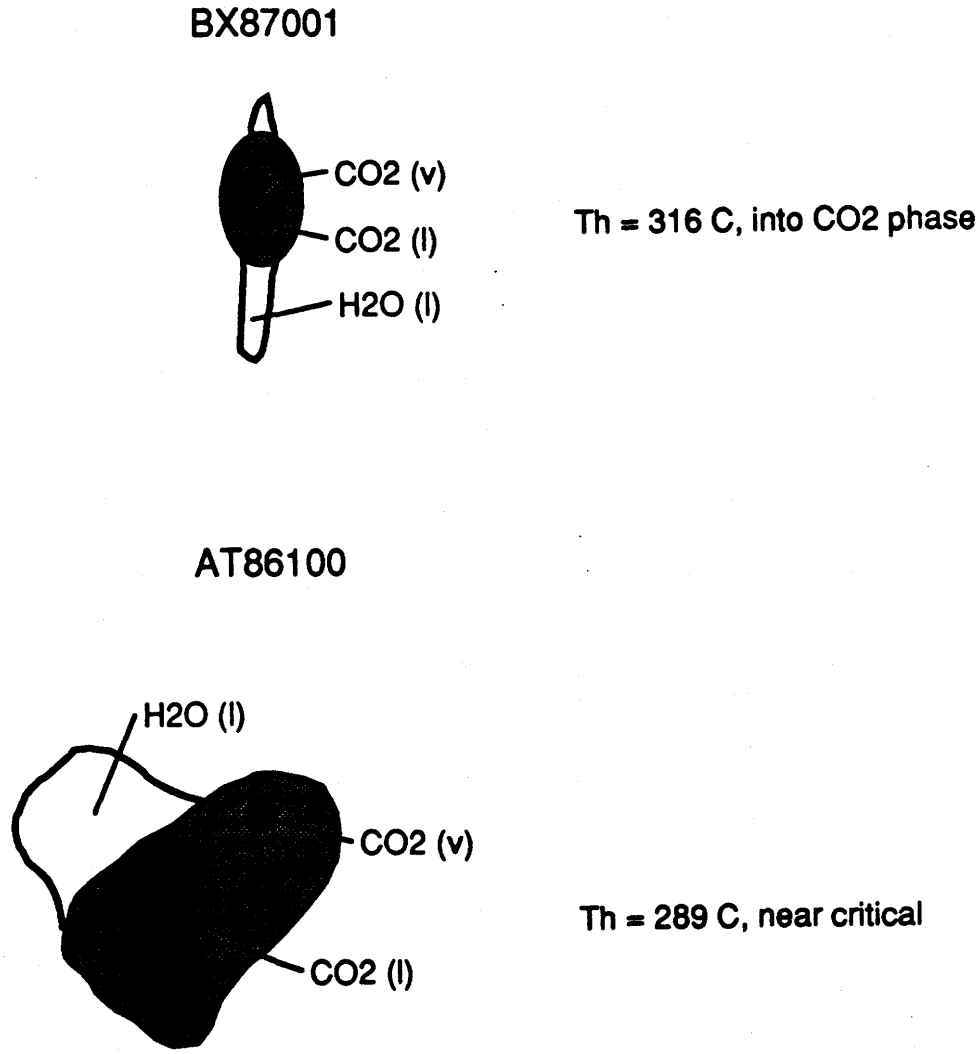

Figure 28: Two examples of morphology of Type I inclusions from the Box (BX87001) and Athona (AT86100) quartz veins, indicating that immiscibility had occured before the inclusion was fully formed. See text for further discussion.

form of pre-entrapment immiscibility must have occurred. Critical homogenization of several Type I inclusions further emphasizes the trapping of a heterogeneous fluid at the CO_2-H_2O solvus.

Fluid immisciblity is an attractive model to explain the roughly bimodal population of Type I and Ia inclusions, and it provides a means of relating the fluid inclusions with the mechanisms of veining and mineral precipitation. Fluid inclusion studies of lode-gold vein systems with a large vertical extent (of as much as a kilometer) detect no differences in the characteristics of the fluid from lower levels to higher levels (e.g. Ho, 1987). This suggests that ambient pressure and temperature gradients have minor effects on vein emplacement, but that a radical volume increase in a dilational (brittle or brittle-ductile) vein system produces a localized pressure drop, triggering immiscibility. However, whether this occurs on a large scale simultaneously, or on a limited scale as proposed by Ho (1987), is not known. Destabilization of ligands by CO_2 effervesence, where H_2S is partitioned into the CO_2 phase, may be the cause of gangue mineral and gold precipitation, a mechanism which has been proposed or alluded to several times in recent literature (e.g. Bowers, 1991; Seward, 1989; Spycher & Reed, 1989; Spooner et al., 1987; Drummond & Ohmoto, 1985). As well, the variable salinities observed in Type I inclusions may reflect inhomogeneous partitioning of solutes during CO_2 release

(Bowers & Helgeson, 1983), recorded by concurrent fluid trapping in proximal inclusions. Guha et al. (1991), using samples from the Sigma mine, and several other lode-gold deposits in the area, have reported a positive correlation between the degree of immiscibility in CO_2-H_2O inclusions, and the gold content of the deposit. At the Sigma mine, which is a felsic intrusive hosted lode-gold stockwork, grossly similar to the Goldfields deposits, the CO_2-H_2O inclusions form a distinctly bimodal immiscibility set, and are primary with respect to late-stage brittle fracturing of the veins that is directly related to gold deposition. In comparison to the Goldfields lode-gold veins, this is remarkably similar to the suspected association of an immiscibility assemblage of Type I inclusions with late-stage gold mineralization.

Determination of the absolute pressure at which inclusions were formed is somewhat problematic. However, minimum pressures, corresponding to the point of fluid unmixing, can be approximated by using the internal fluid properties of inclusions that do not show signs of a necking morphology. This is shown graphically in Figure 29, which is a plot of pressure versus mole fraction CO_2, constructed for 6 wt. % NaCl, and can be used without estimating the volume percent CO_2 in the inclusion (Brown & Lamb, 1989). Minimum pressure, or the pressure at homogenization, is indicated to be approximately 2.5 to 3 kilobars for Type I inclusions that do not show any signs of necking. If the bimodal Type I

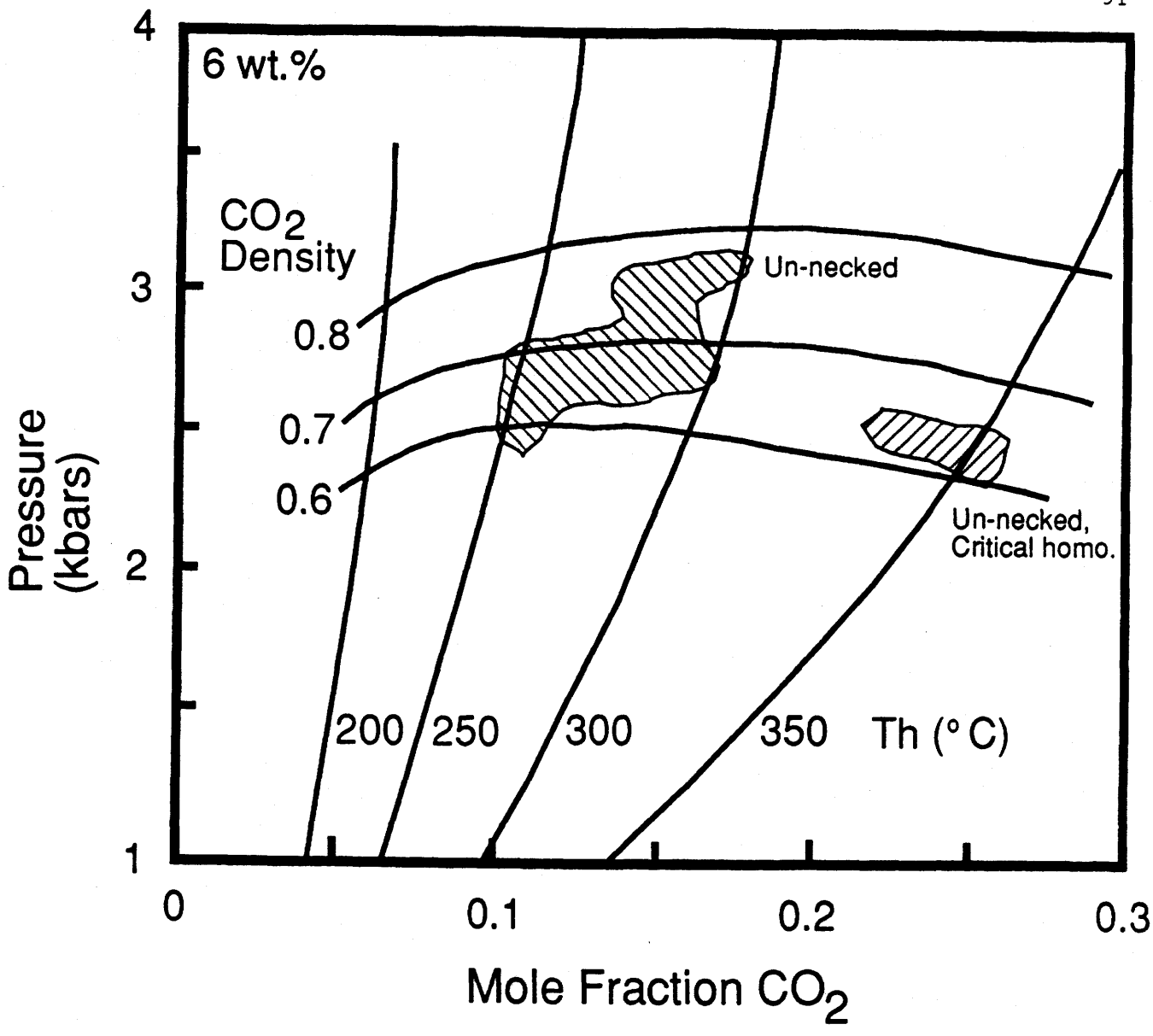

Figure 29: Minimum pressure estimates, based on CO_2 densities (horizontal curves) and CO_2-H_2O homogenization temperatures (vertical curves) of the fluid (Lamb & Brown, 1989), for Type I inclusions. Only data for inclusions with no signs of necking are used (Appendix 2). For these inclusions, some of which had critical homogenizations (see text), the minimum pressures are indicated to be approximately 2.3 to 3.0 kbars. See text for further discussion.

inclusion populations are the result of fluid immiscibility, then the homogenization temperature and minimum pressure are the actual trapping conditions. If the inclusions represent the trapping of a homogeneous fluid, then the homogenization temperature and pressure are minimums. Additionally, several Type I inclusions exhibited critical homogenization, which indicates they were trapped near the critical point on the CO_2-H_2O solvus. For these inclusions, the homogenization temperature and pressure are the trapping conditions, suggesting that Type I inclusions trapped a heterogeneous fluid that represents an immiscibility assemblage. Therefore the minimum pressure range of 2.5 to 3 kb, indicated on Figure 29, is the approximate trapping pressure, and the Th is the temperature at which the fluid was trapped.

Summary

Type I inclusions (Figure 30) represent a moderate temperature (approximately 300°C), high density, CO_2-bearing, low salinity hydrothermal fluid, which is suspected to be the fluid associated with the later stages of veining and gold mineralization of the Goldfields lode-gold deposits, although no direct association was found between Type I inclusions and gold mineralization. Immiscible separation of CO_2 is indicated by the bimodal population of CO_2-rich and H_2O-rich inclusions. Minimum pressures are indicated to be approximately 2.5 to 3 kilobars.

Type II, III, and IV inclusions are interpreted to

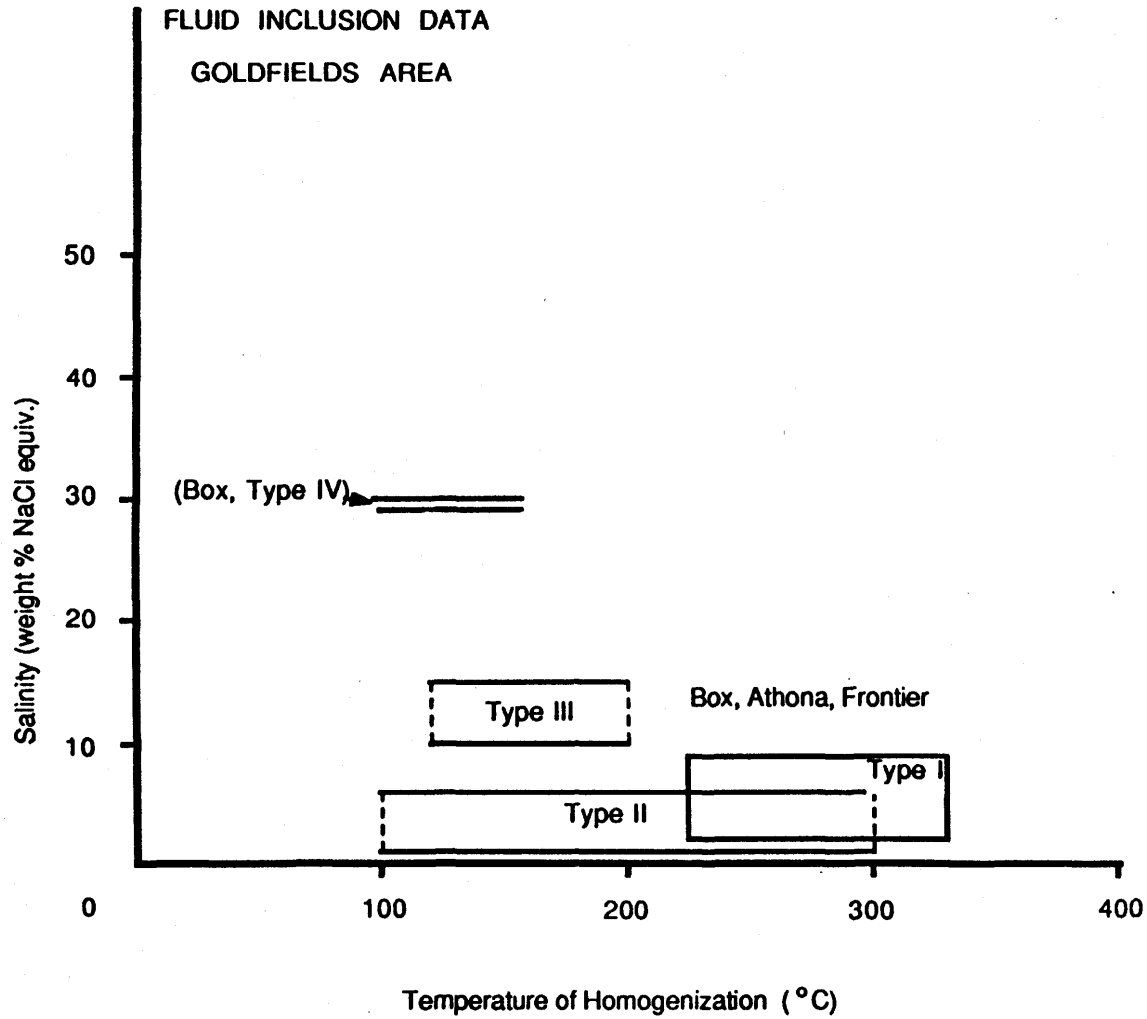

Figure 30: Summary of fluid inclusion data from the lode-gold veins, showing relation between homogenization temperatures and salinities of the various types of inclusions.

represent later fluid events of uncertain origin (Figure 30). Type II inclusions contain fluid of low salinity (1 to 5 wt. % NaCl eq.), but minimum temperatures are generally obscured by considerable necking. A resonable estimate for the homogenization temperatures, based on stable isotope and fluid inclusion data from the Au-PGE-U deposits (see chapter 5.0), would be approximately 100 to 300°C. The homogenization temperatures of Type II inclusions from the Frontier property are better defined, from 100 to 200°C. Type II inclusions post-date deformation of the lode-gold veins, and are present as secondary inclusions in all the barren veins examined. Therefore, they are unlikely to be related to the mineralizing event. Almost identical late fluid inclusions are reported in a fluid inclusion study of lode-gold deposits in the Yellowknife area (English, 1981), and Smith et al. (1984) report similar secondary inclusions from the McIntyre-Hollinger deposit in Ontario. Ho (1987) also reports similar inclusions, from virtually all lode-gold deposits studied in Australia. This suggests that Type II inclusions represent a fluid that is an intrinsic, but unknown, part of the thermotectonic evolution of supracrustal terranes that host lode-gold deposits.

Type III inclusions have moderate salinities (10 to 15 wt. % NaCl eq.), and homogenization temperatures of 120 to 200°C. The presence of a carbonate or iron chloride daughter mineral implies the fluid is oxidized. Kotzer & Kyser (1991)

report inclusions of similar salinity and temperature in early quartz overgrowths from the Athabasca basin, which are interpreted to represent early diagenetic basinal waters. Type III inclusions may also represent this fluid. If so, the age of this fluid event is ca. 1700 to 1500 Ma. (Kotzer et al., 1992a), which marks the onset of diagenesis in the Athabasca basin.

Type IV inclusions have high salinities (30 wt. % NaCl eq.), and are highly necked. Type IV inclusions are similar to those observed as primary fluid inclusions in euhedral quartz from the Athabasca basin (Kotzer & Kyser, 1991), as well as from euhedral quartz and carbonate in the Au-PGE-U veins, and the "sponge rock" alteration zones within the mine granites (see chapter 5.0). This implies similar types of basinal brine-like fluids were involved in all of the above. For the inclusions from the Athabasca basin, the fluid is thought to correspond to peak diagenesis at ca. 1450 Ma (Kotzer et al., 1992a; Kotzer & Kyser, 1991).

4.3 Stable Isotopes

4.3.1 Isotopic Compositions and Isotopic Geothermometry

The stable isotopic compositions of vein minerals were analysed to try and constrain their formation temperature, and to trace the origins of the fluid from which they precipitated (all compositions and temperatures are listed in Appendix 3). Much later secondary fluids have also interacted with the veins, represented by Type II, III, and IV inclusions. The fluids represented by Type II inclusions may have had the most secondary influence, based on the great abundance of these inclusions in the veins. Generally, the oxygen isotopic compositions of most minerals are unaffected by later events, unless the mineral has been completely or partially recrystallized, whereas minerals are much less resistant to hydrogen isotopic exchange.

Temperatures derived from stable isotope equilibrium fractionations are only approximations, as errors in the order of ± 50°C are not uncommon. This is due, in part, to the imprecise calibration of some mineral fractionations, and to the extreme temperature sensitivity of some minerals, such as quartz, where a 2 per mil variation in its oxygen isotopic composition is equivalent to an approximate 100°C change in temperature (Clayton et al., 1972).

Vein Quartz

Figure 31 compares the $\delta^{18}O$ values of vein quartz from all three lode-gold deposits, showing a variation of several per

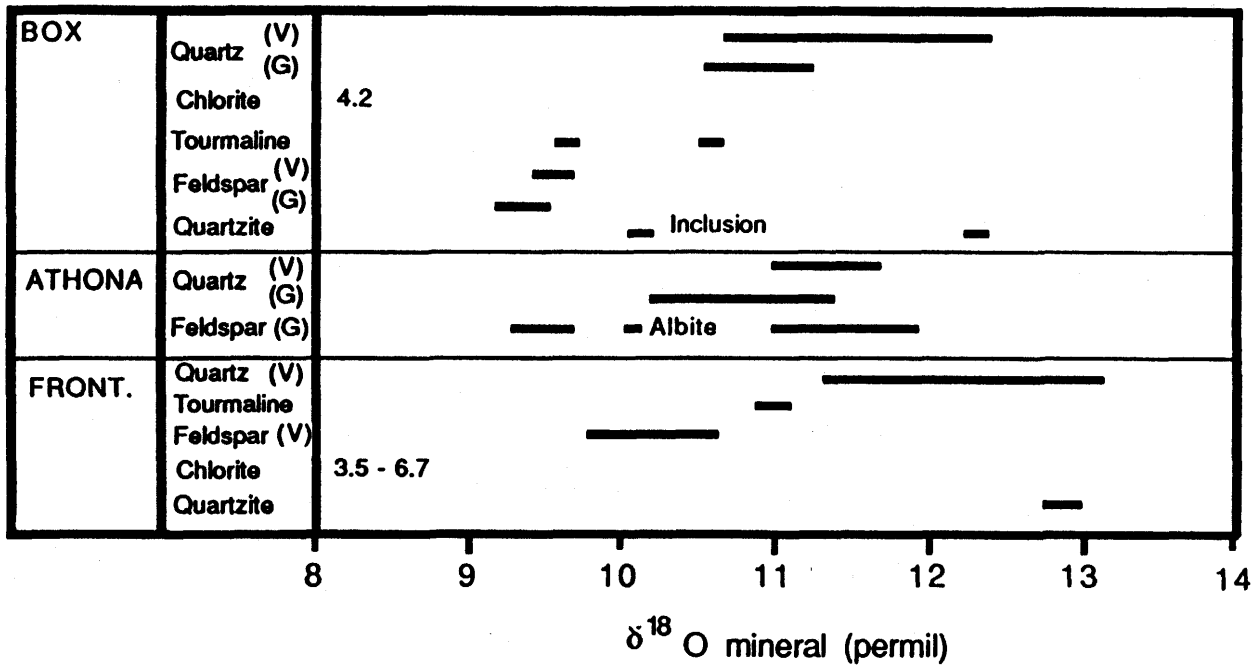

Figure 31: Summary of $\delta^{18}O$ values of minerals from lode-veins and Mine granites. "V" or "G" in brackets following mineral indicate mineral is from vein or granite. $\delta^{18}O$ values for quartzites are whole-rock samples. Data from Appendix 3.

mil, from 10.7 to 12.9. Individually, quartz from a vein system varies by less than 2 per mil, although the range for the Athona veins is based on only two analyses. Four replicate analyses of quartz from sample AT86100 show a variation of 0.6 per mil, slightly greater than the ± 0.2 per mil error, suggesting the presence of small scale isotopic variability within the quartz veins. Variations in the $\delta^{18}O$ composition of lode-gold quartz veins has been documented by Kerrich (1987), and may be related to small variations of fluid temperature and isotopic composition. The immiscible separation of CO_2 during vein formation may also have had a limited effect on the isotopic compositions (e.g. Bowers, 1991). Kerrich (1987) proposes that large temperature variations are unlikely, due to the depths (1 to 3kb) at which mesothermal lode-gold deposits are estimated to form. The $\delta^{18}O$ composition of Goldfields vein quartz may also have been slightly altered by the addition of minor quantities of quartz during secondary fracturing and healing of the veins.

$\delta^{18}O$ values for vein quartz from the Slave, Churchill, and Superior Provinces (Kerrich, 1987) range from approximately 9 to 19 per mil, clustering around 12 to 14 per mil. Within this range, $\delta^{18}O$ values of quartz veins vary systematically between districts within the same Province, and between mines within the same district. These distinct isotopic compositions imply that heterogenous fluid sources exist, each supplying unique mineralizing fluids, on a deposit or camp

scale. However, the overall uniformity of $\delta^{18}O$ values indicates that these deposits share similar genetic processes and physio-chemical conditions (Kerrich, 1987). The Goldfields deposits are consistant with this trend. The overlap of $\delta^{18}O$ values of the Goldfields quartz veins (Figure 31) implies a similar genetic history and fluid source, but an overall increase in $\delta^{18}O$ values of quartz from the Athona mine to the Frontier property suggests similar but unique fluids for vein systems only a few kilometers apart. It is not clear what controls this minor variation, but it is likely not coincidental that the overall increase in quartz isotopic compositions corresponds to the relative position of the deposit away from the center of the Goldfields Synclinorium (Figure 7).

Granitic Quartz

The $\delta^{18}O$ values of quartz from the host granites (Figure 31) are similar to those of the veins, but are somewhat lower. Similarity between the $\delta^{18}O$ values of vein quartz and quartz from the host granite would be expected for systems with low water/rock ratios (i.e. wall rock buffering of the fluid), but the distinctly lower $\delta^{18}O$ values of the granitic quartz implies that the quartz in the granites did not entirely control the isotopic composition of the fluids in the vein systems. Additionally, $\delta^{18}O$ values of whole rock samples of the surrounding quartzites range from 10.1 to 13.0 (Figure 31), encompassing the isotopic compositional ranges of quartz for

both veins and granite, further implying that the Murmac Bay Group sedimentary package may have been the source for the granites, and later, acted as a buffer on the auriferous vein fluids. Although whole-rock $\delta^{18}O$ values for the granites were not measured, their leucocratic nature means that a whole rock signature will be dominated by the $\delta^{18}O$ values of quartz and feldspar. Therefore whole-rock $\delta^{18}O$ values for the granites would fall between approximately 9.5 and 11.5 per mil, similar to the values measured in granites that have sedimentary ("S-type") sources (Faure, 1986).

Chlorite

Gangue chlorite from the veins was analysed by XRD and found to be part of the di/tri Fe-Mg chlorite series, closest to clinochlore in composition. Petrographic examination of vein chlorite from the Box and Frontier properties shows chlorite to occur in two configurations: (1) as "selvage-type" chlorite, which occurs as plates, books, and irregular masses proximal to vein selvages, or fine-grained chlorite coating tension fractures (Group II, sets 4 and 5 of Roberts, 1990); (2) as fine grained rims around early sulphide grains, and in fractures cutting early pyrite cubes. The latter type of chlorite appears to be later than the selvage-type (Figure 21), associated with late brittle micro-fractures, but did not occur in enough quantity to be analysed. For all of the chlorite types, virtually without exception, up to 10% muscovite is associated with the chlorite. In a few

instances, selvage-type chlorite appeared to be forming by the conversion of biotite. The biotite is probably rafted from the vein wall during fluid incursion. All chlorite samples analysed for their oxygen isotopic compositions are selvage-type chlorite.

$\delta^{18}O$ values for chlorites ranged from 3.5 to 6.7 per mil (Figure 31). Two samples (FR87025, UC86-83), with the highest $\delta^{18}O$ values, yield apparent isotope equilibration temperatures with coexisting quartz of 450°C (Wenner & Taylor, 1971). Two other chlorite samples, BX87006 and FR86004, yield apparent isotope equilibration temperatures with coexisting quartz of 390 and 290°C respectively. The difference between isotopic equilibration temperatures of 390°C and 450°C is insignificant when the uncertainty of ± 50°C in the quartz-chlorite fractionation is considered. Biotite rafted from the granites, which may have been altered to form vein chlorite, would likely have had a $\delta^{18}O$ value near 6 per mil, assuming it was formed in equilibrium with quartz in the granites at approximately 600°C (Bottinga & Javoy, 1975). Chlorite forming from the conversion of biotite, may have inclusions of the biotite, so that the samples analyzed are not homogeneous. Therefore some of the "chlorite" will not be in complete oxygen isotopic equilibrium with the vein quartz, as in the most ^{18}O-rich samples, FR87025 and UC86-83. Due to this "biotite effect", the lower isotopic equilibration temperatures of 290 and 390°C are most likely to be indicative

of actual fluid temperatures during the vein forming event, as well as correlating to the trapping temperatures of Type I fluid inclusions.

The hydrogen isotopic composition of the chlorites range from -64 to -81 (Appendix 3). Chlorite from samples FR87025 and UC86-83, which yield apparent equilibration temperatures of 450°C, have δD values of -64 and -76 per mil respectively. In comparison, the δD value of chlorite from sample BX87006, which has an apparent isotope equilibrium temperature at 390°C, is -73 per mil, and for sample FR86004, which yielded the lowest apparent equilibration temperature with vein quartz, the δD value is -81. The range in δD values is relatively small and, because hydrogen isotopic equilibrium between minerals and water is achieved much faster than oxygen, the δD values of the chlorite probably reflect the δD values of the vein fluids.

Tourmaline

Tourmaline occurs within the veins as groups of fine-grained prismatic crystals, usually clustered near and on vein selvages, but also occur out in the center of the vein, probably "rafted" from the selvage area. Petrographic relations show that tourmaline is not reacting with vein quartz, although tourmaline bundles are locally altered to muscovite with minor chlorite in the area of late brittle micro-fractures (Plate 3). Microprobe analysis of the chemical composition of the tourmalines indicate that they

Plate 3: a - photomicrograph of muscovite-altered (M) tourmaline crystals (T), hosted in vein quartz (Q), from a lode-gold vein in the Frontier Mine granite (FR87025F). Photograph was taken in cross-polarized light, and the bottom edge of the photograph is approximately 5mm long; **b** - a similar photomicrograph of altered vein tourmaline (T) from Box Mine lode-gold veins, showing Mine granite at the bottom right, and vein quartz (Q) at the upper left. Large mass of muscovite (M) in center of photograph has completely replaced tourmaline. Note additional muscovite (M) in small fracture in vein quartz at upper left (TKK87003). Photograph taken in cross-polarized light, and the bottom edge is approximately 5mm long.

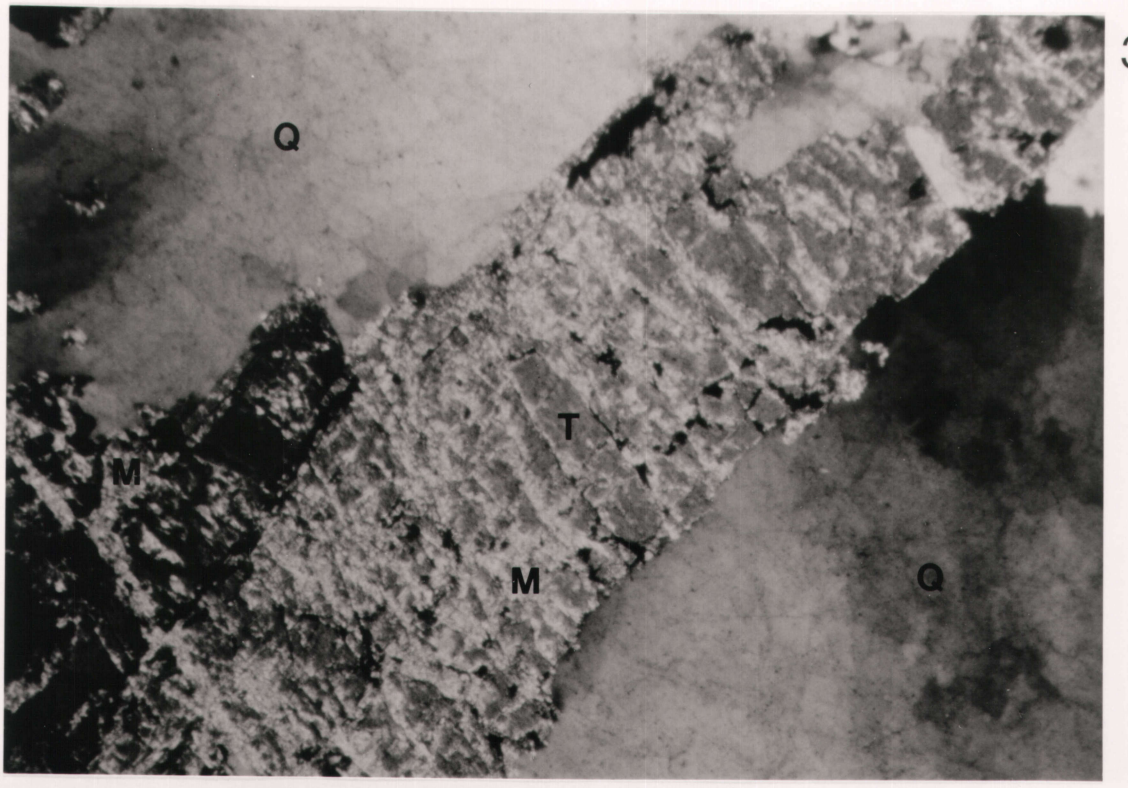

3a

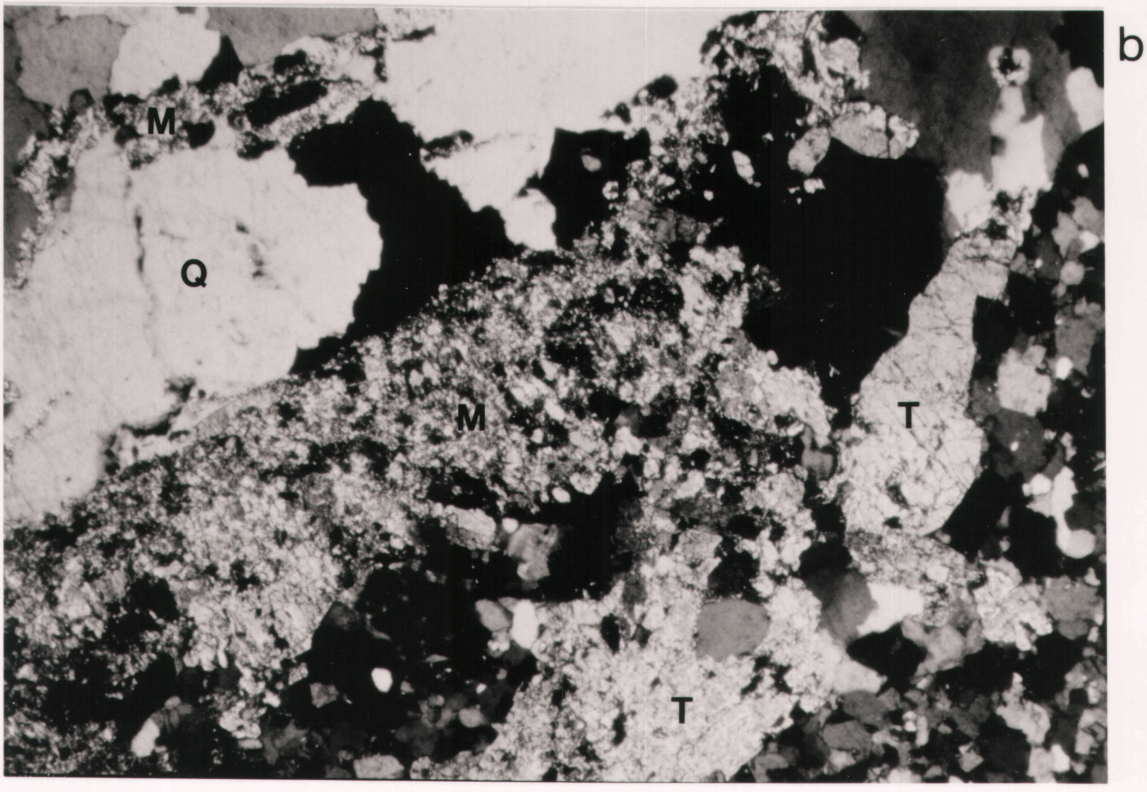

b

have an intermediate composition in the dravite-schorl series (Figure 32). Evidence of compositional zoning in the tourmalines is absent, except for a few narrow, iron-enriched bands, detected during microprobe analysis. The chemical composition of tourmaline from the Box and Frontier quartz veins are similar to those of tourmalines from Archean lode-gold deposits in the Superior Province.

$\delta^{18}O$ values of tourmaline from the Box and Frontier quartz veins vary from 9.6 to 11.0 per mil (TKK87003, TKK87004 and FR87025F), resulting in quartz-tourmaline fractionations of approximately 1.3 to 1.8 with coexisting quartz (Appendix 3). Using a modified quartz-muscovite fractionation (Eslinger et al., 1979) to approximate quartz-tourmaline, the isotope equilibrium temperatures for these fractionations vary from 569 to 775°C (Appendix 3). The modification is based on work at the University of Saskatchewan, from natural systems, which suggest that tourmaline fractionations for both oxygen and hydrogen are almost identical to those of muscovite (Kotzer et al., 1992b). All three of the quartz-tourmaline fractionations indicate geologically unreasonable temperatures of vein emplacement, especially given the fluid inclusion trapping temperatures of less than 400°C, which implies that the tourmalines are not in isotopic equilibrium with the vein quartz. The δD values of two of the tourmaline samples, FR87025F and TKK87003, are -39 and -49 per mil, respectively. As the tourmaline has been extensively altered by later

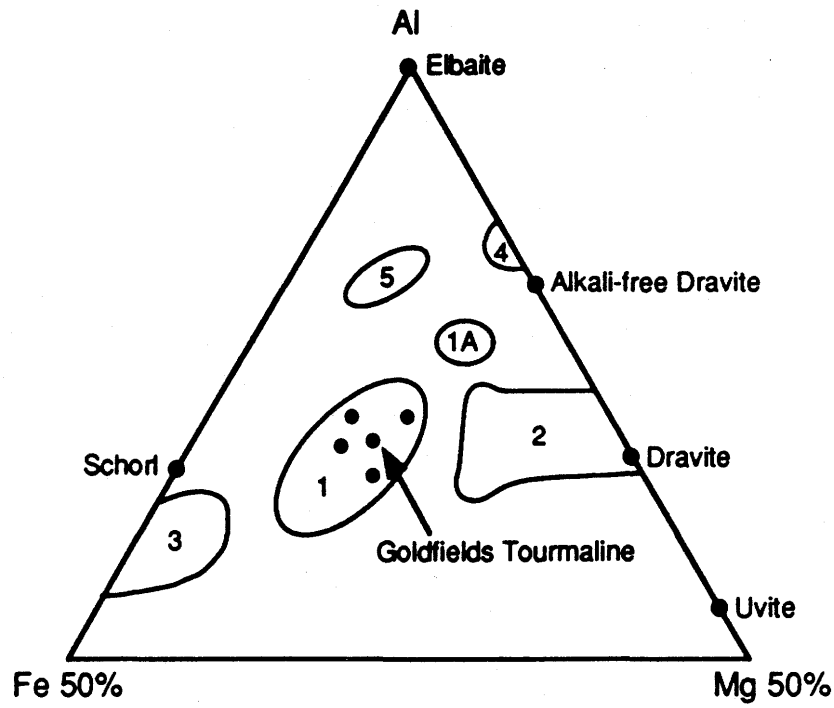

1 - Superior Province, Archean Lode Gold Deposits
1A - Chrome Dravites
2 - Base Metal Deposits
3 - Granitic Environment
4 - MacArthur River Uranium Deposit
5 - Cu, Mo Porphyries

Figure 32: Al-Fe-Mg ternary diagram of chemical compositions of tourmalines from Goldfields lode-gold veins (black dots). Tourmalines have an intermediate schorl-dravite composition, similar to tourmalines from Archean lode-gold deposits. Large black dots are "end-member" tourmaline compositions. Compositional fields for comparison are from (1) Archean mesothermal lode-gold deposits (1A are chrome-rich); (2) base metal sulphide deposits; (3) granitic environments in S.W. England, Portugal, and Thailand; (4) MacArthur River unconformity-type uranium deposit; (5) porphyry Cu-Mo deposits in Peru.

muscovite, its oxygen isotopic compositions may have been partially altered. However, as hydrogen will equilibrate much faster than oxygen, the δD values of the tourmaline may be representative of the muscovite-bearing fluid.

Muscovite

Muscovite replaces tourmaline in both the Box and Frontier veins (Plate 3), and muscovite-filled micro-fractures that appear to cross cut into the tourmaline and vein quartz near the sites of alteration emphasize the secondary nature of the muscovite (Plate 3b). These appear to be the same micro-fractures that host late chlorite in other section of the veins. A muscovite sample from the Frontier veins (FR87025F) has a δ^{18}O value of 7.4 per mil, and a δD value of -80 per mil (Appendix 3). The isotopic composition of the muscovite indicates it is not in isotopic equilibrium with the host tourmaline, because muscovite and tourmaline in equilibrium with the same fluid should have approximately the same δD and δ^{18}O values.

Tremolite

Tremolite was identified in quartz veins from two locations. A barren vein (BX86074, see Figure 14) emplaced outside of the Box granite contains approximately 20% tremolite, which has a δ^{18}O value of 7.7 per mil, and a δD value of -107 per mil. Coexisting vein quartz, which petrographically appears to be in equilibrium with the tremolite, has a δ^{18}O value of 11.9 per mil. Using the quartz-

hornblende fractionation of Bottinga & Javoy (1975) to approximate quartz-tremolite, the calculated equilibrium temperature is 560°C. This temperature, which is similar to the 550°C temperature derived from one of the quartz-tourmaline fractionations, indicates that the barren vein may have been emplaced under high temperature conditions. The time of emplacement of the barren vein is unknown.

Tremolite was identified as a gangue phase in auriferous veins from the Frontier property. Unfortunately, the tremolite is intimately associated with chlorite and muscovite, perhaps as an alteration product similar to the tourmaline, and could not be separated sufficiently for isotopic analysis.

Feldspar

Potassium feldspars (often perthitic) from both the veins and the granites were analysed for their oxygen isotopic compositions. Albite from the granites was avoided, as petrographic examination shows two possible ages of albite (Sibbald, 1985). Gangue albite from the auriferous veins could not be located in sufficient quantity for separation.

Feldspar can readily undergo isotopic exchange with hydrothermal fluids (O'Neil, 1987), such that exchange at temperatures of 200 to 300°C usually result in more positive $\delta^{18}O$ values for the feldspars, whereas exchange above 300°C generally results in lower $\delta^{18}O$ values, depending on the oxygen isotopic composition of the fluid. Quartz is very resistant

to exchange with hydrothermal fluids, so that the effect on its isotopic composition will be minimal. Later fluid interaction is often indicated by the production of feldspar with red hematitic staining, with a clouded or dusty appearance in thin section, such as is observed in feldspars from the Goldfields area. $\delta^{18}O$ values of two feldspars from the Box Mine granite are approximately 9.2 to 9.6 permil, whereas four feldspars from the Athona Mine granite vary from approximately 9.3 to 11.9 per mil (Figure 31, Appendix 3).

Most of the fractionations for quartz-feldspar pairs from the Athona granite do not conform to the magmatitic equilibrium quartz-feldspar fraction trend (500 to 700°C), probably due to secondary fluid-induced shifts in the oxygen isotopic composition of the feldspars (Figure 33). If all the quartz-feldspar fractionation temperatures for the Box and Athona granites are calculated, the range would be from 415 to 806°C, which is anomalously large for "magmatic" temperatures. In addition, quartz-feldspar pairs from samples AT87017 and AT86048 have negative fractionations, as a result of "open system" isotopic exchange between the feldspar and a later hydrothermal fluid (e.g. Taylor, 1986). Quartz-feldspar pairs from samples AT86063, AT86064, and BX87037 plot nearer the magmatic equilibrium trend. This scattering of the data, near magmatic fractionations, in a direction perpendicular to the equilibrium trend (Figure 33), is compatible with "closed system" isotopic exchange, perhaps with limited "open system"

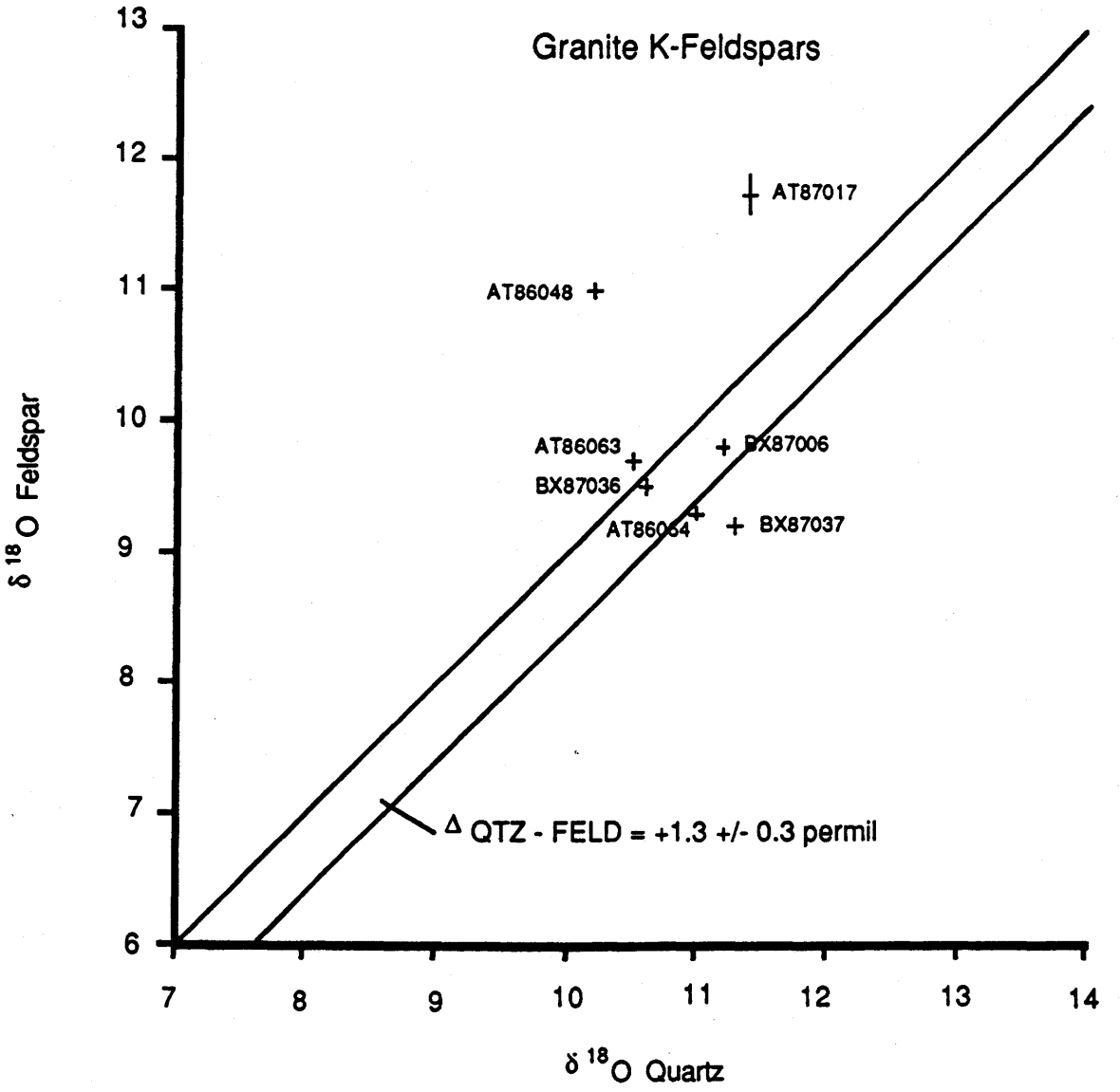

Figure 33: Relation between $\delta^{18}O$ quartz and $\delta^{18}O$ feldspar for coexisting quartz-feldspar pairs from the Box and Athona Mine granites. Diagonal lines are boundries of "magmatic" equilibrium for quartz-feldspar fractionations of 1.3 ± 0.3 per mil. See text for explanation. Data are from Appendix 3.

exchange, during several fluid events. Samples BX87006 and BX87036, however, do plot within the equilibrium trend, indicating magmatic quartz-feldspar closure temperatures of 550 to 660°C, similar to the high temperatures implied by some of the isotopic equilibrium temperatures of vein gangue minerals (see above sections on tourmaline and tremolite). 550 to 660°C is slightly less than the temperature of magma generation suggested for anatexic (S-type) granites (650 to 700°C) in the presence of water (Hyndman, 1981), but comparable to isotopic equilibration temperatures measured for most granites (e.g. Taylor, 1986).

Vein Feldspar

Petrographic relations imply that orthoclase is a primary gangue mineral in the Frontier veins, but potassium feldspar (perthitic microcline) has not been reported as a primary gangue phase in the Box or Athona quartz veins. It is possible that feldspars from the Box and Athona veins occur as re-equilibrated rafted crystals, or as a primary gangue phase, as petrographic relations do not indicate that potassium feldspar is out of equilibrium with the vein quartz.

The isotopic composition of potassium feldspars from the Box and Frontier quartz veins range from approximately 9.4 to 10.7 per mil (Appendix 3). Quartz-feldspar fractionations for the Box and Frontier veins plot within the "magmatic" trend (Figure 34), with the Frontier and Box samples grouped at overall higher and lower $\delta^{18}O$ values respectively. Isotopic

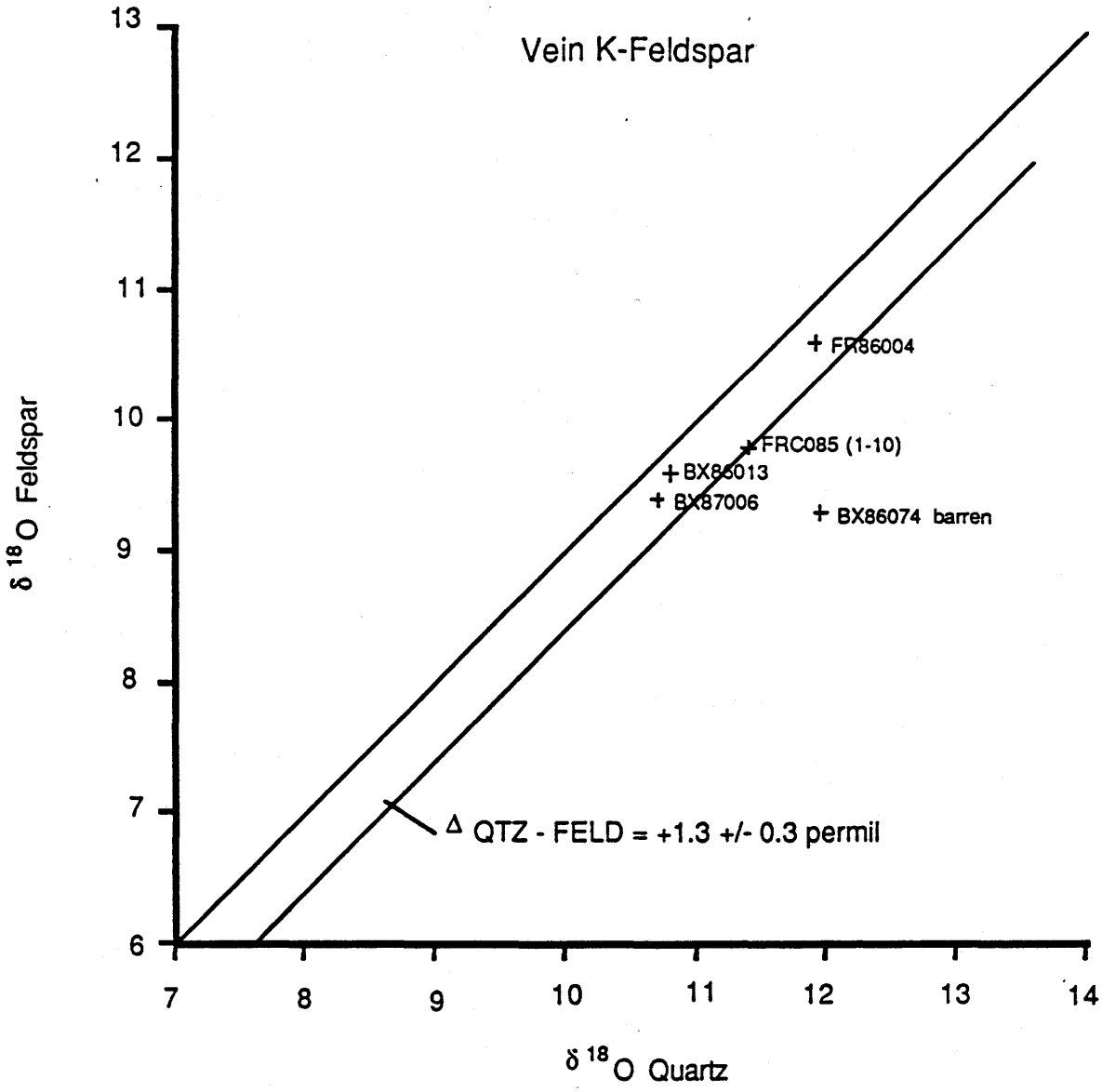

Figure 34: Relation between $\delta^{18}O$ quartz and $\delta^{18}O$ feldspar for coexisting quartz-feldspar pairs from the Goldfields lode-gold veins. Diagonal lines are boundaries of "magmatic" equilibrium for quartz-feldspar fractionations of 1.3 ± 0.3 per mil. See text for explanation. Data are from Appendix 3.

equilibrium temperature calculations (Bottinga & Javoy, 1975) for the pairs range from 510 to 630°C, whereas sample BX86074, from a barren vein, has an apparent temperature of 330°C. As the quartz-feldspar isotope geothermometer is inherently temperature insensitive, especially above 400°C, only a general conclusion may be drawn: that the vein feldspars may have attained, or maintained, oxygen isotopic equilibrium with coexisting vein quartz, at a temperature between approximately 300 and 600°C. Additionally, the oxygen isotopic compositions of potassium feldspars in the veins are very similar to the isotopic compositions of potassium feldspars in the granites, between 9 and 10 per mil, implying that the potassium feldspar in the veins is rafted from the granites. This may also be the case with feldspar in the Frontier veins. The barren vein quartz-feldspar temperature is additionally suspect, as it is in large discordance with the quartz-tremolite isotopic equilibration temperature, and disequilibrium between quartz-feldspar is suggested by its discordance from the quartz-feldspar equilibrium trend (Figure 34).

Sulphides

The sulphur isotopic compositions of various sulphide phases from the lode veins are shown in Figure 35 and Appendix 3. Separates of pyrite, chalcopyrite, galena, and sphalerite were obtained from samples of the Box veins (BX86011, BX87019, BX87034, BX86044, TKK87001), as well as pyrite, sphalerite, and galena from the Athona veins (AT87009, AT87017). Pyrite

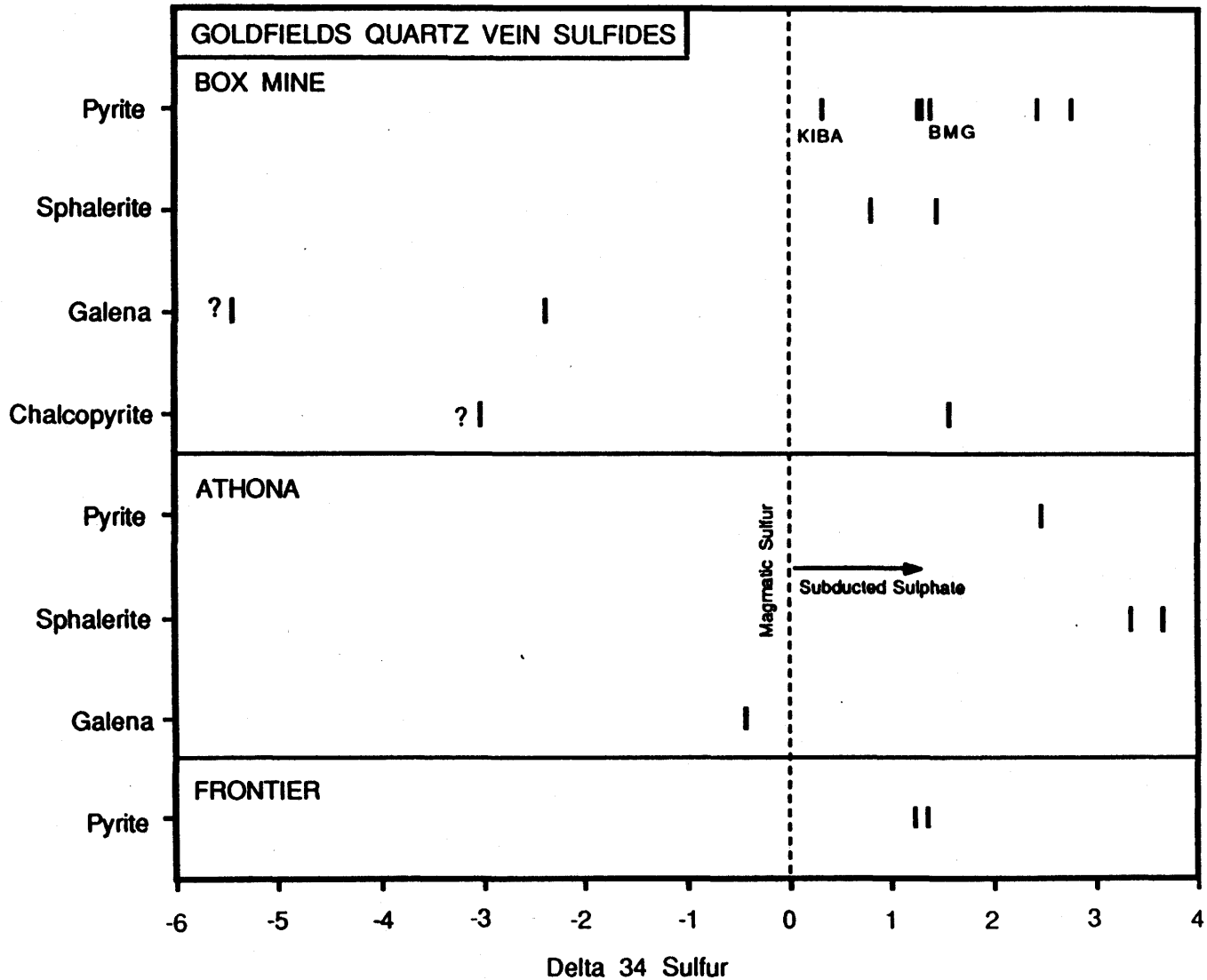

Figure 35: Compilation of $\delta^{34}S$ values for sulphide minerals in lode-veins from the Goldfields deposits. KIBA value is non-sulphide sulphur extracted from a sample of the Box Mine granite, whereas BMG is a pyrite from the Box Mine granite. $\delta^{34}S$ values of magmatic sulphur at approximately 0 per mil, and suducted sulphate at > 0 per mil are shown for reference. Variable $\delta^{34}S$ values for the vein sulphides indicates isotopic disequilibrium amoung the phases. Data are from Appendix 3.

is the only sulphide phase in the Frontier veins (FR86004, FRC86085). Pyrite was also separated from the Box granite, where it occurs as subhedral grains (BX86043). In addition, one sample of sulphur was extracted from a non-pyritic portion of the same granite sample, using the KIBA method (Sasaki et al, 1979).

Petrographic examination of the sulphide phases in the veins suggests a detailed paragenesis as shown in Figure 36, which expands on the sulphide parageneses reported by Koeppel (1968) and Beavan (1938). None of the major sulphide phases appear to be in equilibrium with each other, as many of the coexisting phases showed veining, fracture-filling and replacement textures. At the Box Mine, early, minor sphalerite is overgrown by early, euhedral pyrite, which is the dominant sulphide phase in the veins. The pyrite is sometimes overgrown and replaced by red-brown coloured sphalerite. This latter sphalerite often has small blebs and rods of chalcopyrite in it, probably due to "chalcopyrite disease", a texture ascribed to either exsolution or epitaxial overgrowth (Craig & Vaughan, 1981). Small grains of anhedral pyrite appear to be associated with the latest stages of the sphalerite. Late dendritic and stringer galena, with associated chalcopyrite stringers and ovoid blebs, cross-cuts or replaces all previous phases. In several cases, galena has overgrown chalcopyrite but, in narrow veins, their relationship could not be determined. Narrow dendritic

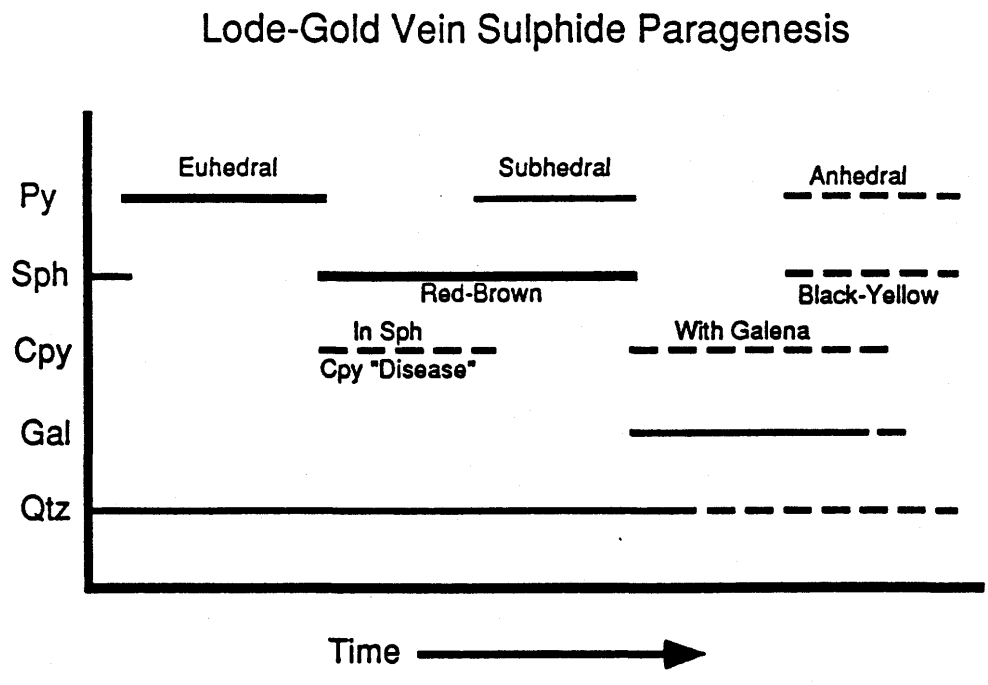

Figure 36: Paragenesis of vein sulphide for the Box and Athona lode-gold deposits. Frontier veins only contain euhedral to subhedral pyrite. Thick lines indicate major phase, thin lines are minor phases, and dashed lines are trace or uncertain phases. See text for explanation of labels.

stringers of galena occur towards the center of most veins, likely related to the galena which veins other phases, suggesting that galena is one of the latest phases to fill brittle fractures in the syndeformational vein system. Another late phase is rare, black coloured sphalerite, spatially associated with the late galena and chalcopyrite. The late sphalerite, as well as minor anhedral pyrite, occur as dendritic stringers or elongate crystals, similar to the galena-chalcopyrite stringers. Vein paragenesis is similar at the Athona Mine, although in the samples examined, there appeared to be very little chalcopyrite, and sphalerite appeared to be more abundant than the early pyrite phase. Quartz veins from the Frontier property only contain euhedral to anhedral pyrite, which appears to be equivalent to the early euhedral pyrite phase in the Box and Athona veins.

Because there are no phases that show conclusive petrographic equilibrium, the calculated sulphide-pair isotopic equilibration temperatures of 200 to 500°C (Kajiwara & Krouse, 1971) are dubious. $\delta^{34}S$ values should decrease in the order Py > Sph > Cpy > Gal if they are in equilibrium (e.g. Faure, 1986). However, sphalerite in sample AT87017 has a $\delta^{34}S$ value that is actually greater than that of coexisting pyrite (Athona, Figure 35). The Box samples show significant variability in the $\delta^{34}S$ values of both galena and chalcopyrite, as well as a 1.5 per mil variation in pyrite (Figure 35). Isotopic exchange with later fluids may be responsible, in

part, for some of the variation.

The overall sulphur isotopic compositions of the minerals, and disseminated sulphur from the Box granite extracted using the KIBA technique, range from 0 to +4 per mil (Figure 35, Appendix 3), which is comparable to the range of $\delta^{34}S$ values from volcanic rocks in a subduction zone setting, where subducted marine sulphate will impart positive $\delta^{34}S$ signatures to fluids and magmas (Faure, 1986). Comparison of $\delta^{34}S$ values of pyrite from the veins and pyrite from the Box granite, which are all greater than 1.2 per mil, to the lower KIBA value of 0.3 per mil for the Box granite, suggests that the vein sulphur was not derived from the granite, but from a different reservoir, and that the widespread pyritization of the granite is related to the veining event.

4.3.2 Fluids in Equilibrium with Minerals

From the $\delta^{18}O$ values of the vein minerals, it is apparent that many of the gangue phases are not in isotopic equilibrium with each other, as the apparent isotopic equilibration temperatures are geologically unreasonable. Only the two larger quartz-chlorite fractionations yield reasonable temperatures of approximately 300 to 400°C, which generally correlate with the trapping temperatures of Type I inclusions, indicating that the precursor biotite likely achieved, in some instances, isotopic equilibrium with the vein fluids during recrystallization to chlorite. Isotopic data from other minerals indicate disequilibrium, and although their

petrographic relations do not necessarily indicate it, many appear to be: (1) "rafted" from the vein wall as a pre-existing phase, such as potassium feldspar and chlorite; (2) formed very early in the vein paragenesis, such as tourmaline, and have not maintained isotopic equilibrium with the bulk of the later formed quartz. Gangue albite probably has a similar relationship with the quartz.

The isotopic composition of the fluids which were in equilibrium with vein minerals, and from which at least some of the minerals formed, can be calculated by using the isotopic composition of the chlorites and the isotopic equilibration temperatures derived from quartz-chlorite fractionations. For late muscovite, the trapping temperature of Type I fluid inclusions is used, as they appear to be related to the late brittle fracturing event. From the samples discussed in the preceding section, isotopic fluid compositions can also be calculated or estimated for the mine granites and a barren quartz vein.

For the lode-gold veins, isotopic equilibration temperatures of coexisting quartz and chlorite yield reasonable temperatures of 300 to 400°C, which indicates that to be the temperature of the fluid from which the minerals precipitated. Trapping temperatures of Type I fluid inclusions, suggested to be similar to the homogenization temperatures, imply a temperature of 250 to 350°C, at least during the later stages of veining associated with the

muscovite.

The isotopic compositions of water in equilibrium with chlorite (BX87006, FR86004) at 300 to 400°C are approximately -29 to -41 per mil for hydrogen (Taylor, 1974), and 3.5 to 5.4 per mil for oxygen (Wenner & Taylor, 1971). This water plots within the metamorphic water field, clearly indicating that the vein-forming fluids were metamorphic in origin (Figure 37). The fluid isotopic composition approaches that of the fluid isotopic compositions calculated for the basement rocks underlying portions of the Athabasca basin (Wilson & Kyser, 1987; Kotzer & Kyser, 1990).

The isotopic composition of the fluid that was in equilibrium with the late muscovite (replacing tourmaline) can be calculated, if the temperature of this event is assumed to be that indicated by Type I fluid inclusions. At 300°C, the median homogenization temperature, muscovite would be in equilibrium with a fluid that had a δD value of -32 per mil (Suzuoki & Epstein, 1976), and a $\delta^{18}O$ value of 4.0 per mil (O'Neil & Taylor, 1969) This point plots at the same position the chlorite waters do (Figure 37), implying the the late fracturing event is related to the overall veining event, and that the gold-bearing fluid is also metamorphic in origin.

At 600°C, which is the average temperature derived from quartz-feldspar fractionation, the $\delta^{18}O$ value of water in equilibrium with unaltered mine granite feldspars ranges from

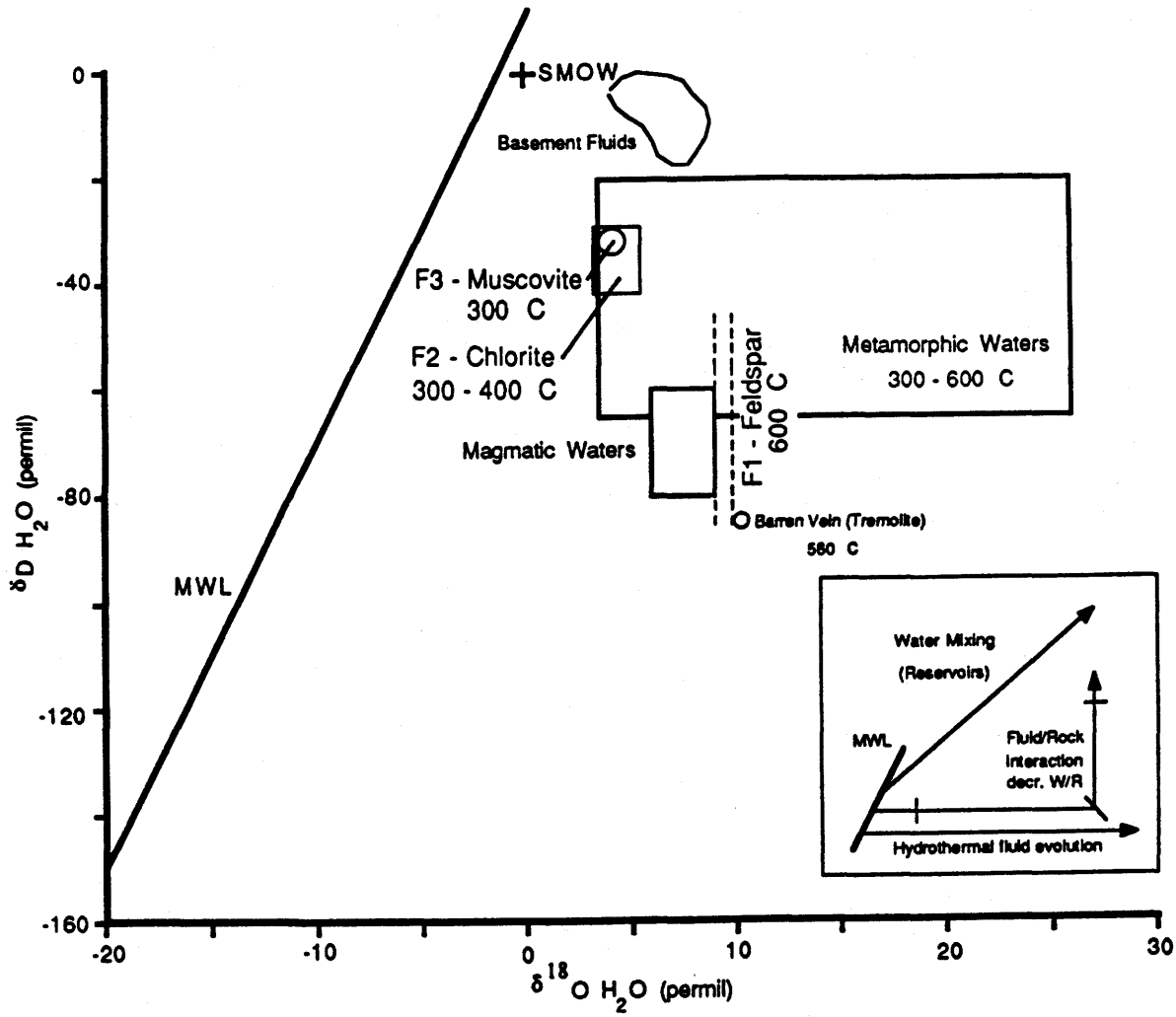

Figure 37: Relation between $\delta^{18}O$ and δD values of water in equilibrium with minerals from the Goldfields lode-gold deposits. F1 - waters in isotopic equilibrium with Box Mine granite feldspars, at 600°C (δD of fluid is unknown), and possibly the barren veins, at 560°C; F2 - waters in isotopic equilibrium with selvage-type chlorite from the Box and Frontier lode-gold veins, at 300 to 400°C; F3 - waters in isotopic equilibrium with late muscovite from the Frontier lode-gold veins at 300°C, the homogenization temperature of Type I fluid inclusions. Values of typical metamorphic water and magmatic water, the meteoric water line (MWL), and standard mean ocean water (SMOW) are shown for reference (Taylor, 1974). Value of basement waters associated with unconformity-type uranium deposits in the Athabasca basin are also shown (Wilson & Kyser, 1987 and Kotzer & Kyser, 1990). Inset shows ways in which the isotopic composition of meteoric waters can be modified.

8.9 to 9.5 per mil (O'Neil & Taylor, 1967). This range is higher than the average $\delta^{18}O$ value (about 8.3 per mil) calculated for the veins, suggesting they are distinct fluids (Figure 37).

The isotopic composition of the water that was in equilibrium with tremolite from the barren vein (BX86074), at 560°C, gives a value of -85 permil for δD (Graham et al., 1984), and 10.3 per mil for $\delta^{18}O$. The hornblende-water fractionation for oxygen (Bottinga & Javoy, 1975) was used to approximate tremolite, as their respective hydrogen fractionations are virtually identical. The isotopic composition of the fluid is not within the metamorphic water field (Figure 37), but is similar to the values for fluids in equilibrium with the mine granite waters. This suggests that the vein was emplaced under similar pressures and temperatures as the mine granites, and may be contemporaneous.

Calculation of the isotopic compositions of the fluids in equilibrium with individual minerals has shown there to be two, possibly three, distinct fluids. The first (F1) was a fluid of presumed metasomatic origin (magmatic-hydrothermal, or magmatic-metamorphic), involved in the formation of the mine granites and perhaps some of the barren quartz veins in the area (Figure 37). This fluid has values indicative of low water/rock ratios (see inset, Figure 37), and may represent an isotopically evolved fluid (locally buffered) originating either from magmatic activity at depth, or from metamorphic

waters at depth.

The next fluid event (F2) is most likely responsible for the lode-gold quartz veins, and is indicated to be a metamorphic fluid. The isotopic composition of the fluid is similar to the compositions reported for Archean mesothermal lode-gold deposits from Australia and the Superior Province (Kerrich, 1987). Proterozoic deposits in Saskatchewan and Manitoba, such as Star Lake (Ibrahim, 1991), Rio, and Graham (Ansdell and Kyser, 1990) also have similar isotopic fluid compositions.

A third fluid event (F3) is related to late muscovite formation, and probably gold deposition, in the lode veins. Although the absolute timing of this fluid event is not clear with respect to the formation of the veins, the fluid appears to be of metamorphic origin, and of the same isotopic composition as the vein forming fluids, suggesting that F2 and F3 are intimately related.

4.4 Radiogenic Isotopes

Rb/Sr isotopic ratios were measured in silicate gangue mineral separates from the Frontier and Box quartz veins, to determine directly the age of the veining and associated gold mineralization. Feldspar separates from the Box granite were also analysed for comparison with the Rb/Sr work of Bell & Bikerman (1985) on minerals and whole-rock samples of the mine granites (Figure 8). Silicate gangue phases from the Athona veins, and albite from the Box veins are rare, and could not

be separated in sufficient quantities for analysis. Appendix 4 lists all measured ratios for the mineral samples. All errors are quoted at the 2-sigma level.

For the Frontier veins, a potassium feldspar (FR86004) and a tourmaline (FR87025F) were used to construct a two point isochron, which indicates an age of 1910 ± 9 Ma, with an initial Sr ratio of 0.757432 ± 0.00005 (Figure 38a). Using a different feldspar from the Frontier veins (FRC86085), the isochron yields an age of 1961 ± 42 Ma, with an initial Sr isotopic ratio of 0.757295 ± 0.00062 (Figure 38b). Tourmalines, from both the Frontier and Box properties, have a very low Rb content, so their $^{87}Sr/^{86}Sr$ ratios approximate the initial Sr isotopic ratios of the fluids present when they formed. For this reason, tourmaline was chosen as the initial Sr isotopic ratio for a model age of the late muscovite which replaces the tourmaline (FR87025F). In the Frontier veins, the muscovite has very high $^{87}Sr/^{86}Sr$ and $^{87}Rb/^{86}Sr$ ratios, so that the model age of 1838 ± 9 Ma (Figure 38c) is relatively independent of the initial Sr ratio used. Recalculation of the model age using initial ratios of 0.70 and 0.79 only changes the age to 1850 Ma and 1831 Ma respectively. These are virtually the same, within the error limits, as the 1838 Ma age. The Frontier muscovite date suggests the late stages of vein emplacement, associated with gold mineralization, occurred at ca. 1.84 Ga. As the vein feldspars are not in stable isotopic equilibrium with the vein quartz, they are

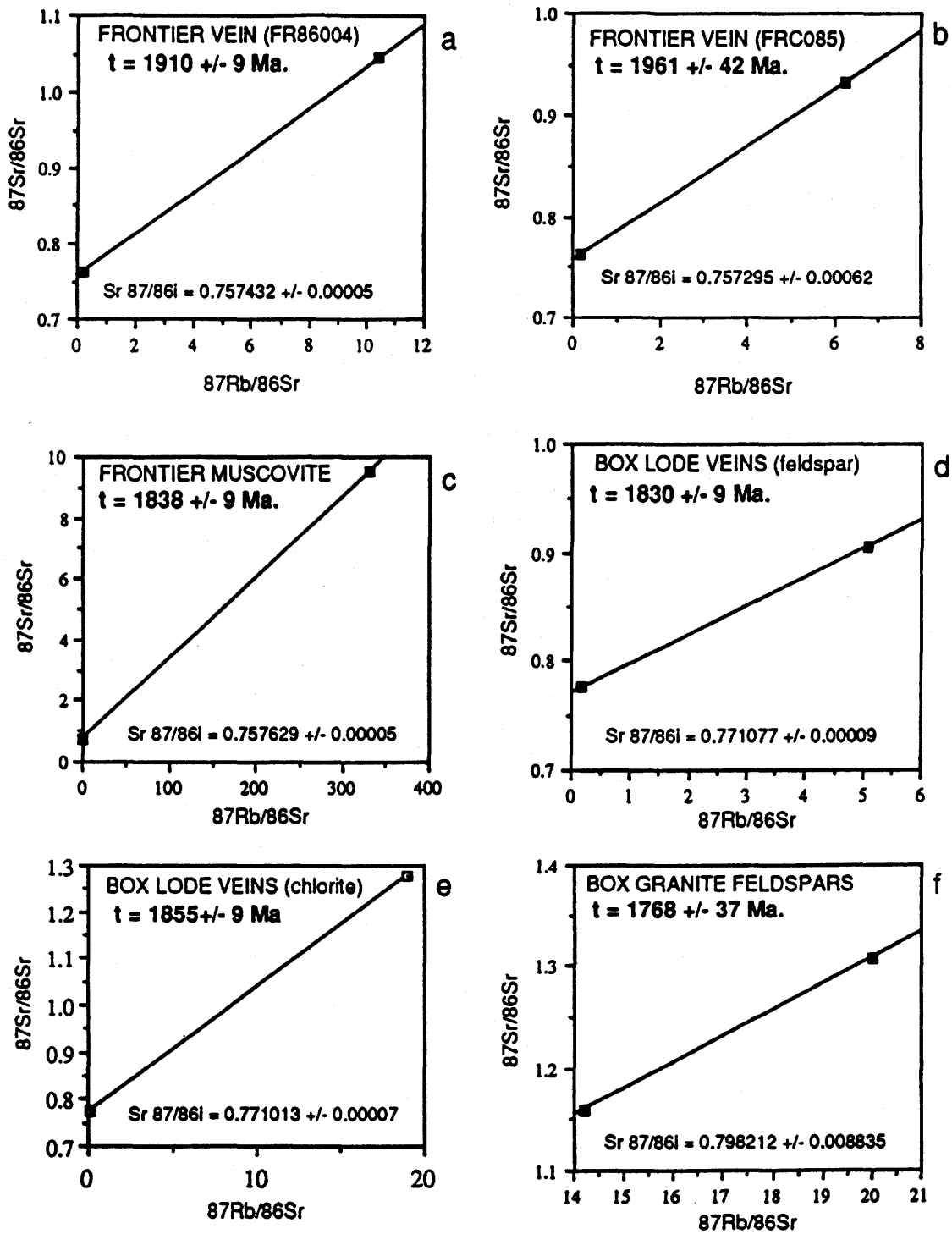

Figure 38: Rb/Sr isochrons for lode-gold vein minerals and Box Mine granite feldspars. Isochrons (a) and (b) are formed by tourmaline and feldspar from the Frontier lode-veins; (c) a model age, using late muscovite that alters tourmaline in the Frontier lode-veins, and assuming an initial $^{87}Sr/^{86}Sr$ ratio based on the tourmaline ratios. Isochrons (d) and (e) are formed using Box lode-vein feldspar and chlorite, respectively; isochron (f) formed by feldspars from the Box Mine granite. See text for further explanation. Data are from Appendix 4.

suspected to be rafted into the vein, and therefore the isochrons represent "mixing-chrons" between the mine granite and the veins. This is further emphasized by the significantly different isotopic ratios between the two feldspars (Appendix 4), suggesting the ratios are the result of mixing.

Tourmaline (TKK87003) and potassium feldspar (BX87006) from the Box veins form a two point isochron with an age of 1830 ± 9 Ma and an initial Sr ratio of 0.771077 ± 0.000085 (Figure 38d). Although potassium feldspar is not thought to be a primary gangue phase, as suggested by its oxygen isotopic composition (Figure 34), its Rb-Sr systematics may have re-equilibrated with the fluid. Because the age derived from the feldspar isochron is very similar to the muscovite model age from the Frontier veins, it implies that the same fluids may have exchanged with the feldspar, resetting its Rb-Sr systematics. Selvage-type chlorite (BX87006), which gave a reasonable oxygen isotopic equilibration temperature of 390°C, forms an isochron with the tourmaline (TKK87003) with an age of 1855 ± 9 Ma, and an initial Sr isotopic ratio of 0.771013 ± 0.00007 (Figure 38e). This age is similar to the 1.84 Ma age of the late muscovite, implying complete Rb/Sr re-equilibration of the chlorite with the vein fluids, as its oxygen isotopic composition suggests. This further indicates an approximate 1.85 to 1.84 Ma age of the gangue minerals in the lode-gold veins.

Potassium feldspar separates (BX87006, BX87036) from the Box mine granite, which appear to be in oxygen isotopic equilibrium with the quartz in the granite (Figure 34), yield a two point isochron with an age of 1768 ± 37 Ma, and an initial Sr ratio of 0.798212 ± 0.008835 (Figure 38f). This age corresponds very closely to the Rb/Sr age reported by Bell & Bikerman (1985) for a whole-rock isochron of the Frontier mine granite (1760 ± 100 Ma), as well as a feldspar isochron of the Box mine granite (1740 ± 220 Ma). The very high errors on the ages likely represent the varying degree of Sr isotopic exchange by the feldspars with one or more fluids, creating an overall inhomogeneity of the Rb/Sr systematics within the feldspars. The ca. 1740 to 1780 Ma age is interpreted to be a late Hudsonian overprint, due to waning metamorphism, or late magmatic activity (Bell & Bikerman, 1985). Koeppel (1968, recalculated by Bell, 1981) reports a similar age of ca. 1780 Ma, derived by U/Pb dating of uraninite from the simple U-vein deposits of the Beaverlodge area. A similar Pb/Pb age was derived from vein-hosted galenas from the Box mine (Koeppel, 1968). Both of these ages are interpreted to be minimum ages, possibly reset during the same event that produced the Rb/Sr ages.

The high initial $^{87}Sr/^{86}Sr$ ratios of the granite feldspars indicate that they were derived from significantly older, isotopically evolved, crustal material (e.g. Faure, 1986). This is illustrated in Figure 39, using Rb/Sr (Bikerman et

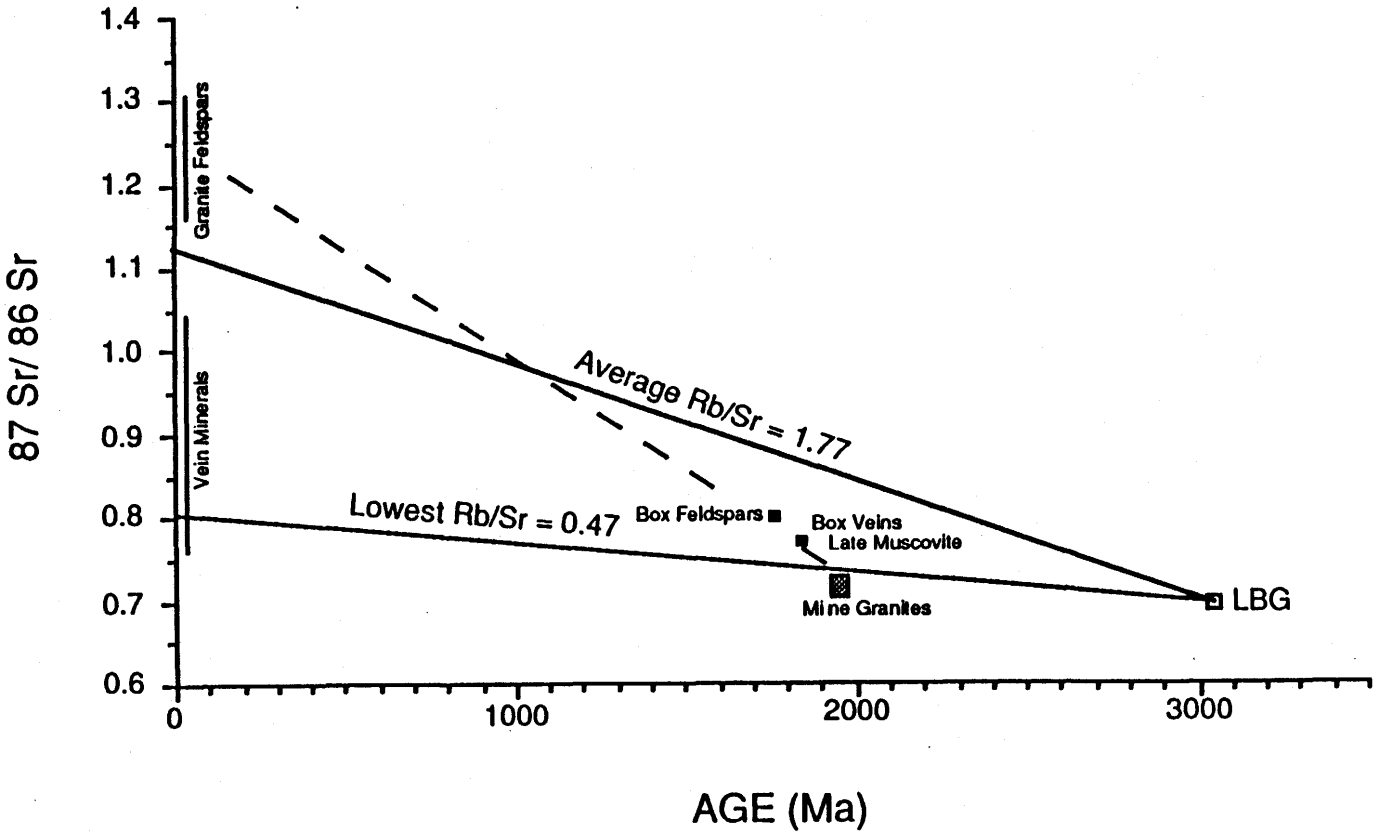

Figure 39: Model of $^{87}Sr/^{86}Sr$ evolution of basement rocks, mine granites, and lode-gold vein minerals in the Goldfields area. LBG = Lodge Bay granite, used as tentative model for basement rocks, showing evolution (solid lines) for low and average Rb/Sr ratios (Van Schmus et al., 1986; Bikerman et al., 1990) towards present Sr ratios of the lode-vein minerals (this study). Age of mine granites from O'Hanley et al. (1991), and initial Sr ratios assumed from Bell & Bikerman (1985). Dashed line indicates evolution towards present Sr ratios of Mine granite feldspars (this study). See text for further explanation.

al., 1990) and U/Pb zircon data (Van Schmus et al., 1986) from the nearby Lodge Bay granite (Figure 5) as a tentative model for Archean basement in the area. Even though the Lodge Bay granite may not be truely basement (see section 2.0), it is at least composed of material derived from basement rocks, and should thus be generally representative of the radiogenic evolution of basement rocks in the area. The evolution of the $^{87}Sr/^{86}Sr$ ratio of the Lodge Bay granite through time is shown for the average and lowest whole-rock Rb/Sr ratios reported by Bikerman et al. (1990). The ages, initial $^{87}Sr/^{86}Sr$ ratios, and present day $^{87}Sr/^{86}Sr$ ratios of vein minerals from the Box and Frontier veins fall within the evolution envelope of the Lodge Bay granite, implying that the minerals were derived from a source similar in age to the Lodge Bay granite. The minerals are also near the tentative evolution line for the mine granites (see below), so that the fluids could have aquired some Sr from the mine granites during wall-rock buffering of the fluids.

Radiometric age data from O'Hanley et al. (1991) and Bell & Bikerman (1985) was used to plot the age and initial $^{87}Sr/^{86}Sr$ ratios of the mine granites (Figure 39), which fall slightly below the Lodge Bay granite evolution path, implying derivation from a source that is different from the source of the Lodge Bay granite; perhaps a younger source, or one with lower Rb/Sr ratios than the Lodge Bay granite. This would be expected if the granites incorporated substantial amounts of

sedimentary material which had varied sources (O'Hanley et al., 1991), some older (ca. 3.0 Ga), and some younger (ca. 2.5 to 2.6 Ga). The fluids which deposited the veins appear, most likely, to be associated with dominantly older crustal material.

4.5 Summary of Lode-Gold Deposits

The three largest lode-gold deposits of the Goldfields Peninsula, the Box, Athona, and Frontier properties, have been characterized using fluid inclusion, stable isotope, and radiogenic isotope data. The deposits are geochemically similar to many Archean-aged mesothermal lode-gold deposits, especially the felsic dyke- or stock-hosted deposits, which occur in similar structural settings (e.g. Sigma-Lamaque, Quebec; Colomac, N.W.T.; Goldlund, Ontario). Some aspects of the Goldfields deposits, such as the high, apparent stable isotopic equilibration temperatures of vein minerals, bear more of a similarity to other Proterozoic deposits in Saskatchewan and Manitoba (e.g Sulphide-Preview: Armstrong, 1990; Star Lake: Ibrahim, 1991).

Fluid inclusion data have shown that the Box, Athona, and Frontier lode-gold veins likely formed, at least in part, from a high density (0.6 to 1.0 g/cm^3), low salinity (6 wt. % NaCl eq.), CO_2-bearing aqueous fluid (bulk mole fraction CO_2 = approximately 0.4), at a minimum temperature of approximately 300°C. The variable but bimodally distributed CO_2/H_2O ratios in Type I inclusions, which are suspected to be primary or

pseudosecondary (i.e. "late primary" to "early secondary"), may be the result of pre- to syn-entrapment immiscibility of some form, perhaps as a result of a local pressure drop within late brittle fractures during the last stages of vein emplacement and gold deposition. Fluid immiscibility is considered to be a likely mechanism of gold deposition. Late stage brittle fractures in lode-gold veins, which host primary inclusions with immiscible assemblages, and which are associated with the actual gold mineralization of the veins, occur at the Sigma Mine (Guha et al., 1991). The data from the Goldfields deposits suggest a similar paragenesis of the vein systems.

Stable isotopic data indicate that the actual fluid temperature during vein emplacement was approximately 300 to 400°C, which would correlate with an immiscible assemblage of Type I fluid inclusions, because the homogenization temperature of the inclusions (approximately 300°C) is equal to the fluid trapping temperature under conditions of immiscibility. Minimum pressures are indicated to be from 2.5 to 3.0 kbars, but would be the actual fluid trapping pressures under conditions of immiscibility.

Secondary fluid inclusions in the veins show that at least three different late fluids have infiltrated the rocks of the Goldfields area. Two of the fluids are similar to basinal diagenetic brines, similar to those recorded in fluid inclusions and by the stable isotopic compositions of minerals

in the Athabasca basin. The origin of the other secondary fluid, represented by Type II inclusions, is unknown, but similar low-salinity fluids have been reported from other mesothermal lode-Au deposits. The Type II fluid may be related to the late overprinting event, recorded by feldspars in the mine granites, at ca. 1740 to 1780 Ma.

Stable isotopic analyses of cogenetic minerals from the deposits have shown that the lode-gold vein forming fluids were likely of a metamorphic origin, at a temperature of approximately 300 to 400°C. Based on measured $\delta^{18}O$ values, the gangue silicate minerals, for the most part, are not in isotopic equilibrium. This is attributed to incomplete re-equilibration of pre-existing minerals (wall-rock derived) and the veining fluids, or interaction of the minerals with later fluids. Sulphide mineral petrography indicates disequilibrium between most sulphide phases in the veins. The overall $\delta^{34}S$ values of the sulphides indicate a sulphur source that was related to a subduction environment.

Rb/Sr ages of vein minerals and feldspars from the Mine granite indicate the veins were emplaced between ca. 1.85 and 1.84 Ga, and that the mine granites have been affected by several overprinting events: (1) the lode-gold veins at ca. 1.84 Ga, and (2) a later regional event ca 1.78 to 1.74 Ga. The high initial Sr ratios of both the vein minerals and granite feldspars indicate they were derived, in part, from significantly older, but different sources.

5.0 Au-PGE-U Mineralization

5.1 Geology of Deposits

5.1.1 Nicholson & Fish Hook Bay Deposits

The Nicholson Au-PGE-U deposits are located on the east side of Nicholson Bay (Figure 2, location 4), where Murmac Bay Group rocks are relatively flat-lying. On the west side of the bay, and at several other locations nearby, small outliers of highly silicified and hematized Athabasca sandstone indicate that the present level of exposure is very close to the paleosurface upon which the Athabasca Group was deposited, and that the Athabasca basin at one time covered much of the area (Sibbald, 1982). The hematite-silica alteration of these outliers, and of the basement rock below them, is remarkably similar to the alteration associated with the Nicholson deposits. The geology and mineralization of the area have been described by Christie (1953), Joliffe (1946), Beck (1969), and Robinson (1955), and more recently by Sibbald (1982, 1988), Sibbald et al. (1983), Schwann (1985), Peiris & Parslow (1987, 1988), Hulbert et al. (1988), and Hulbert (1990).

Mineralization occurs proximal to a small, sill-like mafic to ultramafic complex which has intruded quartzites, carbonates, and calc-silicates (diopside and tremolite) of the Murmac Bay Group. The sill is several tens of meters thick,

and is composed of serpentinite, gabbro, and amphibolite phases (Figure 18).

The rocks are cut by several generations of faults, but the mineralization is hosted in roughly north-trending subvertical fracture zones. The paragenesis of the deposit is very complex, but the mineralization can be grouped into two types (Sibbald 1988), as 2 cm to 2m wide, quartz-dolomite-hematite-pitchblende veins filling the fractures, and as broad, irregular, Au-PGE bearing alteration zones of hematite and quartz ("chert"), often with vein-like vugs of euhedral quartz and dolomite. The alteration zones are associated with the fractures and some shallow dipping lithological contacts, but do not show clear structural controls. All of the six mineralized zones (zones 5 and 6 are small, and not shown on Figure 18) on the Nicholson property are of limited strike length, roughly from 50 to 300m long. The maximum depth of mineralization appears to be about 130m, but can vary greatly over short strike lengths (Sibbald, 1988).

The uranium mineralization is of the complex vein-type, and is very similar to Athabasca unconformity-type uranium deposits, containing pitchblende, Ni-Co arsenides, sulpharsenides, sulphides and vanadates, and native gold and silver. Hulbert (1990) has identified a wide variety of PGE- and Au-bearing selenium, antimony, bismuth, and mercury minerals, as well as native precious metal alloys. Amorphous, U-bearing hydrocarbon "buttons" have also been reported

(Robinson, 1955).

Relatively complex paragenetic sequences have been proposed by Hulbert (1990) and Peiris and Parslow (1988), which imply that the mineralization may have occured in stages or pulses. Hulbert (1990) concluded that U, PGE, and Au were introduced together, along with the euhedral quartz-carbonate-hematite veins and alteration. The restricted occurrence of PGE mineralization proximal to the ultramafic complex is likely due to the derivation of the PGE's from the ultramafic rocks. Peiris and Parslow (1988) are unsure of the timing of Au introduction, but suggest that U is slightly later than the initial quartz-carbonate-hematite event, and propose an overall negative correlation between Au and U. This implies, as do some field relations, that the complex vein-type uranium mineralization may have overprinted a pre-existing Au-PGE(±U) deposit.

Peiris and Parslow (1988) report a significant feature of the hematitic alteration, first reported by Dawson (1951) from his work on the uranium deposits in the area, wherein the total iron content of unaltered country rocks and hematitically altered country rocks is relatively constant. Only the form of the iron changes, from pyrite and magnetite, to hematite. Another important feature reported by Hulbert (1990) is the three- to ten-fold elevation of chlorine content within the alteration system. These two features are indicative of redox-type mineralization reactions between

reduced basement rocks and an oxidized, highly saline fluid.

The geologic setting of the Fish Hook Bay mineralization (Figure 2, location 6) is very similar to that of the Nicholson zones, in that a small ultramafic body has intruded quartzites and carbonates of the Murmac Bay Group. A large unit of iron formation is interbedded with the sediments. The rocks are more steeply dipping, but are again cut by north-striking fractures which host similar complex vein-type mineralization in two main zones. PGE enrichment appears to be somewhat less than at the Nicholson property (Hulbert et al., 1988). Peiris and Parslow (1987) indicate that the paragenetic sequence is unclear as a result of the fine-grained nature of the Fish Hook mineralization.

5.1.2 Quartzite Ridge Showing

The Quartzite Ridge occurrence is located about 20 km to the west of the Goldfields Peninsula, approximately 3 km south of Beaverlodge Lake (Figure 3). As no publicly available data has been published, the following description is partly based on verbal reports by company geologists, and partly on examination of hand samples and drill core.

Au-PGE mineralization is found within the faulted and brecciated contact between Murmac Bay Group quartzites, and a large gabbroic unit (Figure 3). The full strike extent and width of the mineralization are not known, although diamond drilling showed it to be shallow and erratic. Portions of the Gunnar granite and Lodge Bay granite occur approximately 1 km

to the north and south, respectively. Unconformably overlying Martin Group rocks extend south from Beaverlodge Lake, to within about a kilometer of the showing. Sibbald (1988) points out the proximity of this showing, as well as several others found just to the east of Beverlodge Lake, to the present limit of the Martin basin, but the original extent of the Martin and Athabasca basins, and their stratigraphic relationship to each other, is obscure.

Pervasive hematization and silicification, with small (cm scale) quartz-hematite veins and vugs, comprise the macroscopic mineralization. Within the veins, quartz occurs as euhedral crystals. Hematite occurs as earthy flakes, or as well-formed metallic rosettes, suggesting there may be two periods of hematite deposition. A cursory microprobe analysis identified very small grains of sphalerite, remnant magnetite, native Au and Ag, and an unknown U-, As-, and Ce-bearing metallic phase. Minor features determined by probe analysis include the development of a minor, Mg-rich clay alteration, and that very fine-grained, green-coloured, ovoid apatites cause the dark banding (bedding?) observed in the quartzite. While examining the quartz for fluid inclusion petrography, narrow strands of tourmaline were seen as growth-oriented inclusions within the quartz. The fibres often form long helical coils, sub-parallel to the c-axis of the quartz crystal.

5.1.3 Cross-cutting U-bearing Veins ("Comb Veins")

The comb veins are mineralogically similar to the complex vein-type uranium deposits, but in the Goldfields area occur almost exclusively in narrow (< 1m) east-striking, sub-vertical faults, and they do not have an extensive envelope of hematitic alteration. For convenience, the veins are refered to as comb veins, due to the prominent euhedral quartz crystals which comprise the bulk of the veins, forming well developed comb structure. Similar veins have been reported from many locations around the Athabasca basin, indicating a widespread event, and the veins are often proximal to unconformity-type U deposits, occurring in both basement and basinal rocks (e.g. Hoeve and Sibbald, 1978). The paragenesis of the veins includes initial euhedral quartz, followed by euhedral dolomite, hematite, chlorite, pitchblende, native gold, and various sulphides (Koeppel, 1968). The veins examined in this study cross-cut the older lode-gold veins in both the Box and Athona granites.

5.1.4 Carbonate Albitite or "Sponge Rock"

Carbonate albitite, or "sponge rock" as it is commonly called, is a minor alteration feature observed in the Box and Athona granites, as well as being a major feature of the Gunnar uranium deposit. On the Goldfields Peninsula, the "sponge rock" occurrences are small, irregular to linear shaped zones within the granites that are essentially composed of albite and dolomite, with minor euhedral quartz as a late

phase. Within these zones the granite has been highly cataclastized, probably representing localized shearing, and is deficient in quartz, which has apparently been replaced by subhedral to euhedral dolomite and "dusty" hematite. The zones are associated with uranium mineralization at the Gunnar deposit, and have elevated U contents at the Box and Athona (Quirt, pers. comm.). Hoeve (1982) suggests that the albitization may have occurred earlier, associated with either the lode-gold event, or the simple-type uranium mineralization, and that dolomite deposition occurred along the same structures during the Athabascan complex-type mineralization.

5.2. Fluid Inclusions

5.2.1. Fluid Inclusion Petrography

Fluid inclusions in euhedral quartz and euhedral dolomite were identified from all of the above occurrences. Drill core samples from the Fish Hook Bay and Nicholson properties were supplied by L. Hulbert of the G.S.C.. Surface and drill core samples from the Quartzite Ridge occurrence were obtained from Kasner Group company geologists.

In all of the samples used for microthermometric measurements, most of the fluid inclusions occur along growth planes, and thus are primary in origin. Because the quartz and dolomite are associated with Au-PGE(±U?) deposition (Hulbert, 1990), the fluids in the inclusions represent the mineralizing fluids. Secondary inclusions along cross-cutting

fractures are not common, but in all cases the fluids are essentially identical to those in the primary inclusions, or so similar as to be indistiguishable from them. The minerals showed no other signs of strain or deformation, indicating they are in a virtually pristine state with respect to the preservation of fluid inclusions.

Inclusions were identified as primary by their location along growth zones within the crystal (Roedder, 1984). Figure 40 schematically illustrates typical quartz (A) and dolomite (B) crystals from the Au-PGE-U deposits, showing the composite morphology and orientation of growth zones seen in the samples. Initial trapping of inclusions in the quartz crystals occured in an relatively unordered, non-planar swarm (Figure 40A, label 1) that forms a rounded conical shape at the base of the crystal (Plate 4a). As growth of the crystal becomes more ordered, inclusions are trapped in linear to sub-planar vectors (2), which may have a concentric, inverted conical form in three dimensions. In some samples, the continuation of type 2 growth extends up through the c-axis of the crystal (4). Once the hexagonal form of the crystal has been established, typical growth zones occur parallel to the edges of the crystal form (3, 5, Plate 4b). Growth zones parallel to the pyramid of the crystal (5, lower line) indicate a temporary termination of crystal growth, or a rapid change in the physiochemical characteristics of the fluid, due to the mass of solid inclusions which accumulated. Growth

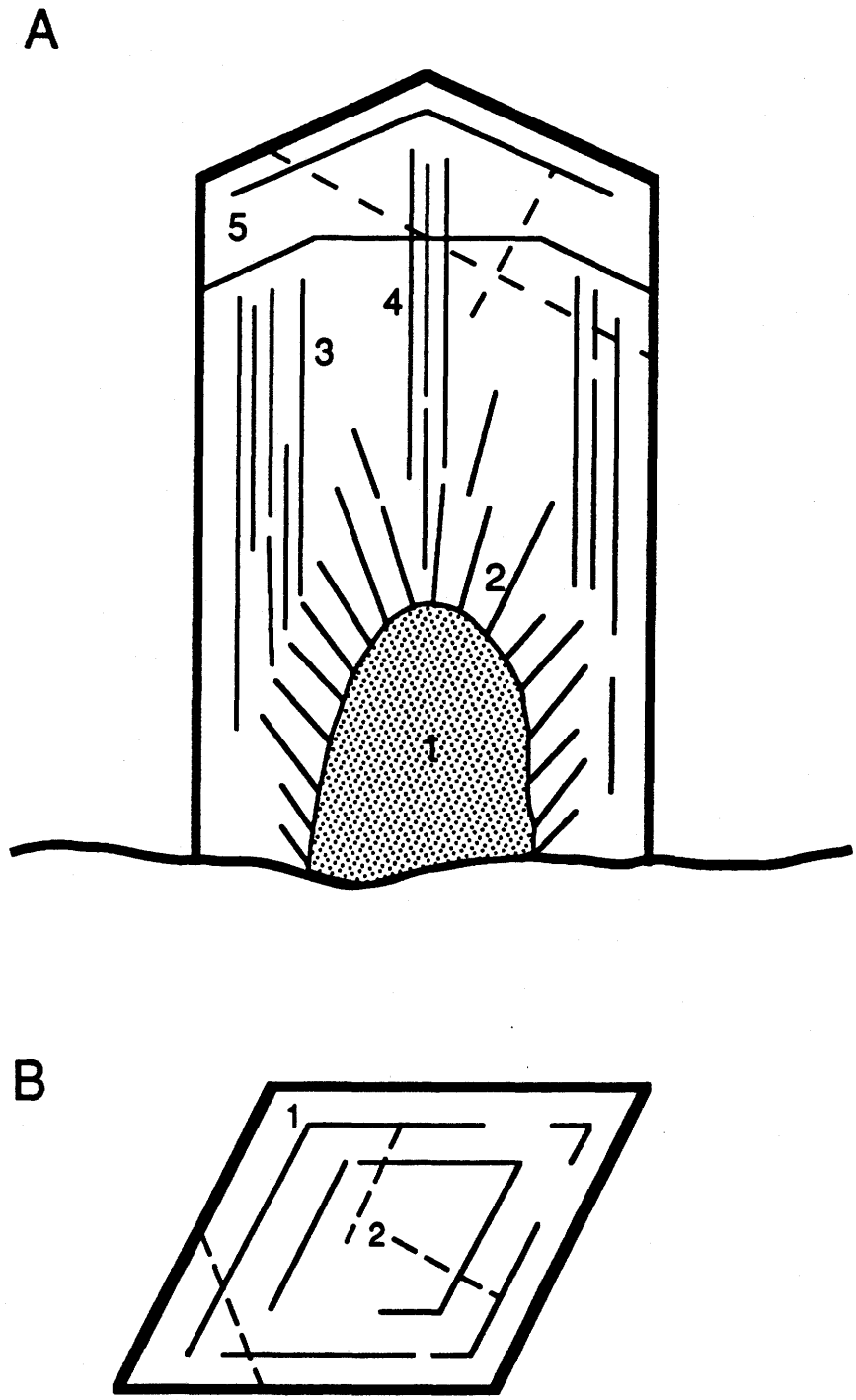

Figure 40: Schematic diagram of primary fluid inclusion locations on growth planes within euhedral quartz and dolomite crystals from the Au-PGE-U deposits in the Goldfields area. Numbering along solid lines corresponds to growth plane locations and orientations (see text). Dashed lines represent internal fracture planes (psuedosecondary inclusions) and secondary fracture planes. See text for further discussion of the growth and fracture planes, and the fluid inclusions found along them.

Plate 4: a - Photomicrograph of a euhedral quartz crystal from a late comb vein, Box mine (BX86082). Two types of primary growth patterns (2 & 3, see text for explanation) are visible, associated with numerous primary fluid inclusions. Along left edge of photo is a growth face (F) of the crystal. Bottom edge of photo is approximately 3.35mm in length; **b** - photomicrograph of a euhedral quartz crystal from the Quartzite Ridge showing (QR-87-3). Two types of primary growth patterns (3 & 5, see text for explanation) are visible, cross cut by several fracture planes (S) that host pseudosecondary inclusions. A group of very thin tourmaline crystals (T) is also visible. The growth base of the quartz crystal is at the bottom left of the photograph. The bottom edge of the photograph is 1.35mm in length; **c** - photomicrograph of three-phase, primary fluid inclusions hosted in euhedral vein dolomite from the No.4 zone, Nicholson mine (TKK87035). Dashed lines indicate the orientations of the two growth plane directions. Bottom edge of photograph is 0.4mm in length.

4a

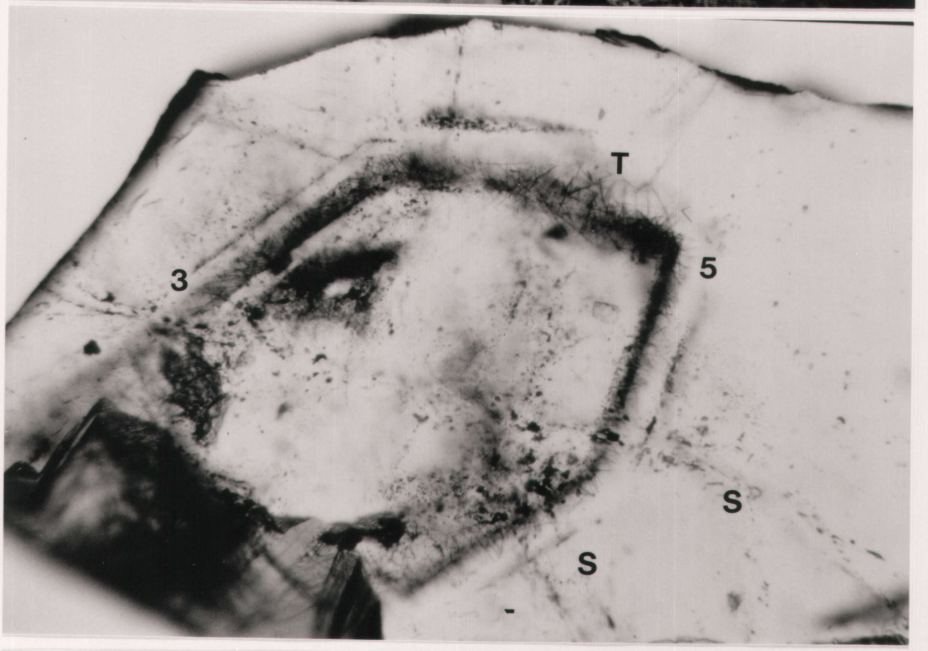

b

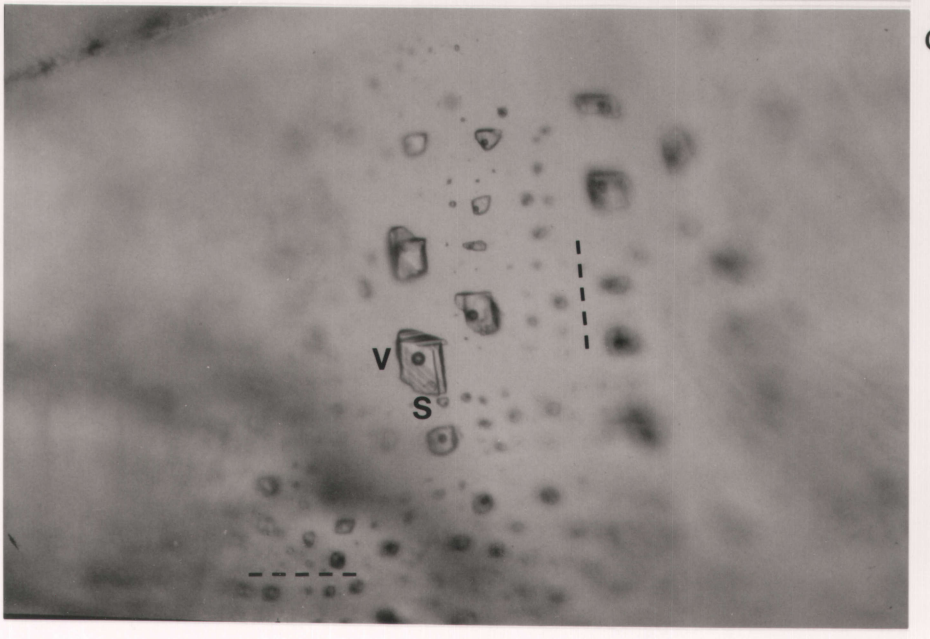

c

zones of type 3 become subordinate near the termination of the crystal, where type 5 zones are most common. Typical pseudosecondary and secondary fractures are shown with dashed lines.

Primary fluid inclusions in dolomite crystals are hosted in planar growth structures which parallel the cleavage planes of the crystal (Roedder, 1984). The planes are associated with growth of the crystal, as they form corners (Figure 40B, 1; Plate 4c) from which the planar zones do not continue further outward toward the edge of the crystal. It is very unlikely that secondary inclusions along a fractured cleavage plane would follow another cleavage plane around their intersection point. Furthermore, pseudosecondary inclusions along intracrystal fractures (2) are indistinguishable from those on the growth planes, suggesting the latter are primary. Secondary fractures host inclusions that are also very similar to the primary and pseudosecondary inclusions.

Nearly all of the inclusions showed signs of necking (Plate 5), which in many cases is very prominent, and creates a wide variety of individual inclusion types and shapes. Fluid inclusions with negative crystal shapes are common, but the inclusions commonly have arms, tubes, pointed tips, and irregular shapes created by necking. Inclusion size is generally large, from 10 to 100 microns or more in diameter, averaging approximately 20 to 30 microns. On the basis of their chemical and petrographic characteristics, the

Plate 5: a - Photomicrograph of a large, necked fluid inclusion along a fracture plane in euhedral quartz, Quartzite Ridge showing (QR-87-3). Necking of the inclusion is indicated by its three chambers, all of which contain different phase proportions (1 - liquid and vapour H_2O, 2 - liquid H_2O, 3 - liquid H_2O and halite crystal). Bottom edge of photograph is approximately 0.4mm in length; **b** - photomicrograph of two primary fluid inclusions in euhedral quartz from a late comb vein, Box mine (BX86082). Necking is shown by the narrow tubes (N) projecting fom the inclusion. Example at upper left of photograph shows phases that are nearly partitioned from each other, with the solid (S) phyllosilicate and H_2O vapour (V) phases in seperate chambers of the inclusion. The bottom edge of the photograph is approximately 0.4mm in length; **c** - photomicrograph of primary fluid inclusions in euhedral quartz from a late comb vein, Box mine (BX86082). Necking is indicated by the variablity in phase ratios amoung the inclusions, as well as "nipples" extending from inclusion walls. Note inclusions that are monophase liquid or vapour (dark bubbles), and inclusions that contain halite (H) or phyllosilicate (S) daughter crystals. Bottom edge of photograph is approximately 0.4mm in length.

5a

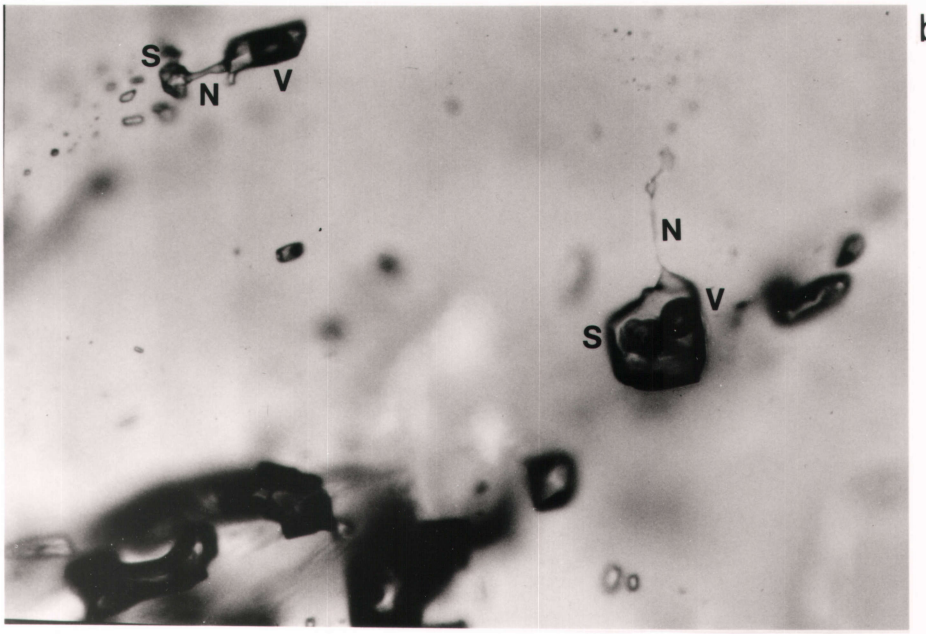

b

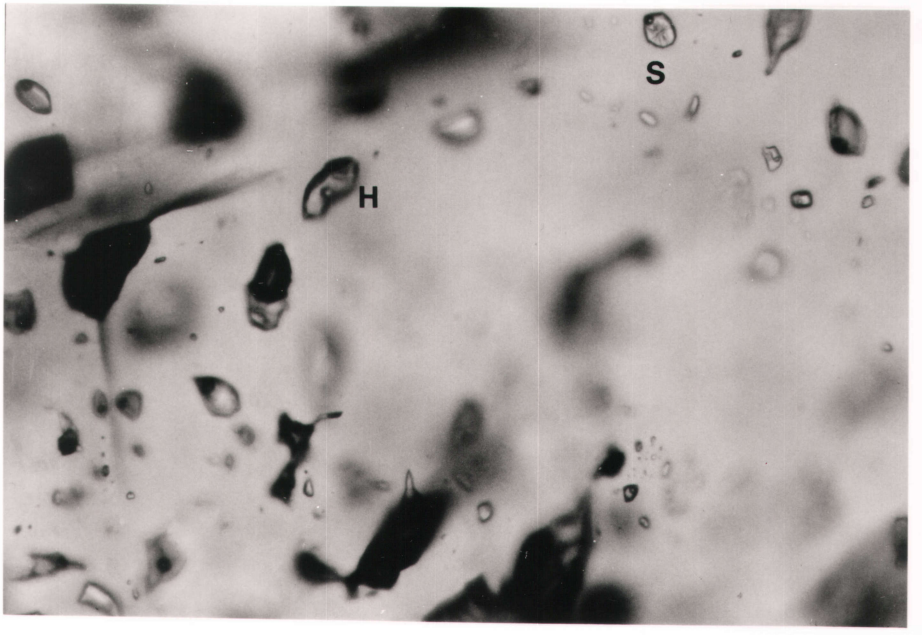

c

inclusions are considered as a group, some of which are similar in age and character to the Type IV inclusions seen in the Box lode-gold veins. The most common type of inclusion (approximately 20 to 40 % of total number of inclusions) is a four phase aqueous inclusion with a 10 to 20 volume % vapour phase, a halite daughter, and sometimes a "captured" phase (Figure 41, inclusion at bottom of center column; Plate 6a, 6b). Three end-member inclusion types can be used to define roughly the range of inclusion types: one phase aqueous (H_2O), one phase vapour-rich, and inclusions containing one, or multiple, daughter or "captured" phases (Figure 41). The latter category includes inclusions that are nearly 100% captured phase (i.e. virtually a solid mineral inclusion; Plate 6c). "Captured" phases were distinguished from true daughter minerals by two means: (1) either the inclusion contains too much of the solid phase for it to have been precipitated from the contained volume of liquid; (2) the solid phase is embedded in the wall of the inclusion, suggesting that the inclusion enveloped it (Figure 42). Both of these morphological criteria could also result from the necking of a larger inclusion, which may have originally precipitated a solid phase.

Captured or daughter phases are numerous in the inclusions. Some are nearly ubiquitous, such as NaCl and hematite, but some are restricted to certain occurrences. The only completely soluble daughter phase is NaCl. Two

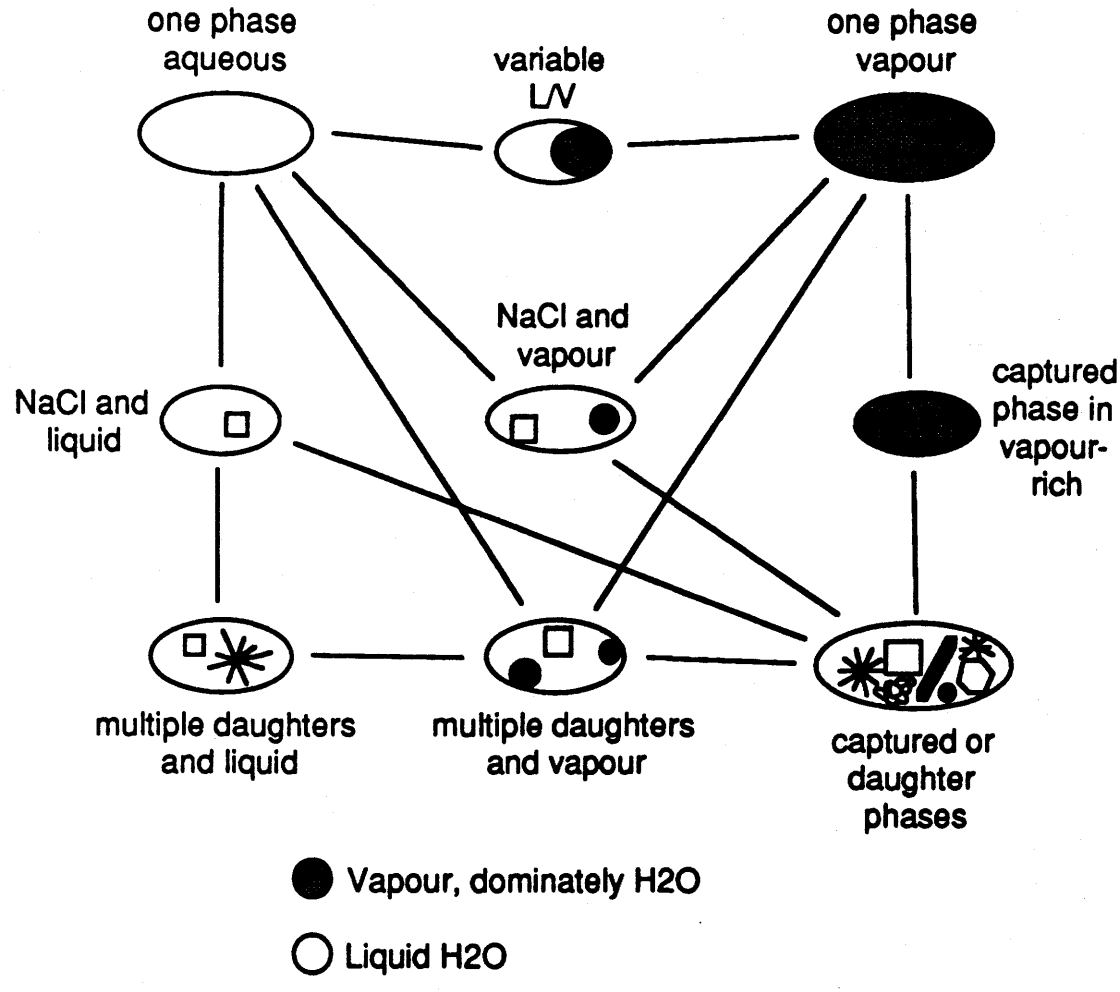

Figure 41: Schematic diagram of primary and secondary fluid inclusion types from the Au-PGE-U deposits in the Goldfields area. Due to necking, innumerable "types" of inclusions were created, but typically appear as a four phase inclusion (H_2O liquid and vapour, with NaCl daughter and "captured" solid) of the type shown in the middle of the bottom row. Lines indicate possible relations of various types of inclusions. See text for further discussion.

Plate 6: **a** - Photomicrograph of a typical three-phase inclusion (L - H_2O liquid, V - H_2O vapour, S - halite cube) in euhedral vein dolomite from the No. 4 Zone, Nicholson mine. This inclusion is associated with a short fracture plane, and is likely secondary or pseudosecondary in origin. The inclusion is also atypically large, as bottom edge of photograph is 0.4mm in length; **b** - photomicrograph of a typical three-phase inclusion (V - H_2O vapour, S - halite cube) along a primary growth plane (P) in euhedral quartz, Quartzite Ridge showing (QR-87-3). A plane of secondary inclusions (S) is visible along the bottom of the photograph, which is approximately 0.4mm in length; **c** - photomicrograph of primary fluid inclusions in euhedral quartz from late comb veins, Box mine (BX86082). Note the wide variation of phase proportions amoung the inclusions, including an inclusion that is nearly full of phyllosilicate "daughter" phase (S), encased in a large vapour bubble (dark inclusion walls). Bottom of photograph is 0.4mm in length.

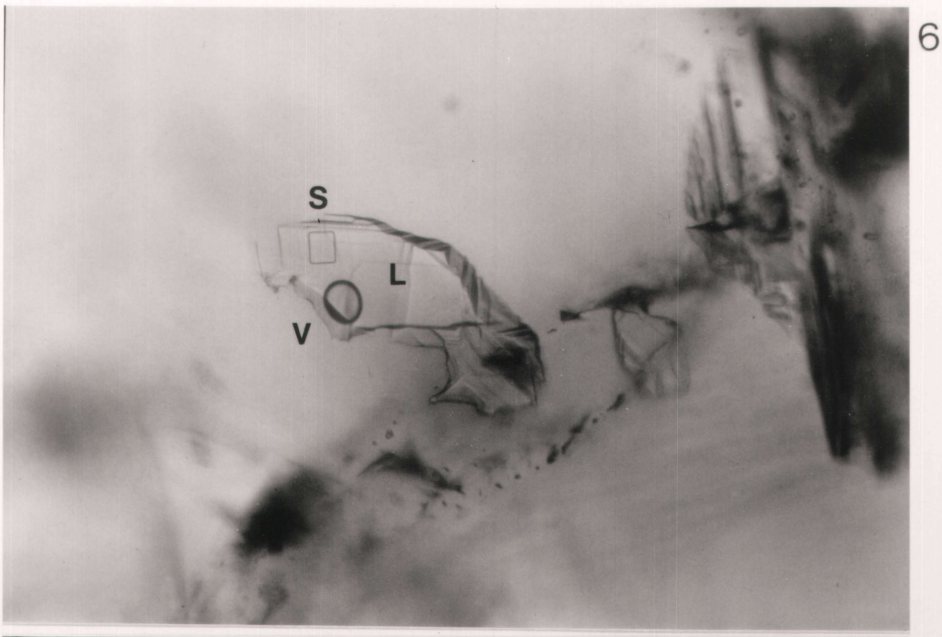

6a

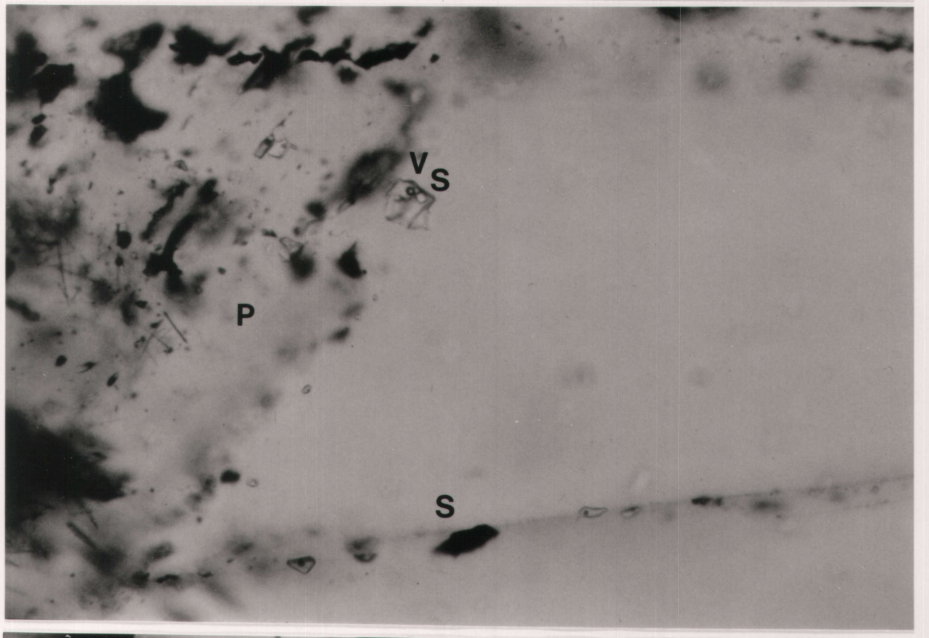

b

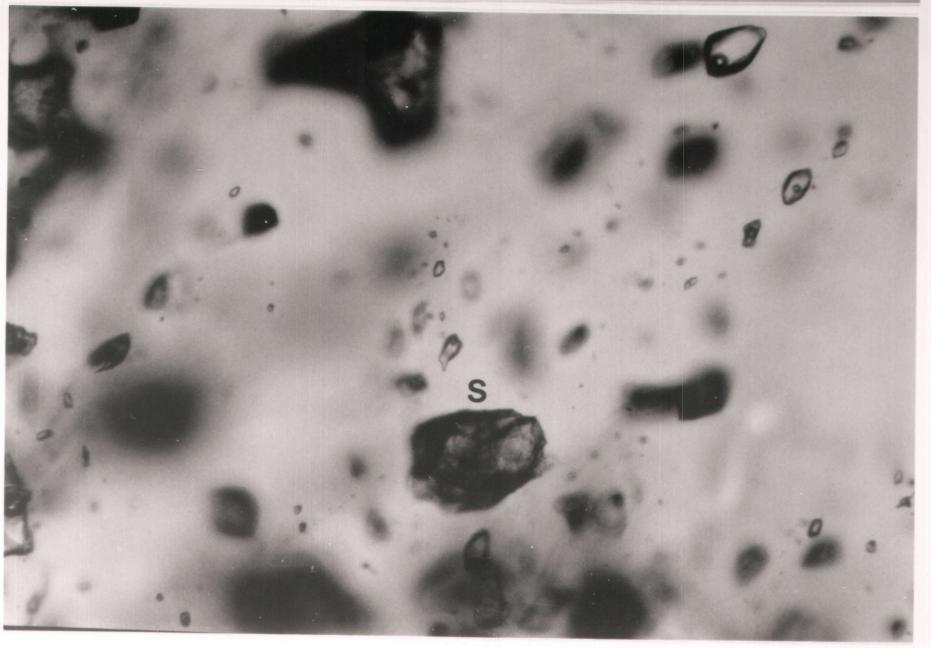

c

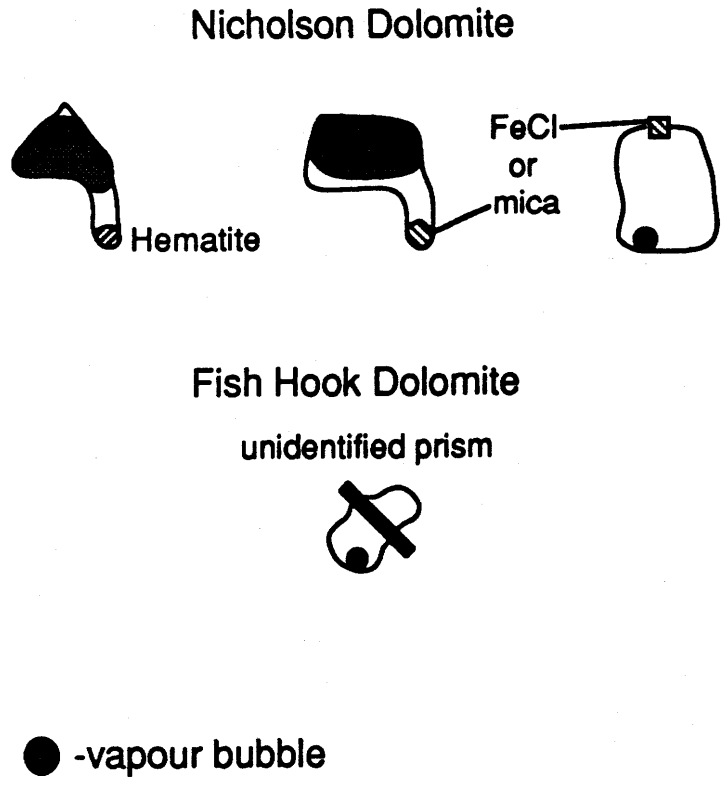

Figure 42: Schematic diagram of primary and secondary fluid inclusions from the Nicholson and Fish Hook Bay deposits that have overgrown an already formed solid phase. The solid may be a true daughter, or a "captured" phase.

inclusions contained soluble $FeCl_n$, whereas all other solids were insoluble over a maximum heating period of fifteen minutes, at temperatures above 300°C. In the Nicholson samples, both quartz and dolomite contain many forms of "daughter" solids, which include, in approximate order of abundance (question mark indicates a tentative identification): (1) NaCl cubes (Plate 6a); (2) Red-brown coloured hematite flakes; (3) Light green coloured, hexagonal to rounded, stubby prisms or plates of $FeCl_n$; (4) Granular masses (of small plates ?) of green tinted, low birefringent mineral, possibly chlorite or other mica; (5) Very small round to oval opaques, probably sulphide (thucholite?); and (6) Small, green tinted, roughly rhombic carbonate crystals.

Inclusions in the Fish Hook samples contain the same daughter minerals, but in addition, there are rare insoluble, long, thin, colourless prisms. Those in the Quartzite Ridge samples contain only NaCl cubes and hematite flakes as daughter phases. Inclusions in the "sponge rock" samples also contain NaCl cubes and hematite flakes, as well as carbonate rhombs.

The fluid inclusions in the comb vein samples from the Box and Athona properties contain a somewhat different assemblage of daughter phases, listed below in order of abundance; (1) Fibrous radial clusters of moderately birefringent phyllosilicate (Plates 5b, 5c, 6b), most likely muscovite, but possibly paragonite, chlorite, or dawsonite

($NaAl(CO_3)(OH_2)$; Coveney, 1981). This daughter is very common, and often fills entire inclusions, either vapour-rich or aqueous (Plates 6b); (2) Very small, adjoined, sub-rectangular pairs, or "twins", are rarely seen as single crystals. These commonly precipitated upon cooling, but only dissolved slightly (?), or were insoluble, upon heating. Athough the crystals are too small to be adequately identified, some form of carbonate is a possibility; (3) NaCl cubes are not as common as from the other occurrences, and are often small. They may be obscured by the muscovite clusters (Plate 5c); (4) Hematite flakes are surprisingly rare, especially as the veins contain abundant hematite as a later phase.

Some of the above listed daughter phases exist as solid inclusions along growth planes in their respective occurrences. The most common solid inclusions are hematite, opaques, and phyllosilicates.

5.2.2 Microthermometric Data

The types of microthermometric data collected from the Au-PGE-U occurrences are similar to those already defined in section 4.2.2. The data must be interpreted in a general way, as necking has heavily influenced homogenization temperatures (Th), dissolution temperatures (Td), and the low temperature data by partitioning vapour and solid phases into later formed, necked-off inclusions. An additional hindrance in interpreting the data is that the phase relations of complex, highly saline, multicomponent brines is poorly understood, and

recent efforts (e.g. Davis et al, 1990) to quantify their behaviour have only been partially successful.

Homogenization temperatures (Th) from all occurrences range from 40 to 400°C (Figures 43 and 44), reflecting the effect of necking of the inclusions (Plate 5c). The median Th for all inclusions from the Nicholson, Fish Hook, and Quartzite Ridge deposits is approximately 140°C. The median Th for the comb veins is slightly higher, at about 160°C. Most inclusions have a fairly constant liquid to vapour ratio (about 10 to 20 volume % vapour), and these inclusions may have formed without undergoing significant necking. Therefore, the measured Th, which closely group around the median values, represent a close approximation of the true Th. Inclusions with lower Th (low vapour/liquid ratio), and especially higher Th (high vapour/liquid ratio), are probably those that underwent necking. In support of this interpretation, one dolomite sample that was analysed (TKK87035, Nicholson No.4 zone) was found to have inclusions with consistant liquid/vapour ratios, which yielded Th of 130 to 140°C (Figure 45), concordant with the average Th for all inclusions (Figure 44). Only a few inclusions, of the approximately 50 measured, have Th outside the median range, suggesting that most of the inclusions were formed without signficant necking.

Halite dissolution temperatures were used to estimate the salinity of the fluids, as recommended by Roedder (1984),

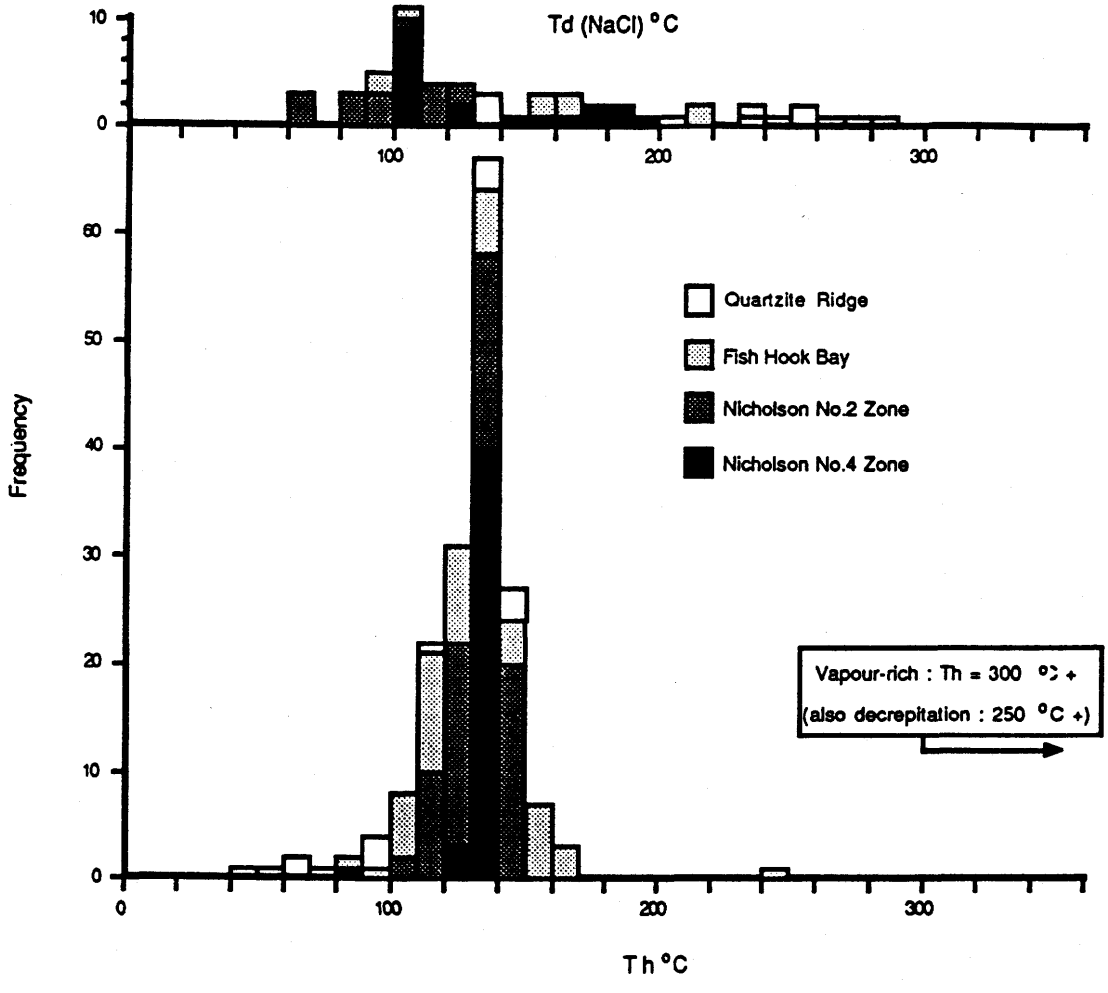

Figure 43: Compilation histogram of homogenization temperatures (Th) and halite dissolution temperatures (Td) from primary and secondary fluid inclusions, Nicholson, Fish Hook Bay, and Quartzite Ridge deposits. The wide range of Th is the result of necking. Some vapour-rich inclusions had Th of 300°C or more, which are not shown, as the median Th of approximately 140°C is more representative of actual fluid temperatures. See text for further discussion.

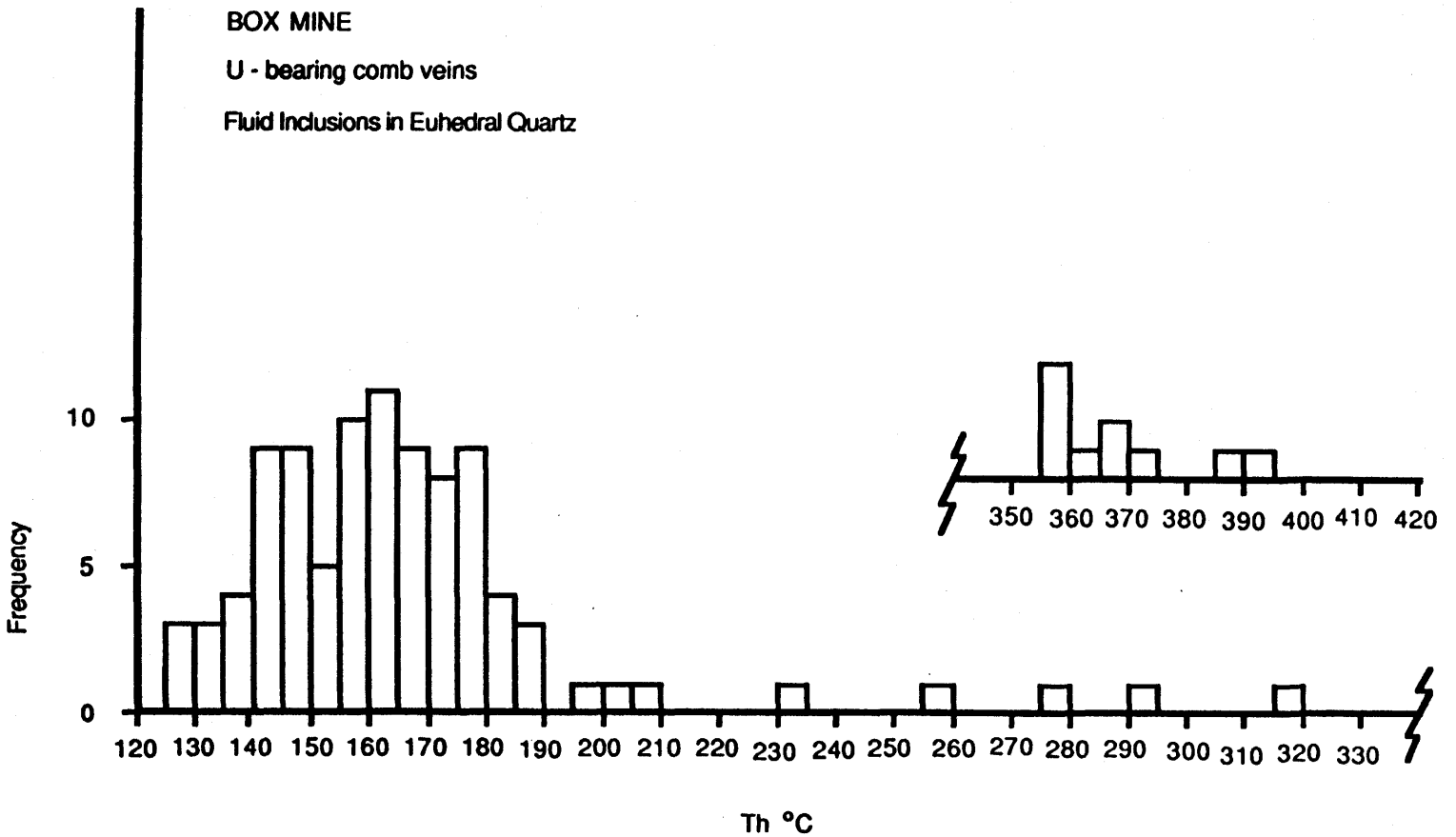

Figure 44: Histogram of homogenization temperatures (Th) of primary fluid inclusions from the cross-cutting comb veins, Box Mine. Median Th is about 160°C, and approximates the actual fluid temperatures indicated by stable isotopic equilibration temperatures of the vein minerals.

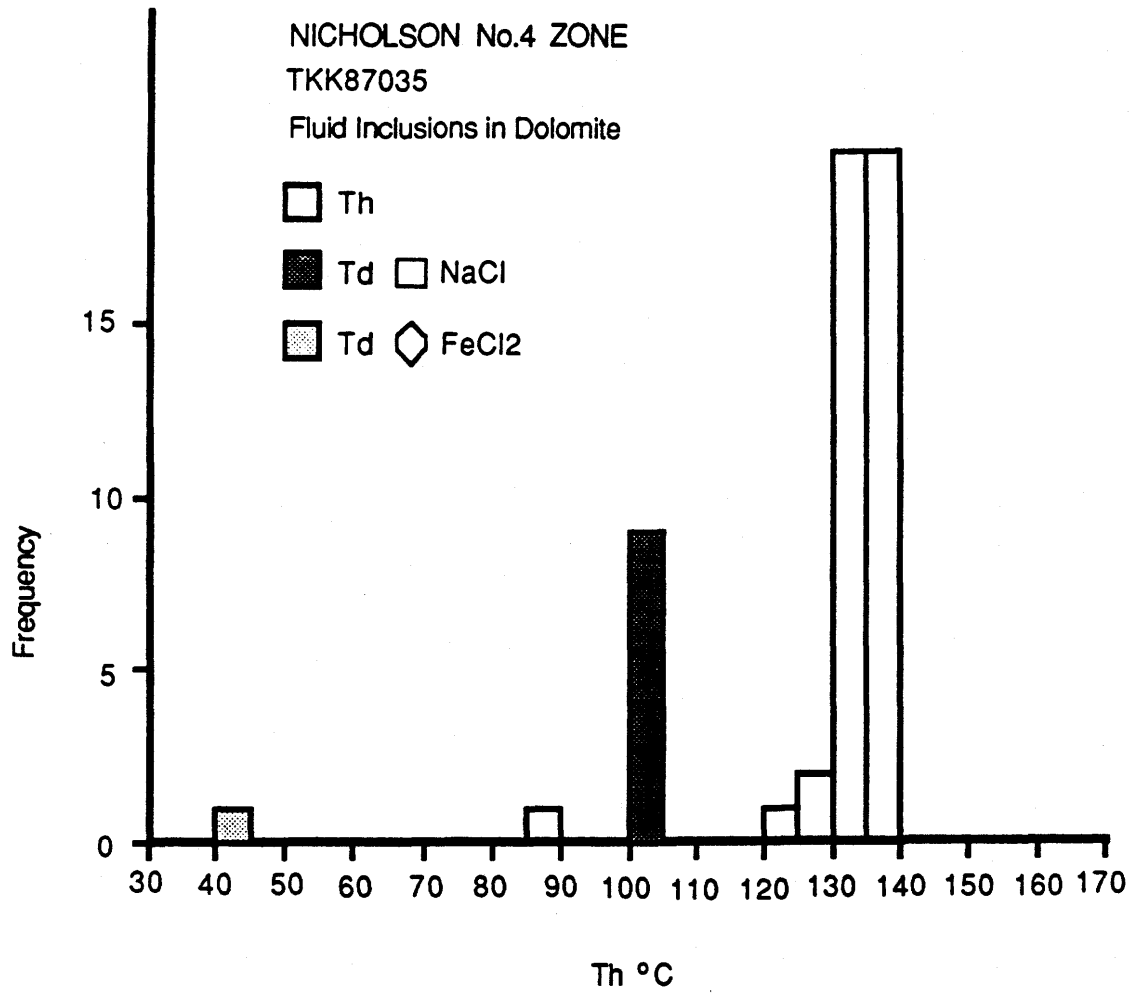

Figure 45: Histogram of homogenization (Th) and NaCl dissolution (Td) temperatures of primary and secondary fluid inclusions in dolomite, Nicholson No.4 zone. Restricted range of Th from un-necked inclusions is the same as the median Th for all Au-PGE-U deposits.

using the graph provided in Shepard et al. (1986). Due to the low slope of the curve at temperatures below 300°C, variations of 100°C (due to necking) only result in a 2 or 3 weight percent variation in salinity, which is negligible in comparison to the high salinities observed. Regardless of the measured salinity, the presence of NaCl daughters indicates salinities of at least 26.6 weight percent NaCl equivalent, which is the saturation point of NaCl in H_2O. Salinity is expressed as NaCl weight percent equivalent (NaCl wt. % eq.), due to the presence of other solutes in the fluid. The presence of other solutes is indicated by the freezing data (see below). Congruency of halite dissolution temperatures (Td) from sample TKK87035 (100 to 105°C, about 28 wt. % NaCl eq.) also indicate that these inclusions probably did not form by necking, as partitioning of solid salts into necked off inclusions will change the bulk salinity of the inclusion, changing the dissolution temperature (Figure 45). Most of the other samples have variable Td, from 60 to 290°C (Figure 43), typically spanning about 100°C, or more, within each deposit (Figures 46 to 49). This corresponds to salinities of approximately 27 to 38 wt. % NaCl eq. For inclusions that are necked, the lower end of their salinity range is probably more indicative of the bulk salinity of the fluid, as partioning a salt cube into a smaller volume of fluid will artificially increase the bulk salinity of the inclusion.

Individually, inclusions from the deposits indicate

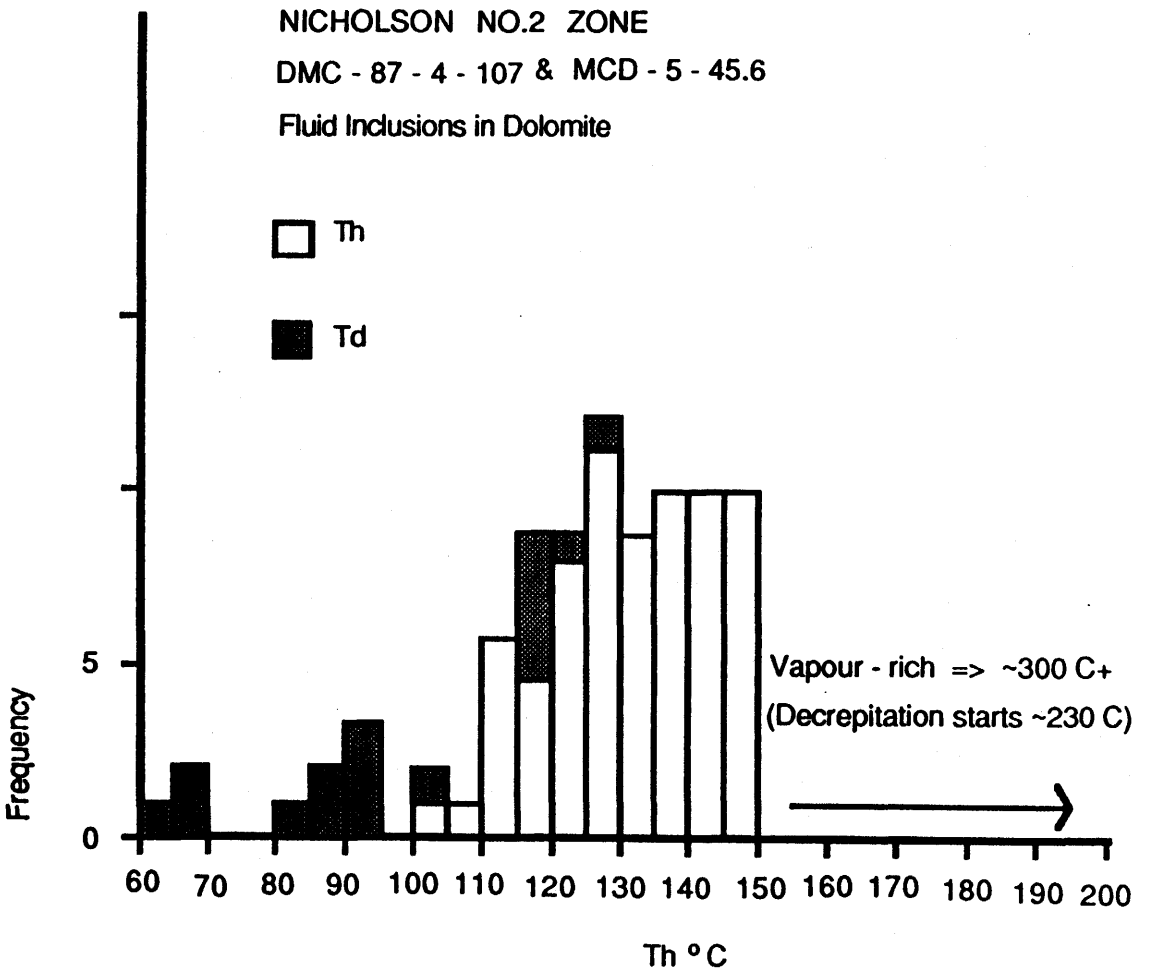

Figure 46: Histogram of homogenization (Th) and NaCl dissolution (Td) temperatures of primary and secondary inclusions in dolomite, Nicholson No.2 zone. Some vapour-rich inclusions have Th greater than 300°C.

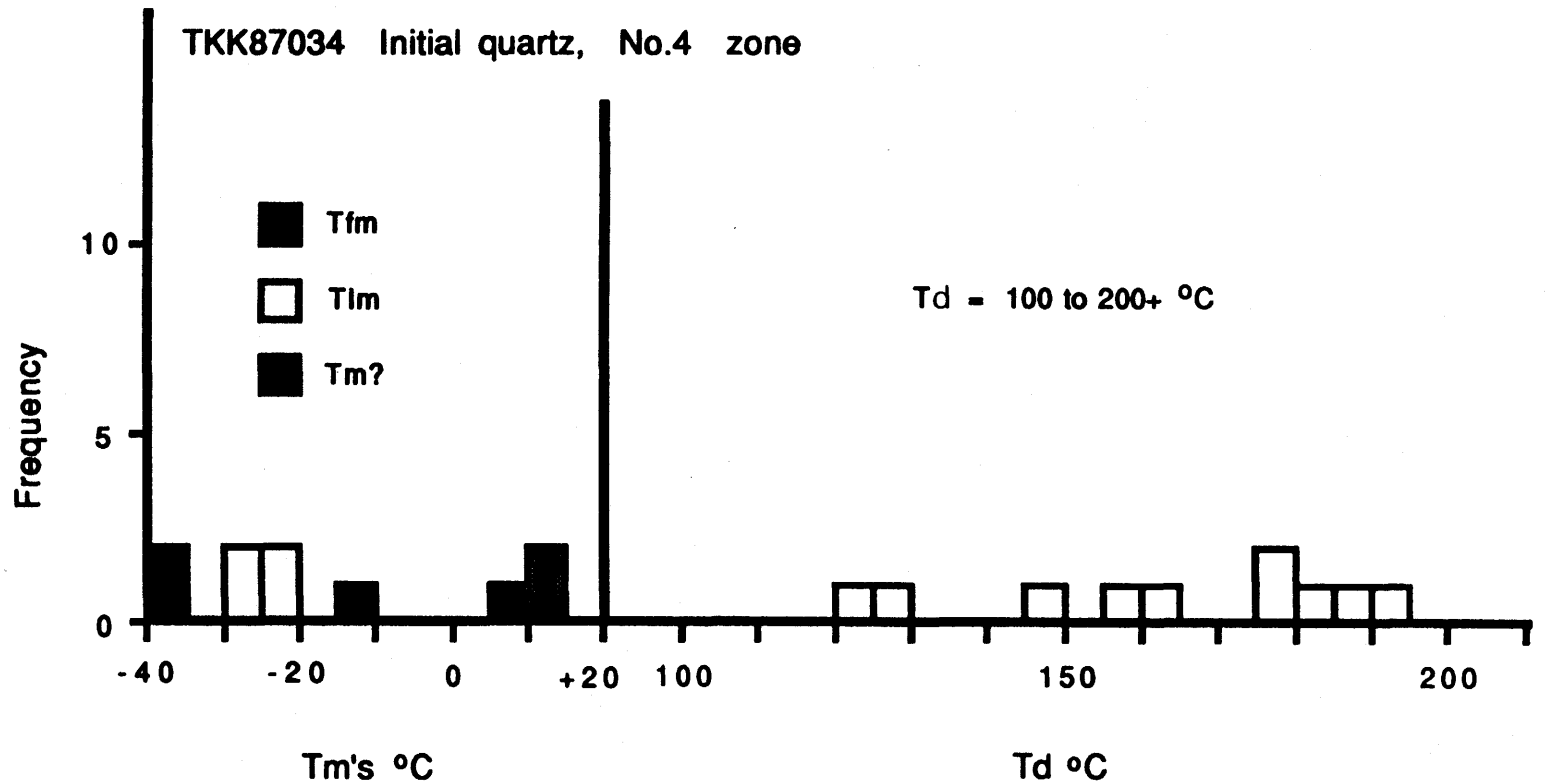

Figure 47: Histogram of NaCl dissolution temperatures (Td) and low temperature microthermetric data from primary fluid inclusions in early quartz, Nicholson No.4 zone. Tfm - temperature of "first melt", or eutectic. Tlm - temperature of "last melt" (ice). Tm? - melting temperature of unknown phase.

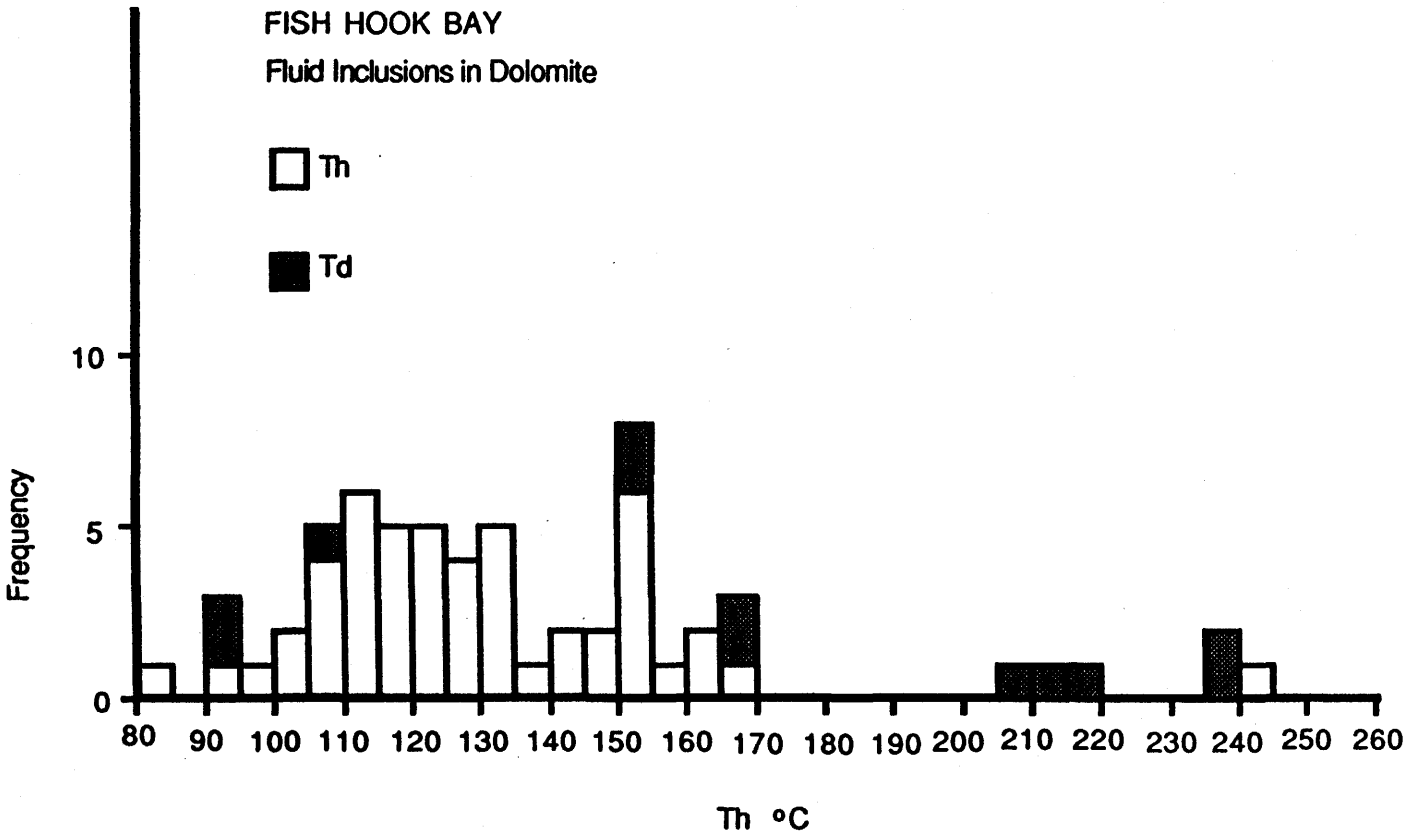

Figure 48: Histogram of homogenization (Th) and NaCl dissolution (Td) temperatures of primary and secondary inclusions in dolomite, Fish Hook Bay deposit.

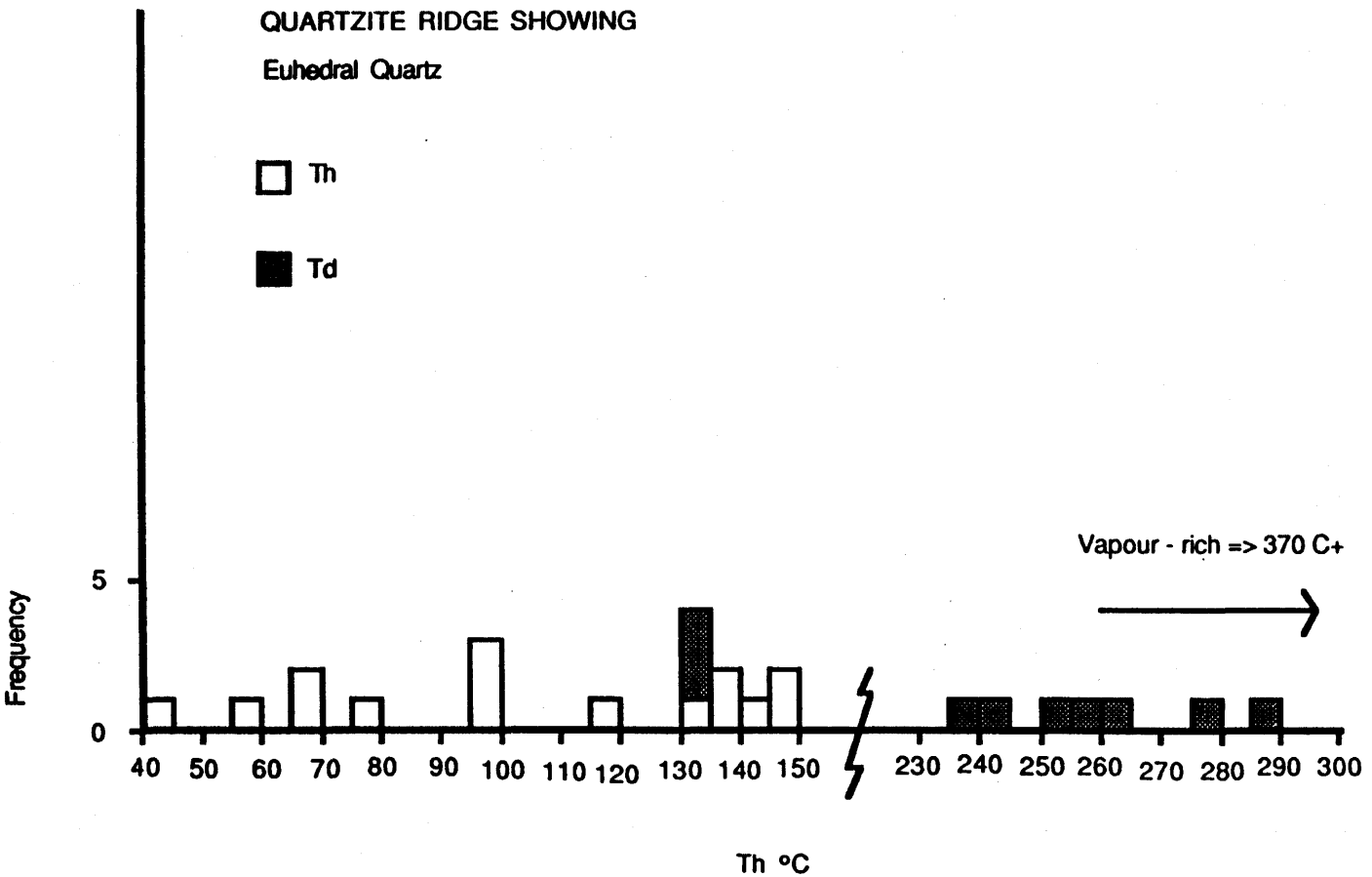

Figure 49: Histogram of homogenization (Th) and NaCl dissolution (Td) temperatures of primary and secondary inclusions in quartz, Quartzite Ridge showing. Some vapour-rich inclusions have Th greater than 370°C (not shown).

salinities as follows: the Nicholson dolomite samples, from zones No.2 and No.4, have Td from 60 to 130°C (Figures 45 and 46), indicating salinities of 27 to 29 wt. % NaCl eq., whereas Nicholson quartz samples have Td from 120 to 195°C (Figure 47), indicating salinities from 29 to 32 wt. % NaCl eq. The Fish Hook dolomite samples have Td from 90 to 240°C (Figure 48), indicating salinities from 28 to 34 wt. % NaCl eq.. Similarly, Quartzite Ridge quartz samples have Td from 130 to 290°C (Figure 49), indicating salinities of 29 to 38 wt. % NaCl eq.. Only one halite dissolution could reliably be observed from the comb vein samples, at a temperature of 360°C, indicating a salinity of 42 wt. % NaCl eq.. One $FeCl_2$ dissolution was observed, at 41°C, in sample TKK87035 (Figure 45), but cannot be interpreted due to the absence of solubility data for the daughter phase.

Freezing data collected from the inclusions is complex and poorly understood, and can only be interpreted semi-quantitatively, due to: (1) the effects of necking (Roedder, 1984), (2) the difficulty in accurately observing the multiple phase changes (Shepard et al., 1986), (3) the metastability of some phases (Davis et al., 1990), (4) the presence of trace components and volatiles that are partitioned into frozen phases (Seitz & Pasteris, 1990), and (5) the incomplete data set on which to model multicomponent brines (Spencer et al., 1990; Oakes et al., 1990). For these reasons, it is impossible to fully and quantitatively interpret the data, and

only general interpretations and conclusions will be discussed.

Data collected from the inclusions consist of a range of phase melting temperatures, including H_2O ice (Tmf - first melt, and Tml - last melt), one or more hydrous salt compounds (Tms), hydrous gas compounds (Tmg), and possibly, hydrous carbonates (Tmc). Although every effort was made to accurately observe phase changes using recommended techniques such as cyclic freezing and slow warming rates, the small size of most inclusions, the difficulty in freezing highly saline inclusions, and the non-refractive nature of many of the phases are problems which often compound each other to virtually invalidate such techniques. Therefore, many melting temperatures were inferred by rapid and sudden bubble movement or expansion, although no solid was readily visible. In some cases only two data points could be collected, at the start and end of a continuum of melting phases, as individual phase melting points could not be distingushed within the block of melting phases.

As a general statement, the ice melting temperatures within inclusions from all of the occurrences confirm that the brines are very saline, as shown by freezing point depressions (Tml) to as low as -28°C. Additionally, several solute species besides Na^+ and Cl^- are indicated by Tmf (eutectic) well below the eutectic temperature of the $NaCl-H_2O$ system at -20.8°C, as well as the light brown colouration of the frozen

inclusion, which indicates the presence of Mg^{+2} or Ca^{+2} in the fluid (Shepard et al., 1986).

The Nicholson samples have the largest low temperature data suite, with well over 50 separate measurements from dolomite- and quartz-hosted inclusions. The Tml_{H2O} range from -28.0 to -22.6°C, indicating high salinities, while Tmf, when observed, ranged from -41.0 to -35.3°C, and in one inclusion was tenatively observed at approximately -50°C. Eutectic temperatures this low indicate that the fluids are not simple H_2O-NaCl systems, but contain cations such as Fe^{+2}, Mg^{+2}, and Ca^{+2}. Other melting temperatures observed in the inclusions range from -16 to -11°C, -3 to -0.5°C, +0.9 to +1°C, +4.5 to +10°C, +13.1 to +14.6°C, and +23 to +45°C. The first and last temperature ranges were only indicated by a rapid shift in the bubble position within the inclusion, and not all temperature intervals were observed in every inclusion, but the data indicate that up to 7 different phases may have been precipitated upon freezing. As an example, the range of low temperature data from inclusions hosted in euhedral quartz from the Nicholson No.4 zone is illustrated in Figure 47.

The phases that are melting at these temperature intervals are one or more of various hydrous salts (e.g. Hydrohalite: $NaCl.2H_2O$, Antarcticite: $CaCl_2.6H_2O$, and $MgCl_2.12H_2O$), with the possibility of gas hydrates (e.g. Clathrate: $CO_2.5^3/_4H_2O$) and hydrous carbonates (e.g.

$Na_2CO_3.10H_2O$). A curious phenomenon was observed during cooling of the Nicholson inclusions, as the bubble would often expand in area by about 15 to 25%. This is thought to represent minor to trace amounts of gases in quantities too small (or too soluble) to form a separate bubble, being partitioned into the vapour phase as a result of decreased solubility within the liquid. Likely gases would be CO_2 or SO_2, which may be later incorporated into frozen phases (Seitz & Pasteris, 1990).

Freezing data collected from the Fish Hook samples appeared to bear an overall similarity to that from the Nicholson samples, but the small inclusion size made accurate data collection impossible.

The Quartzite Ridge freezing data is similar to the Nicholson data, but only a few inclusions were studied due to the extreme difficulty encountered in getting the inclusions to freeze. Tml occurred at -37°C, with three other phases melting at -18 to -15°C, -3 to -2°C, and +4.6 to +5.0°C.

The comb veins also have a large freezing data set, with 30 separate measurements. As with the Quartzite Ridge samples, the Tmf was never observed, but Tml ranged from -25.3 to -22.4°C, with four more phases melting at -10.5 to -9.4°C, -5.2 to -4.2°C, -2.1 to -0.2°C, and +5 to +6°C.

5.2.3 Discussion of Data

Petrographic and microthermometric examination of quartz- and dolomite-hosted fluid inclusions associated with Au-PGE-U

mineralization has shown that the mineralizing fluids were highly saline (about 30 to 40 wt. % NaCl eq.) chloride brines, at low to moderate temperatures, probably between 100 and 200°C. These data are summarized in Figure 50, which includes the fluid inclusion data from the lode-gold veins for comparison. Freezing data clearly show that the chemical composition of the brines is very complex, but is in the system H_2O-NaCl-$FeCl_2$-$MgCl_2$-$CaCl_2$-CO_3^{+2}-($\pm CO_2$, $\pm SO_2$?). The fluid inclusions in the comb veins appear to have a somewhat different chemical composition, due to the presence of unique phyllosilicate daughter phases. The absence of phyllosilicate daughters in the "sponge rock" dolomite suggests that it is more closely related to the fluids observed at the Nicholson and Quartzite Ridge deposits.

Other trace components present in the fluids may include hydrocarbons (i.e. hydrocarbon buttons in Nicholson and Fish Hook veins), hydrogen gas, and methane (Debussey et al., 1988).

The brines are very oxidizing, as shown by the extensive hematitic alteration around the deposits, and hematite daughter crystals within the fluid inclusions. Brines of this nature are readily able to transport Au, PGE, and U as chloride complexes, as shown by Mountain & Wood (1988), Wilde & Bloom (1988), and Jaireth (1988). Wilde & Bloom (1988), working on Australian unconformity-type deposits in the Alligator Rivers Uranium Field, such as Jabiluka and

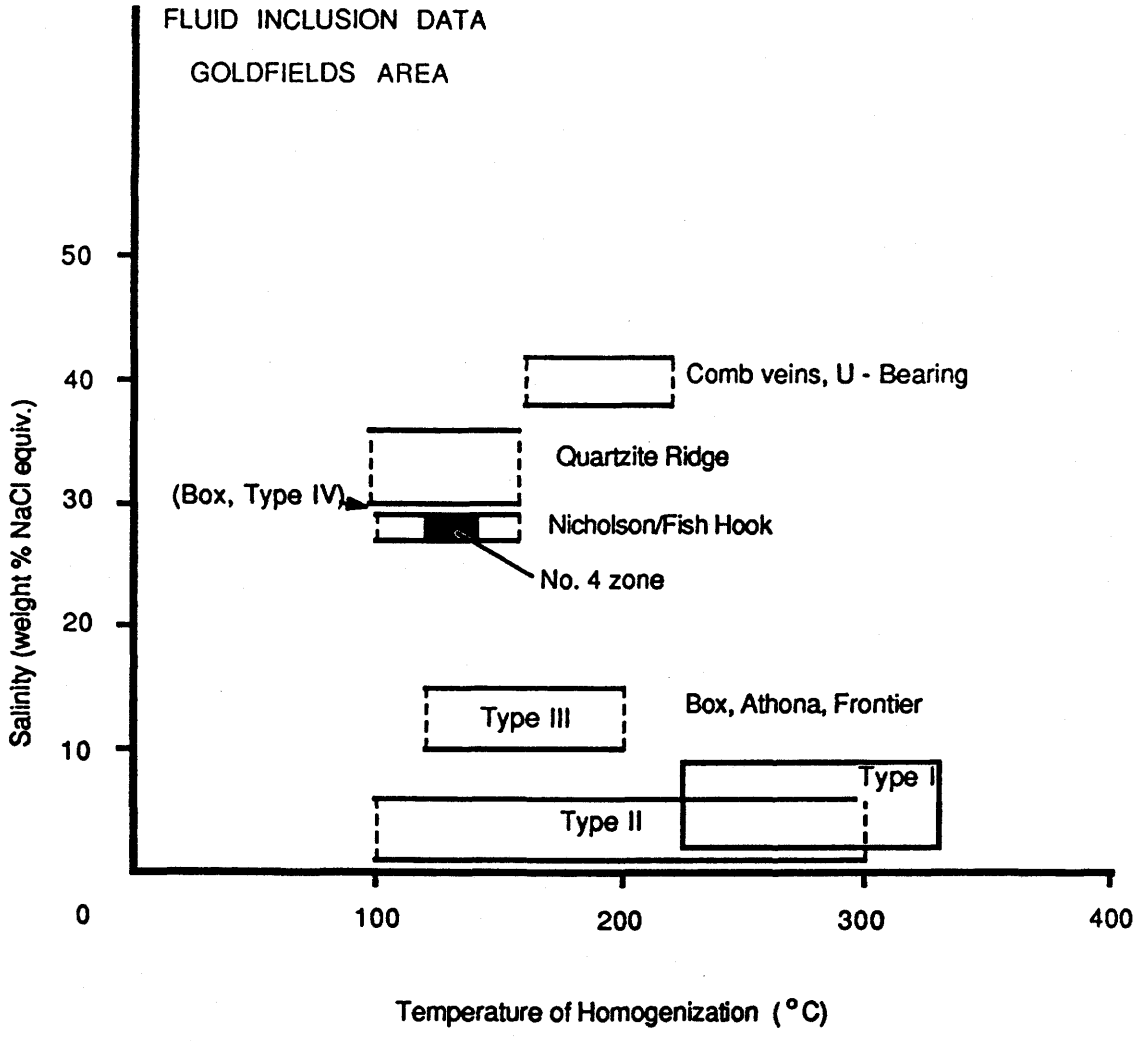

Figure 50: Summary of fluid inclusion data from the Au-PGE-U deposits, Goldfields area, showing relation between approximate homogenization temperatures and fluid salinities. Inclusion types from the lode-gold veins are shown for reference. Note the similarity between Type IV secondary inclusions from the Box veins, and primary inclusions from the Nicholson, Fish Hook Bay, and Quartzite Ridge deposits. Dashed lines indicate the uncertainty of the homogenization temperatures.

Coronation Hill, suggest that deposition of the metals occurs by redox reaction as the oxidized brines encounter reducing conditions (e.g. at Nicholson, faults in pyritic basement rocks). Fluid inclusions from the Jabiluka, and several other nearby deposits (Wilde et al., 1989) are very similar to the Goldfields Au-PGE-U related fluid inclusions.

Fluid inclusions from the Goldfields Au-PGE-U deposits are remarkably similar in their salinities to fluid inclusions observed in euhedral quartz associated with the MacArthur River and Eagle Point unconformity-type uranium deposits (Kotzer & Kyser, 1990), as well as at other locations within in the Athabasca basin (Pagel et al., 1980). This suggests that similar basinal-type fluids were involved in both types of mineralization, and that they may be broadly contemporaneous.

5.3 Stable Isotopic Data

5.3.1 Isotopic Compositions & Isotopic Geothermometry

To complement the fluid inclusion data, oxygen isotopic analyses were made of co-existing euhedral quartz, euhedral dolomite, and crystals of specular hematite from the Nicholson, Quartzite Ridge, and comb vein deposits, as well as "sponge rock" dolomite from the Athona mine granite. The data are summarized in Figure 51 and Appendix 3. Carbon isotopic data were also collected for the dolomite separates. Hydrogen isotopic compositions were determined by the direct analysis

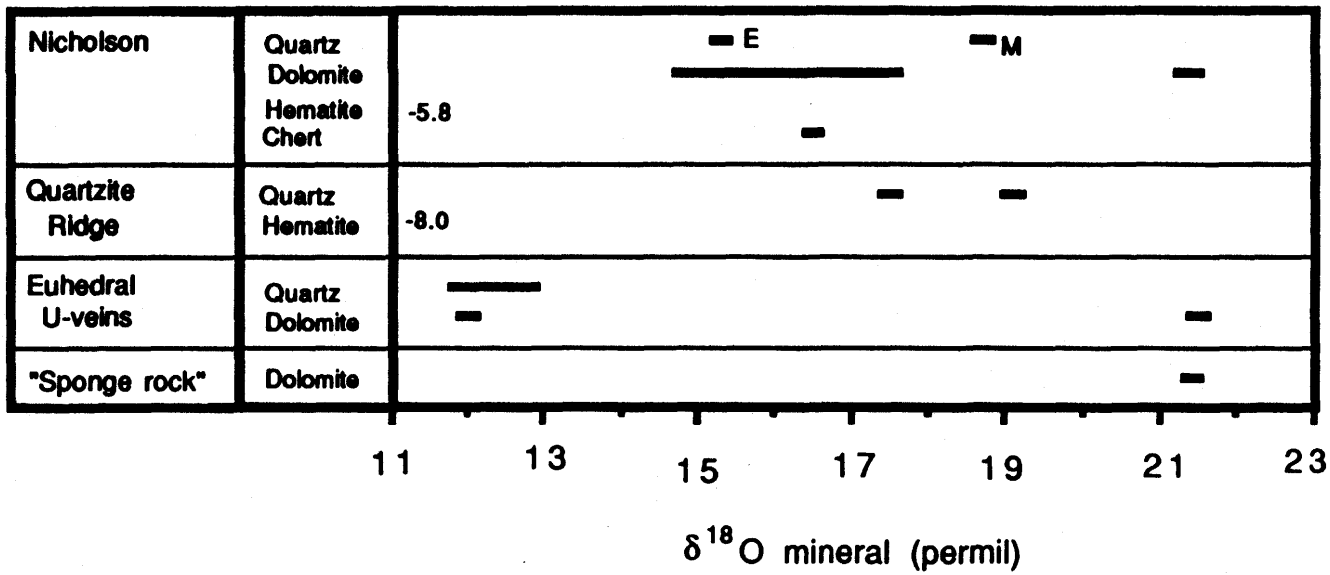

Figure 51: Summary of $\delta^{18}O$ values of vein minerals from the Au-PGE-U deposits, Goldfields area. E = early euhedral quartz along vein edges, M = later euhedral quartz from middle of vein. "Chert" is a sample of the fine-grained silica alteration that envelopes the vuggy vein cavities. Data are from Appendix 3.

of water derived by thermal decrepitation of fluid inclusions hosted in quartz and dolomite from Nicholson, Quartzite Ridge, and comb vein samples. Direct analysis of inclusion water is possible because only one generation of inclusions (primary) is present within the vein minerals.

The oxygen isotopic composition of vein quartz from the Au-PGE-U deposits ranges from 11.8 to 19.1 per mil, and is distinct from that of the lode-gold veins (Figure 51). One sample of silica alteration from the Nicholson deposit fell within this range, at 16.5 permil, showing that the veins and silica alteration are associated with the same fluids. Within the data set, there are two groups, that of the comb veins, with lower $\delta^{18}O$ values of quartz from +11.8 to +12.9, and the Nicholson and Quartzite Ridge veins, which have $\delta^{18}O$ values for quartz of +15.3 to +19.1 per mil (Figure 51). This implies that the comb veins were emplaced at a higher temperature, or from a fluid of a different isotopic composition, possibly reflecting buffering of the fluid by the local host rocks (i.e., the isotopic composition of the comb veins bears an overall similarity to that of their mine granite hosts).

The $\delta^{18}O$ values of dolomite from the Nicholson veins, comb veins, and "sponge rock" zones vary from +12 to +21.5 per mil (Figure 51), with $\delta^{13}C$ values from -3.5 to -8.2 per mil (Appendix 3). The cause of this wide variation in the isotopic compositions of dolomite is not clear; it may be due to changes in fluid composition or temperature, but is most

likely due to isotopic exchange with late meteoric waters. The variation in $\delta^{13}C$ values probably reflects the incorporation of country rock carbon (e.g. graphite), with a lower $\delta^{13}C$ value, into the vein dolomite.

The oxygen isotopic compositions of two vein hematite samples were -5.8 permil and -8.0 permil, from the Nicholson and Quartzite Ridge deposits, respectively (Figure 51).

Overall, the range of euhedral quartz $\delta^{18}O$ values from the Goldfields deposits are similar to those reported for euhedral quartz associated with unconformity-type uranium deposits in the Athabasca basin, from +11.5 to +16 per mil, as well as diagenetic euhedral quartz overgrowths of the sandstone, at approximately +14 per mil (Kotzer & Kyser, 1990). Similarly, euhedral dolomites also have oxygen and carbon isotopic compositions similar to euhedral dolomite associated with unconformity-type uranium deposits, which have $\delta^{18}O$ values of approximately +13 to +15 per mil, and $\delta^{13}C$ values of approximately -4 to -8 per mil (Kotzer & Kyser, 1990).

Co-existing mineral pairs from the Nicholson, Quartzite Ridge and comb veins were used to calculate oxygen isotopic equlibration temperatures, indicating the temperature of vein emplacment (see below, or Appendix 3). Notably, the calculated isotopic temperatures are similar to the median homogenization temperatures suggested for the fluid inclusions, indicating that the majority of the inclusions provide useful data, even though necking has occurred.

Two Nicholson samples, TKK87034 (No.4 zone) and MCD5-45.6 (high-grade portion of No.2 zone), were used to calculate isotopic equilibration temperatures. Early euhedral quartz and later euhedral dolomite from sample TKK87034, collected from outcrop, were not in equilibrium, as indicated by a negative value for their quartz-dolomite fractionation. This is not unexpected, as the early quartz is a minor phase within the vein, representing the earliest phases of vein emplacement. As well, the quartz is coated with a thin layer of hematite, suggesting a hiatus may have occurred before dolomite deposition, during which time a change in fluid temperature or composition may have occurred. Sample MCD5-45.6, a piece of drill core from the footwall of the No.2 zone, provided co-existing euhedral quartz, euhedral dolomite, and specular hematite. Petrographic relations indicate that all of the phases are in textural equilibrium. In this sample, quartz occurs as sporadic clusters of several crystals within the central portions of the vein. Because three different minerals co-exist, three separate equilibrium temperatures can be calculated, providing an internal check on the calculated isotopic equilibrium temperatures. The quartz-hematite fractionation of 24.5 per mil yields a temperature of 80 to 110°C (Becker & Clayton, 1976), the quartz-dolomite fractionation of 2.2 per mil yields a slightly higher temperature of 100 to 120°C (Matthews & Katz, 1977), and the dolomite-hematite fractionation of 22.3 per mil results in a

similarly concordant temperature of 80 to 115°C. These isotopic temperatures suggest a vein formation temperature of approximately 100 to 110°C.

Co-existing euhedral quartz and specular hematite from the Quartzite Ridge core samples (QR-87-3, 1.9 + 4.6m) yield isotopic equilibration temperatures of 110 to 125°C, from a quartz-hematite fractionation of 25.5 per mil. This is similar to the isotopic equilibrium temperatures for the Nicholson samples, suggesting a genetic similarity between the two deposits.

The $\delta^{18}O$ values of co-existing euhedral quartz and dolomite from the comb veins at both the Box (BX87008) and Athona (AT87011) properties were used to calculate isotopic equilibration temperatures. The quartz-dolomite fractionation from the Box sample is -9.7 per mil, indicating significant disequilibrium between the two phases, probably as a result of isotopic exchange between the dolomite and later, low-temperature fluids. The dolomite also appears very weathered, implying significant interaction with meteoric water. As with sample TKK87034, a hiatus between quartz and dolomite deposition is indicated by a very thin layer of hematite that coats the quartz crystals. The quartz-dolomite fractionation of the Athona sample is 0.9 per mil, which indicates a temperature of approximately 175°C. The slightly higher temperature of the comb veins, along with their differing fluid chemistry, are compatible with them being products of a

different fluid event than the lower temperature Au-PGE-U veins.

Stable isotopic compositions of clay minerals and quartz from unconformity-type uranium deposits in the Athabasca basin indicate that the basinal brines were at temperatures near 200°C (Kotzer & Kyser, 1990), about 75 to 100°C higher than the fluid temperatures indicated for the Nicholson and Quartzite Ridge deposits. Only the comb veins have temperatures similar to the unconformity-type deposits, which, in conjunction with the similarities in the chemical characteristics of the fluids, implies a possible genetic relationship.

5.3.2 Fluids in Equilibrium with Minerals

Two methods were used to determine the stable isotopic composition of the fluids that were in equilibrium with the veins. The oxygen isotopic composition of a fluid was calculated from the $\delta^{18}O$ value of quartz, using the temperatures calculated from the corresponding quartz-dolomite or quartz-hematite mineral pairs. The δD value of the fluid was determined by thermal decrepitation of fluid inclusions within quartz and dolomite.

For the Nicholson deposit, quartz from sample MCD5-45.6, at 100 to 110°C, is calculated to be in equlibrium with water that has a $\delta^{18}O$ value of 1 to 2.2 per mil. If the same temperatures are used for the early quartz from sample TKK87034, they yield a $\delta^{18}O$ of -4.3 to -5.6 per mil for the

fluid. The fine-grained silica alteration, at 100 to 110°C, would be in equilibrium with similar water, having a $\delta^{18}O$ value of about -4 per mil. The total range of $\delta^{18}O_{H2O}$ values for all Nicholson dolomites, at 100°C, is from -4.3 to +2.7 per mil, so that the total range of $\delta^{18}O$ values of the fluids that were in isotopic equilibrium with minerals from the Nicholson samples is between about -5 and +3 per mil.

Quartz from the Quartzite Ridge samples would be in isotopic equilibrium, at 115°C, with water that has a $\delta^{18}O$ value of 0.1 to 1.6 per mil, very similar to that of the Nicholson deposit.

At 175°C, euhedral quartz in the comb vein samples would be in equilibrium with a fluid that had a $\delta^{18}O$ value of 0 to -1.6 per mil. Comb vein dolomites with the lowest $\delta^{18}O$ values, which appear to have retained their original isotopic compositions, would be in equilibrium with fluids that had $\delta^{18}O$ values near 0 per mil.

As there is only one generation of fluid inclusions within the minerals, the hydrogen isotopic composition of the fluid was determined by the direct analysis of water collected by thermal decrepitation of primary fluid inclusions within euhedral quartz and dolomite. Six samples were analysed for the δD value of inclusion fluids, including three from Nicholson, two from the comb veins, and one from Quartzite Ridge. The Nicholson samples included early quartz (TKK87034), late quartz (MCD5-45.6), and a dolomite (MCD5-

45.6), which had δD_{H2O} values of -94, -92, and -90 per mil, respectively (Appendix 3). Three dolomite samples collected on the surface gave aberrant values of -117 to -140 per mil, due to contamination by relatively recent meteoric waters, with low δD values, that are held between cleavage planes, and released upon heating. Quartz crystals, and dolomite samples from drill core, are not susceptible to this contamination. Inclusion fluids in quartz from the Quartzite Ridge sample (QR-87-3) produced a similar result, with a δD value of -89. Two samples of quartz from the comb veins, BX87008 and AT87011, have fluid δD values markedly lower at -58 and -55, respectively (Appendix 3). The large difference in δD values between the comb veins and the Au-PGE-U veins indicates they were not formed during the same fluid event, even though the fluids have similar calculated $\delta^{18}O$ compositions.

5.4 Discussion and Summary

The δD and $\delta^{18}O$ values of the fluids that were in equilibrium with gangue minerals in the Au-PGE-U deposits, and the U-bearing comb veins are summarized in Figure 52. The comb vein fluids are similar in isotopic composition to basinal brines from the Athabasca basin, as determined by Wilson & Kyser (1987), and Kotzer & Kyser (1990), by stable isotopic studies on minerals from unconformity-type uranium deposits and basinal sandstones. The similarity of fluid isotopic compositions, temperatures, and high salinities (approximately 30 to 40 wt. % NaCl eq.) implies that the comb

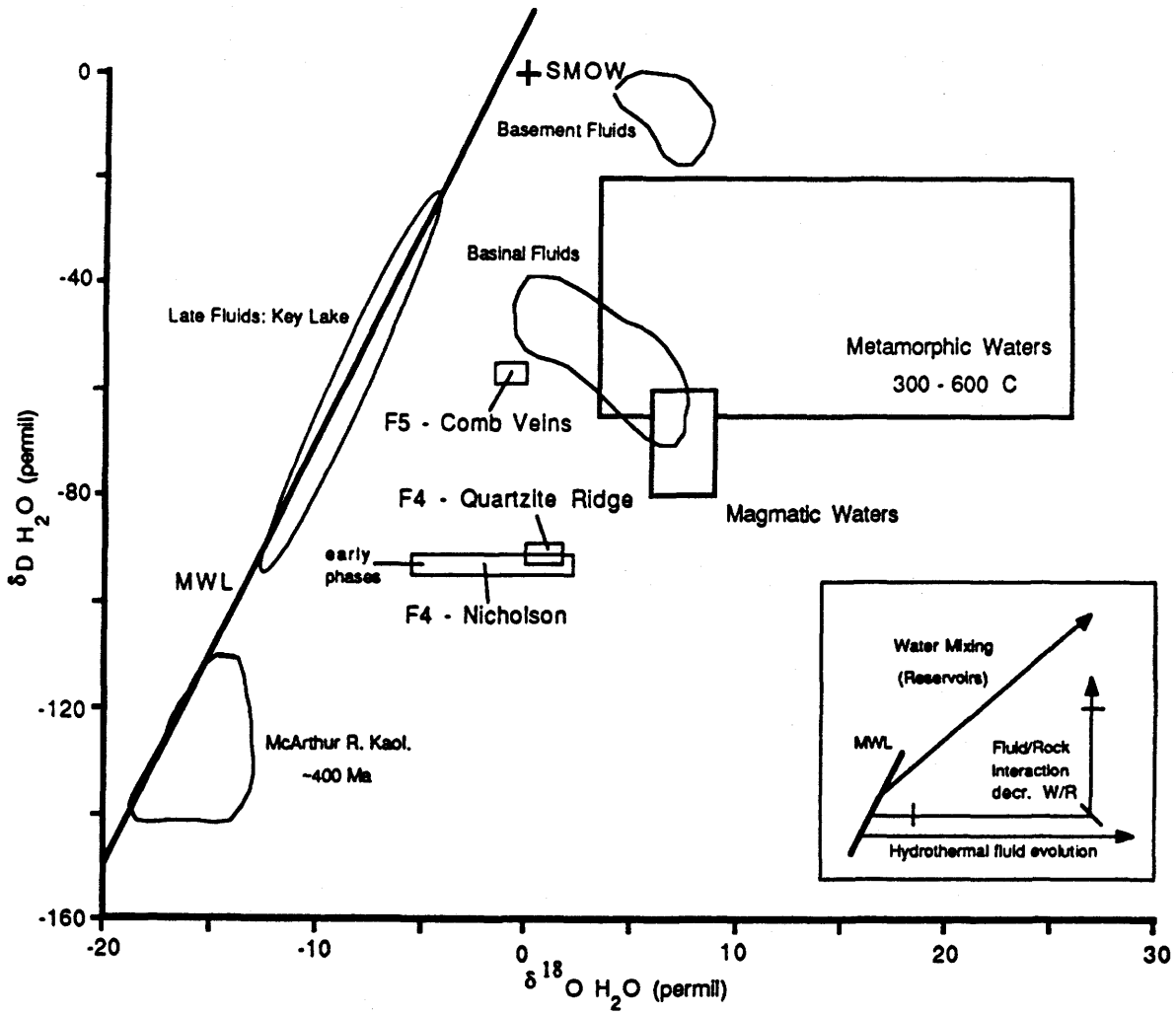

Figure 52: Relation between $\delta^{18}O$ and δD values of water in equilibrium with vein minerals from Au-PGE-U deposits, Goldfields area: F4 - fluids in isotopic equilibrium with quartz and dolomite, at 100 to 110°C, from the Nicholson deposit, and with quartz, at 115°C, from the Quartzite Ridge deposit. Included are isotopic compositions for water in equilibrium with silica alteration and early quartz from the Nicholson deposit; F5 - fluids in isotopic equilibrium with quartz and dolomite, at 175°C, from the U-bearing comb veins. Value of basin waters in equilibrium with minerals from unconformity-type uranium deposits in the Athabasca basin are also shown (Wilson & Kyser, 1987; Kotzer & Kyser, 1990). Other water values indicated are those in equilibrium with clay minerals from the Athabasca basin (Wilson & Kyser, 1987). All other information is referenced in Figure 37.

veins are associated with the same fluid event that produced peak diagenesis and unconformity-type uranium mineralization within the Athabasca basin. However, the isotopic composition of fluids associated with the Nicholson and Quartzite Ridge deposits (and by association, the Fish Hook Bay deposit and "sponge rock" alteration of the mine granites) are distinctly different in their δD values and calculated temperatures from the comb veins fluids, even though the salinities and δ^{18}O values of the fluids are similar. Therefore, the Au-PGE-U vein deposits have fluid histories that are somehow distinct from the fluids associated with the mineralizing and diagenetic processes within the Athabasca basin.

Efforts to date the uranium mineralization in the Nicholson deposits, by Koeppel (1968), and Kyser et al. (1990), using U-Pb techniques, have so far proved inconclusive due to later multiple reworking of the U-Pb system by secondary fluids (minimum ages were determined of ca. 1.0 to 1.25 Ga). The age of the mineralizing event is important, because changes in latitude due to continental drift will affect the isotopic composition of the basinal fluid, especially its δD value.

The hydrogen isotopic composition of a fluid is also a function of its source, so that the basinal brines associated with the Au-PGE-U mineralization may have originated, in whole or in part (mixed with Athabasca fluid?), within the slightly older Martin basin, or an unrecognized "proto-Athabasca"

basin, instead of the Athabasca basin. This implies that the Martin Group sediments (or other sediments) once onlapped the Goldfields area, covering a larger area than their present exposure suggests. If this is the case, the mineralization may be older than that of the unconformity-type uranium deposits, or the complex-vein type uranium deposits. If the mineralization is not related to fluids from the Martin basin, a fluid source within the Athabasca basin is a possibility. However, it is unlikely that this fluid originated within a "sub-basin" of the Athabasca basin, because such a fluid is not recorded anywhere else in the Athabasca basin. This would imply that the most reasonable explanation for the difference in the isotopic composition of the fluids associated with the Au-PGE-U deposits and the comb veins is related to differences in the probable ages of the mineralization types, which resulted in distinct hydrogen isotopic compositions as a result of latitude changes. Whether or not these basinal fluids were mixed with an Athabascan basinal fluid is not known. There are only two time periods at which the Beaverlodge area was at the approximate latitude (Kotzer et al., 1992a) to have a δD value around -90 per mil: (1) initially, ca. 1.7 to 1.5 Ga, very early in the development of the Athabasca basin, by which time the Martin (or other) basin had already formed and was most likely diagenetically evolving, implying that the mineralization was influenced by fluids from the Martin basin, or an unknown "proto-Athabasca"

basin; (2) from ca. 1000 to 900 Ma, suggesting a much younger age for the mineralization, such as is observed in some uranium deposits associated with the Athabasca basin. Illite from the Eagle Point deposit has an age of ca. 950 Ma, but the δD value of the mineralizing fluids are approximately -65 per mil (Kotzer & Kyser, 1990), similar to other unconformity-type uranium deposits in the Athabasca basin, implying that basinal fluids of this age are not related to Au-PGE-U vein mineralization in the Goldfields area.

Chert and hematite altered outliers of sandstone near the Nicholson deposit are suggested by Sibbald (1988) to be remnants of Athabasca sandstone, and that the similarity of this alteration to the alteration that accompanies the Nicholson Au-PGE-U mineralization implies the mineralizing fluids were derived from the Athabasca basin. However, the $\delta^{18}O$ value of the chert alteration from one of the outliers is approximately 21 per mil (Kotzer, pers. comm.), which is several per mil more enriched in $\delta^{18}O$ than quartz and chert samples from the Nicholson mineralization (Figure 51), or quartz alteration from the Athabasca basin (Kotzer & Kyser, 1990). Therefore, the isotopic data indicate that the sandstone outliers cannot be presently related to the Nicholson mineralization with certainty.

6.0 Summary and Conclusion: Fluid Event Models

The objective of this study was to delineate the fluid history of the Goldfields area, using various vein-type deposits as "records" of fluid events, and the relationship of these "local" events to the fluid history of the greater Beaverlodge area during its complex thermotectonic evolution. The interpretation of fluid inclusion, stable isotope, and radiogenic isotope data from the veins and mine granites has identified up to six fluid events (Figure 53), occurring from ca. 2.0 to 1.0 Ga.

The first fluid event identified (F1, Figure 53) occurred at ca. 1.97 to 1.95 Ga (O'Hanley et al., 1991), when the mine granites were formed as nearly in-situ melts in the presence of a "metasomatic" fluid. The origin of the event is attributed to the burial of the Murmac Bay Group, presumably in a subduction setting, during the Thelon-Talston orogeny at ca. 2.0 to 1.9 Ga (Hoffman, 1991; see Figure 54). $\delta^{18}O$ values of the granite minerals indicate an isotopic closure temperature for this event of 550 to 650°C, and that the "metasomatic" fluids may be related to magmatic activity that occurred at deeper structural levels in the subduction zone. The development of a regional foliation, D1, may have occurred during the earlier stages of this event as well. The Thluicho Lake Group may be the remnants of a turbidite basin that

THERMOTECTONIC EVENT (STRUCTURAL)	TEMP & SALINITY OF FLUID INCLUSION EVENT	TEMPERATURE OF STABLE ISOTOPE FLUID EVENT	AGE (Ga)	BEAVERLODGE AREA
Murmac Bay Group Deposition	——	——	2.5 - 2.0	Continental Platform, Marginal to Extensional Tectonics?
D1 (Thelon Orogen?)	——	——	< 2.5 > 2.0	L. Amph. to Gran. Metamorphism Regional Foliation (S1)/Older Granite
Thelon Orogen (Talston Magmatism)	——	F1- Metasomatic closure at 550-650 C	1.97 - 1.95	Burial: Mine Granites Thuiluco Basin?
D2: Early Hudsonian Orogen, Churchill/Arc or Rae/Hearne	I + Ia 250 - 350 C 0 - 10 wt. % NaCl eq.	F2 + F3 - Metamorphic 300 - 400 C	1.85 - 1.84 (Lode Au)	Compressional Uplift: Greenschist Retrograde Goldfields Synclinorium/Au-mineralization
D2: Middle Hudsonian, Churchill/Superior Continued Uplift	II 100 - 300 C 0 - 10 wt. % NaCl eq.	——	1.84 - ca. 1.75 ?	Simple-type U Veins? Late 1.78 - 1.74 Ga Overprint Fault Reactivation: Martin Basin ?
Martin Group deposition	IV + Au-PGE--U inclusions 100 - 200 C 28 - 36wt. % NaCl eq.	F4 - Basinal Fluids 100 - 120 C	ca. 1.8 - 1.7 ?	Fault Reactivation: Martin Basin Diagenesis ? U-PGE-Au Mineralization "Sponge Rock"
Athabasca Group deposited Early to Peak Diagenesis & BasinalFluid Flow	III 100 - 200 C 10 - 15 wt. % NaCl eq. Comb Vein inclusions 100 - 200 C 40 wt. % NaCl eq.	F5 - Basinal Fluids 175 C	ca. 1.6 - 1.0	Early diagenesis (Type III inclusions) to Peak diagenesis Unconformity -type U-mineralization (Complex-type veins) Comb Veins

Figure 53: Summary diagram of fluid events in the Goldfields area, recorded by fluid inclusions in vein-type deposits and stable isotopic compositions of minerals, as they relate to thermotectonic events in Beaverlodge region. Ages indicated are from O'Hanley et. al. (1991), and Kotzer et. al. (1992). See text for discussion of correlations.

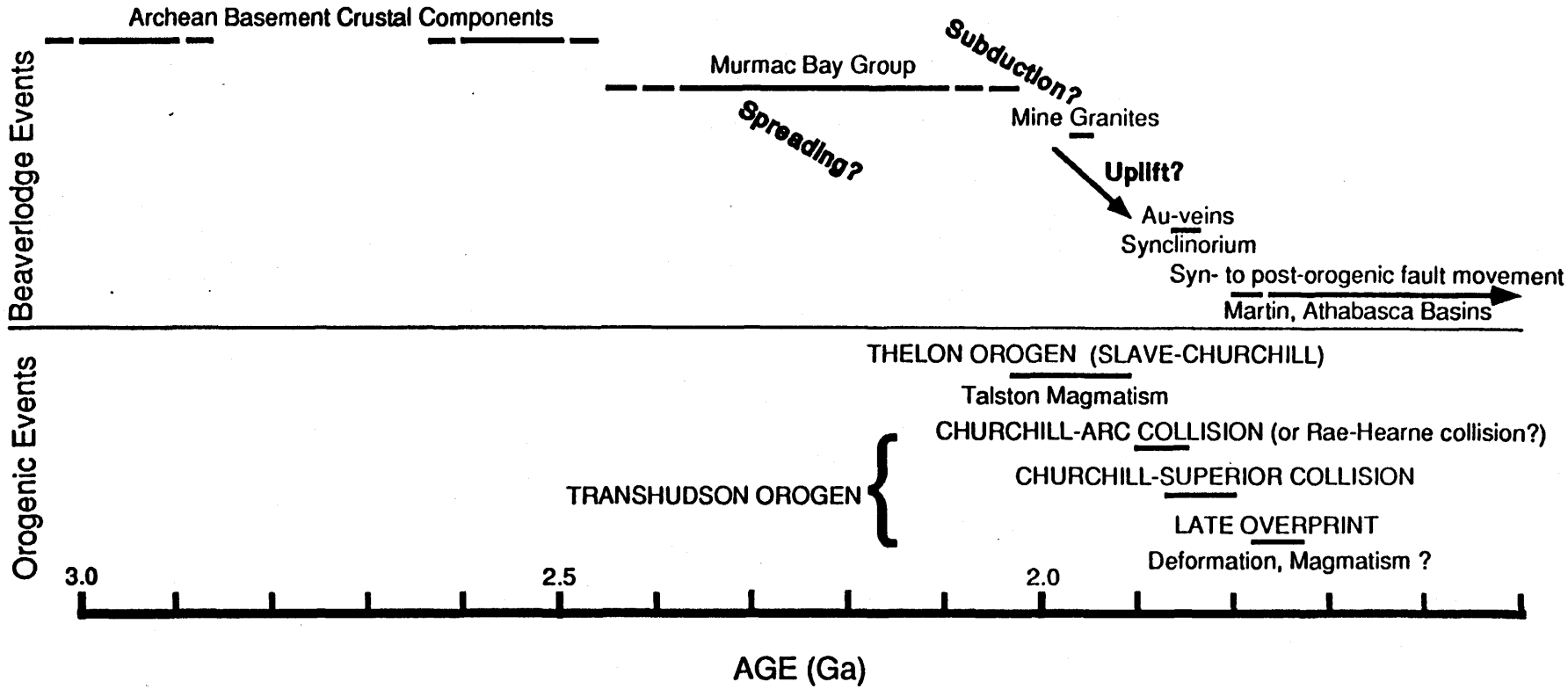

Figure 54: Summary diagram of geological events in the Goldfields and greater Beaverlodge region, as they relate to major orogenic events that have affected the Churchill Province. Ages of tectonic events are from Bickford et al. (1990), Hoffman (1991), and O'Hanley et al. (1991). See text for further explanation.

developed in the back-arc basin of the subduction zone (Figure 55).

The next fluid event documented is the lode-gold quartz vein mineralization, associated with D2 deformation (Figure 53), which is recorded in the veins by Type I and Ia fluid inclusions, and by the stable isotopic compositions of vein minerals as F2 and F3 (which are likely parts of the same overall fluid event). This fluid, at least during the late stage of vein development, is suspected to have been associated with gold deposition, and is indicated to have been at minimum temperatures of about 300°C (Figure 53), and minimum pressures of 2.5 to 3.0 kbars. As the fluid is CO_2-bearing, and the inclusion populations appear to indicate pre-entrapment immiscibility, these temperatures and pressures are trapping conditions. This is confirmed by some stable isotopic equilibration temperatures of quartz and chlorite gangue minerals that yield temperatures of 300 to 400°C (Figure 53). The minerals were in equilibrium with a fluid of metamorphic origin. Rb/Sr ages of vein minerals indicate they are at least 1.84 Ga, and probably between 1.855 and 1.84 Ga, suggesting that the D2 folding, and the retrograde metamorphic fluid that likely caused the lode-gold mineralization, are related to compressional uplift during terminal collision of the Thelon-Talston orogeny, or to uplift caused by an early Hudsonian collision, in part indicated by movement along the Snowbird Shear Zone (Figures 53, 54 and 55). The source of

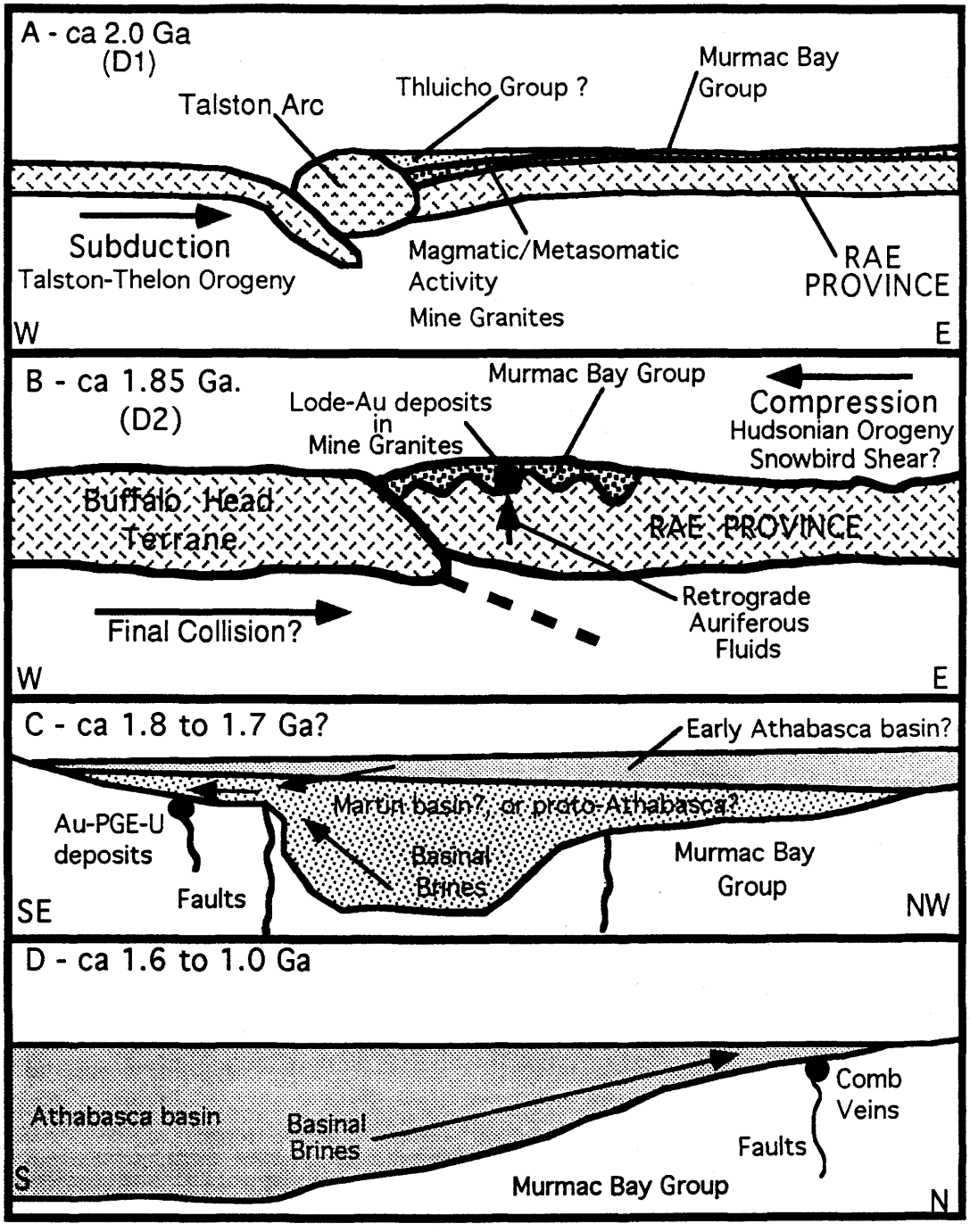

Figure 55: Generalized cross-sectional models of the geologic evolution of the Goldfields area, based on information summarized in Figures 53 and 54: A - Talston Orogeny ca. 2.0 Ga, causing burial of the Murmac Bay Group and formation of the mine granites (D1); B - Hudsonian orogenic events, beginning ca. 1.85, cause uplift, deformation and lode-gold mineralization (D2); C - formation and diagenesis of Martin basin, forming Au-PGE-U mineralization, ca. 1.75 Ga?; D - formation and diagenesis of Athabasca basin, forming comb veins, which are "equivalent" to unconformity-type uranium deposits in the basin.

the retrograde fluids is not clear, but they may have been derived from dehydration of subducted material (e.g. Kyser & Kerrich, 1990) during the Thelon-Talston Orogeny, or the dehydration of stacked thrust sheets created by the Hudsonian Orogeny; the initial $^{87}Sr/^{86}Sr$ ratios of the vein minerals, and of the feldspars from the Mine granites imply that F1 to F3 fluids (Figure 53) were derived from, or interacted with, significantly older (i.e. deeply buried) crustal material.

The fluid represented by Type II inclusions is of an uncertain origin, but clearly post-dates the lode-gold veins (1.84 Ga), and pre-dates the maximum age of the Au-PGE-U mineralization (ca. 1.75 ?). However, this fluid event appears to be regionally extensive and may be related to events in the Beaverlodge area that are thought to have occurred ca. 1.78 to 1.74 Ga (Figure 53), such as albitization or the formation of the simple vein-type uranium deposits. This age span, often referred to as the "late overprint", is suggested to correspond with the later stages of the Hudsonian Orogen (Figure 53, 54). The "late overprint" is also recorded by feldspars from the Box mine granite, which yield an Rb/Sr age of ca. 1.77 Ga. The Martin basin may have started to form at this time, due to epeirogenic fault movement during the waning stages of the Hudsonian Orogen, and this fluid event may also be related to early diagenesis within the basin.

The next fluid event, F4 (Figure 53), is recorded by primary fluid inclusions in the complex Au-PGE-U vein-type

deposits which contain fluids of a moderately high salinity (28 to 36 wt % NaCl eq.). A similar fluid is found in secondary Type IV inclusions from the lode-gold veins and in fluid inclusions from the "sponge rock" zones that have locally altered the mine granites. Stable isotopic equilibration temperatures of vein minerals from the Nicholson and Quartzite Ridge deposits indicate that this fluid was at a temperature of 100 to 120°C. The age of this fluid event may be as old as ca. 1.8 to 1.7 Ga, because the depleted δD value of the fluid, at approximately -90 permil, indicates a high latitude for the area. For this reason, it is possible that Au-PGE mineralization, such as in the Nicholson and Quartzite Ridge deposits, may have formed from peak diagenetic basinal fluids within the Martin basin (Figure 55). Other causes of the distinct δD value of the fluid include the presence of a "proto-Athabasca" basin, or the mixing of either of these basinal fluids with Athabasca basinal fluids. Whether or not uranium accompanied the gold and platinoids, or was later overprinted on pre-existing Au-PGE mineralization, is not known presently.

F5 is the youngest fluid event, recorded by the late comb veins. The fluids are of a high salinity (40 wt. % NaCl eq.), and stable isotopic equilibrium fractionations between vein minerals indicate their temperature was approximately 175°C. Their stable isotopic values are similar to those of the diagenetic fluids in the Athabasca basin between ca. 1.6 and

1.0 Ga, during which time the unconformity-type and complex vein-type uranium deposits were formed (Figures 53 and 55). As mentioned above, this may be the time during which uranium mineralization overprinted the Au-PGE mineralization, forming "hybrid" Complex U-PGE-Au Vein-Type deposits. An early stage of the F5 fluid event is represented by Type III secondary inclusions in the lode-gold veins. The moderate salinity of the fluid (10 to 15 wt. % NaCl eq.) is similar to that of the fluid inclusions observed in quartz overgrowths from the Athabasca basin, where the fluid is interpreted to be of an early diagenetic origin (Figure 53).

REFERENCES

Alcock, F.J., 1936: The gold deposits of Lake Athabasca. C.I.M.M. Transaction, Vol. 39, p. 531-546.

Appleyard, E.C., 1988: The origin of the Frontier Granite, Goldfields, Saskatchewan: a metasomatic assessment. In Summary of Investigations 1988, Saskatchewan Geological Survey, Saskatchewan Energy and Mines, Miscellaneous Report 88-4, p. 161-167.

Appleyard, E.C., 1989: Field observations on the Frontier, Box and Athona granites, Goldfields Area, Saskatchewan. In Summary of Investigations 1989, Saskatchewan Geological Survey, Saskatchewan Energy and Mines, Miscellaneous Report 89-4, p. 82-86.

Appleyard, E.C., 1990: Petrogenetic aspects of the Goldfields granites, Saskatchewan. In Summary of Investigations 1990, Saskatchewan Geological Survey, Saskatchewan Energy and Mines, Miscellaneous Report 90-4, p. 84-93.

Ansdell, K.M. and Kyser, T.K., 1990: Epigenetic gold mineralization in the Flin Flon Domain: fluid characteristics. Modern Exploration Techniques, Saskatchewan Geological Society Special Publication 10, p. 219-234.

Armstrong, D.C., 1990: The geochemistry and gold metallogenesis of the Sulphide-Pap Lakes area, northern Saskatchewan, Canada. Unpublished Ph.D. thesis, University of Birmingham, England.

Armstrong, R.L. and Ramaekers, P., 1985: Sr isotopic study of Helikian sediment and diabase dikes in the Athabasca Basin, Northern Saskatchewan. Canadian Journal of Earth Sciences, Vol. 22, p. 399-407.

Beavan, A.P., 1938: The geology and gold deposits of Goldfields, Lake Athabasca, Saskatchewan; Unpublished Ph.D. thesis, Princeton University.

Beck, L.S., 1959: Mineral occurences in the Precambrian of northern Saskatchewan (excluding radioactive minerals); Saskatchewan Energy and Mines, Report No.36, p.48-52.

Beck, L.S., 1969: Uranium deposits of the Athabasca Region. Saskatchewan Geological Survey, Saskatchewan Mineral Resources, Report 126.

Beck, L.S., 1986: General geology and uranium deposits of the Beaverlodge District. In Uranium Deposits of Canada, E.L. Evans, editor; C.I.M.M. Special Vol. 33, p. 85-94.

Becker, R.H. and Clayton, R.N., 1976: Oxygen isotope study of a Precambrian banded iron-formation, Hamersley Range, Western Australia. Geochimica et Cosmochimica Acta, Vol. 40, p. 1153-1165.

Bell, K., 1981: A review of the geochronology of the Precambrian of Saskatchewan-some clues to uranium mineralization. Mineralogical Magazine, Vol. 44, p. 371-378.

Bell, K. and Bikerman M., 1985: Saskatchewan Shield Geochronology (Rb-Sr) Project. In Summary of Investigations, Saskatchewan Geological Survey, Saskatchewan Energy and Mines, Miscellaneous Report 85-4, p. 59.

Bell, K. and Blenkinsop, J., 1984: Saskatchewan Shield Geochronology (Rb-Sr) Project. In Summary of Investigations, Saskatchewan Geological Survey, Saskatchewan Energy and Mines, Miscellaneous Report 84-4, p. 80.

Bell, K. and Macdonald, R., 1982: Geochronological calibration of the Precambrian Shield in Saskatchewan. In Summary of Investigations 1982, Saskatchewan Geological Survey, Saskatchewan Energy and Mines, Miscellaneous Report 82-4, p. 17-22.

Bikerman, M., Bell, K., and Blenkinsop, J., 1990: Rb-Sr Geochronology of the Lodge Bay granite, a ca. 3.0 Ga basement in the Beaverlodge area, Saskatchewan. In Summary of Investigations 1990, Saskatchewan Geological Survey, Saskatchewan Energy and Mines, Miscellaneous Report 90-4, p. 143-145.

Bickford, M.E., Van Schmus, W.R., Collerson, K.D., Macdonald, R., 1987: U-Pb Zircon Geochronology Project: New Results and Interpretations. In Summary of Investigations 1987, Saskatchewan Geological Survey, Saskatchewan Energy and Mines, Miscellaneous Report 87-4, p. 76-79.

Bigeleisen, J., Pearlman, M.L., and Prosser, H.C., 1952: Conversion of hydrogenic materials to hydrogen for isotope analysis. Analytical Chemistry, Vol. 24, p. 1356-1357.

Bottinga, Y. and Javoy, M., 1975: Oxygen isotope partitioning among the minerals in igneous and metamorphic rocks. Rev. Geophys. Space Phys, Vol. 13, p. 401-418.

Bowers, T.S., 1991: The deposition of gold and other metals: Pressure-induced fluid immiscibility and associated stable isotope signatures. Geochimica et Cosmochimica Acta, Vol.55, p. 2417-2434.

Bowers, T.S., and Helgeson, H.C., 1983: Calculation of the thermodynamic and geochemical consequences of non-ideal mixing in the system H_2O-CO_2-NaCl on phase relations in geologic systems: Equation of state for H_2O-CO_2-NaCl fluids at high pressures and temperatures. Geochimica et Cosmochimica Acta, Vol. 47, p. 1247-1275.

Brown, P.E. and Lamb, W.M., 1986: Mixing of H_2O-CO_2 in fluid inclusions: Geobarometry and Archean gold deposits. Geochimica et Cosmochimica Acta, Vol. 50, p. 847-852.

Brown, P.E. and Lamb, W.M., 1989: P-V-T properties of fluids in the system $H_2O \pm CO_2 \pm$NaCl: New graphical presentations and implications for fluid inclusion studies. Geochimica et Cosmochimica Acta, Vol. 53, p. 1209-1221.

Byrne, N.W., 1937: Diamond drilling at Lake Athabasca. C.I.M.M. Transactions, Vol. 40, p. 165-184.

Christie, A.M., 1952: Goldfields-Martin Lake map area, Saskatchewan. Geological Survey of Canada, Memoir 269.

Clayton, R.N. and Mayeda, T.K., 1963: The use of bromine pentafluoride in the extraction of oxygen from oxides and silicates for isotopic analysis. Geochimica et Cosmochimica Acta, Vol. 27, p. 43-52.

Clayton, R.N., O'Neil, J.R. and Mayeda, T.K., 1972: Oxygen isotope exchange between quartz and water. Jounal of Geophysical Research, Vol. 77, p. 3057-3067.

Collins, P.L.F., 1979: Gas hydrates in CO_2-bearing fluid inclusions and use of freezing data for estimation of salinity. Economic Geology, Vol. 74, p. 1435-1444.

Cooke, H.C., 1937: Preliminary Report, Goldfields Area, Saskatchewan, Geological Survey of Canada Paper 37-3.

Cooke, H.C., 1946: Canadian Lode Gold Areas (Summary Account). Geological Survey of Canada, Economic Geology Series No.15, p.34.

Coombe, W., 1984: Gold in Saskatchewan. Saskatchewan Energy and Mines, Open File Report 84-1, p. 16-28.

Craig, J.R. and Vaughn, D.J., 1981: Ore Microscopy and Ore Petrography, Wiley and Sons, 1981.

Davis, D.W., Lowenstein, T.K., and Spencer, R.J., 1990: Melting behavior of fluid inclusions in laboratory-grown halite crystals in the systems NaCl-H_2O, NaCl-KCl-H_2O, and NaCl-$CaCl_2$-H_2O. Geochimica et Cosmochimica Acta, Vol. 54, p. 591-601.

Dawson, K.R., 1951: A petrographic description of the wall-rocks and alteration products associated with pitchblende-bearing veins in the Goldfields region, Saskatchewan. Geological Survey of Canada, Paper 51-24.

Drummond, S.E. and Ohmoto, H., 1985: Chemical evolution and mineral deposition in boiling hydrothermal systems. Economic Geology, Vol. 80, p. 126-147.

English, P.J., 1981: Gold-quartz veins in metasediments of the Yellowknife Supergroup, Northwest Territories: A fluid inclusion study. Unpublished M.Sc. thesis, Edmonton, Canada, University of Alberta, 108 p.

Eslinger, E., Savin, S., and Yeh, H.W., 1979: Oxygen isotope geothermometry of diagenetically altered shales. SEPM Special Publication No. 26, p. 113-124.

Fahrig, W.F., 1961: The geology of the Athabasca formation. Geological Survey of Canada, Bulletin 68, 41 p.

Faure, G., 1986: Principles of Isotope Geology: J. Wiley & Sons, N.Y., Second Edition, 589 p.

Fayek, M., Kyser, T.K., and Kusmirski, R.T., 1991: Petrography, fluid inclusion and stable isotope data from the Bakos lode gold deposit. In Summary of Investigations 1991, Saskatchewan Geological Survey, Saskatchewan Energy and Mines, Miscellaneous Report 91-4, p. 175-177.

Graham, C.M., Harmon, R.S. and Sheppard, S.M.F., 1984: Experimental hydrogen isotope studies: hydrogen isotope exchange between amphibole and water. American Mineralogist, Vol. 69, p. 128-138.

Guha, J., Lu, H., Dube, B., Robert, F., and Gagnon, M., 1991: Fluid characteristics of vein and altered wall rock in Archean mesothermal gold deposits. Economic Geology, Vol. 86, p. 667-684.

Hanmer, S., Kopf, C., and Darrach, M., 1991: The East Athabasca Mylonite Zone: An Archean segment of the Snowbird Tectonic Zone. In Summary of Investigations, Saskatchewan Geological Survey, Saskatchewan Energy and Mines, Miscellaneous Report 91-4, p. 192-195.

Harper, C.T., 1983: Iron ores of Northern Saskatchewan. Saskatchewan Energy and Mines, Report 220, p. 35-41.

Ho, S.E., 1987: Fluid inclusions: their potential as an exploration tool for Archean gold deposits. In Ho, S.E. and Groves, D.I., editors; Recent Advances in Understanding Precambrian Gold Deposits. Extension Department, University of Western Australia, Publication No. 11, p. 239-263.

Ho, S.E., Bennett, J.M., Cassidy, K.F., Hronsky, J.M.A., Mikucki, E.J., and Sang, J.H., 1990: Nature of ore fluid, and transportational and depositional conditions in sub-amphibolite facies deposits. In Gold Deposits of the Archean Yilgarn Block, Western Australia; Ho,S.E., Groves, D.I., and Bennett, J.M., editors; Extension Department, University of Western Australia, Publication No. 20, p. 198-211.

Hoeve, J., 1982: Perspective on uranium mineralization at Beaverlodge. Saskatchewan Research Council Publication No. G-745-1-E-82.

Hoeve, J., 1984: Host rock alteration and its application as an ore guide at the Midwest Lake uranium deposit, northern Saskatchewan. Canadian Mining and Metallurgical Bulletin, Vol. 77, p. 63-72.

Hoeve, J., and Sibbald, T.I.I., 1978: On the genesis of Rabbit Lake and other unconformity-type uranium deposits in northern Saskatchewan, Canada. Economic Geology, Vol. 73, p. 1450-1473.

Hoeve, J., Rawsthorne, K., and Quirt, D., 1981: Uranium metallogenic studies: Clay mineral stratigraphy and diagenesis in the Athabasca Group. In Summary of Investigations 1981, Saskatchewan Geological Survey, Saskatchewan Energy and Mines, Miscellaneous Report 81-4, p. 76-89.

Hoeve, J. and Quirt, D., 1986: A common diagenetic-hydrothermal origin for unconformity-type uranium and stratiform copper deposits. Saskatchewan Research Council Publication No. R-855-5-A-86.

Hoffman, P.F., 1988: United plates of America, the birth of a craton: Early Proterozoic assembly and growth of Laurentia. Annual Review of Earth and Planetary Sciences, Vol. 16, p.543-603.

Hoffman, P.F., 1990: Geological constaints on the origin of the mantle root beneath the Canadian shield. Phil. Trans. R. Soc. Land, A 331, p. 523-532.

Hoffman, P.F., 1991: Subdivision of the Churchill Province and the extent of the Trans-Hudson orogen. In Lewry, J.F. and Stauffer, M.R., editors; The Early Proterozoic Trans-Hudson Orogen of North America. Geological Association of Canada, Special Paper 37.

Hrdy, F., Kyser, T.K., and Kusmirski, R.T., 1991: Mineral parageneses, fluid characteristics and radiogenic isotopic data from the Proterozoic Jasper gold zone, La Ronge Domain. In Summary of Investigations, Saskatchewan Geological Survey, Saskatchewan Energy and Mines, Miscellaneous Report 91-4, p. 178-180.

Hulbert, L., 1986: Geological environments for platinum group element mineralization: A brief overview. Presented at "Economic Minerals of Saskatchewan Symposium" by the Saskatchewan Geological Society, November 19, 1986.

Hulbert, L., 1990: The uranium-gold-platinum-group element association in the greater Beaverlodge area, northern Saskatchewan (Extended Abstract). In Modern Exploration Techniques, Saskatchewan Geological Society, Special Publication Number 10, p. 235-236.

Hulbert, L., Duke, J.M., Eckstrand, O.R., Lydon, J.W., Scoates, R.F.J., Cabri, L.J., and Irvine, T.N., 1988: Geological environments of the platinum group elements. Geological Survey of Canada, Open File 1440, 148 p.

Hyndman, D.W., 1981: Controls on source and depth of emplacement of granitic magma. Geology, Vol. 9, p. 244-249.

Ibrahim, M.S., 1990: History of the fluids associated with the Proterozoic Star Lake lode-gold deposit, northern Saskatchewan, Canada. Unpublished M.Sc. thesis, University of Saskatchewan, 124 p.

Ibrahim, M.S. and Kyser, T.K., 1991: Fluid inclusion and isotope systematics of the high-temperature Proterozoic Star Lake lode gold deposit, northern Saskatchewan, Canada. Economic Geology, Vol. 86, p. 1468-1490.

Jaireth, S., 1988: Hydrothermal transport of platinum and gold in the unconformity-related uranium deposits: a preliminary thermodynamic investigation. Bureau of Mineral Resources, Geology and Geophysics, Record 1988/9.

Jewitt W.G. and Gray S., 1946: The Box Mine. C.I.M.M. Transactions, Vol. 43, p. 447-467.

Jiricka, D.E., 1984: SMDC Exploration: Lodge Bay Project CBS 5664, 5665, 5667, S-97948 Athabasca Mining District, Saskatchewan.

Jolliffe, A.W., 1946: Cornwall Bay-Fish Hook Bay area, Lake Athabasca, Saskatchewan. Unpublished map and report, Geological Survey of Canada.

Kajiwara, Y. and Krouse, H.R., 1971: Sulfur isotope partitioning in metallic sulfide systems. Canadian Journal of Earth Sciences, Vol. 8, p. 1397-1408.

Kerrich, R., 1987: The stable isotope geochemistry of Au-Ag vein deposits in metamophic rocks. In Mineralogical Association of Canada, Short Course in Stable Isotope Geochemistry of Low Temperature Fluids, Vol. 13, p. 287-336.

Killin, A.F., 1939: Petrographic study of rocks from the Box Mine, Athabasca Lake. Unpublished Ph.D. thesis, University of British Columbia.

Koeppel, V., 1968: Age and history of the uranium mineralization of the Beaverlodge area, Saskatchewan. Geological Survey of Canada, Paper 67-31, 111 p.

Kotzer, T.G. and Kyser, T.K., 1990: The use of stable and radiogenic isotopes in the identification of fluids and processes associated with unconformity-type uranium deposits. Modern Exploration Techniques, Saskatchewan Geological Society Special Publication 10, p. 115-131.

Kotzer, T.G. and Kyser, T.K., 1991: Retrograde alteration of clay minerals in uranium deposits: Radiation catalyzed or simply low-temperature exchange? Chemical Geology (Isotope Geoscience Section), Vol. 86, p. 307-321.

Kotzer, T.G., Kyser, T.K., and Irving E., 1992a: Paleomagnetism and the evolution of fluids in the Proterozoic Athabasca Basin, northern Saskatchewan, Canada. Canadian Journal of Earth Sciences (in press).

Kotzer, T.G., Kyser, T.K., King, R.W., and Kerrich, R., 1992b: An empirical oxygen and hydrogen isotope geothermometer for quartz-tourmaline and tourmaline-water. Submitted to Geochimica et Cosmochimica Acta, 1992.

Kyser, T.K., 1987: Equilibrium fractionation factors for stable isotopes. In Mineralogical Association of Canada Short Course Volume 13, Stable Isotope Geochemistry of Low Temperature Fluids, p. 1-84.

Kyser, T.K. and O'Neil, J.R., 1984: Hydrogen isotope systematics of submarine basalts. Geochimica et Cosmochimica Acta, Vol. 48, p. 2123-2133.

Kyser, T.K. and Kerrich, R.W., 1990: Geochemistry of fluids in tectonically active crustal regions. In Mineralogical Association of Canada Short Course Volume 18, Fluids in Tectonically Active Regimes of the Continental Crust, Nesbitt, B.E., editor, p. 133-230.

Kyser, T.K., Kotzer, T. and Sibbald, T.I.I., 1990: Oxygen, U-Pb and Pb-Pb isotope systematics in uraninite from complex U-Au-PGE vein-type and unconformity-type uranium deposits in northern Saskatchewan. In Summary of Investigations 1990, Saskatchewan Geological Survey, Saskatchewan Energy and Mines, Miscellaneous Report 90-4, p. 64-69.

McCrea, J.M., 1950: On the isotopic chemistry of carbonates and a paleotemperature scale. Journal of Chemical Physics, Vol. 18, p. 849-857.

Macdonald, R., 1983: Geology and Regional Context of the Oldman Lake Area. In Summary of Investigations 1983, Saskatchewan Geological Survey, Saskatchewan Energy and Mines, Miscellaneous Report 83-4, p. 19-23.

Macdonald, R., 1987: Update on the Precambrian geology and domainal classification of northern Saskatchewan. In Summary of Investigations 1987, Saskatchewan Geological Survey, Saskatchewan Energy and Mines, Miscellaneous Report 87-4, p. 87-104.

Macdonald, R. and Slimmon, W.L., 1986: Geology Map 241A, Greater Beaverlodge Area, 74N-6 to -11, 1:100,000. Saskatchewan Energy and Mines.

Matthews, A. and Katz, A., 1977: Oxygen isotope fractionation during dolomitization of calcium carbonate. Geochimica et Cosmochimica Acta, Vol. 41, p. 1431-1438.

Mountain, B.W. and Wood, S.A., 1988: Chemical controls on the solubility, transport, and deposition of platinum and palladium in hydrothermal solutions: A thermodynamic approach. Economic Geology, Vol. 83, p. 492-510.

Nicholls, J. and Crawford, M.L., 1985: Fortran programs for calculation of fluid properties from microthermometric data on fluid inclusions. Computers Geosciences, Vol. 11, p. 619-645.

Oakes, C.S., Bodnar, R.J., and Simonson, J.M., 1990: The system $NaCl-CaCl_2-H_2O$: The ice liquidus at 1 atm total pressure. Geochimica et Cosmochimica Acta, Vol. 54, p. 603-610.

O'Hanley, D.S., Kyser, T.K., and Sibbald, T.I.I., 1991: The age of mine granites, Goldfields Area. In Summary of Investigations 1991, Saskatchewan Geological Survey, Saskatchewan Energy and Mines, Miscellaneous Report 91-4, p. 76-80.

O'Neil, J.R., 1987: Preservation of H, C, and O isotopic ratios in the low temperature environment. In Stable Isotope Geochemistry of Low Temperature Fluids, Kyser, T.K., editor; Mineralogical Association of Canada Short Course 13, p. 85-128.

O'Neil, J.R. and Taylor, H.P., 1967: The oxygen isotope and cation exchange chemistry of feldspars. American Mineralogist, Vol. 52, p. 1414-1437.

O'Neil, J.R. and Taylor, H.P., 1969: Oxygen isotope equilibrium between muscovite and water. Journal of Geophysical Research, Vol. 74, p. 6012-6022.

Pagel, M., 1975: Determinations des conditions physiochemiques de la silification diagenetic des gres Athabasca (Canada) an moyen des inclusions fluides: C.R. Acad. Sci. Paris, T. 280, Ser. D., p. 2301-2304.

Pagel, M., Poty, B., and Sheppard, S.M.F., 1980: Contribution to some Saskatchewan uranium deposits mainly from fluid inclusion and isotopic data. In Proceedings of International Uranium Symposium on the Pine Creek Geosyncline, 1980, p. 639-953.

Peiris, E.P.W. and Parslow, G.R., 1987: Metallogenic studies, Nicholson-Fish Hook Bays area. In Summary of Investigations 1987, Saskatchewan Geological Survey, Saskatchewan Energy and Mines, Miscellaneous Report 87-4, p. 58-59.

Peiris, E.P.W. and Parslow, G.R., 1988: Geology and geochemistry of the uranium-gold mineralization in the Nicholson Bay-Fish Hook Bay area. In Summary of Investigations 1988, Saskatchewan Geological Survey, Saskatchewan Energy and Mines, Miscellaneous Report 88-4, p. 70-76.

Quirt, D., 1988: Reconnaissance investigation of Pt, Pd and Au in host rocks of Saskatchewan uranium deposits. In Summary of Investigations 1988, Saskatchewan Geological Survey, Saskatchewan Energy and Mines, Miscellaneous Report 88-4, p. 176-178.

Quirt, D., 1990: Metasomatic host-rock alteration at the Frontier gold prospect, Goldfields area, Saksatchewan. In Summary of Investigations 1990, Saskatchewan Geological Survey, Saskatchewan Energy and Mines, Miscellaneous Report 90-4, p. 146-157.

Rafter, T.A., 1965: Recent sulfur isotope measurements on a variety of specimens examined in New Zealand. Bulletin of Volcanology, Vol. 28, p. 3-20.

Ramaekers, P., 1981: Hudsonian and Helikian basins of the Athabasca region, Northern Saskatchewan. In Proterozoic Basins of Canada, Campbell, F.H.A., editor; Geological Survey of Canada, Paper 81-10, p. 219-233.

Robert, F. and Kelly, W.C., 1987: Ore-forming fluids in Archean gold-bearing quartz veins at the Sigma Mine, Abitibi greenstone belt, Quebec, Canada. Economic Geology, Vol. 82, p. 1464-1482.

Roberts, R.G., 1990: Structural controls of the Box and Athona deposits, Goldfields area, Saskatchewan. Saskatchewan Geological Survey, Saskatchewan Energy and Mines, Open File Report 90-2.

Robinson, S.C., 1955: Mineralogy of uranium deposits, Goldfields, Saskatchewan. Geological Survey of Canada Bulletin 31, 128 p.

Roedder, E., 1984: Fluid Inclusions: Mineralogical Society of America, Reviews in Mineralogy, Vol. 12, 1984, 646 p.

Ross, J.R., 1949: Stratigraphy and structure of the Goldfields area, northern Saskatchewan. Unpublished M.Sc. thesis, University of Toronto.

Sasaki, A., Arikawa, Y., Folinsbee, R., 1979: KIBA reagent method of sulfur extraction applied to isotopic work. Bill. Geol. Surv. Japan, Vol. 30, p. 241-245.

Schwann, P.L., 1985: Geochemistry and petrology of the Nicholson Bay ultramafic complex, northwestern Saskatchewan. Unpublished B.Sc. thesis, University of Regina, 67 p.

Scott, B.P., 1978: The geology of an area east of Thluicho Lake, Saskatchewan (Part of NTS area 74N-11). Saskatchewan Energy and Mines, Report 167.

Sheppard, T.J., Rankin, A.H., Alderton, D.H.M., 1986: A Practical Guide to Fluid Inclusion Studies. Blackie & Son Limited, Glasgow, 239 p.

Seitz, J.C., and Pasteris, J.D., 1990: Theoretical and practical aspects of differential partitioning of gases by clathrate hydrates in fluid inclusions. Geochimica et Cosmchimica Acta, Vol. 54, p. 631-639.

Seward, T.M., 1989: The hydrothermal chemistry of gold and its implications for ore formation: boiling and conductive cooling as examples. In Keays, R.R., Ramsay, W.R.H., and Groves, D.I., editors; The Geology of Gold Deposits: The Perspective in 1988. Economic Geology, Monograph 6, p. 398-404.

Sibbald, T.I.I., 1982: Uranium metallogenic studies: Nicholson Bay area. In Summary of Investigations 1982, Saskatchewan Geologcical Survey, Saskatchewan Energy and Mines, Miscellaneous Report 82-4, p. 43-45.

Sibbald, T.I.I., 1984: Gold metallogenic Studies, Goldfields Area. In Summary of Investigations, Saskatchewan Geological Survey, Saskatchewan Energy and Mines, Miscellaneous Report 84-4, p. 116-121.

Sibbald, T.I.I., 1985: Geology and genesis of the Athabasca uranium deposits. In Summary of Investigations 1985, Saskatchewan Geological Survey, Saskatchewan Energy and Mines, Miscellaneous Report, p. 133-156.

Sibbald, T.I.I., 1987: Overview of the Precambrian geology and aspects of the metallogenesis of northern Saskatchewan. In Economic Minerals of Saskatchewan.

Sibbald, T.I.I., 1988: Nicholson Bay uranium-gold-platinum group element deposit studies. In Summary of Investigations 1988, Saskatchewan Geological Survey, Saskatchewan Energy and Mines, Miscellaneous Report 88-4, p. 77-81.

Sibbald, T.I.I. and Lewry, J.F., 1980: Uranium metallogenic studies: Lodge Bay area, Lake Athabasca. In Summary of Investigations 1980, Saskatchewan Geological Survey, Saskatchewan Energy and Mines, Miscellaneous Report 80-4, p. 44-48.

Sibbald, T.I.I., Schwann, P.L., and Dunn, C.E., 1983: Uranium-gold metallogenic studies: Nicholson Bay ultramafic complex. In Summary of Investigations, Saskatchewan Geological Survey, Saskatchewan Energy and Mines, Miscellaneous Report 83-4, p. 75-79.

Sibbald, T.I.I. and Jiricka, D.E., 1986: Geology of the gold deposits, Goldfields, Saskatchewan. In Gold in the Western Shield, C.I.M.M. Special Vol. 38, p. 412-414.

Smith, T.J., Cloke, P.L., and Kesler, S.E., 1984: Geochemistry of fluid inclusions from the McIntyre-Hollinger gold deposit at Timmins, Ontario, Canada. Economic Geology, Vol. 79, p. 1265-1285.

Spencer, R.J., Moller, N., and Weare, J.H., 1990: The prediction of mineral solubilities in natural waters: A chemical equilibrium model for the Na-K-Ca-Mg-Cl-SO_4-H_2O system at temperatures below 25°C. Geochimica et Cosmochimica Acta, Vol. 54, p. 575-590.

Spooner, E.T.C., Bray, C.J., Wood, P.C., Burrows, D.R., and Callan, N.J., 1987: Au-quartz vein and Cu-Au-Ag-Mo-anhydrite mineralization, Hollinger-McIntyre Mines, Timmins, Ontario: $\delta^{13}C$ values (McIntyre) fluid inclusion gas chemistry, pressure (depth) estimation, and H_2O-CO_2 phase separation as a precipitation and dilation mechanism. Ontario Geological Survey Miscellaneous Paper 136, p. 35-56.

Spycher, N.F. and Reed, M.H., 1989: Evolution of a Broadlands-type epithermal ore fluid along alternative P-T paths: implications for the transport of base, precious, and volatile metals. Economic Geology, Vol. 84, p. 328-359.

Suzuoki, T. and Epstein, S., 1976: Hydrogen isotope fractionation between OH-bearing silicate minerals and water. Geochimica et Cosmochimica Acta, Vol. 40, p. 1229-1240.

Swanson, C.O., 1945: Probabilities in estimating the grade of gold deposits. C.I.M.M. Transactions, Vol. 48, p. 323-350.

Taylor, B.E., 1986: Magmatic volatiles: isotopic variations of C, H, and S. In Stable Isotopes in High Temperature Geologic Processes, Valley, J.W., Taylor, H.P., and O'Neil, J.R., editors; Mineralogical Society of America, Vol. 16, Bookcrafters Inc., Michigan, p. 185-226.

Taylor, H.P. Jr., 1974: The application of oxygen and hydrogen isotope studies to problems of hydrothermal alteration and ore deposition. Economic Geology, Vol. 69, p. 843-883.

Tremblay, L.P., 1972: Geology of the Beaverlodge mining area, Saskatchewan. Geological Survey of Canada Memoir 367, 265 p.

Tremblay, L.P., Loveridge, W.D., and Sullivan, R.W., 1981: Report 4, in Current Research, C, Geological Survey of Canada, Paper 81-C.

Tyrrell, J.B., 1894: Report on the country between Athabasca Lake and Churchill River. Geological Survey of Canada Annual Report, Vol. 8, Part D.

Van Schmus, W.R., Persons, S.S., Macdonald, R., and Sibbald, T.I.I., 1986: Preliminary results from U-Pb zircon geochronology of the Uranium City region. In Summary of Investigations 1986, Saskatchewan Geological Survey, Saskatchewan Energy and Mines, Miscellaneous Report 86-4, p. 108-111.

Wenner, D.B. and Taylor, H.P. Jr., 1971: Temperatures of serpentinization of ultramafic rocks based on $^{18}O/^{16}O$ fractionation between coexisting serpentine and magnetite. Contrib. Mineral. Petrol. 32, p. 165-185.

Wilde, A.R. and Bloom, M.S., 1988: Tranport and deposition of gold with uranium and platinum-group elements in unconformity-related deposits. Geological Society of Australia Abstracts, No. 22, p. 325-330.

Wilde, A.R., Mernach, T.P., Bloom, M.S., and Hoffman, C.F., 1989: Fluid inclusion evidence on the origin of some Australian unconformity-related uranium deposits. Economic Geology, Vol. 84, p. 1627-1642.

Wilson, M.R. and Kyser, T.K. (1987): The stable isotope geochemistry of alteration associated with the Key Lake uranium deposit, Canada. Economic Geology, Vol. 82, p. 1540-1557.

APPENDIX 1: Chemical Analyses of Athona Mine granite

Sample	(SRC)	Rock	Al2O3	Fe2O3	CaO	MgO	K2O	Na2O	%LOI	P2O5	MnO	TiO2
84	118	NMG	13.5	.85	.13	.25	3.28	4.56	.3	.01	.01	.03
84	119	NMG	13.1	.94	.68	.31	5.49	2.51	.9	.01	.028	.05
84	120	NMG	15.1	2.23	.87	1.12	4.93	3.22	1.4	.07	.038	.23
84	121	NMG	14.5	.5	.18	.2	5.41	3.5	.1	.02	.01	.03
86	97	NMG	12.8	1.11	.21	.24	4.75	3.91	.5	.02	.009	.04
86	98	NMG	11.7	1.1	.23	.3	4.52	3.24	.5	.02	.012	.04
86	117	SMG	12.8	.77	.25	.3	4.78	3.69	.3	.02	.012	.03
86	118	SMG	6.9	.74	.19	.47	4.94	3.34	.5	.02	.006	.04
86	119	SMG	9.2	.71	.16	.21	4.06	4.14	.2	.02	.009	.04
86	120	SMG	10.8	.91	.41	.41	4.8	3.35	.8	.02	.018	.05
86	121	SMG	7	.97	1.56	1.39	3.95	3.45	2.8	.02	.062	.04
86	125	NMG	6	.33	.06	.05	.11	6.6	.1	.02	.004	.02
86	128	NMG	10.6	.84	.36	.19	.15	6.79	.4	.02	.012	.03
86	130	NMG	11.1	.78	.13	.14	5.3	3.56	.3	.02	.008	.03
86	140	NMG	9.6	.94	.15	.34	4.24	4	.3	.02	.013	.03
86	141	NMG	10.4	.95	.17	.21	4.67	3.74	.5	.02	.006	.05
86	142	NMG	12.6	.94	.16	.18	5.28	3.37	.5	.02	.009	.03
86	143	NMG	12.7	.87	.17	.21	5.32	3.44	.5	.02	.008	.03
86	144	NMG	13.3	.55	.18	.11	5.3	3.96	.2	.02	.003	.03
86	145	SMG	10.5	.93	.81	.54	.11	6.04	.7	.02	.024	.04
86	146	SMG	13.2	1.12	1.84	1.04	.12	6.37	1.5	.02	.041	.04
86	147	SMG	11.1	.87	.54	.54	2.73	4.78	.5	.02	.019	.05
86	148	SMG	10.3	1.29	.3	.6	3	4.75	.6	.02	.012	.07
86	149	SMG	10.7	1.28	.23	.28	4.13	3.82	.7	.02	.008	.04
86	150	SMG	12	.34	.16	.1	.24	6.69	.2	.02	.003	.02

Data from Saskatchewan Research Council, NMG = northern granite body, SMG = southern granite body

APPENDIX 1: Chemical Analyses of the Box Mine Granite

Sample		Rock	SiO2	Al2O3	Fe2O3	CaO	MgO	K2O	Na2O	%LOI	P2O5	MnO	TiO2
SRC86	94	BMG	86.011	4.6	1.22	.86	1.09	.3	1.56	1.9	.02	.029	.01
SRC86	95	BMG	82.238	9	.48	.06	.09	.35	6.84	.4	.01	.002	.03
SEM	GG7	BMG	69.58	17.17	1.44	.38	.38	8.86	3.87	.4	.01	.03	.08
SEM	GG10	BMG	74.21	11.96	1.01	.05	.26	5.62	2.84	.5	.01	.01	.09
SEM	SK615	BMG	81.6	9.46	1.26	.22	.19	2.39	3.84	.85	.03	.01	.08
SEM	SK701	BMG	76.2	12.1	.97	.1	.26	5.35	3.36	.93	.02	.01	.08

Data from Sibbald, 1984 (SEM), or Saskatchewan Research Council. BMG = Box Mine granite

APPENDIX 1: Chemical Analyses of the Frontier Mine Granite and Host Quartzites

Sample	(SRC)	Rock	Al2O3	Fe2O3	CaO	MgO	K2O	Na2O	%LOI	P2O5	MnO	TiO2
86	1	QTZ	8.3	.78	.08	.98	4.92	.26	1.1	.04	.012	.09
86	2	QTZ	7.2	1.19	.04	.56	4.17	.22	.7	.03	.008	.1
86	3	QTZ	15.3	2.98	.23	.71	10.09	.43	1.3	.21	.009	.3
86	4	QTZ	18.3	1.55	.01	.33	13.28	.49	1	.03	.004	.23
86	5	QTZ	10.4	.99	.08	.98	3.83	.26	1.4	.06	.036	.14
86	6	QTZ	19.7	3.86	.19	4.39	9.69	.48	2.6	.05	.054	.33
86	7	QTZ	23.2	1.94	.01	1.81	13.2	.47	2.1	.02	.009	.46
86	8	QTZ	16.2	1.36	.01	1.1	10.04	.36	1.4	.03	.006	.41
86	17	QTZ	14	1.54	.11	1.07	9.03	.48	1	.1	.013	.17
86	18	QTZ	8.8	1.04	.1	.55	6.06	.39	.7	.07	.008	.09
86	19	QTZ	11.6	.65	.16	.25	10.01	.49	.4	.09	.005	.08
86	20	QTZ	11.9	.54	.13	.16	10.04	.5	.3	.09	.006	.08
86	21	GAB	13.3	13.95	6.26	8.21	1.19	1.96	2.9	.32	.129	1.92
86	22	QTZ	9.1	1.27	.06	1.43	5.18	.36	1.1	.03	.013	.12
86	23	QTZ	8.8	1	.09	.68	6.14	.39	.6	.05	.008	.09
86	24	QTZ	9.3	1.65	.15	1.85	3.5	.26	1.9	.07	.017	.14
86	25	QTZ	9.4	5.43	.18	4.2	2.08	.19	3.4	.09	.029	.21
86	31	QTZ	9.9	1.31	.1	.87	6.15	.28	.9	.04	.01	.1
86	33	QTZ	11	1.06	.16	.95	7.91	.3	.9	.1	.028	.13
86	75	TRANS	8.1	.86	.11	.28	6.05	.38	.4	.07	.004	.04
86	76	TRANS	8.9	3.34	.14	2.27	2.28	.2	2.5	.05	.019	.1
86	77	TRANS	9.5	2.33	.06	1.61	3.53	.29	1.8	.04	.02	.12
86	78	FMG	8.7	.78	.07	.57	5.74	.34	.6	.02	.005	.05
86	79	TRANS	18.9	3.87	.15	1.59	8.73	.51	2.2	.18	.021	.6
86	80	TRANS	14	2.26	.14	1.53	8.7	.47	1.3	.14	.013	.34
86	81	FMG	10.9	1.19	.23	.51	8.29	.38	.4	.03	.005	.08
86	82	TRANS	13.4	1.12	.2	.37	9.48	.47	.3	.03	.004	.14
86	84	FMG	8.6	1.24	.05	.26	6.19	.31	.3	.02	.003	.04
86	85	FMG	7.8	.57	.06	.09	6.28	.31	.7	.03	.002	.04
86	86	FMG	7.8	.54	.05	.05	6.27	.32	.1	.02	.003	.03
86	87	FMG	8.1	.91	.06	.22	5.99	.31	.3	.04	.002	.06
86	88	FMG	8	.84	.06	.14	6.48	.29	.2	.03	.003	.05
86	89	TRANS	17.2	2.05	.08	.79	10.62	.49	1.6	.02	.005	.23
86	90	FMG	7.1	.73	.09	.09	5.53	.24	.1	.04	.001	.04
86	91	TRANS	7.5	1.56	.09	.24	4.92	.3	.3	.02	.003	.11
86	92	TRANS	13.6	1.85	.1	.62	8.91	.47	.9	.08	.008	.24
86	93	TRANS	12.8	1.16	.1	.54	7.7	.41	.8	.09	.006	.13

Data from Sask. Research Council. FMG = Frontier Mine granite, TRANS = transitional rock, QTZ = quartzite country rock

APPENDIX 2: Computer Processed Type I Inclusion Data (Nichols & Crawford, 1985)

Sample	vX CO2	XCO2 (+CH4)	XH2O	XNaCl	Wt.% NaCl	ThCO2	Density CO2	Tm CO2	Tm ICE	Tm CLATH	Th CO2-H2O	Bulk Density	Remarks
BX86044-1	.2	.0738	.909	.0171	5.77	20	.77	-57	-3.9	7	298.5H	.981	
-2	.25	.0961	.8872	.0167		20	.77		-3.9		288H	.968	
-3	.3	.1202	.8635	.0163		20	.77		-3.9		269H	.955	
-4	.15	.0533	.9292	.0175		20	.77		-3.9		288.5H	.994	
-5	.15	.0463	.9361	.0177		27.5	.67		-0.4		302H	.977	N?
BX85003-1	.5	.2098	.7756	.0146		28.5	.64		-2.8		274H	.838	
-2	.25	.0839	.8991	.017		27.5	.67				276H	.941	
-3	.3	.1068	.8767	.0165		27	.68				277HD	.926	N?
-4	.1	.0277	.9543	.018		29.3	.62				271HD	.991	N?
-5	.35	.1319	.8521	.0161		26.6	.69				273H	.911	
-6	.75	.4634	.5267	.0099		25.8	.7				235CD	.782	N
-7	.7	.4018	.5872	.0111		25.8	.7				235CD	.799	N
-8	.5	.2285	.7573	.0143		24.5	.72				297C	.876	N?
-9	.9	.7134	.2813	.0053		27.3	.67				200C+	.708	N?
BX87001-1	.3	.1014	.882	.0166		28.7	.64				330C	.914	N
-2	.85	.6083	.3845	.0073		27.6	.66				280C	.72	N?
-3	.85	.6176	.3753	.0071		26.2	.69				243C+	.743	
-4	.05	.0123	.9694	.0183		30.4	.57				258H	1.009	
-5	.45	.1796	.8053	.0152		28.3	.65				289CD	.86	N
-6	.4	.1488	.8249	.0264	9.39	28.8	.64	-57.1		4.8	336Cr	.889	
-7	.65	.3499	.638	.012		25.5	.7	-57.0			316C	.819	N
-8	.5	.2047	.7815	.0138	5.41	29.2	.62	-57.2		7.2	355CCr	.827	
-9	.1	.0299	.9556	.0145	4.69	27.2	.67	-57.0		7.6	294H	.99	
-10	.4	.1565	.8245	.0191	6.97	27.1	.68	-57.0		6.3	264C	.895	
-11	.85	.6188	.3741	.0071		26	.7	-57.0	-0.6		282C	.746	N?
-12	.85	.6199	.3709	.0092	7.48	25.8	.7	-57.2		6	320C	.751	N?
-13	.6	.2973	.6888	.0138	6.12	26.6	.68	-57.2		6.8	296C	.825	N?
-14	.45	.1784	.8049	.0167	6.29	28.5	.64	-56.9		6.7	352Cr	.86	
-15	.25	.0837	.8993	.017		27.6	.67	-56.9			284H	.941	
AT86100-1	.6	.3086	.687	.0044	2.03	24.3	.72	-57.3		9	289Cr	.836	N?
-2	.2	.0683	.9145	.0172		25	.71				201H	.968	N?
FR86040-1	.1	.0269	.9551	.018		29.8	.6				245HD	.989	N?
-2	.8	.5369	.4545	.0086		25.5	.7				280CD	.769	
-3	.75	.4651	.525	.0099		25.5	.7				280CD	.786	N?
-4	.6	.2945	.6925	.0131		27.1	.68				275CD	.818	N?
-5	.4	.1637	.8208	.0155		24.9	.71				280HD	.905	
-6	.3	.1116	.872	.0164		25	.71				280HD	.936	
THX01-9.0	.8	.5888	.4036	.0076		9	.87					.902	
002-9.0	.9	.7631	.2325	.0044		9	.87					.885	
003-9.0	.95	.8719	.1258	.0024		9	.87					.877	
004-9.0	1	1	0	0		9	.87					.869	
THX1-11.0	.8	.5846	.4077	.0077		11	.85					.89	
002-11.0	.9	.76	.2356	.0044		11	.85					.872	
003-11.0	.95	.8699	.1277	.0024		11	.85					.863	
004-11.0	1	1	0	0		11	.85					.854	
THX1-27.5	.8	.5237	.4675	.0088		27.5	.67					.74	
002-27.5	.9	.7122	.2825	.0053		27.5	.67					.704	
003-27.5	.95	.8393	.1577	.003		27.5	.67					.686	
004-27.5	1	1	0	0		27.5	.67					.668	
004-27.5B	1	1	0	0		27.5	.67					.668	No clath
THX1-30.0	.8	.4952	.4954	.0093		30	.6					.683	
002-30.0	.9	.6882	.306	.0058		30	.6					.639	
003-30.0	.95	.8233	.1734	.0033		30	.6					.617	
004-30.0	1	1	0	0		30	.6					.596	No clath
004-30.0B	.99	.9604	.0388	.0007		30	.6					.599	

X = mole fraction, VX = volume fraction, Tm = melting temperature, Th = homogenization temperature, Clath = CO2 clathrate
N = suspected necking, C = homogenized into CO2 phase, H = homogenized into H2O phase, Cr = critical homogenization
D = decrepitation temperatue, THX = theoretical Type Ia inclusion, used to define dashed box in Figure 27

APPENDIX 3: Stable Isotopic Values and Equlibrium Temperatures of Minerals

SAMPLE NUMBER	MINERAL PHASE	COMMENTS LOCATION	δ18O per mil	δD per mil	δ34S per mil	δ13C per mil	T (°C) qtz-min
BX87006	chlor	musc:10%	4.17	-73.45			390
	qtz	VEIN	10.71				
	feld		9.42				590
	qtz	BMG	11.18				
	feld		9.74				550
BX87008	qtz	COMB	11.82				
	dol;25C		21.54			-5.26	Error
BX86009	qtz	VEIN	12.19				
BX86011	pyr	VEIN			1.24		
BX86013	qtz	VEIN	10.80				
	perthite		9.62				635
BX86017	qtz	VEIN	11.32				
BX87019	cpy	VEIN			1.52		
	gal				-2.37		
	pyr				1.30		
	sph				.79		
BX87031F	W/R	Q'ZITE	12.3				
BX87033	qtz	VEIN?	12.44				
BX87034	cpy	VEIN			-3.03		
	gal				-5.45		
BX87035A	W/R	Q'Z Xeno	10.12				
	qtz	clasts	6.36				
	qtz	rep.	7.27				
BX87036	qtz	BMG	10.60				
	feld	BMG	9.48				660
BX87037	qtz	BMG?	11.26				
	feld	BMG?	9.21				415
BX86043	KIBA	S in BMG			.33		
	pyr	BMG			1.37		
BX86044	qtz	VG,VEIN	11.04				
	qtz		11.19				
	qtz		11.17				
	pyr				2.74		
BX86045	qtz	VG,VEIN	10.94				
BX86074	qtz	Barren V	11.95				
	feld		9.27				330
	trem		7.74	-108.55			560
	trem			-105.31			
BX87079	musc	BMG		-128			
BX86082	qtz	COMB	12.21	-58.14			
TKK87001	sph	VEIN			1.42		
	pyr				2.38		
TKK87003	tour	HFUS	9.63	-48.79			670
	qtz		11.14				
	musc/chlr	50/50%	6.81				
TKK87004	tour	V,HFUS	10.61				570
	qtz		12.40				
AT87009	gal	VEIN			-.43		
	sph				3.33		
AT87011	qtz	COMB	12.88	-54.85			
	dol;25C		12.04			-4.33	175
AT87017	pyr	VG,VEIN			2.45		
	sph				3.67		
	qtz	NMG	11.37				
	feld	NMG	11.57				
	feld	rep.	11.87				Error
AT86048	qtz	SMG	10.20				
	feld	SMG	11.04				Error

SAMPLE NUMBER	MINERAL PHASE	COMMENTS LOCATION	δ 18O per mil	δD per mil	δ 34S per mil	δ 13C per mil	T (°C) qtz-min
AT86050	qtz	VG,VEIN	11.62				
AT86062	alb	Sponge	10.13				
AT86063	qtz	NMG	10.53				
	feld		9.67				805
AT86064	qtz	NMG	11.01				
	feld		9.27				475
AT86100	qtz	VEIN	11.58				
	qtz		11.30				
	qtz		11.53				
	qtz		10.99				
AT86110	dol;25C	Sponge	21.42			-3.54	
FR86001	W/R	Q'ZITE	12.95				
	qtz	clasts	12.85				
FR86004	qtz	VG,VEIN	11.91				
	feld		10.59				580
	chlor	musc:10%	3.54	-83.95			290
	chlor	rep.		-78.56			
	pyr				1.36		
FR87025	chlor	musc:10%	6.73	-63.76			450
	qtz	VEIN	12.59				
FR87025F	qtz	V,Float	13.05				
	tour	HFUS	11.06				
	tour	rep.	10.93	-38.78			775
	musc	chl:10%	7.37	-79.94			
FR86037	qtz	VEIN	12.91				
FRC86085	qtz	VEIN	11.36				
1to10m	feld		9.79				515
	pyr	in fx.			1.21		
FRC86085 21to30m	qtz	VEIN	12.13				
UC86-83	qtz	VEIN	11.67				
	chlor	musc:20%	5.84	-75.79			450
GL86002	qtz	VEIN	9.81				
TKK87016	dol;25C	No.2	17.55			-7.27	
	dol;50C		16.32			-7.31	
TKK87021	dol;25C	No.1	17.99			-6.38	
	dol;50C		15:97			-6.68	
TKK87032	dol;25C	No.4	14.67			-6.29	
	dol;50C		13.84			-6.25	
TKK87034	dol;25C	No.4	15.61			-6.12	Error
	dol;50C		14.29			-6.21	
	qtz	early	15.3	-94.12			
TKK87035	dol;25C	No.4	15.83			-5.95	
	dol;50C		13.98			-6.22	
MCD5-45.6	dol;25C	No.2	16.52	-90.36		-8.11	110
	hem		-5.79				100
	qtz	late	18.74	-92.14			100
DMC4-107	dol;25C	No.2	21.18			-6.93	
DMC4-93	dol;25C	No.2	21.45			-8.15	
No.4,misc	W/R	Q'ZITE	16.47				
CSTONE	qtz	VEIN	19.09				
QR-87-3	qtz	VEIN	17.49	-89.04			
1.9+4.6m	hem		-7.96				115
QR-87-4	pyr	PyrVEIN			-29.94		

HFUS = sample treated by ultrasound in hydroflouric acid
25C or 50C = temperature at which sample was reacted with phosphoric acid
No.1,2,3,4 = zone of Nicholson deposit, Sponge = "sponge rock", COMB = comb vein
V = VEIN, VG = visible gold in sample, rep. = repeat analysis, Error = -ve fract.
BMG = Box Mine granite, NMG and SMG = north and south parts of Athona granite

APPENDIX 4: Rb/Sr Data for the Goldfields Lode-Gold Deposits

Sample	Mineral	Rb (ppm)	Sr (ppm)	87Rb/86Sr	87Sr/86Sr	% Error
Box Lode-Gold Vein Minerals:						
TKK87003	tourmaline	.8325	13.94	.174	.775657	.01
BX87006	feldspar	317.7	184.51	5.083	.904861	.005
	chlorite	217.4	34.96	19.014	1.278528	.003
Box Mine Granite:						
BX87006	feldspar	272.5	58.01	14.206	1.159285	.05
BX87036	feldspar	194.2	29.75	20.026	1.307186	.01
Frontier Lode-Gold Vein Minerals:						
FR86004	feldspar	398.7	114.19	10.445	1.044717	.01
FRC86085	feldspar	250.7	119.17	6.227	.933175	.4
FR87025F	tourmaline	5.075	79.66	.186	.76252	.004
	muscovite	686.5	11.23	330.844	9.505564	.007

All errors are 2 sigma

APPENDIX 5: List of Goldfields Samples

SAMPLE #	DESCRIPTION	ANALYSIS
	BOX MINE	
BX87001	lode-qtz vein in BMG, with gangue sulphides	FI
BX87006	lode-qtz vein in BMG, with gangue chlorite and feldspar	SI, RI
BX87008	comb vein in BMG	SI
BX86009	lode-qtz vein in BMG	SI, FIP
BX86011	lode-qtz vein with gangue pyrite	SI
BX86013	lode-qtz vein in BMG, with gangue feldspar	SI, FIP
BX86017	lode-qtz vein in BMG	SI, FIP
BX87019	lode-qtz vein in BMG, with gangue sulphides	SI
BX87031F	quartzite country rock near BMG	SI
BX87033	lode-qtz vein in BMG	SI
BX87034	lode-qtz vein in BMG, with gangue sulphides	SI
BX87035A	quartzite xenolith in BMG	SI
BX87036	BMG	SI, RI
BX87037	BMG?, near contact	SI
BX86043	BMG with abundant pyrite	SI
BX86044	lode-qtz vein in BMG, with visible Au in pyrite	SI, FI
BX86045	lode-qtz vein in BMG, with visible Au in fracture	SI, FIP
BX86074	barren qtz vein outside BMG, with gangue tremolite and feldspar	SI, FIP
BX87079	BMG with muscovite slips	SI
BX86080	lode-qtz vein in BMG	FIP
BX86082	comb vein in BMG	SI, FI
BX86085-1	lode-qtz vein in BMG	FI

SI = stable isotope, RI = radiogenic isotope (Rb-Sr), qtz = quartz
FI = fluid inclusion microthermometry, FIP = fluid inclusion petrography
BMG = Box Mine granite, AMG = Athona Mine granite, FMG = Frontier M. gr.

SAMPLE #	DESCRIPTION	ANALYSIS
BX86085-2	lode-qtz vein in BMG	FIP
BX86085-3	lode-qtz vein in BMG	FIP
TKK87001	lode-qtz vein in BMG, with gangue sulphides	SI
TKK87003	lode-qtz vein in BMG, with gangue tourmaline and late muscovite	SI, RI
TKK87004	lode-qtz vein in BMG, with gangue tourmaline	SI, FIP
	ATHONA MINE	
AT87009	lode-qtz vein in AMG, with gangue sulphides	SI
AT87011	comb vein in AMG	SI
AT87017	lode-qtz vein in AMG, with gangue sulphides and visible Au in fractures	SI
AT86022	lode-qtz vein in AMG, with visible Au in fracture	FIP
AT86048	AMG	SI
AT86050	lode-qtz vein in AMG, with visible Au and gangue galena	SI, FIP
AT86062	sponge rock alteration in AMG	SI
AT86063	AMG, 1m from edge of sponge rock alteration	SI
AT86064	AMG, 4m from edge of sponge rock alteration	SI
AT86100	lode-qtz vein in AMG	SI, FI
AT86110	sponge rock alteration in AMG	SI, FIP
	FRONTIER PROPERTY	
FR86001	quartzite country rock near FMG	SI
FR86004	lode-qtz vein in FMG, with gangue chlorite, felspar and pyrite, visible Au	SI, RI
FR86021	barren qtz vein in amphibolite above FMG	FIP
FR87025	lode-qtz vein in FMG, with gangue chlorite	SI

SI = stable isotope, RI = radiogenic isotope (Rb-Sr), qtz = quartz
FI = fluid inclusion microthermometry, FIP = fluid inclusion petrography
BMG = Box Mine granite, AMG = Athona Mine granite, FMG = Frontier M. gr.

SAMPLE #	DESCRIPTION	ANALYSIS
FR87025F	lode-qtz vein in FMG, with gangue tourmaline and late muscovite	SI, RI
FR86037	lode-qtz vein in FMG	SI, FI
FR86040	lode-qtz vein in FMG	FI
FRC86085 1to10m	lode-qtz vein in FMG, with gangue feldspar and pyrite sample from drill core	SI, RI
FRC86085 21to30m	lode-qtz vein in FMG sample from drill core	SI
UC86-83	lode-qtz vein in FMG, with gangue chlorite	SI
	GREENLEE PROPERTY	
GL86002	lode-qtz vein, Greenlee property	SI, FIP
	NICHOLSON MINE	
TKK87016	euhedral dolomite vein, No. 2 zone	SI, FIP
TKK87021	euhedral dolomite vein, No. 1 zone	SI, FIP
TKK87032	euhedral dolomite vein, No. 4 zone	SI, FIP
TKK87034	euhedral qtz-dolomite vein, No. 4 zone	SI, FI
TKK87035	euhedral dolomite vein, No. 4 zone	SI, FI
MCD5-45.6	euhedral qtz-dolomite-hematite vein sample from drill core, No. 2 zone	SI, FI
DMC4-107	euhedral dolomite vein sample from drill core, No. 2 zone	SI, FI
DMC4-93	euhedral dolomite vein sample from drill core, no. 2 zone	SI
No.4,misc	chert altered quartzite, float boulder	SI
	QUARTZITE RIDGE SHOWING	
CSTONE	euhedral qtz veinlet	SI
QR-87-3 1.9+4.6m	euhedral qtz-hematite veinlet sample from drill core	SI, FI
QR-87-4	pyrite veinlet in quartzite	SI
	FISH HOOK BAY MINE	
FH27-142.	dolomite vein	FI

SI = stable isotope, RI = radiogenic isotope (Rb-Sr), qtz = quartz
FI = fluid inclusion microthermometry, FIP = fluid inclusion petrography
BMG = Box Mine granite, AMG = Athona Mine granite, FMG = Frontier M. gr.